Dissertation zur Erlangung des Doktorgrades

der Fakultät für Chemie und Pharmazie

der Ludwig-Maximilians-Universität München

Development of a sprayable hydrogel containing the recombinant bacteriophage endolysin HY-133 for topical MRSA sanitation

Simon Eisele

aus Lörrach, Deutschland

2022

Erklärung

Diese Dissertation wurde im Sinne von §7 der Promotionsordnung vom 28. November 2011 von Herrn Prof. Dr. Gerhard Winter betreut.

Eidesstattliche Versicherung

Diese Dissertation wurde eigenständig und ohne unerlaubte Hilfe erarbeitet.

München, den 26. August 2022

…….

(Simon Eisele)

Dissertation eingereicht am: 13. Januar 2022

1. Gutachter: Prof. Dr. Gerhard Winter

2. Gutachter: Prof. Dr. Wolfgang Frieß

Mündliche Prüfung: 17. Februar 2022

Acknowledgements

This thesis was prepared between January 2016 and September 2019 at the Department of Pharmacy, Pharmaceutical Technology and Biopharmaceutics at the Ludwig-Maximilians Universität München (LMU) in cooperation with the Deutsches Zentrum für Infektionsforschung (DZIF) and HyPharm GmbH.

Foremost, I would like to thank my supervisor Prof. Dr. Gerhard Winter for giving me the opportunity to work in this exciting and highly relevant research field. I am very grateful for receiving his valuable advice and guidance during the project work as well as the fruitful and inspiring scientific discussions.

I would also like to thank Prof. Dr. Wolfgang Frieß for kindly taking over the co-referee of this thesis and for establishing excellent working conditions. Additionally, his encouragement of scientific discussions is highly appreciated. Moreover, I enjoyed the numerous social activities the groups did together. Many thanks also go to Prof. Dr. Olivia Merkel, Dr. Gerhard Simon, and Sabine Kohler.

The DZIF is gratefully acknowledged for promoting this project, for funding and material supply, and for taking over the organizational part of the project. Especially, I want to thank Dr. Thomas Hesterkamp, Dr. Lisa Heitmann and Dr. Sebastian Goy for their scientific and organizational support.

My acknowledgement goes also to HyPharm GmbH, formerly Hyglos GmbH, especially to Dr. Wolfgang Mutter and Dr. Sonja Molinaro for the excellent collaboration, the valuable discussions and their input. It was a great opportunity to work with HyPharm's interesting product and being part of the further development. I wish HyPharm and the team all the best for the future.

Moreover, I was supported with material and knowledge from Microcoat. Later stages of the drug product development process were supplied with material from Fraunhofer ITEM. The project was additionally supported by the University of Tübingen and Köln. Here, Prof. Dr. Andreas Peschel together with Dr. Bernhard Krismer and Dr. Dirk Kraus were part of the project team and contributed with their exceptional research of the nasal microbiota. Prof. Dr. Karsten Becker and Prof. Dr. Evgeny Idelevich greatly supported the project in the clinical phase. Many thanks for the lively discussions and great collaboration throughout the project.

Special thanks go to Dr. Dierk Roessner, Dr. Lorenzo Gentiluomo and Wyatt Technologies, where I learned a lot using their CG-MALS system at their labs.

Furthermore, I am very thankful for the opportunity to supervise pharmacy and pharmaceutical sciences students during their regular practical course as well as during the master studies. In particular, I would like to thank Maximilian, Marcel and Britta for their lively curiosity, who conducted their bachelor or master thesis and projects under my supervision.

Two lab-mates were part of the journey. I especially want to thank my first lab-mate Ben for all the great times and good discussions we had. With him, Ellen and Randy I spend a great time at Breckenridge and I was glad to join his lab later that year. Ruth took over his place and the research on antibiotics was joined by AAVs. Thank you for the great time and many coffee breaks!

Particularly, I want to thank Ivi for her great support throughout the time at the department and now at the lyophilization group at Coriolis. Together with Andi, we spend some vacations together and later joined the same company. Carolin and Andy supported this project with *in silico* data and gave valuable insights regarding molecular dynamics. Also, the rest of the team needs to be mentioned in here, as they all contributed to the great atmosphere at the chair: Hristo and Julian, Micha, Dennis and Wei-Wei, Teresa, Bernard and Alice – Thank you all for the unforgettable time!

Finally, I would like to thank my family for their confidence, love, and support throughout the studies and the PhD project. Here, I also want to thank Tom, Basti, Max, Freddie, Chris and Claudia for their friendship!

Last but not least, thank you Nathalie for your patience, support, never-ending encouragement and for your love.

General Table of Content

Chapter 1

Introduction

Table of Contents

1. General introduction

Alexander Fleming's discovery of the modern antibiotic penicillin in 1928 and the introduction of sulfonamides in 1937 made many bacterial, fungal and protozoal infections treatable and controllable for the first time. During the golden era of antibiotic discovery in the 1940s to 1960s, many different antibiotics were isolated and widely used for the treatment of different diseases, leading to significantly increased survival rates and the near disappearance of some former life-threatening diseases [1], [2]. Many antibiotic agents discovered during this period continue to be used today and, in most cases, they are still effective. However, bacterial penicillinase, also known as β-lactamase, was identified in 1940, only shortly after the discovery of penicillin [3]. With a more widely usage of antibiotics, resistant strains of several bacteria became prevalent. This not only led to antibiotic resistance, but also to multi-drug resistant (MDR) bacteria. In 2004, more than 70% of known pathogenic bacteria were estimated to be resistant to at least one of the then available antibiotics [4]. Multi-drug resistant forms of pathogen bacteria are rising in both developing and industrialized countries and are evolving to extremely hazardous pathogens. In this case, nosocomial infections, that means infections acquired in hospitals, are very dangerous and potentially deathly to elderly patients and patients suffering from other diseases. These pathogens are also known as "superbugs", microbes associated with enhanced morbidity and mortality [3]. Problematically, only few therapeutic agents can be used against these infections. This is always linked to the danger that new resistances develop. Beside multi-drug resistant *mycobacterium tuberculosis* and *clostridium difficile*, one of the most known superbugs is methicillin-resistant *staphylococcus aureus* (MRSA) [5]. *Staphylococcus aureus* (*S. aureus*) was treat- and controllable with the discovery of penicillin until the occurrence of penicillinase-containing *S. aureus* strains. With the introduction of methicillin in 1959, this detriment was thought to be abolished, but only 3 years later methicillin-resistant *S. aureus* appeared [3]. By now, this pathogen has become one of the major nosocomial infections, also known as healthcare-associated MRSA (HA-MRSA) [6]. HA-MRSA mainly affects patients with certain risk factors like surgery, general hospitalization, invasive medical devices and residence in long-term care facilities, for example in nursing homes. It is endemic in most hospitals in industrial nations, making effective eradication complicated. In later stages of the MRSA infection, it can spread to the bloodstream, lungs and heart, causing life-threatening endocarditis, meningitis and fatal sepsis [7]. In the US, MRSA is one of the most deathly single infections, causing the deaths of approximately 100,000 patients each year [4], [6].

Next to the HA-MRSA prevalent in hospitals, specific MRSA strains can also colonize persons who were not in contact with healthcare facilities, then called community-acquired MRSA (CA-MRSA) [5]. These strains are more virulent, but show less antibiotic resistances than HA-MRSA and tend to infect younger and healthier people by skin-to-skin contact [6]. CA-MRSA causes skin and soft tissue

infections, but can also lead to serious necrotizing pneumonia [8]. While CA-MRSA rates are still low, they are quickly rising in some regions [9]. Since antibiotic resistant bacteria are increasingly limiting current antimicrobial treatments, development of other types of antibacterial agents is necessary. In addition, other methods besides the acute treatment with antibiotics can be employed to reduce the risk of an MRSA outbreak, for example strict adherence to hand hygiene and general contact precaution measures in healthcare facilities.

1.1 Nasal colonization of *S. aureus*

S. aureus is very common on the human skin. Approximately 30% of the adult population in industrialized countries are colonized with methicillin-susceptible *S. aureus* (MSSA) strains [8]. Although multiple body sites can be colonized by *S. aureus*, the nasal cavity is the most frequent one [9]. Colonization of the nasal cavity with *S. aureus* is known as a major risk for infection. Approximately 20% of the healthy population is persistently colonized in the nasal cavity with *S. aureus* over several months or years [10]. Colonization rates differ between ethnical groups and age; for example, higher persistent colonization rates were determined in children [9], [11].

S. aureus cells are predominantly found in the anterior part of the nasal cavity, the anterior nares [8]. This part of the nose is also called “nose picking area”, which indicates the main cause of persistent infections in hospitals and other healthcare facilities [9], [12]. As *S. aureus* cells are extremely resistant and can survive several months on any type of surface, hands can transfer *S. aureus* from surfaces at infected places to the nose [9]. These surface contaminations are most likely caused by colonized persons suffering from rhinitis [9].

In addition to 20% persistent carriers, about 30% of the people are intermittent carriers. Therefore, only 50% of all people are non-carriers [9], [13]. Amongst these two subgroups, persistent carriers are the more endangered ones. They are colonized with a higher load of *S. aureus* and tend to disperse more *S. aureus* [9].

Amongst people colonized with *S. aureus*, only a fraction is infected with an MRSA strain. This fraction varies across countries and population groups [14]. In the EU, for example, the MRSA share amongst all *S. aureus* infections ranges between 1% to over 50% [15]. There, HA-MRSA decreased over the past years, while at the same time an increase in CA-MRSA and livestock-associated MRSA (LA-MRSA) strains was reported [15]. The US shows an MRSA spread of about 53% among those infected with *S. aureus*, with rising numbers of CA-MRSA over the past years [16].

1.2 Adherence of *S. aureus* to the nasal epithelium

Effective adherence of the pathogen to the nasal epithelial cells facilitates persistent colonization with *S. aureus* [10]. Two major adherence possibilities are known. First, *S. aureus* can directly adhere by

mucosal and mucin binding [10], [17], [18]. Most *S. aureus* cells are found in histological samples in the mucus layer on top of the epithelium because S. aureus cells are able to directly bind to mucin. Second, binding to cell wall proteins was found [10]. The anterior part of the nasal cavity is lined with a stratified, keratinized, non-ciliated squamous epithelium, surrounded by various proteins like loricrin, involucrin and cytokeratin. Direct interaction of *S. aureus* via the cell wall-anchored clumping factor B with cytokeratin and interaction with the cell wall proteins loricrin and involucrin led to strong adherence [10], [19], [20]. However, the degree to which the nasal cavity provides adequate adherence for MRSA strains differs across host genotypes. It is, for example, known that the adherence of *S. aureus* to nasal epithelial cells of carriers is significantly better than that of non-carriers [8]. This also explains why not all persons in health-care environments are carriers.

1.3 *S. aureus* colonization and infections

There are several indications that colonization of the nasal cavity with *S. aureus* and the development of MRSA infections are linked [11]: First, *S. aureus* carriers exhibit higher infection rates than non-carriers. Second, patients are often infected with their own *S. aureus* strain. Comparing the bacterial strain in the colonized nasal cavity with isolates during an acute infection, both strains were shown to be identical [21]. Third, eradication of *S. aureus* in nasal cavity with mupirocin is linked to a decrease in nosocomial infection of patients and a lower risk of MRSA infections after hospital discharge [8], [22]. As a parenteral application is not necessary, this is an important factor for the development of future antibacterial agents.

1.4 Eradication of *S. aureus* in the nasal cavity

Long-term eradication of *S. aureus* in the nasal cavity with mupirocin effectively prevents *S. aureus* infections in dialysis patients [9]. The use of antibiotics after cardiac surgery was also reduced after successful *S. aureus* eradication [23].

Since the nasal cavity plays a key role in MRSA contagion, only effective treatment of both ill and healthy MRSA carriers can prevent future MRSA spreading and lead to a decrease of MRSA rates. In addition, as autoinfection rates are at a high level of about 80%, *S. aureus* eradication prior to surgery or other invasive activities can decrease the probability of *S. aureus* infection [8]. Currently, mupirocin is used for MRSA and MSSA eradication in the nasal cavity. It is applied as a nasal ointment 2 to 3 times per day for 5 to 14 days [24]. Although mupirocin is known as the most effective topical antimicrobial agent currently available for the decolonization of gram-positive bacteria, poor patient compliance leads to a significantly reduced decolonizing effect. Additionally, a positive effect on the outcome of surgical site infections could not be shown, although the overall infection rate with MRSA and autoinfection was reduced [8]. Next to poor patient compliance, the bad outlook regarding long-term

efficacy of mupirocin treatment is problematic. Additionally, the long-term efficacy of mupirocin regarding nasal decolonization is low, as recolonization was frequently observed after 3 months [8]. In addition, increasing mupirocin resistance which is connected with a broad mupirocin application does not allow to use mupirocin for long-term treatment [25].

With the emergence of more and more antibiotic resistances and therefore reduced efficacies, the need for alternative antibiotic drugs beside today's classical antibiotics becomes evident. A long-neglected opportunity lies in the use of bacteriophages.

2. Bacteriophage therapy

The history of bacteriophage therapy is even older than the history of antibiotic therapy. Antibacterial activities against *vibrio cholera* were first reported in 1896 [26]. In 1917, bacteriophages were officially discovered and it was quickly assumed that the antibacterial effect was caused by a virus. The first use in humans was the treatment of a skin disease caused by staphylococcal bacteria in 1921. Shortly after, the commercial development of bacteriophages with antibiotic properties against *staphylococci*, *streptococci* and *E. coli* was started, but only a few years later phage therapy was abandoned in Western countries due to the development of modern antibiotics [27]. However, the former Soviet Union continued to use phage therapy due to the lack of modern antibiotics. Until today, the Eliava Institute in Tbilisi, Georgia, studies phages and treats patients with multi-resistant bacterial infections [28]. Here, cocktails consisting of various bacteriophages are used. Yet, the exact combination is unknown and is changed from application to application. Since the efficacy spectrum of these phage cocktails alters with different batches, a potential approval by regulatory agencies is very difficult [29].

Bacteriophages are naturally occurring viruses which are able to infect bacterial cells. They form progeny bacteriophages within the bacterial cell in the replication phase, subsequently lyse the bacterial cell wall and then release the progeny phages to infect new host cells. During the lysis process, the phage-encoded membrane protein holin opens the cell membrane, which makes the peptidoglycan structure of the bacteria accessible for phage-encoded endolysins [26]. Subsequently, these endolysins specifically hydrolyze the peptidoglycan structure of the cell wall [30]. As gram-positive bacteria do not an have an outer membrane, an exogenous application of these endolysins to destroy the bacterial cell walls is possible.

As bacteriophages are constantly evolving, they are able to rapidly adapt to new multidrug-resistant bacteria. Bacteriophages are characterized by their high specificity, which is one of their biggest advantages as they can only target one bacterial strain while the remaining microbiome remains intact. However, at the same time a high specificity to one strain is also connected to a reduced efficacy in infection where multiple strains are apparent. Therefore, bacteriophages are always applied in multi-

phage cocktails. Because bacteriophages differ from classical antibiotics in their bactericidal mechanism, they can also be used against multidrug-resistant bacteria. However, bacteria which are resistant against bacteriophages were found in several studies [31]. One major resistance mechanism is the variation of surface structures of bacterial strains, which leads to reduced phage binding. Another disadvantage is related to the cell lysis itself: rapid disintegration of the bacterial cell wall can be accompanied by the release of endotoxins, which can then lead to a strong immune response after the treatment [32].

Nevertheless, phage therapy is a promising approach to replace or complement therapy with classical antibiotics. Of particular interest are endolysins, which are formed during the release phase of the bacteriophages and provide fast and effective cell wall weakening by targeting the murein cell wall.

3. Recombinant bacteriophage endolysins as new agents with antibiotic properties

The group of recombinant bacteriophage endolysins represents a novel alternative to classical antibiotics, but also to bacteriophages. Recombinant bacteriophage endolysins cause rapid lysis of gram-positive bacteria when applied exogenously [7]. These endolysins are developed as recombinant proteins which are targeting one specific pathogen. Similar to bacteriophages, the high specificity is one of their main advantages, as pathogens can be eradicated without affecting other bacterial strains from the normal microbiome [33]. Additionally, chances of resistance formation are low [34]–[36]. Most importantly, in contrast to bacteriophages, recombinant endolysins are easier to manufacture because only one well characterized enzyme is produced. Therefore, the application of phage cocktails is not necessary, simplifying regulatory approval. Contrary to phage-encoded endolysins, recombinantly produced bacteriophage endolysins are highly variable and can be specifically adapted towards their intended usage profile.

In general, recombinant endolysins consist of two functional modules: an enzymatic active domain (EAD) and a cell wall binding domain (CBD). Both domains can be designed according to the intended specificity of the endolysins. The high variability results from this modular design, as domains of different origins can be combined with each other, resulting in chimeric endolysins. Thus, recombinant endolysins can be specifically developed for a certain bacterium.

The N-terminal domain is the catalytically active domain of the enzyme. It cleaves major bonds of the peptidoglycan structure in the bacterial cell wall. Four different cleavage sites are known [7]: (I) N-acetylmuramidases (lysozymes) and (II) N-acetyl-β-D-glucosaminidases (glycosidases) both hydrolyze glycosidic bonds in sugar moieties of the cell wall, (III) N-acetylmuramoyl-L-alanine amidases cleave

amid bonds between sugar and peptide moieties, and (IV) L-alanoyl-D-glutamate endopeptidases target peptide bonds in peptidoglycan structures of the cell wall. Some endolysins can also contain 2 or more different catalytic domains, which enables them to target different structures at the host cell wall simultaneously. This improves and accelerates enzyme activity when fast activity is needed. The C-terminal domain determines the bacterial specificity of the enzyme. It binds to the unique structures found on the surface of the host bacterium, thereby adhering to the host cell wall non-covalently. The binding domain is specific for each bacterial strain and makes it possible to target one particular pathogen. In most cases, enzymatic activity of the endolysin demands an interaction of the binding domain and the cell wall [7], [36]. However, in some rare cases lytic activity can be increased when the C-terminal domain is removed [7]. Combining both features of the C- and the N-terminal region, high specificity to one bacterial strain and high cleaving potential can be achieved.

Various recombinant bacteriophage endolysins were developed over the last years [36]–[39]. PlyC, an endolysin against *streptococcus pyogenes*, showed an efficacy comparable to penicillin and erythromycin. However, the endolysin was also effective against streptococcal biofilms, where classical antibiotics failed [40]. *Bacillus anthracis*, the anthrax pathogen, was successfully targeted using the recombinant endolysins AP50-31 and LysB [41].

S. aureus is one of the most prevalent multi-drug resistant pathogens and therefore the development of specific endolysins against it is of particular interest. As described, endolysins have a typical 2-domain structure, comprising an EAD and a CBD for optimized efficacy. Multimeric structures like PlyC are also possible compromising an octameric ring structure, representing the CBD, and a 3-domain EAD [42].

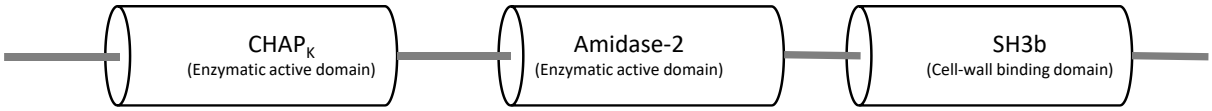

Figure 1: Schematic structure of LysK, the endolysin of PhageK.

A variety of these endolysins are based on LysK, the endolysin of Phage K (Figure 1). LysK consists of an N-terminal cysteine/histidine-dependent amidohydrolases/peptidase ($CHAP_K$) domain, the amidase-2 domain, and the C-terminal binding domain SH3b [43]. Lytic activity was shown in LysK for various *S. aureus* strains [44]. Maintained activity was also determined in a fusion protein containing only the $CHAP_K$-domain and the SH3b-domain, as well as in $CHAP_K$ alone [39], [43]. Therefore, many endolysins which are targeting *S. aureus* contain at least one domain of this pattern.

One of the most studied endolysins is SAL200, a drug product containing SAL-1 as the API [37]. SAL200 is based on the endolysin produced by the bacteriophage SAP-1, which shows higher activity than LysK [45]. Similar to LysK, SAL-1 comprises two EADs, the $CHAP_K$ domain and the amidase-2 domain. As the

CBD, SH3b is included in these endolysins [45]. The endolysin SAL200 showed a bactericidal characteristic and a high efficacy against 336 MRSA isolates [37]. With SAL200 the first-in-human phase I clinical trial of an intravenously administered endolysin was conducted. No severe adverse effects and an overall good tolerance were shown [46]. Results from the second clinical trial (NCT03089697) have not been published yet [47].

Only systemic or very serious infections necessitate intravenous administration. Since *S. aureus* persists in otherwise healthy persons in the nasal cavity, topical eradication of *S. aureus* is of particular interest.

4. The bacteriophage endolysin HY-133

The newly developed HY-133 (HYPharm GmbH, Bernried, Germany) is a bacteriophage endolysin against MSSA and MRSA. HY-133 is a successor of PRF-119 (Hyglos GmbH, Bernried, Germany) with a shorter peptide linker and higher proteolytic stability [48]. The bactericidal activity of HY-133 was shown in vitro against all tested major African *S. aureus* strains, including the novel strain *S. schweitzeri*, which has a different peptidoglycan structure. In addition, HY-133 showed good activity against ceftobiprole/ceftaroline-resistant MRSA strains [49]. The minimum inhibitory concentration (MIC) of HY-133 ranged from 0.125 to 0.5 µg/ml [49]. The progenitor endolysin PRF-119 was positively tested for activity against 398 MSSA strains and 776 MRSA strains with MIC ranges of 0.024 – 0.780 µg/ml (MSSA) and 0.024 – 1.563 µg/ml (MRSA), respectively [48]. It was also demonstrated that HY-133 was active against livestock-associated MRSA (LA-MRSA) [50]. In addition, no cytotoxicity was observed for this recombinant endolysin in low concentrations [51].

The activity of HY-133 was tested against mupirocin and daptomycin in vitro [52]. HY-133 showed a strong and fast bactericidal effect at low concentrations. MIC and MBC values of HY-133 were comparable to those of mupirocin and daptomycin. However, mupirocin only showed an bacteriostatic effect and time-kill curves demonstrated a faster onset of the bactericidal activity of HY-133 within the first hour compared to daptomycin [52].

HY-133 also effectively targeted small colony variants (SCV) of *S. aureus* and showed fast bactericidal activity [53]. Compared to *S. aureus* wild types, SCVs have an altered cell wall composition, a slower growth characteristic and a different metabolism [53]. SCVs are therefore resistant against major antibiotics. It was shown that time-kill curves of HY-133 are substantially faster than for oxacillin, where the onset of the bactericidal effect was only reached after 4-24 h and not after 1 h as in HY-133.

4.1 Enzyme structure

The two bacteriophage endolysins PRF-119 and HY-133 share their two functional domains, the EAD and the CBD (Figure 2). However, they differ in the length of the peptide linker, which was shortened in HY-133 to achieve an increased proteolytic stability.

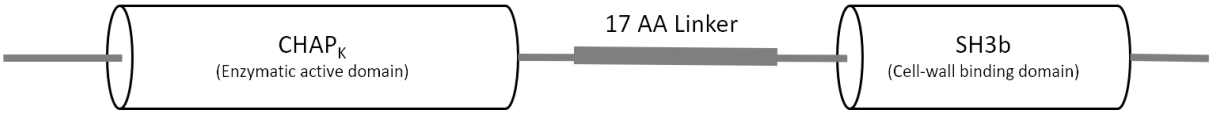

Figure 2: The 2-domain structure of HY-133 comprises a N-terminal EAD and a C-Terminal CBD. The EAD comprises CHAPK of the endolysin LysK and the CBD comprises SH3b of lysostaphin. The domains are linked by a 17 amino acid linker.

The EAD consists of the CHAP$_K$ domain from LysK. In contrast to SAL-1, amidase-2 is not included in this EAD. The CHAP$_K$ domain alone is therefore in control of the lysis of the murein cell wall. It cleaves the peptidoglycan structure between the D-alanine of the tetrapeptide backbone and the first glycine of the pentaglycine cross-bridge [53], [54]. The crystal structure of the CHAP$_K$ domain of LysK was determined by Sanz-Gaitero et al. [54], [55].

The CBD was taken from the bacteriocin lysostaphin, an enzyme originating from *staphylococcus simulans*. Lysostaphin directly binds to the peptidoglycan structure of *S. aureus* via the CBD SH3b and cleaves the penta-glycine cross-bridges of the peptidoglycan structure with its enzymatically active domain. However, the formation of resistances against lysostaphin is very likely [56]–[58]. Due to this, only the CBD of lysostaphin was used in HY-133. Binding of the CBD SH3b was further evaluated and a binding mechanism suggested [59]. It was proposed that two β-strands of the SH3b domain were involved in the binding to the pentaglycine binding side [59]. The crystal structure of lysostaphin was determined as well [60].

HY-133 was patented as a chimeric polypeptide (protein) which specifically targets one pathogen without destroying the microbiome.

4.2 Application of HY-133

Increasing antibiotic resistant rates demand for antibiotics with new modes of action. The broad activity range of HY-133 against various *S. aureus* strains, including MRSA, MSSA, ceftobiprole/ ceftaroline-resistant MRSA strains and borderline oxacillin-resistant isolates, shows that this recombinant bacteriophage endolysins is part of a powerful novel class of antimicrobial agents [49], [52]. The rapid and specific bactericidal activity is particularly suitable for MRSA decolonization. Since the nasal cavity is of special interest for targeting MRSA colonization, nasal application of HY-133 is intended.

5. References

[1] J. Bérdy, "Thoughts and facts about antibiotics: Where we are now and where we are heading," *J. Antibiot. (Tokyo).*, vol. 65, no. 8, pp. 441–441, 2012.

[2] K. Lewis, "Platforms for antibiotic discovery.," *Nat. Rev. Drug Discov.*, vol. 12, no. 5, pp. 371–87, 2013.

[3] Davies, J, & Davies, D., "Origins and Evolution of Antibiotic Resistance," *Microbiol. Mol. Biol. Rev.*, vol. 74, no. 3, pp. 417–433, 2010.

[4] S. Demain, A. L.; Sanchez, "Microbial drug discovery: 80 years of progress.," *J. Antibiot. (Tokyo).*, vol. 62, no. 1, pp. 5–16, 2009.

[5] H. C. Maltezou and H. Giamarellou, "Community-acquired methicillin-resistant Staphylococcus aureus infections," *Int. J. Antimicrob. Agents*, vol. 27, no. 2, pp. 87–96, 2006.

[6] F. R. DeLeo, M. Otto, B. N. B. Kreiswirth, and H. F. H. Chambers, "Community-associated meticillin-resistant *Staphylococcus aureus*," *Lancet*, vol. 375, no. 9725, pp. 1557–1568, 2010.

[7] M. Fenton, P. Ross, O. Mcauliffe, J. O'Mahony, and A. Coffey, "Recombinant bacteriophage lysins as antibacterials," *Bioeng. Bugs*, vol. 1, no. 1, pp. 9–16, 2010.

[8] T. Coates, R. Bax, and A. Coates, "Nasal decolonization of Staphylococcus aureus with mupirocin: Strengths, weaknesses and future prospects," *J. Antimicrob. Chemother.*, vol. 64, no. 1, pp. 9–15, 2009.

[9] H. F. Wertheim *et al.*, "The role of nasal carriage in Staphylococcus aureus infections," *Lancet Infect. Dis.*, vol. 5, no. 12, pp. 751–762, 2005.

[10] C. Weidenmaier, C. Goerke, and C. Wolz, "Staphylococcus aureus determinants for nasal colonization," *Trends Microbiol.*, vol. 20, no. 5, pp. 243–250, 2012.

[11] S. J. Peacock, I. De Silva, and F. D. Lowy, "What determines nasal carriage of Staphylococcus aureus?," *Trends Microbiol.*, vol. 9, no. 12, pp. 605–610, 2001.

[12] H. F. L. Wertheim, M. van Kleef, M. C. Vos, A. Ott, H. A. Verbrugh, and W. Fokkens, "Nose picking and nasal carriage of Staphylococcus aureus.," *Infect. Control Hosp. Epidemiol.*, vol. 27, no. 8, pp. 863–867, Aug. 2006.

[13] A. Sakr, F. Brégeon, J. L. Mège, J. M. Rolain, and O. Blin, "Staphylococcus aureus nasal colonization: An update on mechanisms, epidemiology, risk factors, and subsequent infections," *Front. Microbiol.*, vol. 9, no. OCT, pp. 1–15, 2018.

[14] A. Hassoun, P. K. Linden, and B. Friedman, "Incidence, prevalence, and management of MRSA bacteremia across patient populations—a review of recent developments in MRSA management and treatment," *Crit. Care*, vol. 21, no. 1, p. 211, Dec. 2017.

[15] R. Köck *et al.*, "Methicillin-resistant Staphylococcus aureus (MRSA): burden of disease and control challenges in Europe," vol. 15, no. 41. Robert Koch-Institut, 2010.

[16] A. S. Lee *et al.*, "Methicillin-resistant Staphylococcus aureus," *Nat. Rev. Dis. Prim.*, vol. 4, no. 1, p. 18033, Jun. 2018.

[17] C. von Eiff, K. Becker, K. Machka, H. Stammer, and G. Peters, "Nasal Carriage as a Source of Staphylococcus aureus Bacteremia," *N. Engl. J. Med.*, vol. 344, no. 1, pp. 11–16, Jan. 2001.

[18] A. Alotaibi and S. Clark, "Functional characterisation of cell wall proteins that enhance nasal colonisation by Staphylococcus aureus, through binding to host mucin," *Access Microbiol.*, vol. 1, no. 1A, p. 786, Mar. 2019.

[19] K. A. Lacey, M. E. Mulcahy, A. M. Towell, J. A. Geoghegan, and R. M. McLoughlin, "Clumping factor B is an important virulence factor during Staphylococcus aureus skin infection and a promising vaccine target," *PLOS Pathog.*, vol. 15, no. 4, p. e1007713, Apr. 2019.

[20] C. Laux, A. Peschel, and B. Krismer, "Staphylococcus aureus Colonization of the Human Nose and Interaction with Other Microbiome Members," *Microbiol. Spectr.*, vol. 7, no. 2, pp. 723–730, Apr. 2019.

[21] C. von Eiff, K. Becker, K. Machka, H. Stammer, and G. Peters, "Nasal carriage as a source of Staphylococcus aureus bacteremia. Study Group.," *N. Engl. J. Med.*, vol. 344, no. 1, pp. 11–16, Jan. 2001.

[22] S. S. Huang *et al.*, "Decolonization to Reduce Postdischarge Infection Risk among MRSA Carriers," *N. Engl. J. Med.*, vol. 380, no. 7, pp. 638–650, 2019.

[23] S. Avtaar Singh, "Methicillin Resistant Staphylococcus Aureus (MRSA) Eradication Prior to Cardiac Surgery," *Int. J. Cardiovasc. Thorac. Surg.*, vol. 3, no. 3, p. 18, 2017.

[24] E. Tacconelli, Y. Carmeli, A. Aizer, G. Ferreira, M. G. Foreman, and E. M. C. D'Agata, "Mupirocin Prophylaxis to Prevent Staphylococcus aureus Infection in Patients Undergoing Dialysis: A Meta-analysis," *Clin. Infect. Dis.*, vol. 37, no. 12, pp. 1629–1638, 2003.

[25] S. Khoshnood *et al.*, "A review on mechanism of action, resistance, synergism, and clinical implications of mupirocin against Staphylococcus aureus," *Biomed. Pharmacother.*, vol. 109, no. October 2018, pp. 1809–1818, 2019.

[26] J. A. Hermoso, J. L. García, and P. García, "Taking aim on bacterial pathogens: from phage therapy to enzybiotics.," *Curr. Opin. Microbiol.*, vol. 10, no. 5, pp. 461–72, Oct. 2007.

[27] A. Sulakvelidze, Z. Alavidze, and J. G. Morris, "The challenges of bacteriophage therapy," *Antimicrob. Agents Chemother.*, vol. 45, no. 3, pp. 649–659, 2001.

[28] M. P. Nikolich and A. A. Filippov, "Bacteriophage therapy: Developments and directions," *Antibiotics*, vol. 9, no. 3, 2020.

[29] S. Reardon, "Phage therapy gets revitalized," *Nature*, vol. 510, no. 7503, pp. 15–16, Jun. 2014.

[30] H. Haddad Kashani, M. Schmelcher, H. Sabzalipoor, E. Seyed Hosseini, and R. Moniri, "Recombinant Endolysins as Potential Therapeutics against Antibiotic-Resistant Staphylococcus aureus: Current Status of Research and Novel Delivery Strategies," *Clin. Microbiol. Rev.*, vol. 31, no. 1, Jan. 2018.

[31] F. Oechslin, "Resistance development to bacteriophages occurring during bacteriophage therapy," *Viruses*, vol. 10, no. 7, 2018.

[32] T. K. Lu and M. S. Koeris, "The next generation of bacteriophage therapy," *Curr. Opin. Microbiol.*, vol. 14, no. 5, pp. 524–531, 2011.

[33] K. Abdelkader, H. Gerstmans, A. Saafan, T. Dishisha, and Y. Briers, "The Preclinical and Clinical Progress of Bacteriophages and Their Lytic Enzymes: The Parts are Easier than the Whole," *Viruses*, vol. 11, no. 2, p. 96, Jan. 2019.

[34] L. Y. Filatova *et al.*, "A Chimeric LysK-Lysostaphin Fusion Enzyme Lysing Staphylococcus aureus Cells: a Study of Both Kinetics of Inactivation and Specifics of Interaction with Anionic Polymers," *Appl. Biochem. Biotechnol.*, vol. 180, no. 3, pp. 544–557, 2016.

[35] J. Y. Bae *et al.*, "Efficacy of Intranasal Administration of the Recombinant Endolysin SAL200 in a Lethal Murine Staphylococcus aureus Pneumonia Model," *Antimicrob. Agents Chemother.*, vol. 63, no. 4, pp. 1–8, Apr. 2019.

[36] L. C. Hjelm, J. Nilvebrant, P.-Å. Nygren, A. S. Nilsson, and J. Seijsing, "Lysis of Staphylococcal Cells by Modular Lysin Domains Linked via a Non-covalent Barnase-Barstar Interaction Bridge," *Front. Microbiol.*, vol. 10, no. MAR, pp. 1–9, Mar. 2019.

[37] S. Y. Jun *et al.*, "Antibacterial properties of a pre-formulated recombinant phage endolysin, SAL-1.," *Int. J. Antimicrob. Agents*, vol. 41, no. 2, pp. 156–61, Feb. 2013.

[38] J. M. Obeso, B. Martínez, A. Rodríguez, and P. García, "Lytic activity of the recombinant staphylococcal bacteriophage PhiH5 endolysin active against Staphylococcus aureus in milk.," *Int. J. Food Microbiol.*, vol. 128, no. 2, pp. 212–8, Dec. 2008.

[39] Y. Shan *et al.*, "Recombinant of the Staphylococcal Bacteriophage Lysin CHAPk and Its Elimination against Streptococcus agalactiae Biofilms," *Microorganisms*, vol. 8, no. 2, p. 216, Feb. 2020.

[40] Y. Shen, T. Köller, B. Kreikemeyer, and D. C. Nelson, "Rapid degradation of Streptococcus pyogenes biofilms by PlyC, a bacteriophage-encoded endolysin," *J. Antimicrob. Chemother.*, vol. 68, no. 8, pp. 1818–1824, 2013.

[41] S. Park *et al.*, "Characterisation of the antibacterial properties of the recombinant phage endolysins AP50-31 and LysB4 as potent bactericidal agents against Bacillus anthracis," *Sci. Rep.*, vol. 8, no. 1, pp. 1–11, 2018.

[42] R. D. Heselpoth, Y. Yin, J. Moult, and D. C. Nelson, "Increasing the stability of the bacteriophage endolysin PlyC using rationale-based FoldX computational modeling," *Protein Eng. Des. Sel.*, vol. 28, no. 4, pp. 85–92, 2015.

[43] S. C. Becker, S. Dong, J. R. Baker, J. Foster-Frey, D. G. Pritchard, and D. M. Donovan, "LysK CHAP endopeptidase domain is required for lysis of live staphylococcal cells," *FEMS Microbiol. Lett.*, vol. 294, no. 1, pp. 52–60, 2009.

[44] L. Y. Filatova, S. C. Becker, D. M. Donovan, A. K. Gladilin, and N. L. Klyachko, "LysK, the enzyme lysing Staphylococcus aureus cells: Specific kinetic features and approaches towards stabilization," *Biochimie*, vol. 92, no. 5, pp. 507–513, 2010.

[45] S. Y. Jun, G. M. Jung, J. S. Son, S. J. Yoon, Y. J. Choi, and S. H. Kang, "Comparison of the antibacterial properties of phage endolysins SAL-1 and LysK," *Antimicrob. Agents Chemother.*, vol. 55, no. 4, pp. 1764–1767, 2011.

[46] S. Y. Jun *et al.*, "Pharmacokinetics and Tolerance of the Phage Endolysin-Based Candidate Drug SAL200 after a Single Intravenous Administration among Healthy Volunteers," *Antimicrob. Agents Chemother.*, vol. 61, no. 6, Jun. 2017.

[47] ClinicalTrails.gov, "Phase IIa Clinical Study of N-Rephasin® SAL200." [Online]. Available: https://clinicaltrials.gov/ct2/show/NCT03089697. [Accessed: 19-Dec-2021].

[48] E. A. Idelevich *et al.*, "In vitro activity against Staphylococcus aureus of a novel antimicrobial agent, PRF-119, a recombinant chimeric bacteriophage endolysin," *Antimicrob. Agents Chemother.*, vol. 55, no. 9, pp. 4416–4419, 2011.

[49] E. A. Idelevich *et al.*, "The Recombinant Bacteriophage Endolysin HY-133 Exhibits In Vitro Activity against Different African Clonal Lineages of the Staphylococcus aureus Complex, Including Staphylococcus schweitzeri," *Antimicrob. Agents Chemother.*, vol. 60, no. 4, pp. 2551–2553, Apr. 2016.

[50] U. Kaspar, J. A. de H. Sautto, S. Molinaro, G. Peters, E. A. Idelevich, and K. Becker, "The Novel Phage-Derived Antimicrobial Agent HY-133 Is Active against Livestock-Associated Methicillin-Resistant Staphylococcus aureus," *Antimicrob. Agents Chemother.*, pp. 1–4, 2018.

[51] S. Sielker and G. B. Torsello, "Vascular Graft Impregnation with Antibiotics : The Influence of High Concentrations of Rifampin , Vancomycin , Daptomycin , and Bacteriophage Endolysin HY-133 on Viability of Vascular Cells," *Med Sci Monit Basic Res*, vol. 23, pp. 250–257, 2017.

[52] D. Knaack *et al.*, "Bactericidal activity of bacteriophage endolysin HY-133 against Staphylococcus aureus in comparison to other antibiotics as determined by minimum bactericidal concentrations and time-kill analysis," *Diagn. Microbiol. Infect. Dis.*, vol. 93, no. 4, pp. 362–368, Apr. 2019.

[53] N. Schleimer *et al.*, "In Vitro Activity of the Bacteriophage Endolysin HY-133 against Staphylococcus aureus Small-Colony Variants and Their Corresponding Wild Types," *Int. J. Mol. Sci.*, vol. 20, no. 3, p. 716, Feb. 2019.

[54] M. Sanz-Gaitero, R. Keary, C. Garcia-Doval, A. Coffey, and M. J. Van Raaij, "Crystallization of the CHAP domain of the endolysin from staphylococcus aureus bacteriophage K," *Acta Crystallogr. Sect. F Struct. Biol. Cryst. Commun.*, vol. 69, no. 12, pp. 1393–1396, 2013.

[55] M. Sanz-Gaitero, R. Keary, C. Garcia-Doval, A. Coffey, and M. J. van Raaij, "Crystal structure of the lytic CHAPK domain of the endolysin LysK from Staphylococcus aureus bacteriophage K," *Virol. J.*, vol. 11, no. 1, p. 133, 2014.

[56] A. Gründling, D. M. Missiakas, and O. Schneewind, "Staphylococcus aureus Mutants with Increased Lysostaphin Resistance," *J. Bacteriol.*, vol. 188, no. 17, pp. 6286–6297, Sep. 2006.

[57] H. P. DeHart, H. E. Heath, L. S. Heath, P. A. LeBlanc, and G. L. Sloan, "The lysostaphin endopeptidase resistance gene (epr) specifies modification of peptidoglycan cross bridges in

Staphylococcus simulans and Staphylococcus aureus," *Appl. Environ. Microbiol.*, vol. 61, no. 4, pp. 1475–1479, Apr. 1995.

[58] S. Boyle-Vavra, "Development of vancomycin and lysostaphin resistance in a methicillin-resistant Staphylococcus aureus isolate," *J. Antimicrob. Chemother.*, vol. 48, no. 5, pp. 617–625, Nov. 2001.

[59] P. Mitkowski *et al.*, "Structural bases of peptidoglycan recognition by lysostaphin SH3b domain," *Sci. Rep.*, vol. 9, no. 1, p. 5965, Dec. 2019.

[60] I. Sabala *et al.*, "Crystal structure of the antimicrobial peptidase lysostaphin from Staphylococcus simulans," *FEBS J.*, vol. 281, no. 18, pp. 4112–4122, 2014.

[61] G. Winter, S. Eisele, S. Molinaro, and W. Mutter, "Stabilizing therapeutic proteins with piperazin- or morpholine-containing zwitterionic buffering substances," WO 2021/018619 A1, 2021.

Chapter 2

Objectives of the Thesis

As *S. aureus* adheres to the mucosa of the anterior part of the nasal cavity, topical administration of HY-133 is sufficient and a transcellular drug delivery is therefore not intended. However, adequate drug product delivery at the application site is essential. For this, different dosage forms are possible. The formulation has to be administered locally to the anterior part of the nasal cavity. Ideally, absorption to the interior parts of the nose and the throat region should be avoided. Additionally, higher residence times would increase drug interaction with the affected area. Therefore, semisolid formulations generally are an adequate dosage form for HY-133. Liquid formulations are less suitable as clearance would be too fast.

Hydrogels are water-based matrix systems with very few or only one gelling agent. Therefore, possible interactions can quickly be identified and reduced to a minimum. Commonly used gelling agents often possess mucoadhesive properties, which additionally increase the residence time on the nasal mucosa. Dosing of these hydrogels can only be assured with low viscosity hydrogels. Ideally, these drug products can be sprayed, providing consistent dosing and administration in the nasal cavity. Challenging the formulation development of this new recombinant bacteriophage endolysin was addressed in the course of this thesis.

In the first step, an analytical tool set had to be developed to measure endolysin stability. Over the course of the research, the analytics were adapted and extended to account for changes in the protein formulation (**Chapter 3**). The uncommon 2-domain structure of the protein required additional investigation of the biophysical properties of HY-133 to characterize the purity, integrity profile and the conformation of the active ingredient (**Chapter 4)**.

Next, a suitable liquid formulation of the novel bacteriophage endolysin HY-133 was developed. The active agent needed sufficient stability for a certain period of time without losing activity or concentration. Furthermore, chemical and physical stability had to be ensured throughout the shelf life. Four different formulation screenings and stability studies were conducted to identify a stabilizing composition of excipients. The final formulation was further adapted taking elevated HY-133 concentrations, osmolality for application, and designated packaging material into account (**Chapter 5**).

As HEPES is a crucial component of the formulation, its interaction with HY-133 was further examined in great detail. Additionally, HEPES was compared to other Good's buffers to test whether a similar

stability profile can also be achieved with these buffer substances (**Chapter 6**). The exceptional stabilizing effect of HEPES was investigated further by defining the mode of action of HEPES supported by in-silico analysis. This novelty of HEPES interacting with the protein was further published in the patent *WO2021018619A1: Stabilizing therapeutic proteins with piperazin- or morpholine-containing zwitterionic buffering substances* [61].

Based on the liquid formulation, a sprayable hydrogel drug product was developed. The stability of HY-133 in suitable hydrogel prototypes was evaluated to select a final formulation matrix. Preservative-free nasal applications require microbial integrity and thus sterility. Given that final sterilization of a hydrogel containing a biopharmaceutic is not possible, an aseptic manufacturing process was developed. The scale-up procedure of the hydrogel production was transferred to a contract manufacturing organization (CMO) for phase I and II clinical study preparation (**Chapter 7)**.

Another approach was tested by using nanoparticle trying to set up a sustained release of HY-133 out of a nanoparticulate system. A formulation development was performed (**Chapter 8**), but sustained release out of the nanoparticles not achieved.

Chapter 3

Materials and Methods

Table of Contents

1. Materials

1.1 Excipients

$CaCl_2$ and methionine were purchased in Ph.Eur./USP quality from Merck KGaA, Darmstadt, Germany. NaCl was obtained from Bernd Kraft, Duisburg, Germany and HEPES from VWR International, Ismaning, Germany. L-arginine, arginine-hydrochloride (AppliChem PanReac, Darmstadt, Germany) and Poloxamer 188 (Kolliphor 188, BASF, Ludwigshafen, Germany) were used in Ph.Eur./USP quality.

In the liquid formulation study, the following excipients were used: L-cysteine, EDTA, histidine, polysorbate 80 and trehalose-dihydrate. The excipients were sourced in multi-compendial grade (i.e., Ph.Eur./USP grade) from Merck KGaA, Darmstadt, Germany.

In the hydrogel formulation study, the following gelling agents were used: NaCMC (Cekol 2000) was used in multi-compendial grade (CP Kelco, Lavallois-Perret, France). PVP40 (Povidone), xanthan, and gellan gum were purchased from Sigma-Aldrich (St. Louis, Missouri, US). Various HPMC grades and manufacturers were tested during the hydrogel screening. Benecel K100M, Benecel K200M, and Benecel K4M were sourced from Ashland (Wilmington, Delaware, US). Methocel K4M, Methocel K15M, and Methocel E4M, all in premium quality, were obtained from Colorcon (Dartford, Kent, UK). Mantrocel K100M, Mantrocel K4M (both Parmentier, Frankfurt am Main, Germany) and Vivapharm K4M, Vivapharm K15M, Vivapharm E50 (all JRS Pharma, Rosenberg, Germany) completed the excipient screening.

For the Good's buffers section, the following buffer alternatives to HEPES were tested: MES, MOPS, POPSO, PIPES, and EPPS (all Sigma-Aldrich Chemie GmbH, Steinheim, Germany).

Highly purified water (HPW) was used for formulation preparation.

Unless otherwise described, the protein bulk buffer was exchanged by dialysis. A Spectra/Por dialysis membrane with a molecular weight cut-off of 10 kDa (SpectrumLabs, New Brunswick, NJ, US) was used and a 4-fold buffer exchange was implemented.

The eluents for RP-HPLC were gravimetrically mixed using highly purified water, acetonitrile, and trifluoracetic acid (Sigma-Aldrich). The SEC eluent consisted of NaCl (Bernd Kraft, Duisburg, Germany), di-sodium hydrogen phosphate dihydrate per analysis (AppliChem, Darmstadt, Germany), and sodium phosphate monobasic dihydrate (Honeywell Riedel-de Haen, Seelze, Germany). For the IEX chromatography, eluent A and eluent B both contained Tris-base and Tris-HCl (both Sigma-Aldrich). NaCl (Bernd Kraft) was added to eluent B.

An overnight culture of *staphylococcus xylosus* (*S. xylosus*) (DSZM number 20266, Leibniz Institute DSMZ, Braunschweig, Germany) in brain-heart infusion broth (BHI) (Carl Roth, Karlsruhe, Germany) was used for direct activity measurements of HY-133. For this, 37 g BHI were dissolved in HPW, autoclaved, and stored for up to 2 weeks. The *S. xylosus* overnight culture was further diluted with a lysis buffer, which consisted of Tris-HCl (Sigma-Aldrich), NaCl (Bernd Kraft) and $CaCl_2$ (Caesar & Loretz, Hilden, Germany) at pH 7.4. Semi-micro PMMA cuvettes (Brand, Wertheim, Germany) were used for optical density measurements.

As an alternative activity measurement method, activity of HY-133 was determined with an enzymatic assay kit developed and obtained by Microcoat (Bernried, Germany).

1.2 Active ingredient

The recombinant bacteriophage endolysin HY-133 was developed for the decolonisation of *S. aureus* in the nasal cavity. The active pharmaceutical ingredient (API) HY-133 was provided by HYPharm GmbH. The stock solution of HY-133 has a concentration of at least 4.7 mg/ml with a purity of >95%. It was stored at -80 °C in a bulk formulation buffer consisting of 25 mM HEPES, 150 mM NaCl, 10 mM $CaCl_2$, and 300 mM arginine at pH 8.0. The final HY-133 batch (SCUP5) was produced by Fraunhofer ITEM (Braunschweig, Germany). The protein itself has a molecular weight of 31045.8 Da and an isoelectric point of 9.45. Prior to each experiment, the protein bulk was filtrated with a 0.2 µm PVDF syringe filter (Acrodisc 25 mm, Pall Laboratory, Dreieich, Germany).

The HY-133 lots which were used throughout the developmental process are displayed in Table 1.

Table 1: Overview of the HY-133 lots used during the formulation development and all additional experiments.

Lot number	Concentration [mg/ml]	Used for
ESS_1878	4.8	Analytical development, preliminary stability
ESS_1886	5.0	Analytical development, preliminary stability
ESS_1909	5.2	Analytical development
ESS_2136	4.7	Formulation development (liquid + hydrogel)
SCUP5 (Fraunhofer)	10.2	Scale-up hydrogel study, HEPES interaction

2. Methods

First, a comprehensive analytical setup for the novel active agent HY-133 was developed. Based on Ph.Eur./USP, identity, purity, and content were determined. At the beginning, no analytical methods except for the SDS-PAGE and the bacteriolytic assay were established. An analytical setup was developed to determine protein concentration, chemical and physical changes as well as changes in protein activity. In addition, the protein was biophysically characterized to generate basic information about its structure and melting temperature. The analytical setup was transferred to Fraunhofer ITEM to facilitate analytics during scale-up production of HY-133.

2.1 UV/Vis-spectroscopy (concentration at 280 nm and turbidity at 350 nm)

Protein concentration was analyzed at 280 nm by UV/Vis-spectroscopy with a NanoDrop 2000 (Thermo Fisher Scientific, Waltham, MA, USA). An extinction coefficient of 2.25 g/100 $ml^{-1}cm^{-1}$ (Abs 0.1%) was used for the concentration calculation. Turbidity of the samples was measured by optical density measurements at 350 nm. Each sample was measured in triplicates with its corresponding formulation buffer as a blank solution.

2.2 Reversed phase high pressure liquid chromatography (RP-HPLC)

An Ultimate 3000 system (Thermo Fisher, Dreieich, Germany) and a Jupiter C4, 5 µm 300A, 250 x 4.6 mm column (Phenomenex, Torrence, US) were used for RP-HPLC. Protein detection was performed with an Ultimate 3000 fluorescence detector using the intrinsic fluorescence of HY-133 at 280/343 nm. The column oven was set to 37 °C and the autosampler was cooled to 6 °C to prevent degradation of the samples during the measurement. A 10% acetonitrile in HPW with 0.1% trifluoroacetic acid (mobile phase A) and a 100% acetonitrile with 0.1% trifluoroacetic acid (mobile phase B) were used in a stepwise gradient with a flowrate of 1 ml/min and a runtime of 22 min.

2.3 Size exclusion chromatography (SEC)

An Ultimate 3000 system (Thermo Fisher) with a Tosoh TSKgel G3000SWXL (7.8 mm ID x 30 cm; 5 µm) (Tosoh Bioscience, Stuttgart, Germany) was used for size exclusion chromatography (SEC). The column was later exchanged for a GE Superdex 75 Increase 10/300 GL column (General Electric, Boston, MA, USA) due to the improved resolution and separation of the Superdex column. A filtered buffer solution containing 50 mM Na_3PO_4 and 300 NaCl in HPW at pH 7.0 was used as a mobile phase at a flow rate of 0.5 ml/min for 45 min. Detection was performed with an Ultimate variable wavelength detector at 280 nm. A gel filtration standard (#1511901, Bio-Rad Laboratories, Hercules, CA, USA) was used for regular column tests. 50 µl of a 0.5 mg/ml HY-133 sample were injected, while higher concentrated samples were diluted to 0.5 mg/ml.

2.4 Ion exchange chromatography (IEX)

A Dionex Summit system (Thermo Fischer) with a ProPac WCX-10 BioLC Analytical 4x250 mm column and an attached column guard ProPac WCX-10G (Thermo Fisher) was used for IEX chromatography. 20 mM Tris buffer pH 8.0 (mobile phase A) and mobile phase A plus 300 mM NaCl pH 8.0 (mobile phase B) were used in a stepwise gradient with a flowrate of 1 ml/min and a runtime of 60 min. Samples containing 0.5 mg/ml HY-133 were diluted 1:10 with HPW prior to injection and 100 µl of each sample was injected. A fluorescence detector (280/343 nm) was used to determine the analyte variants. An increase in pre-peak area indicated a rise in acidic protein species.

2.5 Capillary electrophoresis on a chip (Bioanalyzer)

An Agilent 2100 Bioanalyzer system in combination with the Protein 230 kit (Agilent Technologies, Waldbronn, Germany) was used to determine the molecular size distributions of the protein in a range from 14 to 230 kDa. With this setup, aggregated protein species, fragments, and impurities can be determined in HY-133 samples. The samples were prepared according to the protocol, and were diluted in a sample buffer which contained a lower and an upper marker. Each chip can be loaded with up to 10 samples and one ladder which enables a molecular weight allocation over the described range. The results were given as electropherograms, which were then used to calculate the respective shares of each molecular weight species. In addition, densitometry plots were provided for visualization purposes. The system's main advantage compared to SDS-PAGE is its speed and the possibility of a direct quantification of the molecular weight shares.

2.6 Circular dichroism (CD) spectroscopy

A Jasco J-810 spectropolarimeter (Jasco Deutschland GmbH, Pfungstadt, Germany) was used to obtain near-UV circular dichroic spectra. Quartz cuvettes (Hellma GmbH, Muellheim, Germany) with 10 mm pathlengths were installed and measurements were performed with 10 accumulations per sample at a scanning speed of 20 nm/min. For each formulation, blank measurements were performed with the respective formulation buffer and the so obtained spectrum was then subtracted from the protein spectrum. Curve smoothing was performed using the Savitzky-Golay algorithm with 7 smoothing points and the molar ellipticity was calculated as described by Kelly et al. [1]. The molecular weight of the HY-133 was 31,045.8 Da.

2.7 Light obscuration (LO) and micro-flow imaging (MFI)

Subvisible, insoluble particles ≥ 1 µm were analyzed with both LO and MFI.

LO was analyzed with a PAMAS SVSS-35 particle counter with an HCB-LD-25/25 sensor (PAMAS – Partikelmess- und Analysensysteme GmbH, Rutesheim, Germany). The system was rinsed with HPW

before each analysis. Rinsing was performed with a volume of 0.2 ml and followed by 4 measurements of each 0.2 ml sample according to USP <787>.

MFI measurements were performed with a FlowCam 8100 (Fluid Imaging Technologies, Scarborough, ME, USA). The system was equipped with a 10x magnification and a FOV80 flow-cell (80 µm x 700 µm). A sample volume of 200 µl was used and images were collected with a flow rate of 0.15 ml/min and an auto image frame rate of 9 frames/s. For particle detection, 3 µm distance to the nearest neighbor and thresholds of 10 and 13 for light and dark pixels, respectively, were used.

2.8 Activity measurement I: Bacteriolytic assay

An overnight culture of *S. xylosus* in BHI medium was prepared, which was diluted 1:10 after 16 h of incubation at 37 °C. The bacteria dispersion was further incubated at 37 °C until an optical density of about 1.0 ± 0.1 was reached. Subsequently, 10 ml dispersion aliquots were centrifuged at 3,400 x g for 10 min, the supernatant was discarded and the obtained pellets stored on ice until further usage. For each measurement, the pellet was dispersed in lysis buffer and incubated for 30 min at room temperature.

A concentration row of 6 decreasing HY-133 concentrations was prepared. For optical density measurements, a UV/VIS photometer 8453 with an 8-fold cuvette changer, both from Agilent Technologies (Santa Clara, California, USA), was used. 990 µl cell suspension was filled into the semi-micro cuvettes and a baseline was recorded for 1 min. Afterwards, 10 µl of each HY-133 dilution were added to the cell suspension and one value per 30 s was recorded for 30 min. Absorbance over time was determined at 600 nm. A linear fit was used to calculate the activity of HY-133.

2.9 Activity measurement II: FRET-Assay

The activity of HY-133 was determined with an enzymatic assay (HY-133 activity assay, Microcoat, Bernried, Germany). As a substrate, a short peptide sequence with an attached fluorophore and quencher was used. The substrate mimics the murein cell wall of the bacteria and is specific to *S. aureus*. It is hydrolyzed by HY-133, which results in the elimination of the fluorescence quenching. An excitation wavelength of 340 nm and an emission wavelength of 440 nm was applied. The specific activity was calculated according to the activity assay protocol. As the FRET-Assay was under development throughout the study, the results cannot be compared between different development stages. However, a comparison of the different formulations at one timepoint is possible.

2.10 Composition-gradient multi-angle light scattering (CG-MALS)

Homo-association experiments by CG-MALS were performed with 10 mg/ml HY-133 in buffer compositions at pH 6.0 without HEPES and with varying the HEPES buffer concentration (0 mM and

25 mM). Before use, all samples were filtrated with 0.2 µm PVDF filters. Light scattering and protein concentration were analyzed with an automated CG-MALS instrument equipped with a dual syringe-pump (Calypso-II sample and preparation unit), a Dawn Heleos-II multi-angle laser light scattering detector, and an OptiLab® T-rEX dRI detector (all Wyatt Technologies, Santa Barbara, CA, US). Calypso 2.1.5 software was used to obtain Zimm plots and A_2 values [2].

In addition, hetero-association experiments were performed by varying the HY-133 concentration from 0 – 10 mg/ml and the HEPES concentration from 0 – 25 mM. The experimental settings were similar as described above.

2.11 NanoDSF

NanoDSF was used to study the thermal unfolding of HY-133. The samples were filled in standard glass capillaries. A Prometheus NT.48 (NanoTemper Technologies, Munich, Germany) was used the unfolding experiments. The samples were heated from 25 °C up to 95 °C at a ramp of 1 °C/min. Intrinsic protein fluorescence intensity at 330 nm and 350 nm was measured after excitation at 280 (± 10) nm. The fluorescence ratio FI350/F330 was used to determine protein thermal unfolding, calculated by PR.ThermControl V2.1 software (NanoTemper Technologies). Backscattering intensity was measured to detect protein aggregation and precipitation.

2.12 Viscosity

Rheology examinations were performed using the MCR 100 by Physica Anton Paar (Ostfildern, Germany) with an attached parallel plate PP25 (Part NO.: 79044; Serial NO.: 41561). Measurements were performed at 20 °C. A continuous shear rate model was used to measure the viscosity of the different hydrogels. For this, the shear rate was increased from 1 to 100 s^{-1} and 30 measurement points were recorded. Each measurement point was recorded for 10 s. Additionally, a plateau at 100 s^{-1} and a downward shear rate back to 1 s^{-1} were recorded.

2.13 Fourier-transformed infrared spectroscopy (FT-IR)

A Tensor 27 spectrometer (Bruker Optics, Ettlingen, Germany) with a nitrogen-cooled MCT-detector and an AquaSpec Cell (Micro Biolytics, Esslingen am Neckar, Germany) was used to obtain the spectra of the protein sample. The temperature of the detector cell was set to 25 °C and controlled by a Thermo Haake K20 (Thermo Electron, Karlsruhe, Germany). 35 µl of HY-133 at a concentration of 4.8 mg/ml were slowly injected. The corresponding buffer was used as background. Spectra were recorded as triplicate measurements with 100 scans from 4,000-850 cm^{-1} at a resolution of 4 cm^{-1}.

2.14 Differential scanning calorimetry (µDSC)

Unfolding events of HY-133, for example the onset of the melting temperature ($T_{m,\ onset}$), were determined using µDSC. For this, a VP-DSC (MicroCal Inc., MA, US) was used. Prior to the measurement, a water vs. water scan was performed, which was later used for background subtraction. The sample solution at a concentration of 0.5 mg/ml and the corresponding formulation buffer were degassed for 30 s using a ThermoVac station from MicroCal. Subsequently, the solutions were filled into the respective measurement cells and equilibrated for 15 min at 20 °C. Afterwards, the measurements cells were heated from 20 °C to 70 °C with a heating rate of 1 K/min. Following the measurement, both cells were cleaned with 50% nitric acid heated up to 90 °C. Subsequently, the cells were rinsed with 1% SDS and HPW. The thermograms obtained through background subtraction were normalized according to the protein concentration and the maximum was considered as T_m. Automatic calculation of $T_{m,\ onset}$ was performed using Origin 7, fitting the curve to the Boltzmann function.

2.15 Enzyme-linked immunosorbent assay (ELISA)

An ELISA specific to HY-133 was developed by Microcoat. The ELISA can be used for identification and quantification of the protein. The assay was performed according to a proprietary protocol provided by Microcoat. It was used for the quantification of HY-133 from 150 – 9,600 pg/ml.

2.16 Dilutions of hydrogel samples

Hydrogel samples were diluted 1:10 with water for all LC methods to reduce the viscosity of the sample.

2.17 Release testing of HY-133 containing hydrogels

The matrix scan function of the FLUOstar Omega plate reader (BMG Labtech, Ortenberg, Germany) was utilized to assess the release of HY-133 out of a hydrogel sample. For this, 400 µl of the respective gel formulation were pipetted in the middle of a well (6-well plate). A pre-scan was performed to determine the initial hydrogel distribution in each well. Here, a 25x25 matrix raster in a diameter range of 28 mm was scanned with an excitation wavelength of 280 nm and an emission wavelength of 350 nm (Figure 1). The gel distribution should be near circular at the beginning. Subsequently, the hydrogel sample was surrounded with 2 ml of an acceptor medium (150 mM NaCl, 40 mM KCl, 4 mM $CaCl_2$, pH 6.3) and the time-dependent measurements were started. The orbital scans were repeated each 30 s for the first 2 minutes, 1 min intervals for further 10 minutes and 3 min intervals for the rest of the release experiment. At the end of the experiment, the hydrogel was completely dissolved in the acceptor medium and the maximum protein concentration was measured. The release was calculated via the ratio of the released protein and the maximum protein concentration.

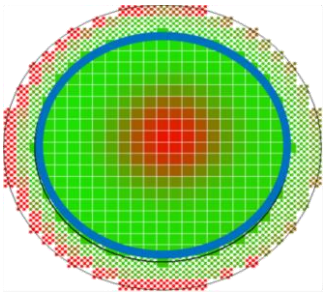

Figure 1: Visualization of a 25x25 matrix scan. The diameter range of 28 mm is marked in blue. Red areas display high protein concentration, whereas green areas display no protein emission.

2.18 Release testing of HY-133 loaded nanoparticles

A nanoparticle aliquot of 0.5 ml was mixed with 1.5 ml 50 mM Tris buffer at pH 7.0. Subsequently, the mixture was centrifuged at 5,000 x g and the supernatant was further analyzed as a starting point for the release study. The remaining pellet was resuspended with the Tris buffer and incubated at 37 °C in a rocker shaker. At each time point, the mixture was centrifuged as described above, the supernatant was completely removed and the pellet resuspended with 0.5 ml Tris buffer. The protein concentration was determined by the described UV/Vis spectroscopy (section 2.1) and RP-HPLC methods (section 2.2).

3. References

[1] S. M. Kelly, T. J. Jess, and N. C. Price, "How to study proteins by circular dichroism," *Biochim. Biophys. Acta - Proteins Proteomics*, vol. 1751, no. 2, pp. 119–139, 2005.

[2] J. Arora *et al.*, "Charge-mediated Fab-Fc interactions in an IgG1 antibody induce reversible self-association, cluster formation, and elevated viscosity," *MAbs*, vol. 8, no. 8, pp. 1561–1574, 2016.

Chapter 4

Biophysical characterization of HY-133

Table of Contents

1. Capillary electrophoresis – sodium dodecyl sulfate (CE-SDS)

Molecular size distributions of HY-133 in the early bulk formulation and in a later developed formulation were determined by CE-SDS using the Bioanalyzer. The thereby obtained electropherograms are shown in Figure and the corresponding densitometry plots in Figure . System and standard peaks which are used for size determination are located below 15 kDa and at 240 kDa. In the early bulk formulation, HY-133 showed a large peak at around 65 kDa beside the monomer peak at 33 kDa (Figure 1 – A). This indicates that a substantial amount of protein dimers was present in the bulk formulation. In addition, a small peak at 27 kDa was observed in the sample, which was later identified as host cell protein. The development of a stable HY-133 formulation led to substantially reduced dimers contents due to buffer composition changes (Figure 1 – B). It should be noted that the monomer peak size at 33 kDa which was determined by the Bioanalyzer slightly deviates from the actual molecular weight of 31.05 kDa.

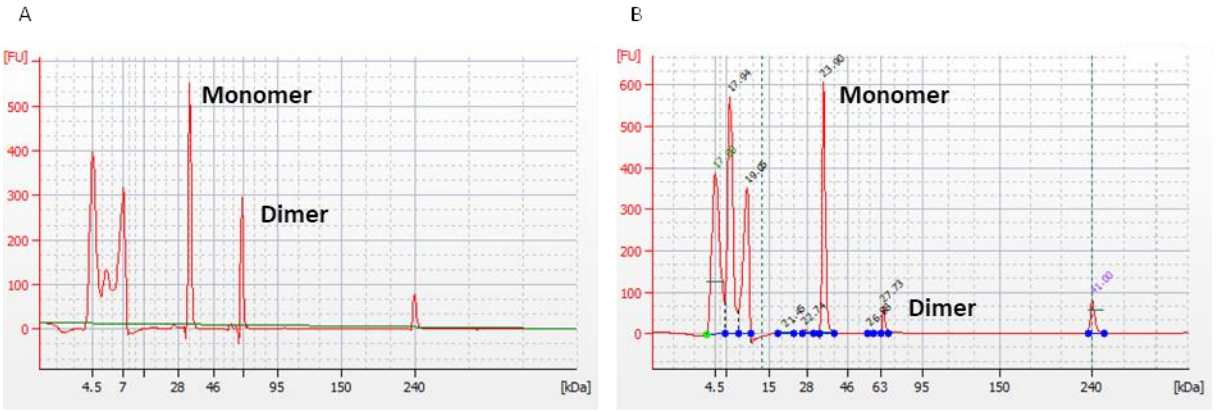

Figure 1: Exemplary electropherogram from CE-SDS (Bioanalyzer) measurements. A: HY-133 early bulk formulation. B: HY-133 bulk formulation incl. methionine at pH 6.

The Bioanalyzer further provides densitometry plots, which visualized the results of the electropherograms (Figure 2). Like the commonly used SDS-PAGE, these images allow a qualitative evaluation of the size distribution of the protein.

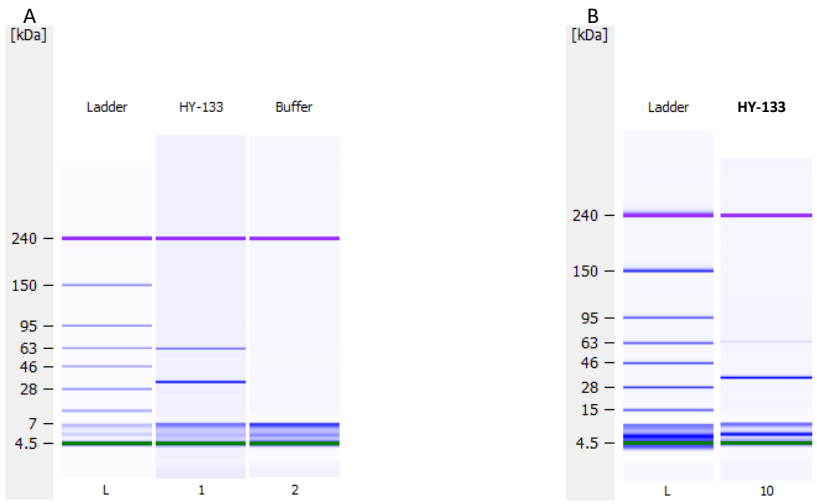

Figure 2: Corresponding densitometry plots of the CE-SDS measurements. A: HY-133 early bulk formulation. B: HY-133 bulk formulation incl. methionine and pH 6.

2. FT-IR

Secondary structural elements of HY-133 were assessed using FT-IR spectroscopy. The absorption spectrum of HY-133 and the corresponding second derivative spectrum are shown in Figure 3. Amid I and amid II bands appeared as distinct bands in the absorption spectrum at 1635 cm^{-1} and 1550 cm^{-1}, respectively. Both bands are predominantly caused by structural elements of the protein backbone. However, only the amid I band can be used for the detailed assignment of secondary structure elements. The second derivative of the FT-IR spectrum identified β-sheets to be the predominant structural elements of HY-133. This is indicated by a large band at 1635 cm^{-1}, typical for β-sheets [1]. Additionally, β-turn (1680 cm^{-1}) and 3_{10}-helix (1660 cm^{-1}) structures were apparent. Both are typically found in proteins, but less often than α-helices or β-sheets [2]. 3_{10}-Helices are short structures, which are tighter folded and are thus conformationally less stable [3].

Crystal structures of both single domains of HY-133 have been determined before [4]–[7]. As described in chapter 1, the EAD consists of a $CHAP_K$ domain. Crystal structures of this domain revealed a globular structure including 2 α-helices, 2 3_{10}-helices and 6 antiparallel β-sheets [5]. Except for the α-helices, these structural elements were also determined by FT-IR measurements in HY-133. Presumably, the α-helices could not be identified because their relevant band was in close proximity to the 3_{10}-helices [8]. The crystal structure of the CBD of lysostaphin, SH3b, identified in total 8 β-sheets [7]. These frequently occurring β-sheets were also determined in the FT-IR spectrum of HY-133. The combination of both domains in HY-133 via the 17 amino acid linker maintained the secondary structure of both single domains. Major deviations or other changes in the secondary structure of the protein were not observed, indicating generally stable structural elements.

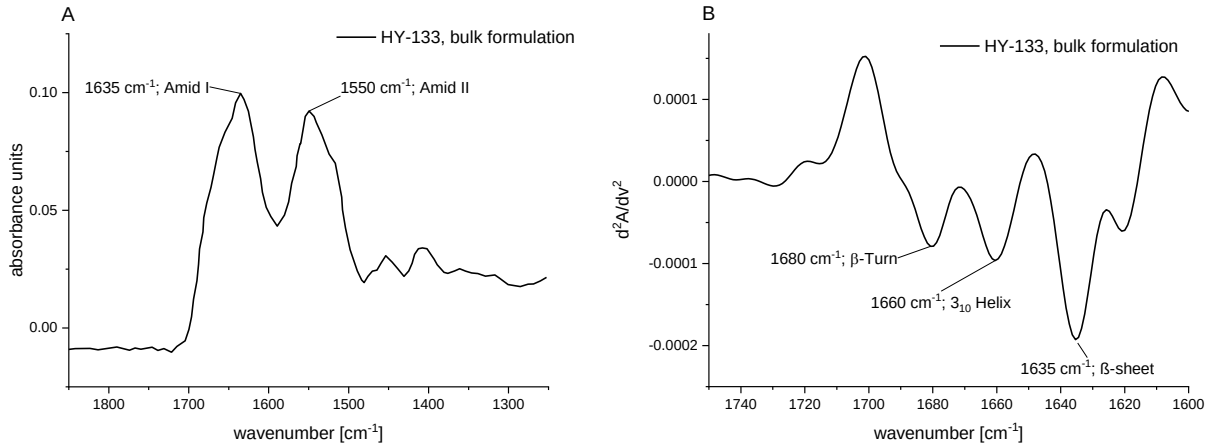

Figure 3: Vector normalized FT-IR absorption spectrum (A) and second-derivative spectrum of the amid I band (B) of HY-133 at a concentration of 5.0 mg/ml in the initial bulk formulation buffer. The bands were assigned according to [8].

3. Circular dichroism (CD) spectroscopy

Near-UV CD-spectra of HY-133 were obtained to determine a fingerprint spectrum of the protein. This fingerprint spectrum is caused by aromatic amino acids, disulfide bonds or associated ligands [9]. The near-UV CD-spectrum of HY-133 showed a large negative peak at around 285 nm (Figure 4 – A). Additionally, 2 smaller peaks at 268 nm and 276 nm were observed. These molar ellipticity signals were caused by the 3 aromatic amino acids tryptophan, tyrosine, and phenylalanine [9]. The substantial overlap of these signals caused the broad peak between 250 nm and 310 nm. Despite the broad peak, distinct local minima for all three amino acids could be determined. As the linker did not comprise any aromatic amino acid, conformational changes of the linker could not be traced by CD measurements.

To elucidate the effect of conformational changes on the CD-spectrum of HY-133, low pH variations of HY-133 in the bulk formulation buffer were examined (Figure 4 – B). Compared to the protein bulk formulation (pH 8.0), no conformational changes could be determined in the pH 7.0 sample. In contrast, in a sample with pH 5.0 a decrease in molar ellipticity was observed, indicating an early unfolding event of HY-133. However, the 3 peak minima were still apparent. A further decrease in formulation pH to 4.0 led to a substantial loss in molar ellipticity and a highly reduced resolution, indicating major unfolding of the protein.

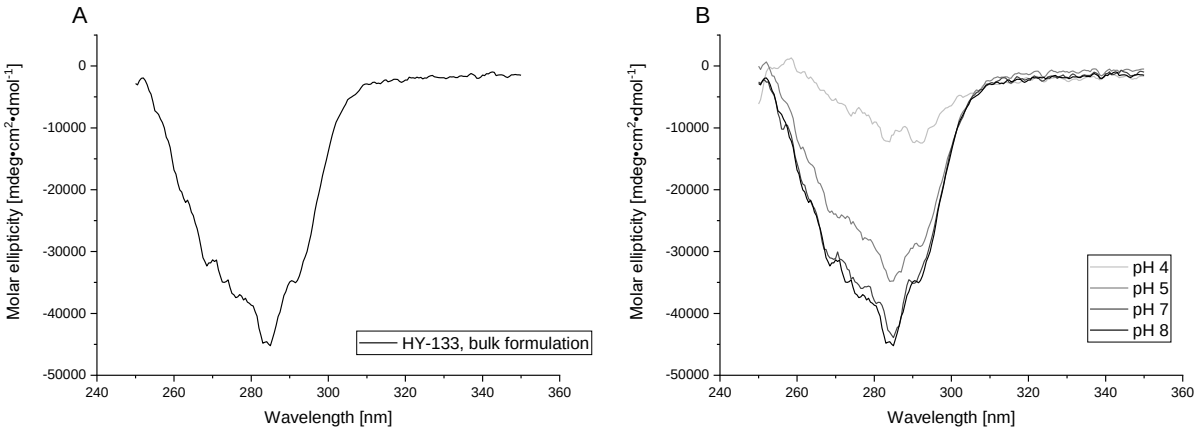

Figure 4: CD Spectra of the initial HY-133 bulk formulation (A) and low pH variations of HY-133 (B).

Studies of the enzymatic activity of the EAD $CHAP_K$ domain alone showed a substantial decrease in lytic activity at pH values below or equal pH 5.0 [10]. This might relate to the unfolding of the EAD $CHAP_K$ domain at these low pH values.

4. µDSC

Folding transitions of HY-133 were evaluated using µDSC measurements. An exemplary thermogram is shown in Figure 5. The maximum at around 53 °C indicates one distinct melting event in HY-133. The $T_{m, onset}$ of HY-133 was calculated using the Boltzmann fit and resulted in an onset melting temperature of 47.8 °C. This unfolding event was irreversible, as the protein precipitates at temperatures above around 65 °C (data not shown).

Despite HY-133 consisting of two different domains which are connected via a linker, only one unfolding event could be observed. This could be explained by either two domain melting temperatures very close to each other or only one melting temperature for both domains. Hence, only one T_m and one corresponding $T_{m, onset}$ was determined.

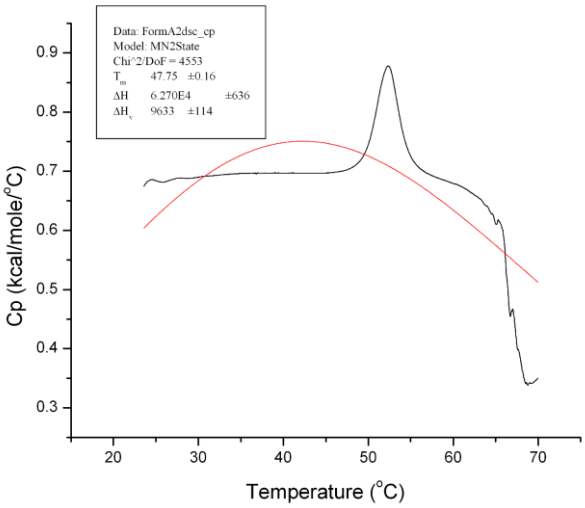

Figure 5: Exemplary thermogram of HY-133 in its initial bulk formulation. $T_{m,onset}$ is calculated by using the Boltzmann fit (shown in red).

A study on the related endolysin PlyC identified thermal stress as reason for an activity loss of the $CHAP_K$ domain [11]. In this endolysin, the $CHAP_K$ domain is one of the two subunits responsible for the bacteriolytic effect. T_m determinations were performed for both the complete subunit and the isolated $CHAP_K$ domain. Whereas the isolated $CHAP_K$ domain showed a T_m of 39.1 °C, the complete EAD of PlyC showed a substantially increased T_m of 46 °C. This indicates that combining $CHAP_K$ with another domain leads to a thermally stabilized endolysin [11]. The structure of PlyC differs from the EAD of HY-133, which does not comprise a second subunit. The absence of a thermal event at around 39 °C in HY-133 could thus potentially be explained by internal stabilization by the combination of $CHAP_K$ with the CBD. Another study examined an EAD consisting of a CHAP-Barnase fusion protein, which showed a T_m of 42.5 °C [12]. In addition, this study analyzed a chimeric endolysin which comprised a $CHAP_K$ domain from LysK and a SH3b domain from lysostaphin. This chimeric construct is almost identical to HY-133 and showed a T_m of 41.0 °C [12]. This indicates that HY-133 is thermally more stable than comparable bacteriophage endolysins. The predecessor of HY-133, PRF-119, also showed a lower stability than HY-133 [13]. Regarding the protein structure, the only change from PRF-119 to HY-133 was a shortened peptide linker [13]. This further indicates that each combination of EAD, CBD and linker needs to be carefully assessed regarding its thermal stability.

The results obtained by µDSC were additionally confirmed by nanoDSF measurements.

5. NanoDSF

Thermal unfolding of HY-133 at a concentration of 0.5 mg/ml was investigated using nanoDSF. Temperature dependent protein unfolding leads to a change in intrinsic fluorescence intensity due to either exposure or covering of aromatic amino acids. The temperature dependent intrinsic fluorescence of HY-133 at 330 nm and 350 nm is shown in Figure 6A. Only one transition event can be observed in both signals, represented by a steeper slope between 40 °C and 50 °C. The precise T_m of 46.4 °C was determined via the inflection point of the signal ratio curve (Figure 6B). However, the onset temperature of the melting temperature ($T_{m, onset}$) could not be determined using nanoDSF.

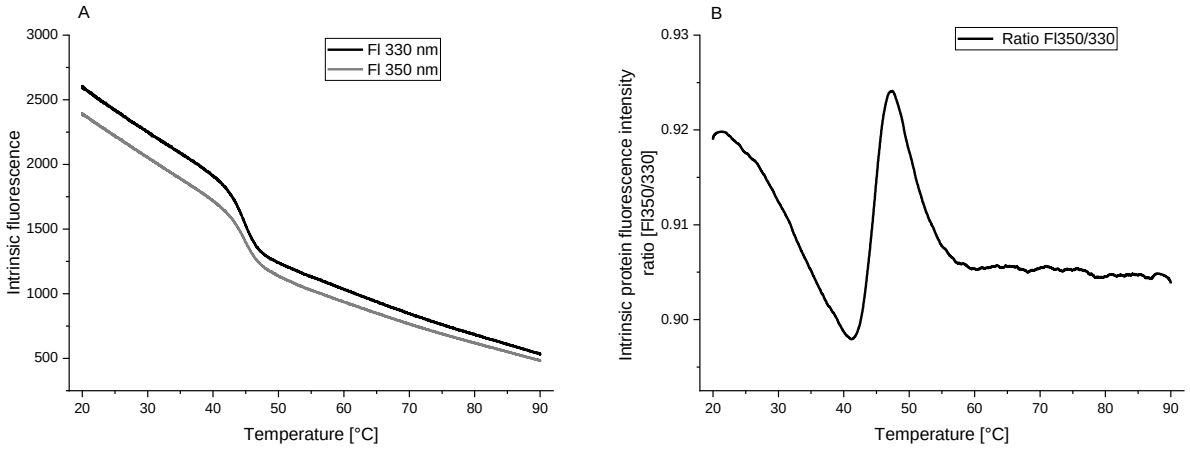

Figure 6: Temperature dependent protein unfolding determined by nanoDSF. The single fluorescence intensities at 330 nm and 350 nm are shown in (A), the ratios in (B).

Like in the µDSC measurements described before, only one unfolding event could be found with nanoDSF. This again indicates a simultaneous unfolding of both domains at a very similar temperature or only one unfolding event of the endolysin. Compared to µDSC measurements, the T_m value obtained by nanoDSF was slightly below the T_m value determined by µDSC and next to the $T_{m, onset}$.

As both µDSC and nanoDSF measurements showed a T_m and $T_{m, onset}$ of HY-133 well above 40 °C, stability studies at an elevated temperature of 40 °C are generally possible.

6. References

[1] A. Barth, "Infrared spectroscopy of proteins.," *Biochim. Biophys. Acta*, vol. 1767, no. 9, pp. 1073–101, Sep. 2007.

[2] L. Pal, G. Basu, and P. Chakrabarti, "Variants of 310-helices in proteins," *Proteins Struct. Funct. Genet.*, vol. 48, no. 3, pp. 571–579, 2002.

[3] C. Tonlolo and E. Benedetti, "The polypeptide 310-helix," *Trends Biochem. Sci.*, vol. 16, no. C, pp. 350–353, Jan. 1991.

[4] I. Sabala *et al.*, "Crystal structure of the antimicrobial peptidase lysostaphin from Staphylococcus simulans," *FEBS J.*, vol. 281, no. 18, pp. 4112–4122, 2014.

[5] M. Sanz-Gaitero, R. Keary, C. Garcia-Doval, A. Coffey, and M. J. van Raaij, "Crystal structure of the lytic CHAPK domain of the endolysin LysK from Staphylococcus aureus bacteriophage K," *Virol. J.*, vol. 11, no. 1, p. 133, 2014.

[6] M. Sanz-Gaitero, R. Keary, C. Garcia-Doval, A. Coffey, and M. J. Van Raaij, "Crystallization of the CHAP domain of the endolysin from staphylococcus aureus bacteriophage K," *Acta Crystallogr. Sect. F Struct. Biol. Cryst. Commun.*, vol. 69, no. 12, pp. 1393–1396, 2013.

[7] P. Mitkowski *et al.*, "Structural bases of peptidoglycan recognition by lysostaphin SH3b domain," *Sci. Rep.*, vol. 9, no. 1, p. 5965, Dec. 2019.

[8] J. KONG and S. YU, "Fourier Transform Infrared Spectroscopic Analysis of Protein Secondary Structures," *Acta Biochim. Biophys. Sin. (Shanghai).*, vol. 39, no. 8, pp. 549–559, Aug. 2007.

[9] S. Kelly and N. Price, "The Use of Circular Dichroism in the Investigation of Protein Structure and Function," *Curr. Protein Pept. Sci.*, vol. 1, no. 4, pp. 349–384, Dec. 2000.

[10] M. Fenton, R. P. Ross, O. Mcauliffe, J. O'Mahony, and A. Coffey, "Characterization of the staphylococcal bacteriophage lysin CHAP K," *J. Appl. Microbiol.*, vol. 111, no. 4, pp. 1025–1035, 2011.

[11] R. D. Heselpoth, Y. Yin, J. Moult, and D. C. Nelson, "Increasing the stability of the bacteriophage endolysin PlyC using rationale-based FoldX computational modeling," *Protein Eng. Des. Sel.*, vol. 28, no. 4, pp. 85–92, 2015.

[12] L. C. Hjelm, J. Nilvebrant, P.-Å. Nygren, A. S. Nilsson, and J. Seijsing, "Lysis of Staphylococcal Cells by Modular Lysin Domains Linked via a Non-covalent Barnase-Barstar Interaction Bridge," *Front. Microbiol.*, vol. 10, no. MAR, pp. 1–9, Mar. 2019.

[13] E. A. Idelevich *et al.*, "The Recombinant Bacteriophage Endolysin HY-133 Exhibits In Vitro Activity against Different African Clonal Lineages of the Staphylococcus aureus Complex, Including Staphylococcus schweitzeri," *Antimicrob. Agents Chemother.*, vol. 60, no. 4, pp. 2551–2553, Apr. 2016.

Chapter 5

Liquid HY-133 formulation development

Table of Contents

1. Stability study of HY-133

1.1 Stability of the initial HY-133 bulk formulation

The initial HY-133 bulk storage formulation is shown in Table 1. It was developed by Hyglos GmbH and used to store the protein after expression and purification in frozen condition (Chapter 1). It comprised HEPES as a buffer excipient, NaCl as tonicity enhancer and $CaCl_2$ as ligand in the active site of the CHAP-domain of the protein. Arginine is important for maintaining the storage stability by preferential exclusion and used in high concentrations. The preliminary pH was set to pH 8.0 and HY-133 was formulated at a concentration of 0.5 mg/ml.

Table 1: Primary HY-133 bulk formulation with a pH of 8.0 and a HY-133 concentration of 0.5 mg/ml.

Excipient	**Concentration [mM]**
HEPES	25 mM
NaCl	150 mM
$CaCl_2$	10 mM
Arginine	300 mM

Although this formulation provided adequate stability upon storage at -80 °C, several pre-tests underlined the instability issues the protein faced in the initial formulation at higher temperatures.

In a first short-term stability study over the course of 8 weeks, the chemical stability and the activity of HY-133 in its initial bulk formulation was examined. Thereby, HY-133 revealed rapid protein degradation in liquid state after storage at 4 °C. Native HY-133 was determined with RP-HPLC, which showed a main peak loss of about 70% after 2 weeks at 4 °C. This finding was accompanied by a similar activity loss in the same time frame (Figure 1). The specific activity of HY-133 was determined with the lysis assay, where the progression of the optical density of a *s. xylosus* culture upon addition of HY-133 was monitored. Activity loss of enzymes upon oxidation was reported before [1]. It was described that oxidation of a single methionine caused activity reduction by 90%. This lack in chemical stability and activity demands further formulation development to obtain a product with a shelf life of more than 6 months at refrigerated storage condition.

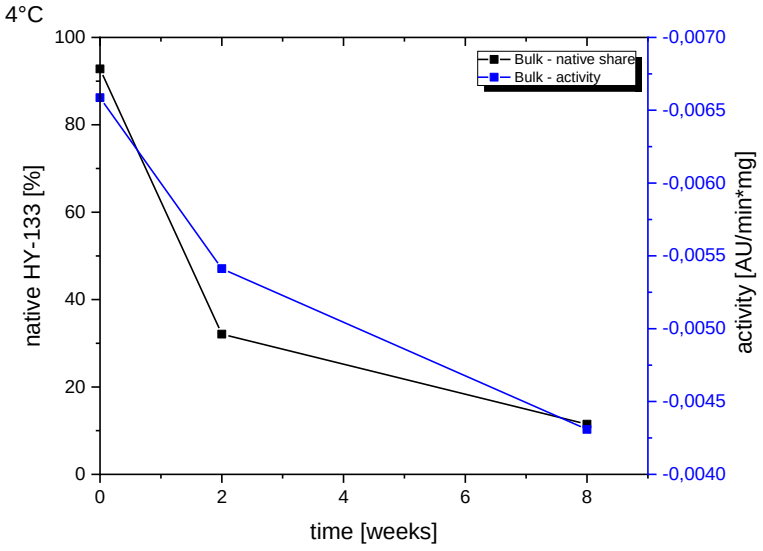

Figure 1: RP-HPLC showed rapid degradation of HY-133 (black) which comes along with activity loss (blue) upon storage of 8 weeks at 4 °C.

1.1.1 Stress study

To get a first impression of the physical stability of the protein, a small stress study was performed. The protein was stressed with different pH values, heat and agitation. In addition, a strong reducing reagent, Dithiothreitol (DTT), was added (Table 2). All samples were stressed in Eppendorf reaction tubes in aliquots of 1 ml each and analyzed on the same day. The different samples were analyzed by using the Bioanalyzer (CE-SDS) in combination with the protein 230 kit, the results are shown as a densitometry plot in Figure 2. Thereby, the amount of lower and higher molecular weight species depending on different parameters was determined. The bioanalyzer is a microfluidic electrophoretic system, which provides separation, staining and detection of the different protein molecular weight species in one step [2], [3].

Table 2: Stressed HY-133 samples in the first pre-test

Stress condition #	Stress	Condition
1	Low pH	pH 2.9
2	Physiological pH	pH 7.4
3	Bulk formulation pH	pH 8.0, reference substance
4	High pH	pH 10.0
5	100 mM DTT	RT
6	Moderate heat stress	37 °C; 30 min
7	Elevated heat stress	60 °C; 30 min
8	100 mM DTT	37 °C; 30 min
9	Shear stress	Vortexing for 2 min
10	Formulation buffer	Negative control

Only the low pH sample (#1; pH 2.9) showed a set of diffuse bands at lower molecular weight regions, indicating unfolding and fragmentation. Sample #7 precipitated after heating to 60 °C and therefore only minor amounts of remaining protein were determined. All other samples showed two distinct bands at 33 kDa and 62 kDa, except for the DTT treated samples. These two samples showed only the protein monomer band at 33 kDa. Therefore, the usage of this reducing reagent effectively reversed the formation of dimers. In addition, this finding also indicated that the formation of disulfide bonds was responsible for the dimer formation [4]. Free cysteine residues in the protein structure (there is at least one surface-accessible cysteine in HY-133) could form disulfide bonds within two or more molecules [5], [6]. An effective inhibition of the formation of disulfide bonds would therefore be beneficial for the monomer content of HY-133. Higher dimer peak contents were determined upon high pH stress (sample #4), in the heat stressed (sample #6) and in the vortexed variation (sample #9). As the protein bulk substance (sample #3) also showed a substantial dimer amount, the first stability-reducing parameter was identified. The negative control (sample #10) did not show any bands beside the marker bands below 12 kDa.

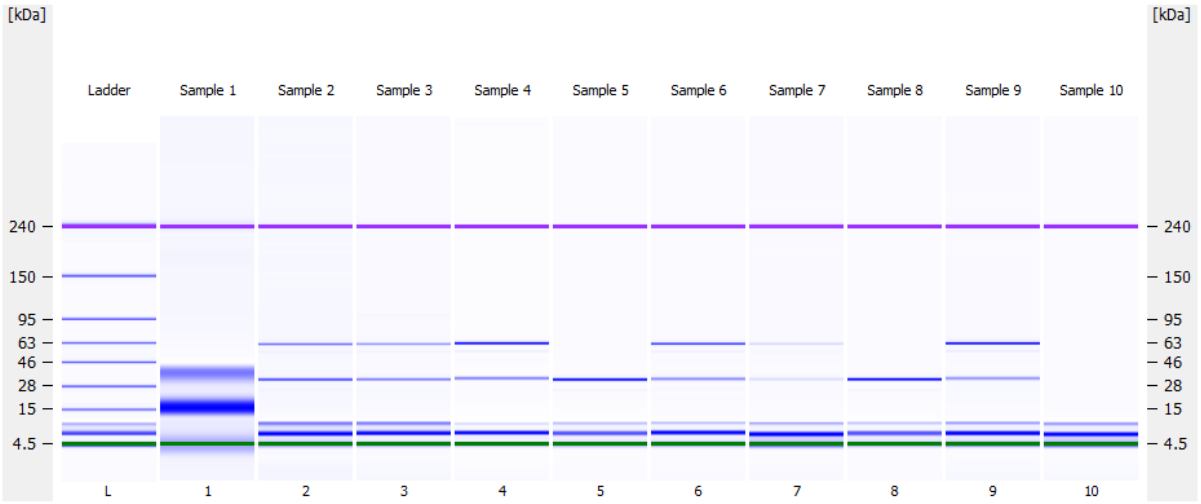

Figure 2: Densitometry plot of the CE-SDS results of the first pre-test.

1.1.2 Formulation variations

The second pre-test comprised a general excipient screening with eight different excipients being spiked to the HY-133 bulk formulation and analyzed using the Bioanalyzer. An overview of the tested formulation compositions is shown in Table 3 and the obtained densitometry plots after excipient spiking is shown in Figure 3. Four different antioxidants, methionine, cysteine, histidine and EDTA were tested. EDTA is used as an adjuvant antioxidant for metal-catalyzed oxidation, when especially free cysteine in the protein is a possible ligand [7]. The amino acids methionine, cysteine and histidine are already established antioxidants in various protein formulations [8], [9]. In addition, two different surfactants, polysorbate 80 (PS 80) and poloxamer 188, the stabilizing agent trehalose and a

formulation variation with less arginine were tested. The latter sample was generated via dialysis of the formulation buffer. All formulations were stored for 24 h at room temperature prior to the analysis.

Table 3: Samples for the excipient screening in the second pre-test.

Variation #	Formulation variation	Excipient concentration
1	Primary formulation (DS)	-
2	DS + Methionine	25 mM
3	DS + Cysteine	20 mM
4	DS + EDTA	0.1 mM
5	DS + PS 80	0.01%
6	DS + PS 80	0.1%
7	DS + Histidine	160 mM
8	DS + Poloxamer 188	0.01 %
9	DS + less Arginine	150 mM
10	DS + Trehalose	750 mM

The majority of the formulations showed two distinct bands at 33 kDa and at 62 kDa, indicating monomer and dimer species of the protein (Figure 3). Slightly higher dimer contents were determined in formulation #6 and #9, indicating compromised stability upon the addition of PS 80 and by the reduction of the arginine content. The addition of trehalose led to oligomerization of the protein, as not only dimers, but also higher molecular weight species were determined. Although often used as cryo- and lyoprotectant, trehalose in high concentrations can promote protein-association by forming clusters and therefore excluding water from the protein surface [10]. However, spiking of cysteine led to a diminished dimer content, mainly due to its strong antioxidative effect. In contrast, the addition of methionine and histidine did not have a direct effect on the dimer content, which remained unchanged in these formulations.

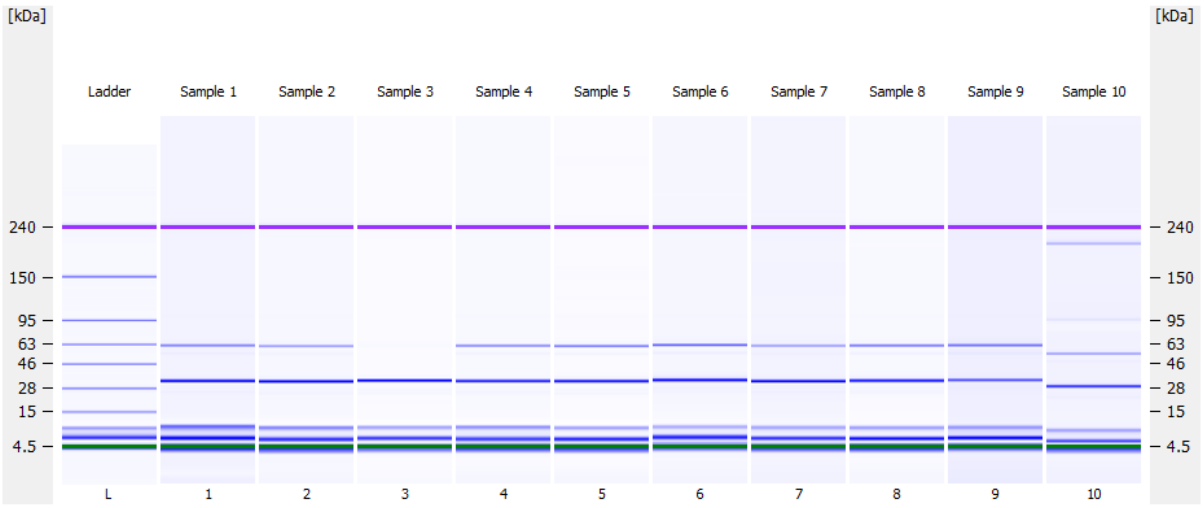

Figure 3: Densitometry plot of the CE-SDS results of the second pre-test.

In summary, the initial bulk formulation contained a substantial dimer content, was susceptible to chemical changes and showed higher loss in activity over storage time. This demands an improvement in physical and chemical stability of the protein, which is needed to ensure adequate shelf life at refrigerated conditions of the liquid formulation of HY-133.

1.2 Formulation screening I

In the first part of the formulation development, the most common degradation pathways like protein oxidation or aggregation were addressed. These degradation pathways were already assessed in several pre-tests above and the excipients selected accordingly. Following, several excipients such as antioxidants (cysteine, methionine), stabilizing amino acids (histidine and arginine in different concentrations) were examined. In addition, pH variations of the initial formulation were tested. The formulation variations are based on the initial HY-133 bulk formulation and all contained 25 mM HEPES, 150 mM NaCl and 10 mM $CaCl_2$. In addition, all formulations except of formulation 4 and 5 contained 300 mM Arginine. An overview of the 10 different formulations is shown in Table 4. HY-133 concentrations in all formulations corresponded to the bulk concentration of 0.5 mg/ml. 3 ml of each formulation was filled into 2R vials and subsequently stored at 4 °C, 25 °C and 40 °C for up to 14 weeks.

Table 4: Formulation list of samples in formulation study I. All formulations contain HY-133 in a concentration of 0.5 mg/ml.

#	Excipient variation	Concentration	pH	Rationale
1	-	-	7.4	Physiological pH
2	-	-	6.5	Lower pH
3	-	-	8.0	Bulk formulation
4	Less arginine	200 mM	7.4	Reduced arginine content
5	Less arginine	100 mM	7.4	Reduced arginine content
6	Addition of cysteine	5 mM	7.4	Antioxidant I
7	Addition of cysteine	25 mM	7.4	Antioxidant I, higher concentration
8	Addition of histidine	10 mM	7.4	Antioxidant II
9	Addition of methionine	10 mM	7.4	Antioxidant III
10	Addition of PS 80	0.1%	7.4	Surfactant

1.2.1 Particle formation and physical stability

The formulations were visually inspected after 8 weeks of storage at the three different storage temperatures. In Figure 4 to Figure 6, exemplary pictures of formulations #1 - #10 after storage at 4 °C, 25 °C and 40 °C for 8 weeks are shown. Storage at 4 °C and 25 °C did not lead to visible particle formation in the formulations. Only in formulation #7 larger, spherical particles could be observed, irrespective of the storage condition. Insolubility of the excipient is unlikely as 25 mM cysteine is well below its solubility limit. Turbidity or opalescence could not be determined in any of the formulations.

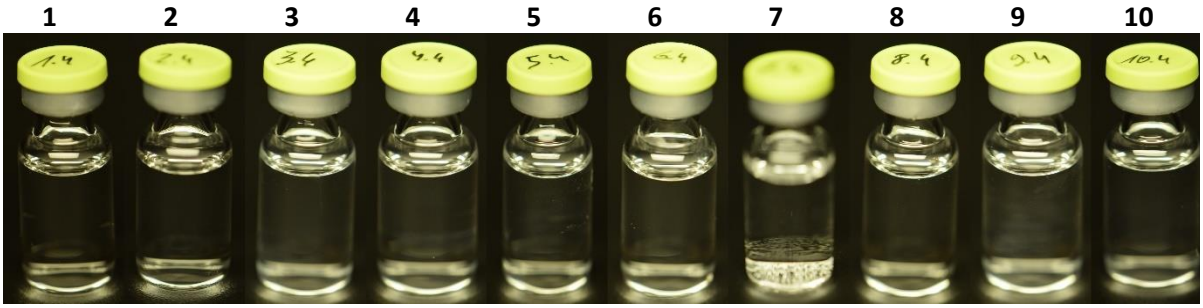

Figure 4: Visual appearance of formulations 1-10 (from left to right) stored at 4 °C for 8 weeks.

Storage at 25 °C was very similar to the above described 4 °C storage (Figure 5). No visible particles were observed in any of the formulations except of formulation #7. A tendency towards slight opalescence was determined in formulation #10.

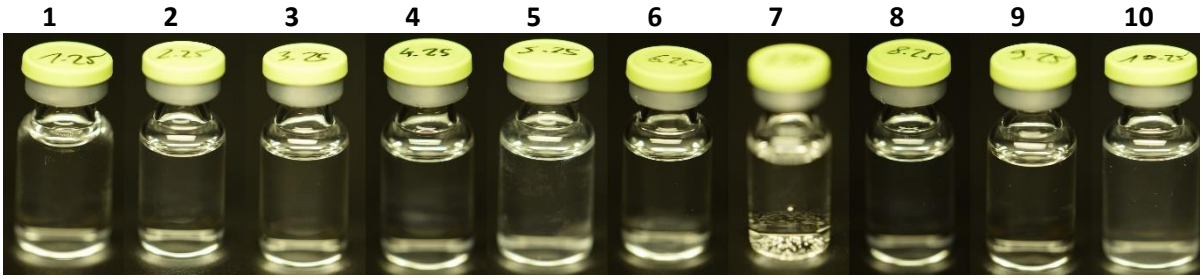

Figure 5: Visual appearance of formulations 1-10 (from left to right) stored at 25 °C for 8 weeks

In contrast, storage at 40 °C led to visible particle formation in the majority of the formulations. Only formulations #1, #2, #3 and #7 were rated as particle free and without turbidity or opalescence. Interestingly, the visible particles vanished in formulation #7 upon storage at 40 °C. The remaining formulations showed large numbers of visible particles and high turbidity. In addition, formulations #5, #6 and #8 resulted in slight discoloration.

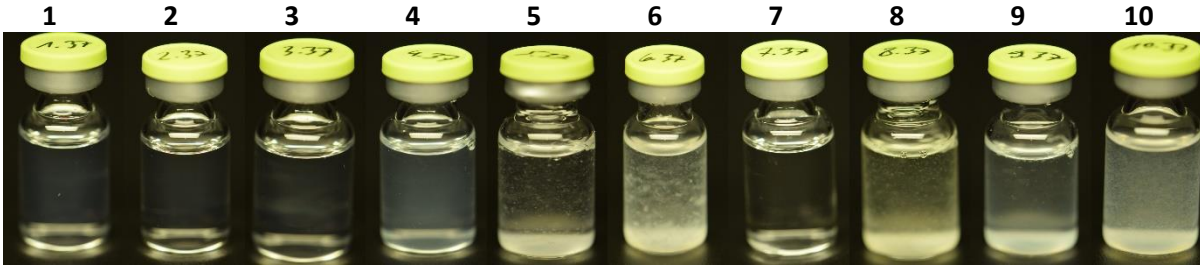

Figure 6: Visual appearance of formulations 1-10 (from left to right) stored at 40 °C for 8 weeks.

Subvisible particles were assessed by light obscuration (LO) measurements and the results are displayed in Figure 7. Storage at 4 °C and 25 °C resulted in low particle numbers in the majority of the formulations, ranging between 1,000 to 5,000 particles ≥ 1 µm per ml. As an exception, a large particle count was determined in formulation #10, which was the only formulation containing polysorbate 80. Storage at 40 °C led increased particle numbers in formulations #4 -#6 and #8 - #10. These results

matched the results from the visual inspection, as visible particles were observed in all formulations with high subvisible particle counts.

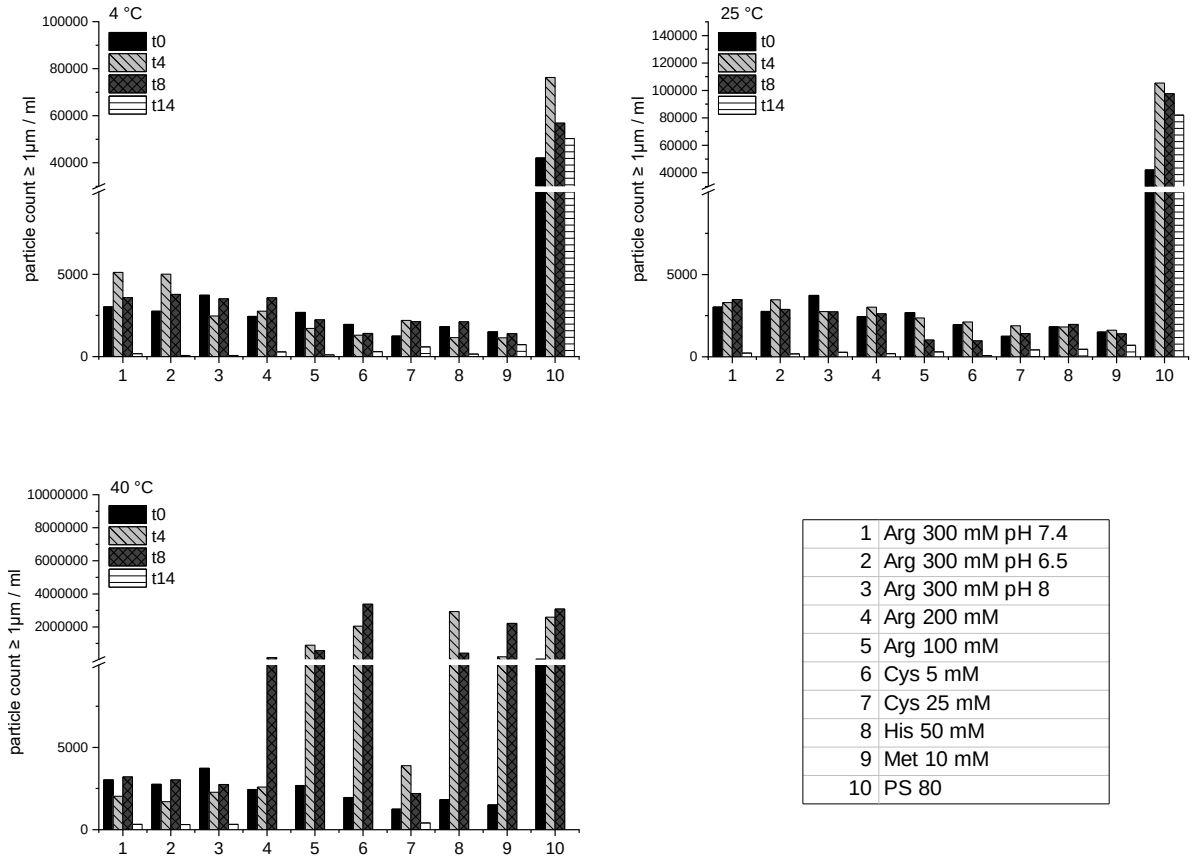

Figure 7: Subvisible particle counts determined by LO.

The monomer content of HY-133 in the first stability study was determined by CE-SDS (Figure 8). Storage at 4 °C led to a decrease in monomer content in most of the formulations. The original bulk formulation (formulation #3) resulted in over 70% aggregated protein after eight-week storage at 4°C. The highest monomer content was observed in formulations containing cysteine, irrespective of the concentration. Formulations #2 (low pH), #8 and #9 (added histidine and methionine, respectively) revealed monomer contents with ≥ 70% after eight weeks of storage at 4 °C. With storage at 25 °C, a similar trend in the monomer content was obtained. After two weeks, only formulations #2, #6, #7 and #9 showed monomer contents over 70%. The relative monomer contents apparently increased in all samples after eight-week storage at 25 °C, which could be explained by a general loss of protein content through insoluble aggregates. Storage at 40 °C led to in general higher monomer contents for any of the formulations. Since the majority of the formulations showed visibly aggregated protein, the higher monomer content can be explained by the formation of insoluble aggregates [11]. These insoluble aggregates cannot be measured with the Bioanalyzer and the monomer content appears to be higher.

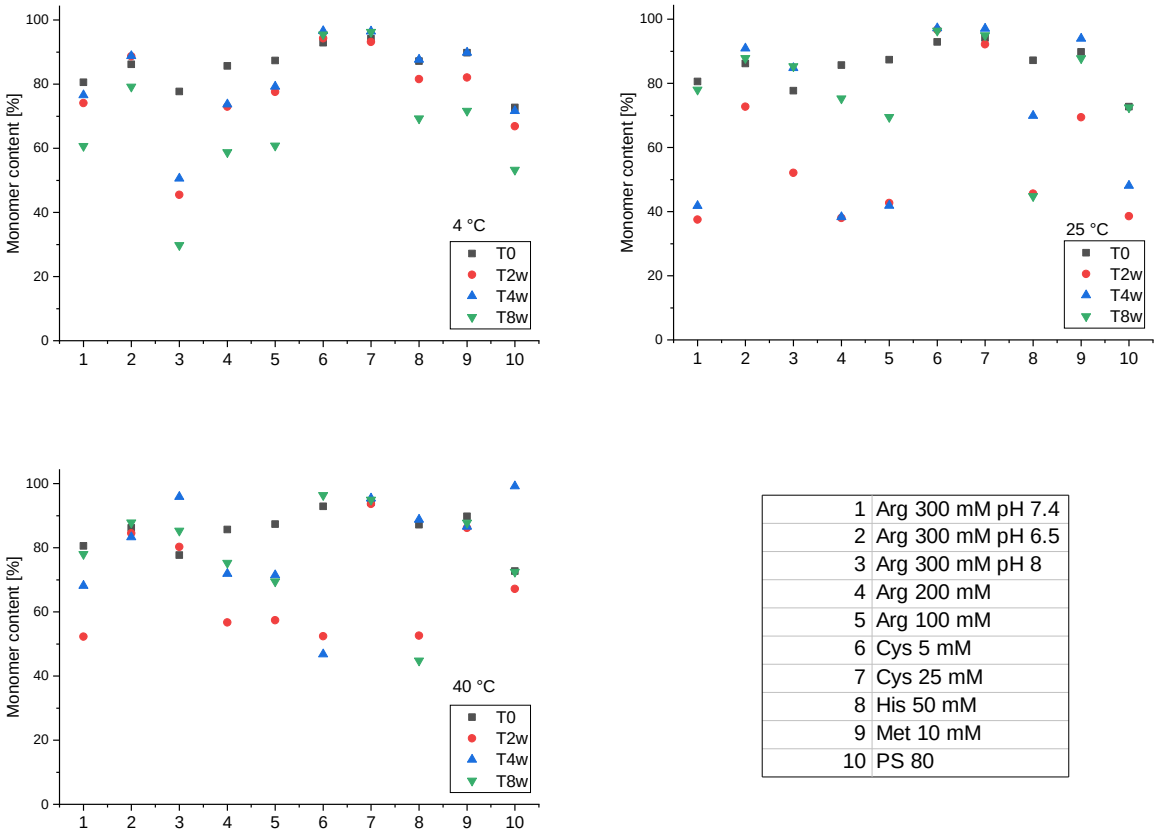

Figure 8: Monomer content of different HY-133 formulations determined with CE-SDS.

Thus, the physical stability of HY-133 was highly formulation and excipient dependent. The addition of cysteine (25 mM) and the three pH variations drastically improved the occurrence of visible particles at storage temperatures of 40 °C. Also, subvisible particles were substantially lower in these formulations upon storage at elevated temperatures. The monomer content was highest in formulations #2, #7 and #9 at all storage conditions. The methionine-containing formulation (#9) showed higher stability upon storage at 4 °C and 25 °C, but high visible and subvisible particle counts upon storage at 40 °C. Overall, it is noticeable that the addition of an antioxidant not only reduced the number of visible and subvisible particles, but also resulted in higher monomer content. This clearly indicated a connection between the occurrence of dimers and other higher molecular weight contents caused by protein oxidation and the formation of subvisible particles. This chemically-induced aggregation pathway is a common reason for protein aggregation and was intensively discussed before [6], [10], [12]. PS 80 is widely used to inhibit protein aggregation [13], [14]. The concentration of 0.1% is well above the critical micelle concentration. The largely elevated subvisible particle numbers in the PS 80 containing formulation was therefore unexpected. It could be linked to subvisible particles originating from degraded PS 80 or to the effect of degraded PS 80 on the induction of aggregation of the protein due to its oxidation by peroxide residues [9], [14]. In addition, visible particles in PS80 formulations could be linked to impurities already present in the PS80 raw material [15].

1.2.2 Chemical stability

Chemical stability of HY-133 was determined by RP-HPLC (Figure 9). The tested formulations varied regarding their native HY-133 protein content over time and dependent on the storage temperatures. The initial bulk formulation (formulation #3) showed rapid chemical degradation upon storage at 4 °C. Already after two weeks, less than 30% native protein content remained. A similar degradation trend was observed by the addition of 5 mM cysteine (#6). Lower arginine concentrations of 200 mM (#4) and 100 mM (#5) led to higher native protein recovery of about 60% after storage at 4 °C over 3 months. Lowering the pH to 6.5 (#2) improved the chemical stability further at 4°C. The addition of 10 mM methionine (#9) or 10 mM histidine (#8) also improved the chemical stability of HY-133. Therefore, formulations #2, #8, and #9 resulted in the highest native HY-133 content with about 90%.

Storage at 25 °C led to fast degradation in all of the formulations. Especially formulations #1, #4, #8, and #10 resulted in faster degradation compared to storage at 4 °C. After two-week storage, only formulations #2, #8 and #9 with the lowered pH 6.5, and added histidine or methionine, respectively, showed a native protein content over 60%. Storage at 25 °C for 14 weeks led to a major decrease in native protein content to below 10% in all formulations except for formulations #2 and #9. Both formulations remained at a native protein content level over 60%.

Storage at 40°C for two weeks led to a major degradation of HY-133 in all formulations except formulations #2 and #9. However, both formulations showed visible degradation over time, resulting in over 50% degraded protein after 8 weeks.

An increase in native HY-133 content in some of the formulations and time points could be explained by the formation of insoluble aggregates. This led to a decreased absolute peak area, especially of degradation species, causing higher native peak contents.

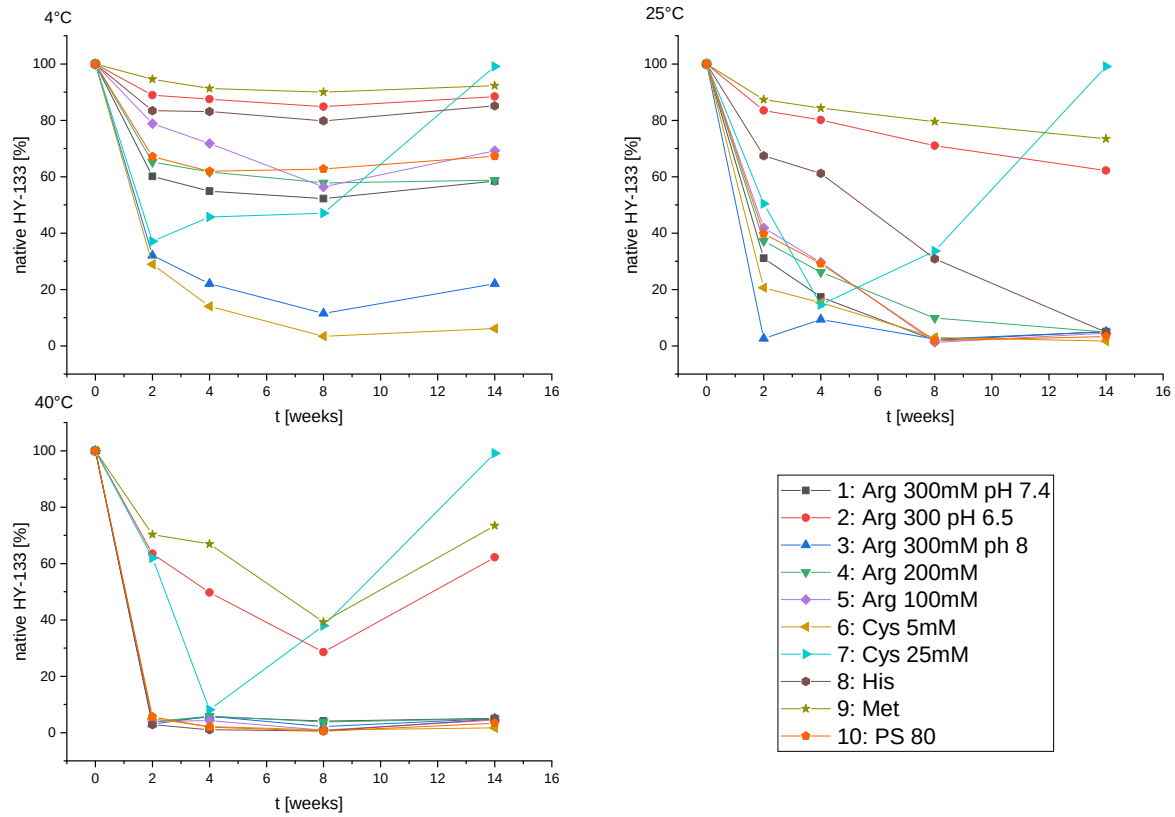

Figure 9: Native protein contents of different HY-133 formulations determined by RP-HPLC upon 14 weeks at 4 °C, 25 °C, and 40 °C.

Methionine was identified as a suitable antioxidant in the HY-133 formulation. This amino acid is a widely and often used antioxidant in the formulation of biopharmaceutics [8], [16]. Lowering the pH below 7 was also already described to effectively decrease oxidation of cysteine residues, which could be shown in the second formulation in this study [17].

1.2.3 HY-133 activity measurements

The activity measurements of HY-133 were under continuous method development and several different FRET-activity assays were conducted. The results of the early FRET-activity measurements (Figure 10) can only be compared with later results regarding their trends since the method was still under development at this stage.

All formulations except of formulation #3 (initial bulk; Arg 300 mM, pH 8) resulted in the same activity level after storage at 4 °C for up to eight weeks. At a storage temperature of 25 °C, formulation #3 showed a loss in activity already after 4 weeks, and activity vanished completely after 8 weeks. At this storage temperature, formulations #1, #4, #5 and #10 showed an apparent increase in activity after 8 weeks, whereas activity remained comparable in the other formulations. Storage at 40 °C led to a total activity loss in all formulations except formulation #2, #7 and #9 with substantial remaining activities.

An apparent increase in activity could be explained by the onset of HY-133 degradation, which required a larger concentration to achieve the same activity. This was then followed by a total loss in activity over time.

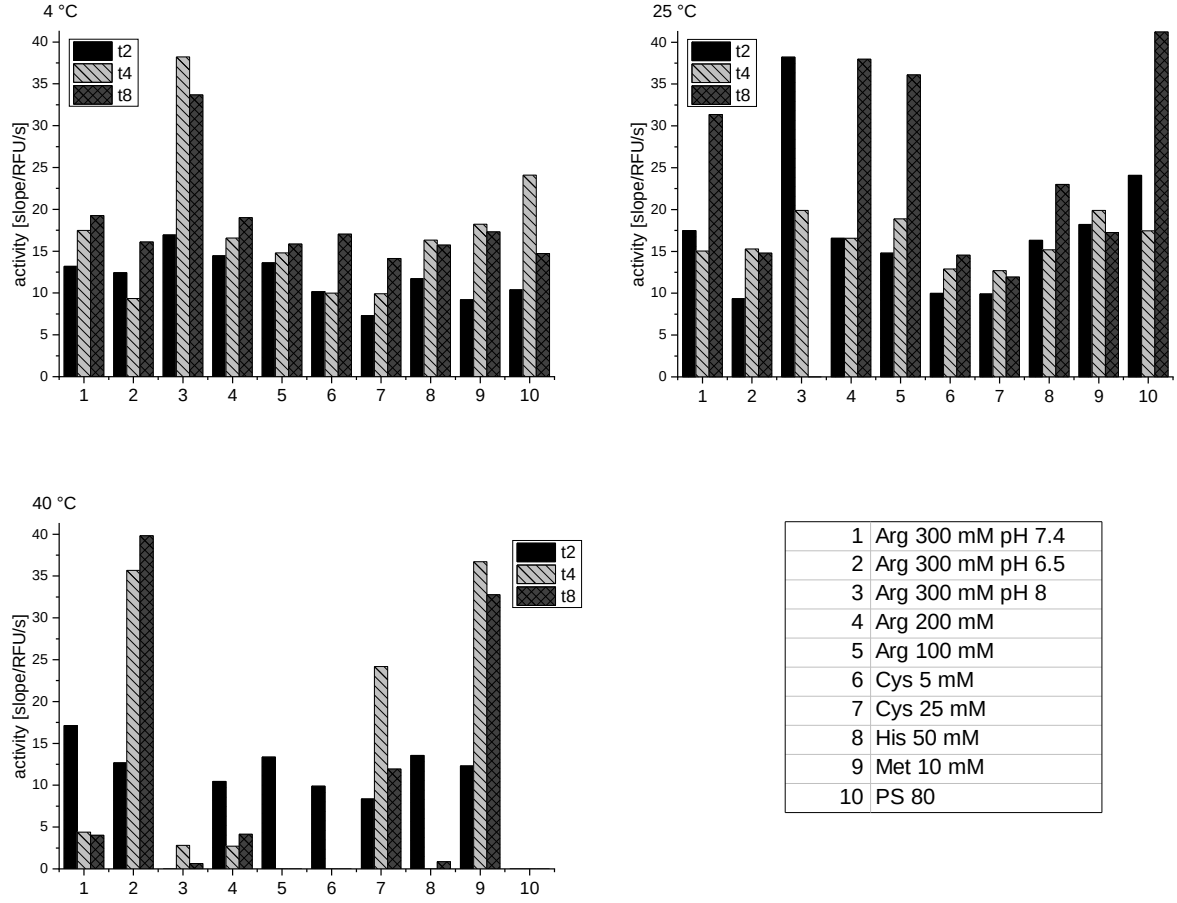

Figure 10: Activity of different HY-133 formulations determined by FRET-assay.

In a second activity test (Figure 11), the direct impact of HY-133 on bacterial integrity was measured. Activity was measured by the decrease of absorbance levels over time, resulting in higher negative slopes (y-axis) in higher activity samples compared to no change in absorbance proposing no remaining activity. At 4 °C, no major differences in activity were observed in the majority of the formulations after 8 weeks of storage. Only formulations #5 and #6 showed a decreased specific activity. Storage at 25 °C led to more pronounced differences in activity. After 8 weeks, formulation #2 showed the highest remaining activity, being comparable to the initial activity. In formulations #3 and #6, activity was not detectable after 8 weeks, whereas the remaining formulations showed lower, but still measurable activity values.

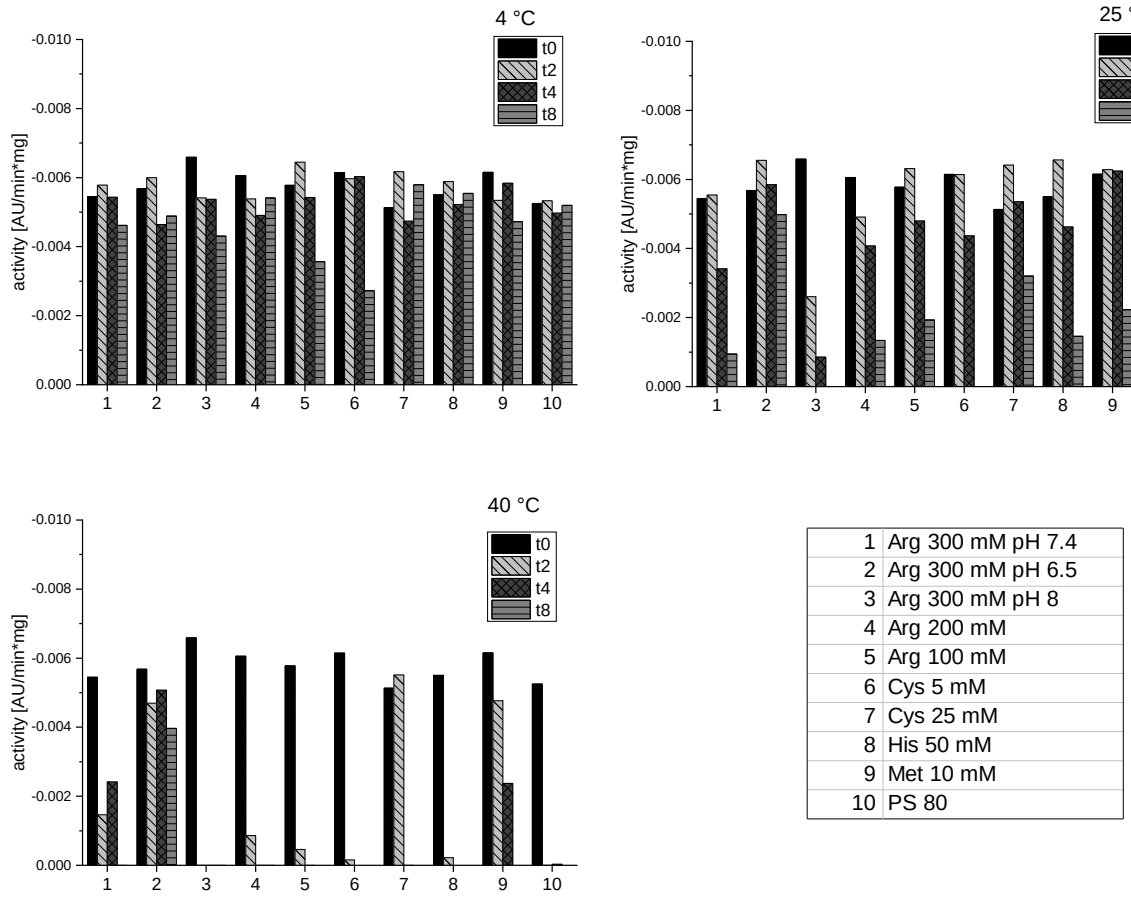

Figure 11: Activity of different HY-133 formulations determined with lysis assay with S. xylosus. The decrease in absorbance was measured, resulting in a higher negative slope value (y-axis) for higher activity levels compared to lower absorbance decreases (lower negative slope values) for less active samples.

In summary, the activity of HY-133 was effectively maintained throughout the study at 4 °C in most of the formulations and at higher temperatures in formulations #2 and #9. These results also correlated to the chemical stability of the protein.

1.2.4 Summary of the first formulation screening

The first study revealed different factors affecting the stability of HY-133 upon storage. As expected, the observed instabilities were more pronounced at higher temperatures. Chemical degradation was strongly reduced by the addition of methionine. In addition, lowering the pH to 6.5 resulted also in protein stabilization. In these two formulations, over 70% main peak content were observed after 14-week storage at 25 °C. Activity was maintained throughout the study at 4 °C storage in any of the formulations except for formulation #3, the initial bulk formulation. At elevated temperatures, highest remaining activity was observed in formulations containing cysteine, methionine, histidine, and in the low pH formulation. Subvisible particle counts were low in all formulations except for formulation #10 after storage at 4 °C and 25 °C. All formulations, except of formulation #7, were determined to be free of visible particles upon storage at 4 °C and 25 °C.

Although formulations #6 and #7 showed promising results regarding their physical stability and activity, cysteine was excluded from further studies as the formulation developed a strong, sulphurous odor. Therefore, the beneficial influences of methionine and a lowered pH value on the stability of HY-133 were investigated further in the next formulation screening (formulation screening II).

1.3 Formulation screening II

The results of the first stability study clearly indicated that a pH lower than 6.5 and the addition of an antioxidant like methionine is beneficial for the protein stability. To further assess these findings, a second stability study was designed. Generally, three main targets were defined: (i) further decrease of chemically modified HY-133 content while maintaining activity over time; (ii) lower arginine content and accompanied decreased osmolality; (iii) the role of Ca^{2+} in HY-133 stability should be evaluated. Therefore, this study included a pH screening, combination of methionine and a lower pH, lower arginine concentration at pH 6.5 and a formulation without $CaCl_2$. All formulations were based on the initial bulk formulation of HY-133 and are varied as described in the following.

Five different pH values were tested in formulations #1 - #5, covering a pH range from 5.0 to 6.8. A reduced arginine concentration of 100 mM instead of 300 mM was tested in formulation #6 at pH 6.5. Formulation #7 contained 10 mM methionine at pH 6.5. In formulation #8, the initial formulation was tested without $CaCl_2$ to verify whether $CaCl_2$ is essential for the protein's functionality. An overview of these different formulations is shown in Table 5.

Table 5: Formulation variations included in the second stability study (formulation screening II).

#	Composition	pH
1	25 mM HEPES; 150 mM NaCl; 10 mM $CaCl_2$; 300 mM arginine	5.0
2	Initial HY-133 bulk formulation	5.5
3	Initial HY-133 bulk formulation	6.0
4	Initial HY-133 bulk formulation	6.2
5	Initial HY-133 bulk formulation	6.8
6	25 mM HEPES; 150 mM NaCl; 10 mM $CaCl_2$; **100 mM arginine**	6.5
7	25 mM HEPES; 150 mM NaCl; 10 mM $CaCl_2$; 300 mM arginine; **10 mM methionine**	6.5
8	25 mM HEPES; 150 mM NaCl; ~~**10 mM $CaCl_2$**~~, 300 mM arginine	6.5

Aliquots of 3 ml of each formulation were filled into 2R neutral glass vials and stored at 4 °C, 25 °C and 40 °C for up to 24 weeks. Samples were analyzed after 2, 6, 10 and 24 weeks with following methods: RP-HPLC for the evaluation of the protein's chemical integrity, CE-SDS (Bioanalyzer) for soluble aggregates, light obscuration for subvisible particles, and the FRET assay for activity measurements.

1.3.1 Particle formation and physical stability

The initial bulk-formulation tests and first stability study indicated that the stability of HY-133 is depending on the respective pH value of the formulation. Therefore, the final pH at the end of the stability study was compared to the starting pH values. The red line in Figure 12 shows the initially adjusted pH at T0. After 24 weeks, all formulations showed an increase in pH with varying extent. Formulations #1 - #4 showed a pH of about 6.5, whereas the pH of formulations #5 - #8 was about 7.0. The formulation pH was therefore not maintained in any of the formulations, although buffering agents were used in all formulations.

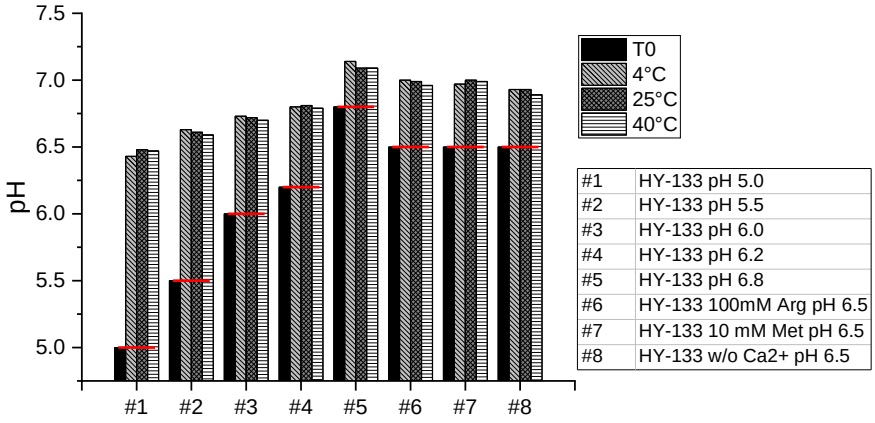

Figure 12: pH shift over time for all formulations analyzed in formulation screening II.

The subvisible particle counts ≥ 1 µm/ml after storage at 40 °C for up to 10 weeks are displayed in Figure 13. Overall, a low number of subvisible particles (below 1,000 particles per ml) were determined in any of the formulations.

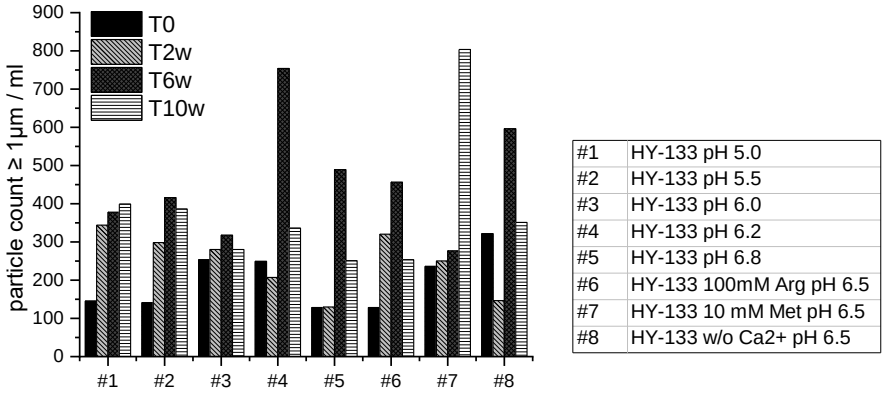

Figure 13: Subvisible particles ≥ 1 µm of the different HY-133 formulations in the second stability study after storage for up to 10 weeks at 40 °C.

Ratios of different size species in the different formulations were determined by CE-SDS. Figure 14 shows the size distribution of HY-133 in the different formulations at T0 and after storage at 4 °C for 24 weeks. At T0, all formulations showed at distinct amount of about 5% dimers and a very small amount of a lower molecular weight species (<5% 25 kDa fraction). After 24 weeks of storage,

formulations #1, #2 and #7 showed a constant monomer peak with no changes of the two different degradation species (fragment or 25 kDa fraction). Formulations #5, #6, and #8 yielded in only 70 – 75% remaining monomer HY-133 content after 24-week storage at 4 °C.

A similar trend in monomer loss was observed after storage at 40 °C (Figure 15). A very pronounced monomer loss was determined in formulations #5, #6 and #8 already after a 2-week storage. Over the course of the study, the dimer content varied in the formulations stored at 40 °C, leading to an apparent decrease in dimer content. These inconsistent results could be explained by the high number of visible particles, whose formation were caused by further aggregation of the protein. The lowest decrease monomer content (no increase or apparent decrease in dimer content, no change in protein concentration) was observed in formulation #1 - #3 and #7, indicating a higher protein stability over time also at elevated temperature.

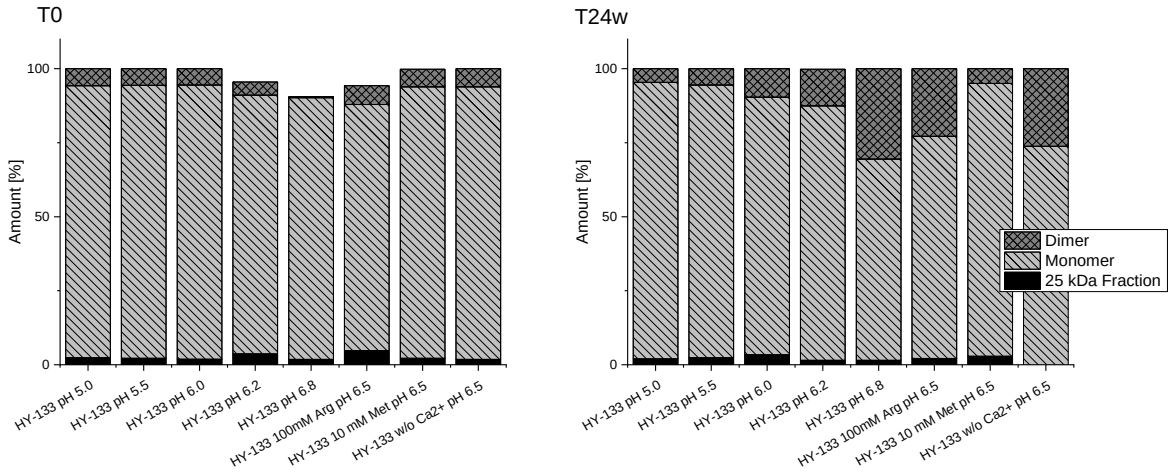

Figure 14: CE-SDS results upon storage for 24 weeks at 4 °C.

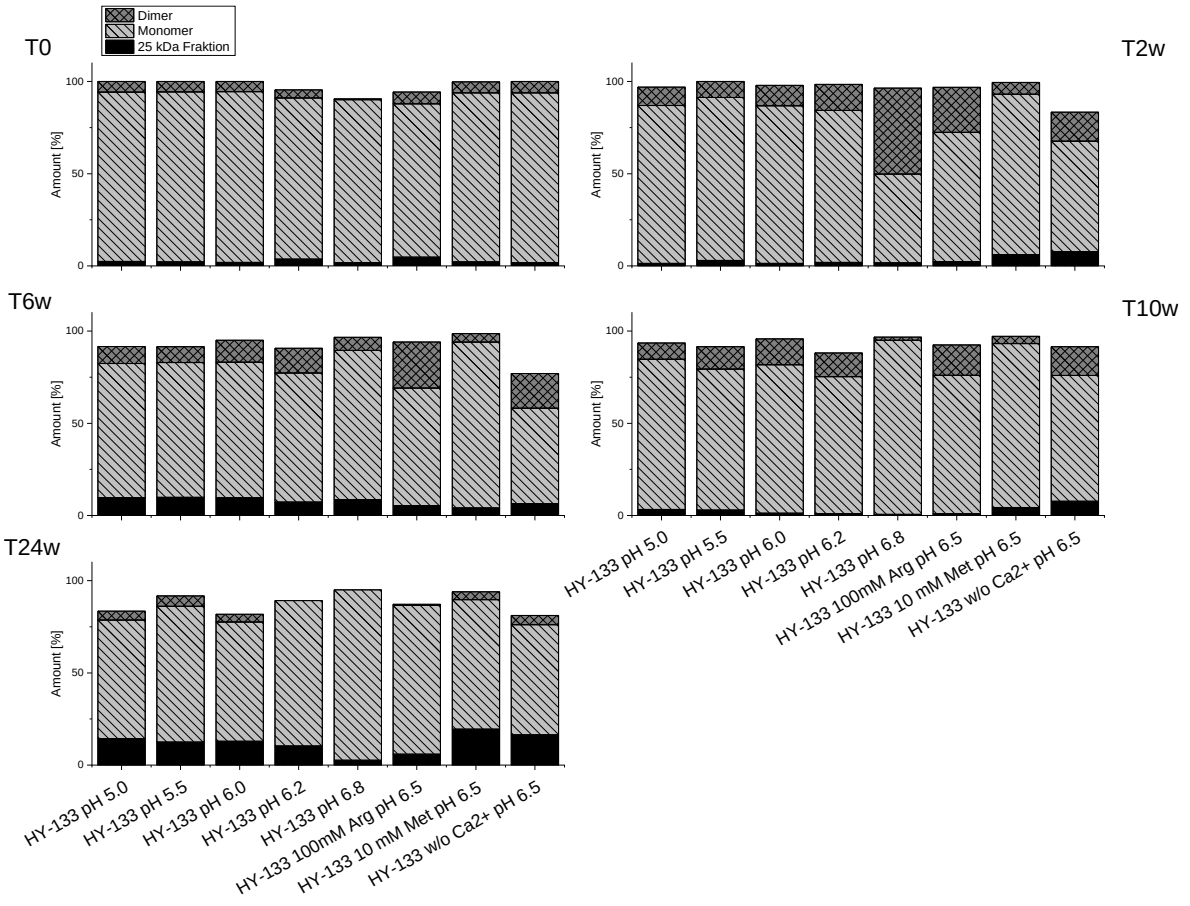

Figure 15: CE-SDS results over time upon storage at 40 °C.

1.3.2 Chemical stability

Chemical degradation of HY-133 was assessed by RP-HPLC. Relative main peak contents over the course of the study at different temperatures are shown in Figure 16. Formulation #7, containing methionine as antioxidant, showed the highest native protein content after storage at all tested temperatures upon 24 weeks. This formulation showed no loss in main peak content upon storage at 4 °C. Initially low pH formulations (formulations #1 - #3) showed less protein degradation compared to formulations with a pH value larger than pH 6.2. Formulation #5 with a pH of 6.8 yielded in an almost complete loss in main peak content upon storage at 4 °C. Storage at elevated temperatures resulted in a similar trend in protein stability over time with formulation #7 performing best in both storage conditions. Again, low pH formulations were superior regarding their chemical stability compared to higher pH formulations. Formulation #7 maintained over 80% main peak content upon storage for 24 weeks at 25 °C, whereas low pH formulations could maintain main peak contents above 50%. Storage at 40 °C led to a total loss in main peak contents in any of the formulations, while formulation #7 could maintain half of the main peak content. In general, reduced arginine amount led to more degradation, as well as the formulation without Ca^{2+}.

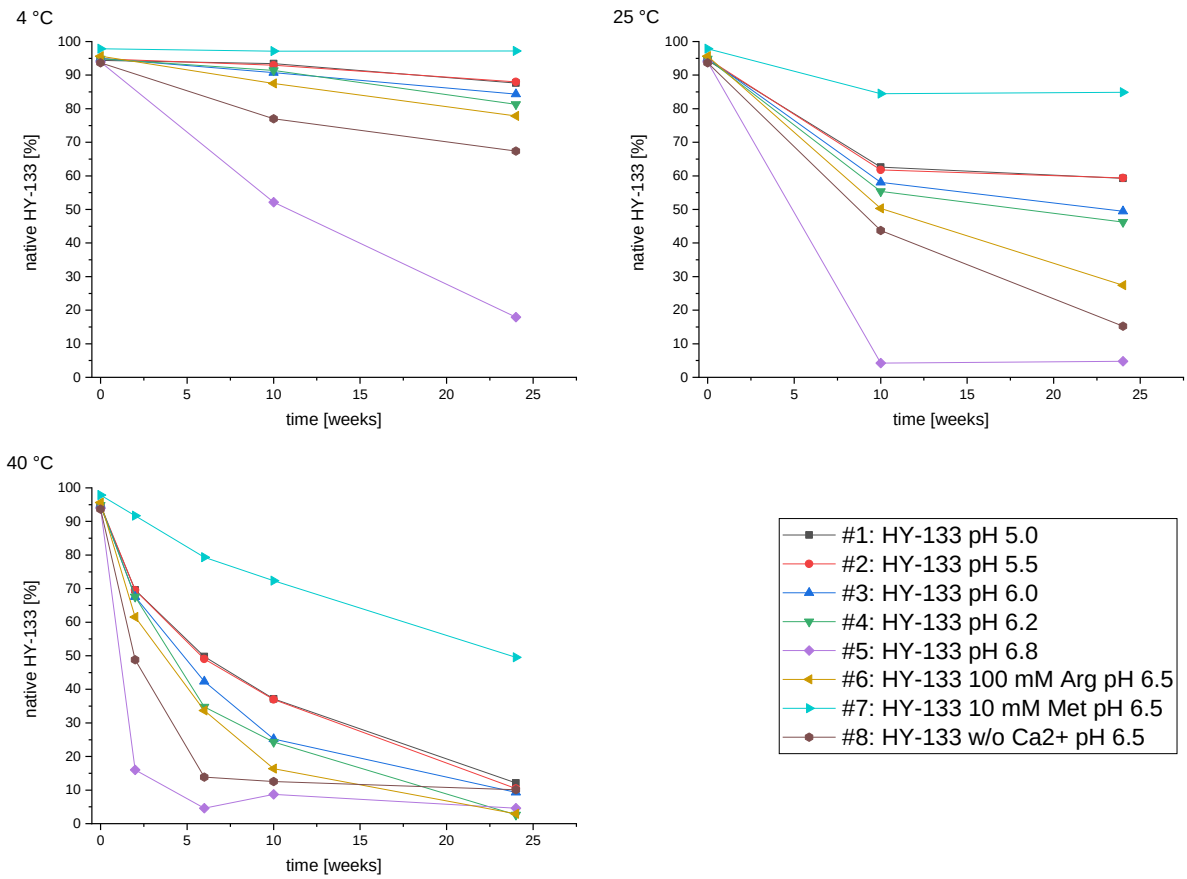

Figure 16: Chemical stability of HY-133 determined by RP-HPLC upon storage for up to 24 weeks at 5 °C, 25 °C and 40 °C.

1.3.3 HY-133 activity measurement

The activity of HY-133 in different formulations after storage for up to 24 weeks is shown in Figure 17. After 24 weeks of storage at 4 °C, the protein was still active in the majority of the formulations. In formulation #5 with the highest pH value, no activity could be detected after 24 weeks while activity was still observed after 10 weeks. All other formulations maintained their specific activities throughout 24 weeks of storage at refrigerated condition.

Activity upon storage at elevated temperatures were examined after 10 weeks. Storage at 40 °C led to a completely vanished activity in formulations #5 and #8 within 10 weeks. The other formulations showed an apparently increase in activity, which represents the onset of losing activity. No major differences in activity were observed after storage at 25 °C.

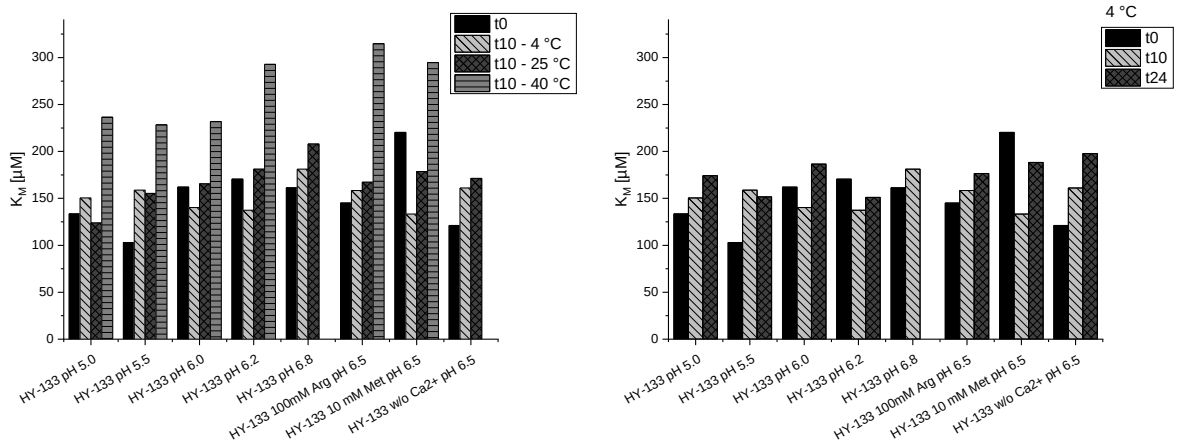

Figure 17: HY-133 activity depending on its formulation. Left: K_m after 10 weeks at 4 °C, 25 °C and 40 °C; right: K_m after 10 and 24 weeks at 4 °C.

1.3.4 Summary of the second formation screening

In summary, the formulations with a lower initial pH and the addition of methionine performed best in the above described formulation study II. Especially the utilization of methionine enhanced the protein's chemical stability, indicated by higher native protein amounts. The antioxidative effect of methionine was shown before and also advisable in this formulation [18]. Initial pH values < 6.2 were shown to be overall preferable regarding their chemical stability and activity. Both formulation variations, lower pH and the addition of methionine, led to a highly increased chemical stability, which was accompanied by maintained activity. However, the in here observed pH changes over time are extensive and affect the outcome of the formulation study. A more precise pH adjustment using a suitable buffer system would be beneficial. Additionally, the combination of a lower pH (< pH 6.2) and the utilization of methionine as an antioxidant should be investigated.

In contrast, the decreased concentration of arginine led to a decrease in protein stability. It was shown that HY-133 aggregation was thereby more pronounced. The concentration dependent stabilizing effect of arginine was described before [9], [10], [19]. It was also shown that HY-133 loses its activity, if Ca^{2+} is not included in the formulation at elevated storage temperatures. The enzymatic active domain (EAD) of HY-133 consists of the CHAP domain from the endolysin of phage K [20]. In a similar CHAP domain, a calcium ion is bound to the amino-terminal part of the domain, nearby the catalytic site [21]. It was proposed that this calcium ion is crucial for maintaining the structure of the protein and therefore being essential for the catalytic mechanism. During the enzymatic reaction, this structural calcium may provide the correct location of the substitute. Besides the loss of activity, the lack of calcium chloride in the formulation buffer also leads to very pronounced chemical changes of HY-133, even at refrigerated conditions. This was accompanied by an elevated dimer amount after 24 weeks of storage at 4 °C. Both physicochemical changes are most likely connected to folding differences in the catalytic region, which could expose oxidation prone regions in the protein. This

phenomenon was reported before in another recombinant phage endolysin, SAL-1. There, the presence of Ca^{2+} ions also increased the proteins activity. Despite our findings, the addition of calcium ions simultaneously reduced the stability of the SAL -1 [22].

1.4 Formulation screening III

In the third stage of the HY-133 formulation study, the buffer composition was adapted to the previous findings of formulation pH values below 6.2 being beneficial to the protein stability. As the initially used buffer component HEPES has an optimal buffer capacity in the range of pH 6.8 to 8.2, this buffer needed to be exchanged by other suitable buffer excipients. Citrate and Histidine buffers are widely used buffer excipients for biopharmaceuticals and provide sufficient buffer capacity at the intended pH of around 6.0 [9], [23], [24] . In this study, four different pH values (5.0, 5.5, 6.0, and 6.5) were tested in formulations containing either citrate, histidine or no additional buffer excipient. The latter formulation contained, like the other two formulations, the zwitterion L-arginine in a concentration of 300 mM. The buffer capacity in the lower pH formulations is neglectable due to pK_a values of around 2 and 9. The three different formulations were dialyzed as described before and the pH controlled thereafter. Each formulation was further spiked with either 0.1 % Polysorbate 80 or 0.1 % Poloxamer 188 and compared to a surfactant-free formulation (Table 6 - Table 8).

Table 6: Formulation composition for formulation study III – buffer free

#	Buffer composition	Adjustment	pH	Surfactant
A1	150 mM NaCl, 10 mM $CaCl_2$, 10 mM methionine, 300 mM arginine	-	5.0	-
A2			5.5	-
A3			6.0	-
A4			6.5	-
A5			5.0	+ 0.1% PX188
A6			5.5	+ 0.1% PX188
A7			6.0	+ 0.1% PX188
A8			6.5	+ 0.1% PX188
A9			5.0	+ 0.1% PS80
A10			5.5	+ 0.1% PS80
A11			6.0	+ 0.1% PS80
A12			6.5	+ 0.1% PS80

Table 7: Formulation composition for formulation study III – citrate buffer

#	Buffer composition	Adjustment	pH	Surfactant
C1	150 mM NaCl, 10 mM $CaCl_2$, 10 mM methionine, 300 mM arginine	15 mM Citrate	5.0	-
C2			5.5	-
C3			6.0	-
C4			6.5	-
C5			5.0	+ 0.1% PX188
C6			5.5	+ 0.1% PX188
C7			6.0	+ 0.1% PX188
C8			6.5	+ 0.1% PX188
C9			5.0	+ 0.1% PS80
C10			5.5	+ 0.1% PS80
C11			6.0	+ 0.1% PS80
C12			6.5	+ 0.1% PS80

Table 8: Formulation composition for formulation study III – histidine buffer

#	Buffer composition	Adjustment	pH	Surfactant
H1	150 mM NaCl, 10 mM $CaCl_2$, 10 mM methionine, 300 mM arginine	10 mM Histidine	5.0	-
H2			5.5	-
H3			6.0	-
H4			6.5	-
H5			5.0	+ 0.1% PX188
H6			5.5	+ 0.1% PX188
H7			6.0	+ 0.1% PX188
H8			6.5	+ 0.1% PX188
H9			5.0	+ 0.1% PS80
H10			5.5	+ 0.1% PS80
H11			6.0	+ 0.1% PS80
H12			6.5	+ 0.1% PS80

1.4.1 Physical stability

Already after preparation, formulations with buffers based on either citrate or histidine showed moderate dimer fractions, with minor deviations between the different pH values and surfactant combinations (Figure 18). Slightly more dimers were determined in formulations containing PS80 (formulations 9-12) compared to Poloxamer 188 and without the use of surfactant. This trend was even more pronounced in formulations with pH values of 6.0 and 6.5. In contrast, formulations buffered with arginine only had substantially higher dimer contents, which was slightly improved by the use of Poloxamer 188. All formulations, irrespective of the buffering component, showed a small peak at around 25 kDa, which was slightly increased in formulations containing Poloxamer 188 (Figure 19). A signal originating from Poloxamer 188 itself can be excluded, as the surfactant has an average molecular weight of about 8.4 kDa [25].

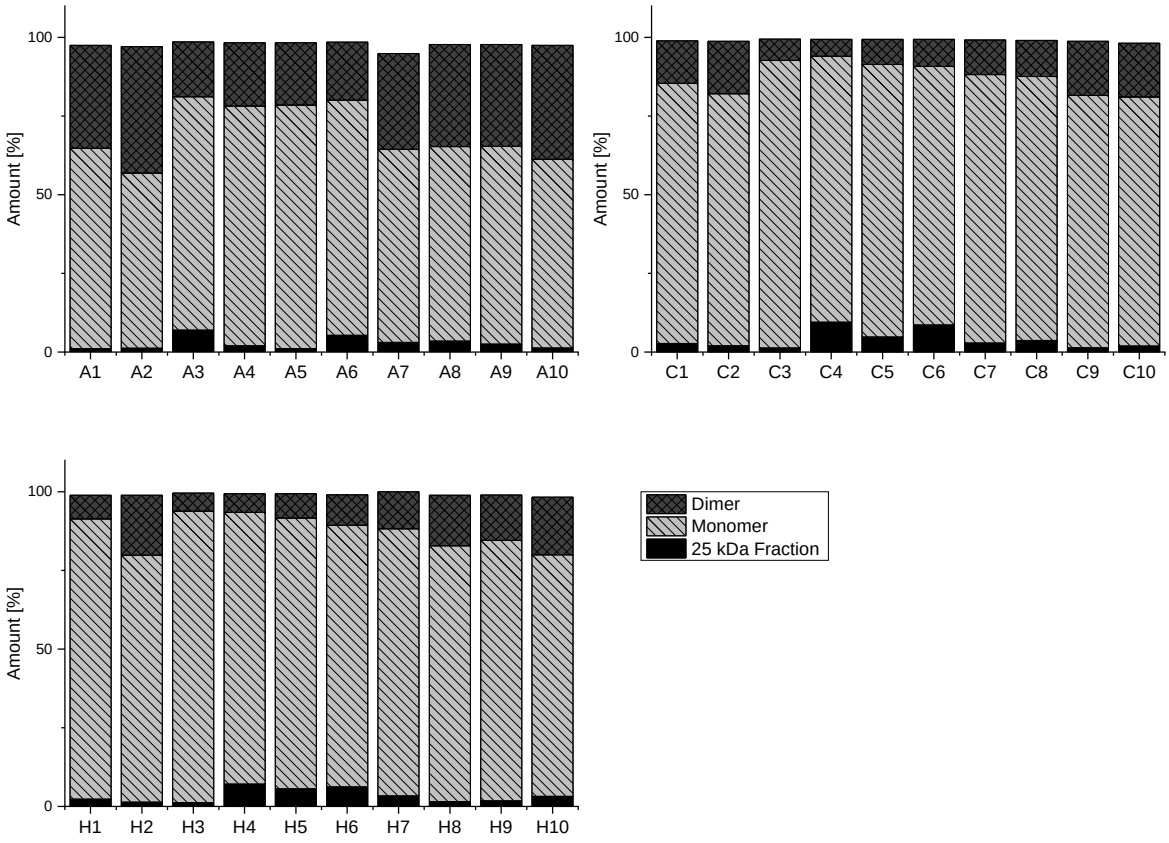

Figure 18: CE-SDS results of formulations comprised in stability study III after preparation.

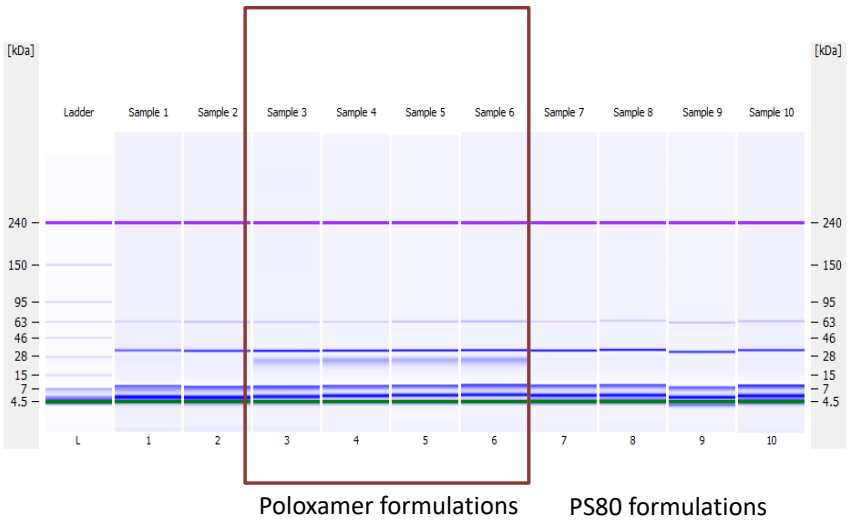

Figure 19: Exemplary densitometry plot of the CE-SDS results of HY-133 citrate formulations after preparation.

1.4.2 Chemical stability

Native HY-133 content was determined by RP-HPLC at T0 and after two weeks of storage at 40 °C. An overview of the results is shown in Table 9. At T0, a native protein content of 85 – 95% was determined in any of the formulations. In general, all formulations containing PS80 (formulations 9-12) started with slightly lower native protein contents after preparation. After two weeks of storage at 40 °C, a substantial loss of at least 30% native HY-133 was determined in all formulations. Highest native protein content was found in the three formulations variations at pH 6.0 with added Poloxamer 188, irrespective of the buffer excipient (formulations 5-8). Low and high pH variations (pH 5.0 and 6.5) showed less chemical stability and therefore higher native protein loss, irrespective of buffer and surfactant. However, the overall decrease in native protein content was highly elevated compared to the two previous stability studies using HEPES as buffer substance.

Table 9: Native HY-133 contents of formulations tested in the formulation screening III.

		Arginine		Citrate		Histidine	
pH	**Surfactant**	**T0**	**T2w**	**T0**	**T2w**	**T0**	**T2w**
5.0	-	90.8	61.1	96.6	47.8	93.1	50.9
5.5		90.4	63.8	94.4	60.6	93.8	59.9
6.0		90.9	64.9	92.6	60.0	92.0	64.0
6.5		90.3	58.1	93.4	58.4	90.9	61.3
5.0	0.1% Poloxamer 188	89.9	60.8	96.2	47.8	92.1	48.7
5.5		89.9	60.9	93.9	61.7	94.3	57.4
6.0		91.1	67.0	92.8	63.7	94.3	65.2
6.5		91.4	56.4	93.3	61.2	91.8	62.5
5.0	0.1% PS 80	91.0	61.6	94.8	53.4	87.0	48.3
5.5		89.2	60.8	93.1	58.8	90.6	51.9
6.0		92.0	61.5	92.3	61.5	92.3	58.2
6.5		92.5	59.2	91.8	61.6	90.4	53.5

1.4.3 HY-133 activity measurement

The activity of the examined formulations was determined using the FRET assay. This method results in the maximum rate of reaction (V_{max}) and K_m. Higher K_m values correspond to lower activity of the respective HY-133 formulation as the affinity to the substrate is lower.

Comparable K_m values were determined in each of the formulations at T0, with slightly higher K_m values in formulation variations without a surfactant (formulations 1+4; Figure 20). After two weeks of storage at 40 °C, K_m values substantially decreased in the majority of the formulations. This was most pronounced in all arginine formulations and in the histidine formulations with added surfactant.

Citrate formulations showed highest remaining activities amongst all formulations. Only citrate pH 5.0 (formulation C5) with Poloxamer 188 resulted in a complete loss of activity.

V_{max} of all formulations were comparable at T0 and decreased in the majority of the formulations after storage. Whereas only a slight decrease was determined in the arginine formulations, the majority of the histidine formulations showed a higher decrease in V_{max} after storage. Also, surfactant-free citrate formulations showed a high V_{max} decrease over time. In contrast, citrate formulations with added surfactant at pH 6.5 showed no change in V_{max} upon storage.

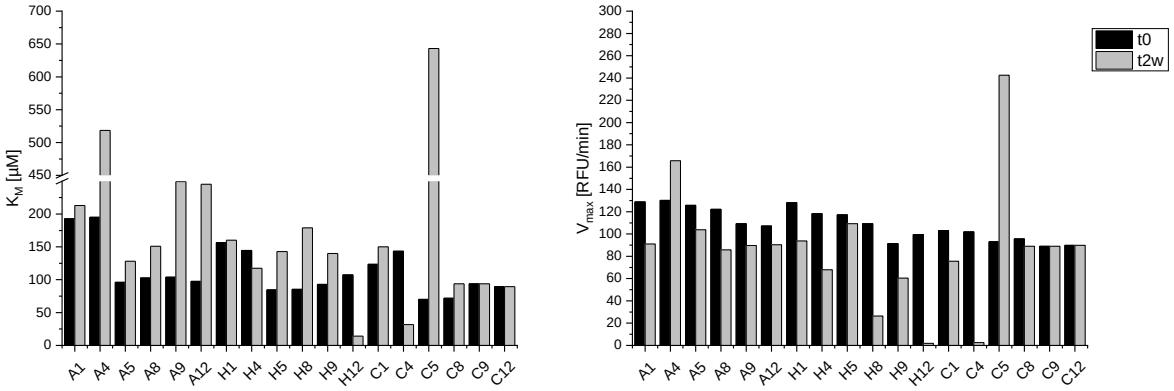

Figure 20: Activity measurements of the different HY-133 formulations in stability study III with a 2-week storage at 40 °C. Left: K_m values; right: V_{max}.

1.4.4 Summary of the third formulation screening

In summary, two different buffer substances (citrate and histidine) and a variation without an additional buffer substance (arginine only) were tested at four different pH values and two different surfactants in the third stability study. The formulations were analyzed at T0 and after two weeks of storage at 40 °C. In general, none of the formulations provided a comparably good stability as formulation #7 in the second stability study (chapter 4-1.3). The observed instabilities could be connected to the used buffer excipient. All arginine formulations showed an elevated decrease of the monomer content compared to histidine and citrate formulations, whereas chemical stability was higher in the arginine formulations than in the other two buffer variations. The overall stability was higher in formulations with a pH of 5.5 and 6.0, irrespective of the buffer substance. This clearly indicated that a very precise adjustment of the pH was needed to avoid degradation of HY-133. As arginine has no buffering capacity at the selected pH region, minor pH changes were more likely and could led to a suboptimal change of the pH value. At this pH, the side chain of arginine is mainly positively charged, due to its pK_a of 9.04 [26]. Arginine is widely known to mitigate protein aggregation without direct binding to the protein, but by preferential exclusion [27], [28]. Despite our findings, arginine itself is not enhancing the chemical stability of a protein [29]. Therefore, the increased chemical stability of the arginine containing HY-133 formulations are rather an effect of indirect

consequences connected to protein folding than due to the arginine itself. The inhere observed increased dimer count of HY-133 in the arginine formulation could be reduced by the addition of an additional buffer excipient. Histidine and citrate were selected, as both excipients are used in this pH range as buffering agents, however, not known for improving chemical stability [23]. Histidine with a pK_a of 6.04 is only half-protonated at this pH, similar to citrate with two pK_a values close to pH 6.0 [23], [26]. The trivalent citrate ion is of special interest, as stabilization of a keratoncyte growth factor was increased by direct binding of citrate due to its polyvalent character [29]. Whereas the physical stability of these formulations was not influenced in the formulations examined in here, the chemical stability of HY-133 was substantially lower compared to the pure arginine formulations. All histidine containing formulations showed similar chemical degradation profile as the citrate formulations. Histidine is an excipient with multi-purpose usage in protein formulations, as it shows some antioxidant effects next to the buffering capacities [30], [31]. There, histidine is used as an hydroxyl radical scavenger by inhibiting redox reactions activated by metal ions [32]. In here, histidine is not effective in inhibiting chemical changes of HY-133, metal-catalyzed reactions in this protein can therefore be excluded.

Thus, the chemical changes in both bi-phasic buffer systems were higher compared to the arginine buffer system. In addition, the buffer system containing also HEPES was superior to any of the examined formulations.

The addition of Poloxamer 188 led to a decrease in dimer content in all formulations. All poloxamer 188 formulations showed a species around 27 kDa, which could either be fragmented HY-133 or formulation impurities. Further experiments (LC-MS) performed by the University of Tübingen indicated that this species could be assigned to a host cell protein originating from protein expression.

The addition of PS 80 resulted in higher dimer contents and lower native protein shares. Polysorbates tend to form peroxides in the examined formulation conditions, which can subsequently lead to auto-oxidation of the surfactant or oxidation of the protein [14]. As the in here observed chemical changes of HY-133 are closely connected to the formation of dimers, the occurrence of both instabilities in all polysorbate formulations is most likely caused by peroxides originating from PS 80. Activity was comparable at T0 between the different formulations and reduced in the majority of the formulations after two weeks of storage. However, the study was subsequently discontinued due to the increased degradation of HY-133 upon storage at elevated temperatures.

1.5 Formulation screening IV

As described in the previous section, histidine and citrate buffers were surprisingly not able to stabilize HY-133 at different pH values. The initially used bulk formulation at pH 8.0 contained HEPES as a buffering agent. However, lower pH values of the bulk formulation showed an increased stability in the first and the second formulation screenings. Since only the buffer excipients were changed in these compositions, the absence of HEPES could be connected to a decreased stability of HY-133. Therefore, the role of HEPES in HY-133 formulations was further evaluated in this study. Additionally, the influence of Poloxamer 188 on the protein stability was examined further.

The following buffer was used as initial formulation buffer for the fourth formulation screening according to the previous described findings: 150 mM NaCl, 10 mM $CaCl_2$, 300 mM arginine and 10 mM methionine. As the second stability study revealed a pH < 6.2 being beneficial for the stability of HY-133, the formulation pH was set to pH 6.0 in all formulations. Five different buffering systems (Table 10) were added to the basic buffer and the protein subsequently dialyzed. HEPES, citrate and histidine were tested alone and in the presence of Poloxamer 188. To evaluate possible synergistic effects of a combination of two different buffer systems, HEPES was tested in combination with histidine and citrate, respectively, with and without Poloxamer 188.

Table 10: Formulation compositions for formulation screening IV.

#	Added buffer	Concentration	pH	Surfactant
1	HEPES	25 mM	6.0	± 0.1% Poloxamer 188
2	Citrate	15 mM		
3	Histidine	10 mM		
4	HEPES + Histidine	25 mM + 10 mM		
5	HEPES + Citrate	25 mM + 15 mM		

1.5.1 Physical stability

The results of the CE-SDS measurements are displayed in Figure 21. In general, storage at 40 °C led to higher fragmentation rates of HY-133 over time. The protein dimer content was stable over time in the majority of the formulations. Only few formulations showed a decrease in dimer content, which was accompanied with an increase in insoluble aggregates and therefore decreased protein concentration as described in the chapters above. Overall, the HEPES formulation with Poloxamer 188 showed the highest monomer content upon storage and the smallest dimer amounts and fragmentated protein. Comparing the formulation to the respective surfactant-free variation, Poloxamer 188 was especially beneficial for reducing fragmentation of HY-133.

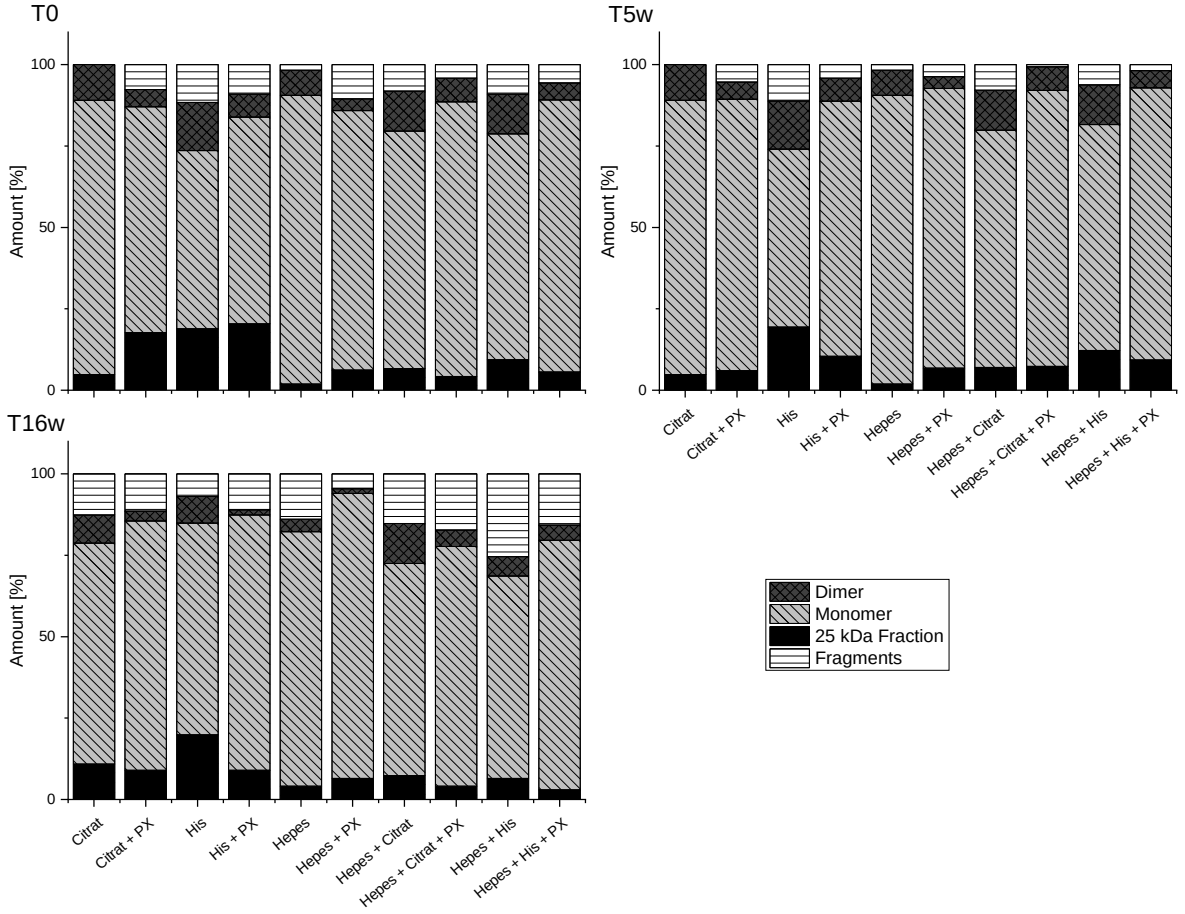

Figure 21: CE-SDS results after storage at 40°C for 5 and 16 weeks, compared to T0 upon storage at 40 °C.

Size-exclusion chromatography was developed during the 4th formulation screening and implemented for the last time point (Figure 22). The monomer content was dependent on the formulation and storage condition. In general, fragment contents were increased upon storage at 40 °C, which was accompanied with a lower monomer content. After storage for 16 weeks at 40 °C, the lowest monomer contents with less than 50% were observed in both citrate formulations. The remaining formulation variations were more stable with monomer contents of over 85%. In contrast, the monomer content of most of the formulations was maintained after storage at 4°C for 16 weeks. In all citrate and HEPES formulations and the respective combinations of these buffer substances, monomer contents of more than 98% were determined. All histidine formulations and their combinations with HEPES showed lower monomer contents of about 91-92%. In general, the addition of Poloxamer 188 had no major impact on the monomer content.

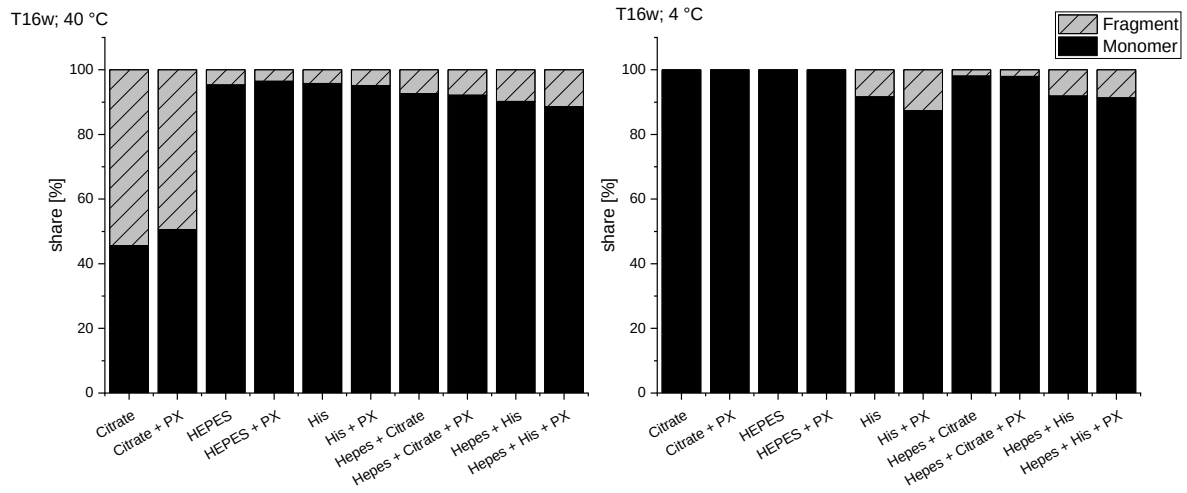

Figure 22: SEC results of the different HY-133 formulations in the formulation screening IV after 16 weeks of storage at 4 °C and 40 °C.

1.5.2 Chemical stability

The percentages of native HY-133 in the different formulations upon storage at 40 °C and 4 °C are shown in Figure 23. Native HY-133 is thereby the main peak content of the protein analyzed by RP-HPLC. Storage at 4 °C for up to 16 weeks resulted in only very minor changes in in all formulations containing HEPES. More than 98% native HY-133 was determined after this storage period. The addition of Poloxamer 188 did not influence the native protein content upon storage. Both formulations without HEPES showed a decrease in native HY-133 of up to 15%.

All HY-133 formulations showed a substantial loss of native protein content upon storage at 40 °C for 16 weeks. However, larger differences in chemical stability were determined amongst the formulations. The highest chemical stability was shown in the formulation containing only HEPES, with more than 60% remaining native protein upon storage. The associated chemical changes were slightly increased by the addition of Poloxamer 188. In general, all formulations containing Poloxamer 188 showed slightly lower native HY-133 content compared to the respective surfactant-free formulation variation.

Both two-phase buffer systems (HEPES-His and HEPES-Citrate) showed lower native HY-133 concentrations compared to the formulation containing only HEPES. Thereby, the addition of histidine resulted in about 50% lower native protein peak contents, whereas the decrease was even higher with the addition of citrate. However, pure histidine and citrate-buffer formulations showed the least stabilization of the native protein content.

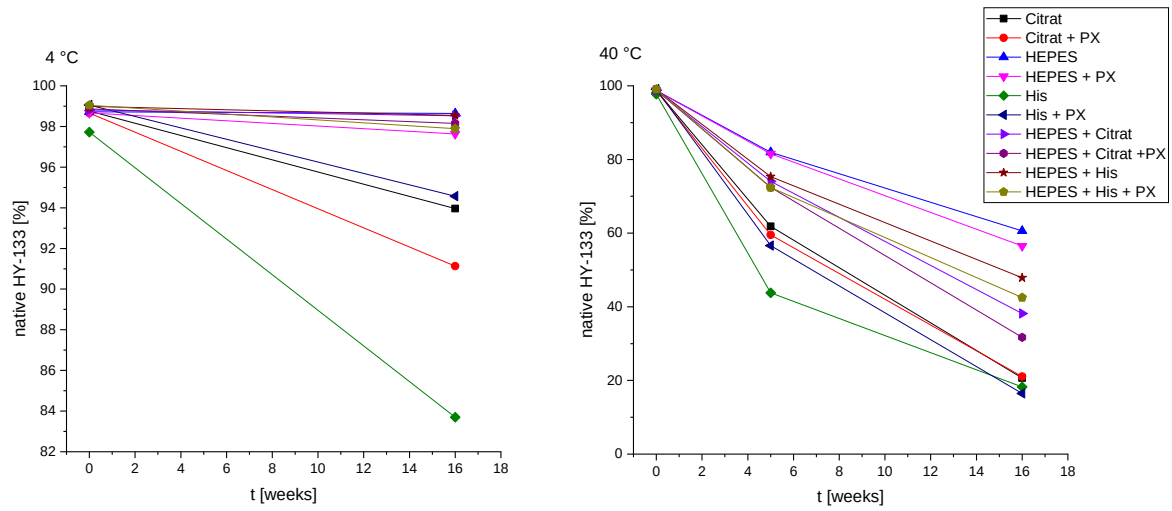

Figure 23: Native HY-133 content after storage at 4 °C for 16 weeks determined by RP-HPLC.

1.5.3 HY-133 activity measurement

K_m values upon storage at 40 °C, representing activity of HY-133, are shown in Figure 24. All formulations showed an increased K_m over storage time. This is generally associated with a loss in activity of HY-133. All formulations containing Poloxamer 188 showed lower K_m values compared to the surfactant-free variant, preserving HY-133 activities better. HY-133 activity was maintained in the formulation containing HEPES and Poloxamer 188, showing only minor deviations between the different time points. An only slight increase in K_m was determined in the bi-phasic buffer system containing HEPES and citrate with added Poloxamer 188. All remaining formulations showed substantially higher K_m values, which were highest in histidine and citrate formulations, as well as in the histidine-HEPES combination. All HEPES combinations resulted in lower K_m values and therefore in higher activities upon storage.

V_{max} varied throughout the study, with higher values in citrate and histidine formulations compared to all formulations containing HEPES, indicating less activity.

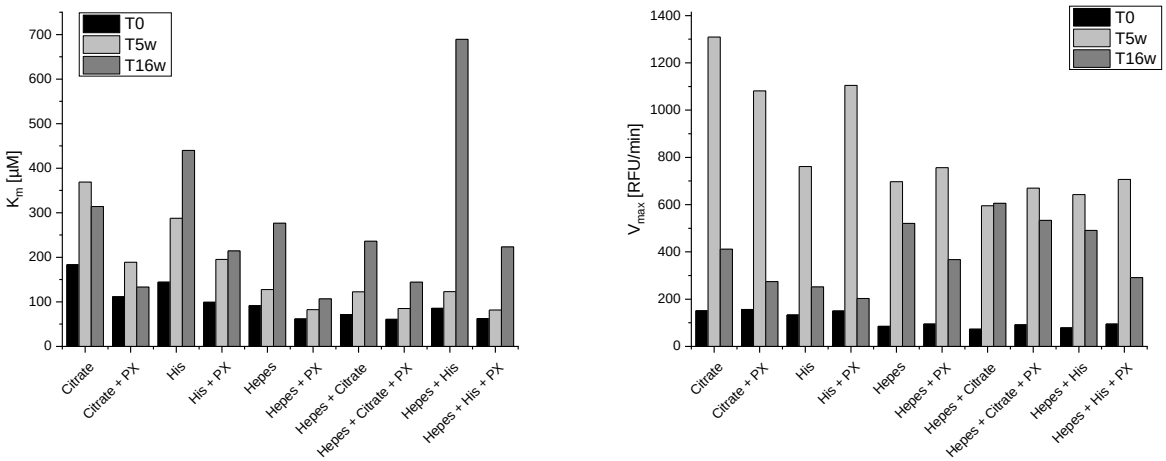

Figure 24: Activity (K_m, left) and velocity (V_{max}, right) of HY-133 in different formulation buffers after 16 weeks of storage at 40 °C.

1.5.4 Summary of the 4th formulation screening

The formulation containing only HEPES as a buffering agent showed the best performance regarding the chemically stability, the conformational stability and the activity. Adding Poloxamer 188 to this formulation had only minor effects on the chemical stability, but reduced dimerization and fragmentation of the protein. Poloxamer 188 can be used to stabilize a protein by forming protein-surfactant complexes with a lower affinity to potentially adsorb at surfaces [33]. Compared to polysorbates, already concentrations below the CMC can lead to higher colloidal stability [31]. Thus, the combination of HEPES and Poloxamer 188 was selected as final formulation. Both two-component buffer systems of HEPES and histidine or citrate, respectively, showed an increased chemical stability compared to pure histidine or citrate buffer formulations, but still lower than the pure HEPES formulation upon storage at accelerated conditions. Reduced activity was determined in pure histidine and citrate formulations. Elevated fragmentation rates were determined in both citrate formulations upon storage at 40 °C with SEC, which could be reduced by the addition of HEPES. In contrast, histidine formulations showed higher fragment contents upon storage at 4 °C, which could not be mitigated by the addition of HEPES. The final formulation of HEPES and Poloxamer 188 was therefore used within the following sections with respect HY-133 liquid formulation.

1.6 Stability of HY-133 after freeze-thaw stress

Freezing and thawing, for example overnight, might happen during scale-up and production of HY-133. Therefore, a small pre-test was performed and chemical stability of HY-133 was analyzed upon up to 3 freeze-thaw cycles. Freezing to -20 °C and -80 °C was tested in two different HY-133 formulations, the final HEPES formulation with and without Poloxamer 188. The amount of native HY-133 was measured with RP-HPLC and the results are shown in Figure 25.

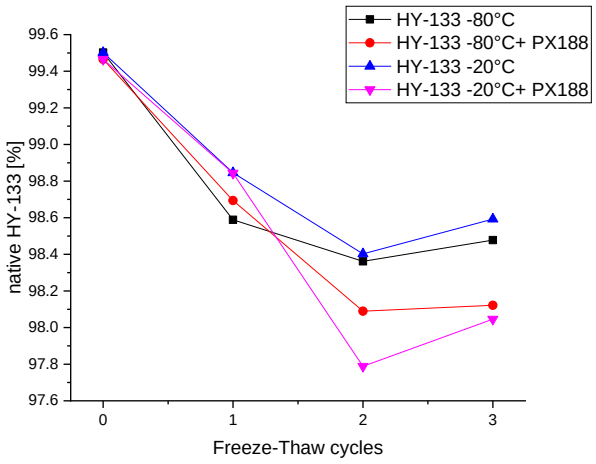

Figure 25: Native HY-133 content after 0 - 3 freeze thaw cycles.

Freezing to -20 °C or -80 °C, respectively, for up to 3 times resulted in a maximal loss of 2% native HY-133 content. Thereby, Poloxamer 188 did not influence the native protein content. Upon two freeze-

thaw cycles, the chemical degradation of HY-133 stopped and no further decrease in native HY-133 was observed. Thus, HY-133 is prone to show small chemical changes upon freeze-thaw stress and this stress condition should therefore be avoided.

2. Concentration dependency on HY-133 stability

In the first four developmental stages (formulation screenings I – IV), a reduced pH and the addition of methionine were determined to be beneficial for the protein stability. So far, the concentration was kept constant at 0.5 mg/ml HY-133. After further in-vitro studies (performed by HyPharm GmbH), a concentration adjustment to 1 mg/ml was required to allow total eradication of *s. aureus* infection in both apical and homogenate compartment. Therefore, the stability of HY-133 at higher concentrations was investigated in the selected formulation shown in Table 11. Formulations with concentrations of 0.5, 1, 2, and 4 mg/ml were stored at 4 °C and 40 °C for up to 7 months.

Chemical and conformational stability (with RP, IEX, SEC and CE-SDS), pH and concentration (UV), particle formation (FlowCam) and specific activity (FRET) were determined. In addition, T_m values of HY-133 in different concentrations were determined by nDSF.

Table 11: Final formulation composition for liquid HY-133 drug product.

Excipient	**Concentration**
NaCl	150 mM
HEPES	25 mM
$CaCl_2$	10 mM
Arginine-HCl	300 mM
Methionine	10 mM
Poloxamer 188	0.05%
pH	*6.0*

2.1 Particle formation and physical stability

Protein concentration and turbidity values were determined by UV-measurements at 280 nm and 350 nm (Figure 26). Storage at 4 °C for 4 months did not influence the protein concentration of the different concentration variations. In addition, turbidity, which was determined by scattering effects at 350 nm, was not observed within the different concentrations. The elevated storage temperature (40 °C) led to an apparent increase in concentration upon storage, which could be connected to scattering effects determined at 350 nm. Turbidity values increased, dependent on the formulation concentration, over time.

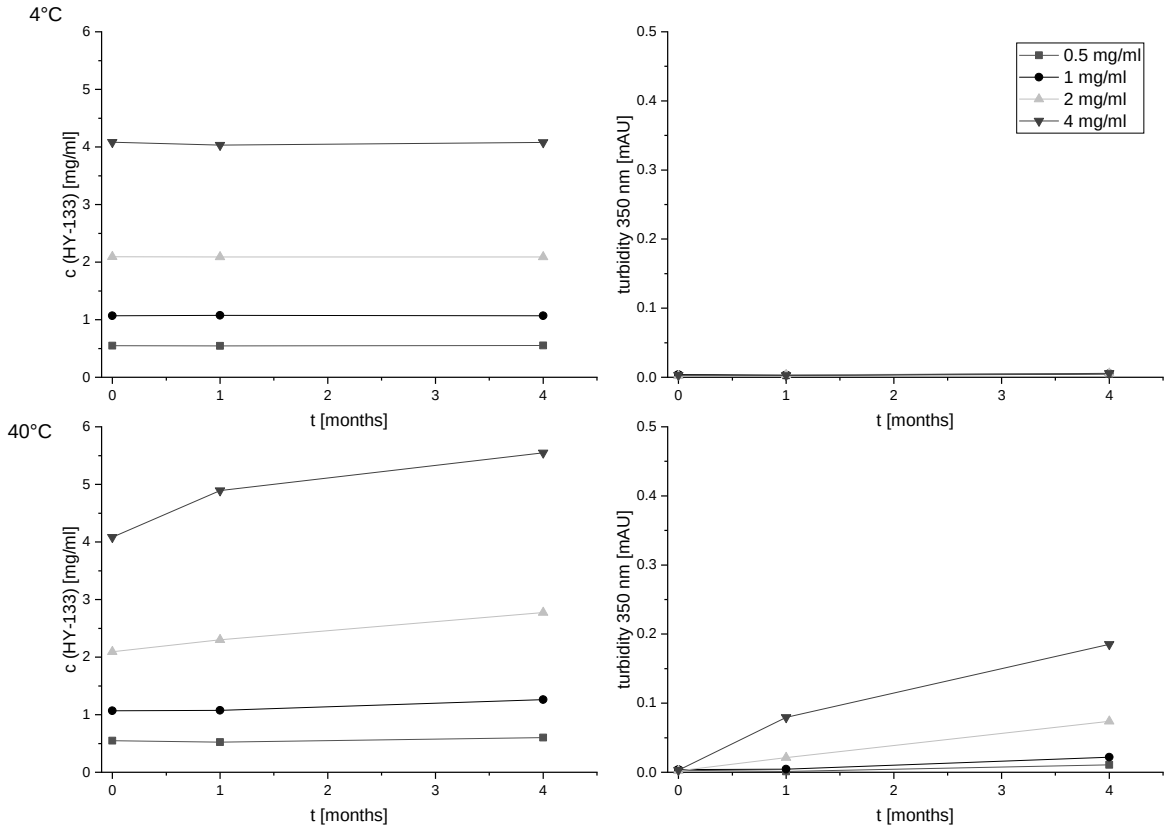

Figure 26: Concentration determination (280 nm) and turbidity determination (350 nm) of the different HY-133 concentration formulations.

Visible particles were evaluated upon storage for 1 month. All formulation variations appeared to be clear and free of visible particles upon storage at 4 °C (Figure 27, left). In contrast, storage at 40 °C led to increasing turbidity with higher concentrations. Whereas the 0.5 mg/ml variation appeared to be clear, an onset in turbidity was already determined in the 1 mg/ml variation. Visible particles were observed in the 2 mg/ml and 4 mg/ml variations.

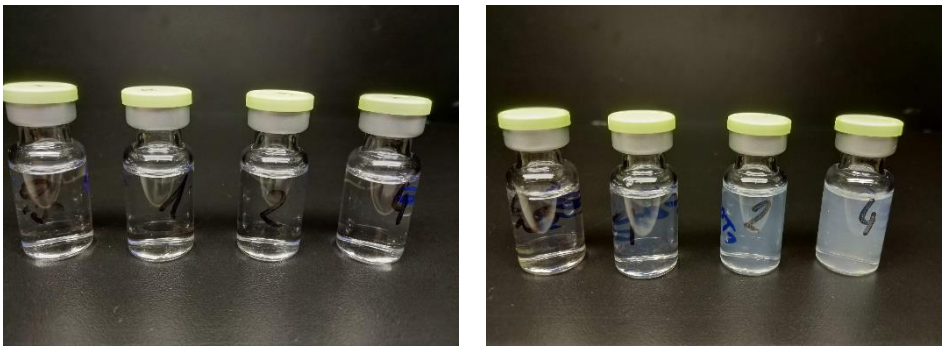

Figure 27: Optical appearance of different HY-133 concentrations after 1-month of storage at 4 °C (left) and 40 °C (right). Formulation variations from left to right: 0.5 mg/ml; 1 mg/ml; 2 mg/ml; 4 mg/ml.

Subvisible particle numbers were determined upon storage at 4 °C for 7 months and at 40 °C for 4 months. The results are displayed in Figure 28. Formulations with concentrations of 0.5 mg/ml and 1 mg/ml HY-133 showed very low numbers of subvisible particles upon storage at 4 °C for up to 7

months and an only minor increase upon storage at elevated temperatures for 4 months. Slightly higher particle numbers were determined in formulations with concentrations of 2 mg/ml and 4 mg/ml HY-133 upon storage for 7 months at 4 °C, but still in moderate level. Storage at 40 °C led to a further increase in subvisible particle numbers in these formulations. Due to the turbidity, subvisible particles could not be determined in the highest concentration of 4 mg/ml after 4 months at 40 °C. Therefore, further FlowCam measurements of formulations stored at 40 °C were dismissed.

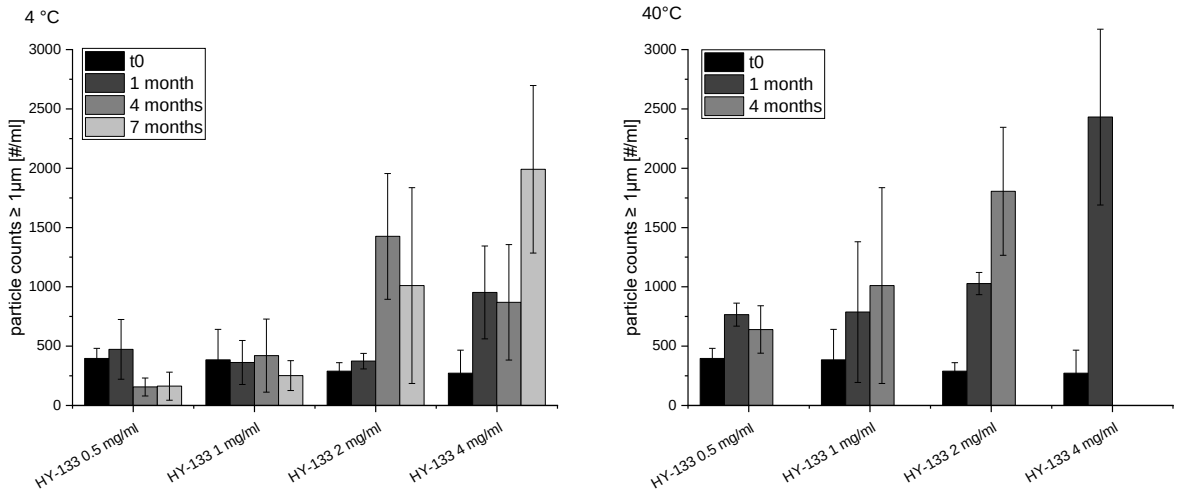

Figure 28: Subvisible particles ≥ 1 µm [#/ml] of different HY-133 concentrations upon storage at 4 °C and 40 °C up to 7 months.

Size exclusion chromatography (SEC) was used for the determination of protein recovery over time, the results are displayed in Figure 29. No differences could be detected in all samples stored at 4 °C for up to 7 months, indicating stable formulations in all four different concentrations over time. In contrast, all samples stored at 40 °C showed significant decrease in total protein amount over storage time. No differences between the different concentration variations could be determined.

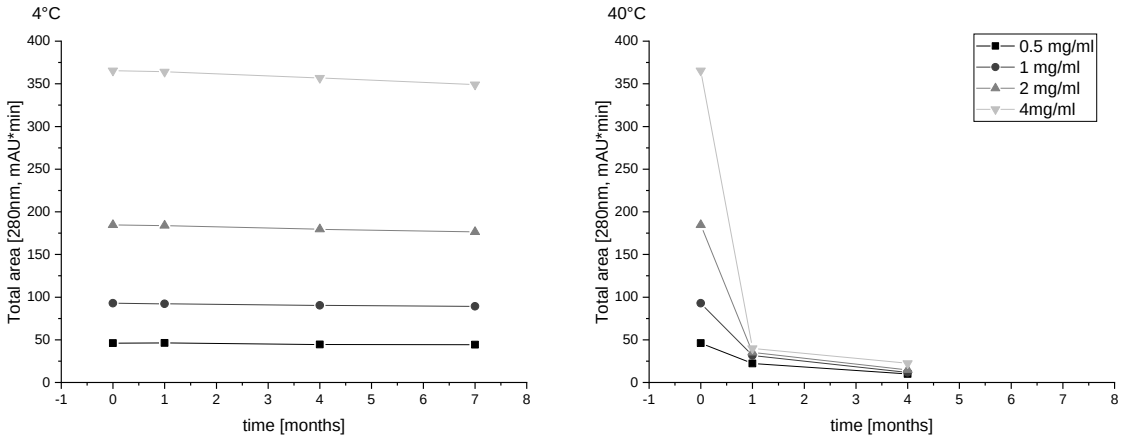

Figure 29: Total recovery of protein content of the different HY-133 presentations determined by SE-HPLC.

In addition, monomer content of HY-133 over time depending on the storage condition was monitored. The results are visualized in Figure 30. An initial monomer content of over 90% was determined in all formulation variations and did not decrease upon storage at refrigerated condition. Therefore, stability of the monomer content over 7 months of storage could be shown. Storage at 40 °C led to rapid decrease of the protein monomer over time. Higher concentrations were thereby connected to less loss in monomer content.

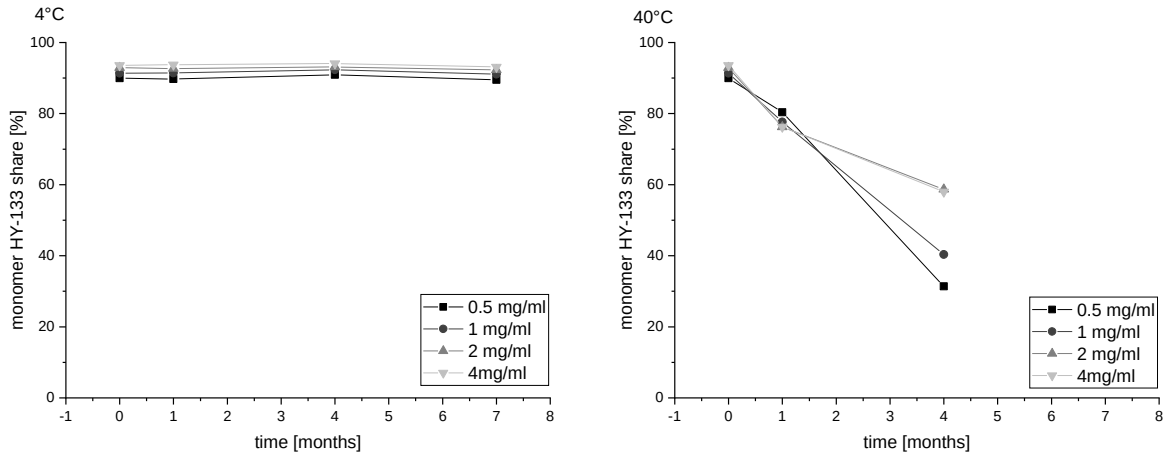

Figure 30: Monomer content of the different HY-133 presentations determined by SE-HPLC.

Storage at 4 °C led to very minor changes in lower and higher molecular weight species (Figure 31). A slight tendency towards lower LMW and larger HMW contents was determined over the course of 7 months. In contrast, storage at 40 °C showed an increase in both LMW and HMW contents. After 1 month of storage, the LMW species remained unchanged in all the formulations, except of the 4 mg/ml formulation, which showed a slightly increased LMW content. After storage for 4 months, elevated LMW contents were determined in all formulations. Here, the increase was protein concentration dependent. Higher HMW contents were already determined upon 1 month of storage, similar in the four different concentration variations. After 4 months of storage, the two lower concentrated variations showed substantially higher HMW contents, whereas the higher concentrated variations remained unchanged. In summary, the loss in main peak content was accompanied to an elevated LWM and HMW contents.

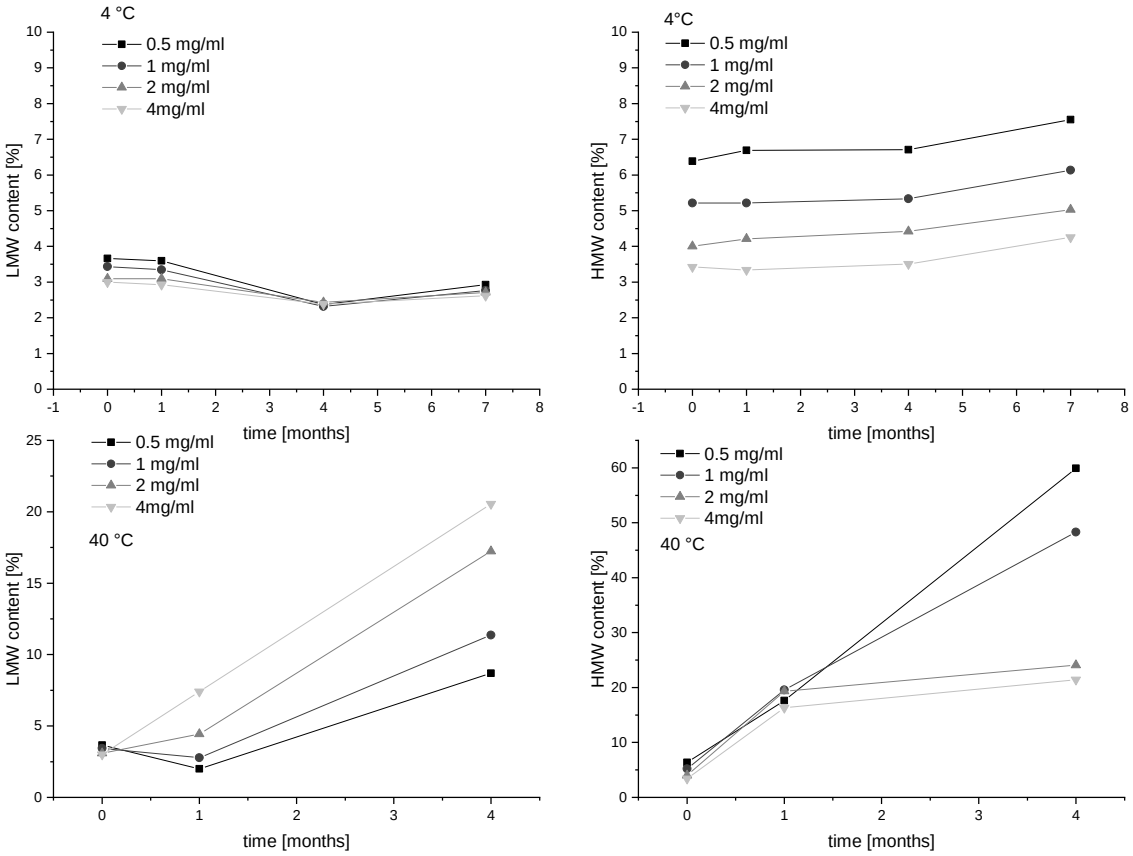

Figure 31: Lower molecular weight (LMW) content and higher molecular weight (HMW) content of HY-133 concentration variations upon storage at 4 °C (upper row) and 40 °C (lower row) determined by SE-HPLC.

Figure 32 shows T_m values of the four different HY-133 concentrations in the selected formulation. T_m values decreased slightly with higher concentrations. Thereby, the T_m value for the 4 mg/ml variation decreased to 44.5 °C, compared to a T_m value of about 46 °C for a 0.5 mg/ml formulation. Thus, lower concentrations of HY-133 were more stable in the chosen formulation according to the higher T_m values. The T_m values close to 40 °C accelerated storage temperature explain therefore the drastic decrease in HY-133 stability upon storage at 40 °C. The even more decreased T_m values for higher HY-133 concentrations clarify the stronger loss in stability at 40 °C compared to the lower HY-133 concentrations.

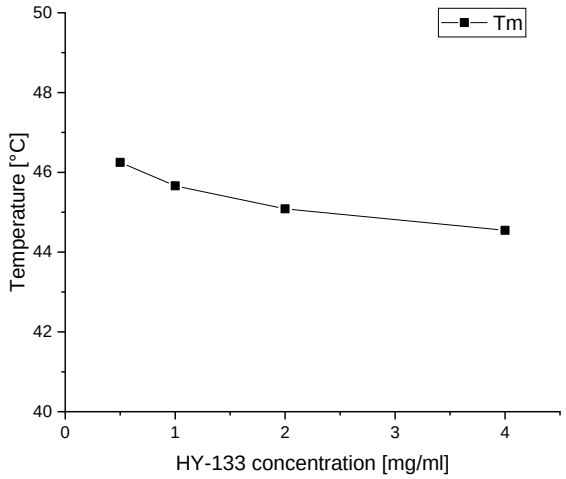

Figure 32: T_m values of concentration variants of the selected HY-133 formulation determined by nDSF.

2.2 Chemical stability

Native HY-133 content was determined by RP-HPLC, the results are shown in Figure 33. Initially, more than 95% native HY-133 were found in all samples after preparation. Storage at 4 °C for up to 7 months did not lead to a loss in native HY-133 content in any of the concentration variations. The four different concentrations did not show any difference regarding their chemical stability over storage time at refrigerated condition. In contrast, all samples stored at 40 °C showed rapid loss in native protein amount already after 1 month. The four formulations differ in the amount of degraded protein with highest degradation in the 4 mg/ml HY-133 variation and lowest protein degradation in the 0.5 mg/ml HY-133 variation. After 4 months of storage, only 20% native protein content was left in all formulation variations.

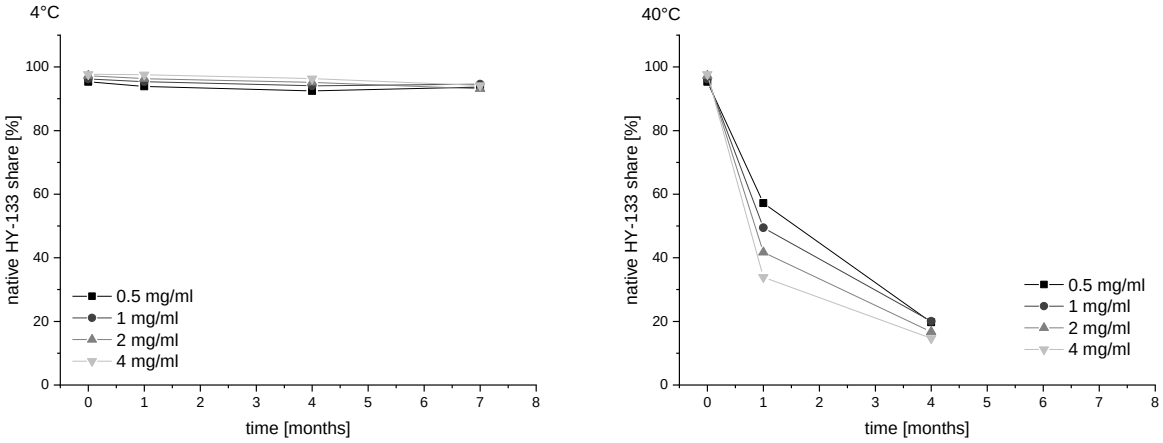

Figure 33: Native HY-133 content determined by RP-HPLC upon storage at 4 °C (left) and 40 °C (right).

2.3 Specific activity

Specific activity of HY-133 after 1 month of storage at 4 °C and 40 °C and after 7 months of storage at 4 °C are displayed in Figure 34. Storage at 40°C led to substantial reduction of the specific activity after

1 month. Thereby, the decrease was higher with higher concentrated formulations. All formulations showed a specific activity after 7 months at 4 °C. Most of the formulations showed equal activities as at T0, only the 0.5 mg/ml variation showed slightly higher specific activities.

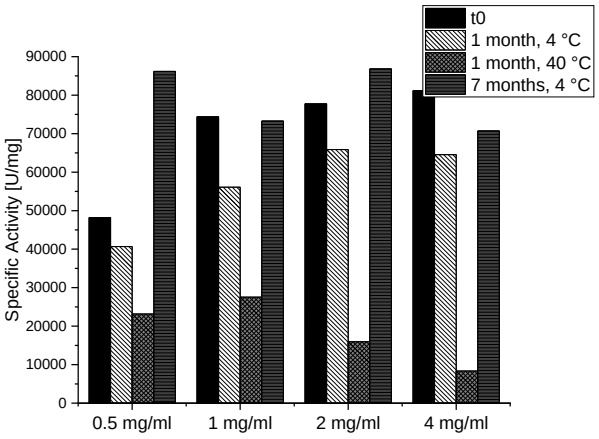

Figure 34: Specific activity of HY-133. Samples containing 2 mg/ml and 4 mg/ml were diluted to 1 mg/ml prior the test due to the test specifications.

2.4 Summary of concentration dependent stability

In summary, adequate stability of all HY-133 concentration variations was shown upon storage at 4 °C for up to 7 months. At this temperature, all HY-133 presentations showed sufficient chemical and colloidal stability, irrespective of the tested concentration. Storage under accelerated condition at 40 °C led to concentration dependent instabilities, which increased with higher protein concentrations. As T_m values showed a decrease with increased HY-133 concentrations from 46 °C to 44 °C for 0.5 mg/ml to 4 mg/ml HY-133, respectively, the concentration dependency at elevated temperatures was expected.

Therefore, storage of all tested concentration variations at refrigerated condition was recommended.

3. HY-133 stability in formulations with reduced salt contents

The so far developed formulation contained a high ionic strength, mainly originating from 300 mM Arg-HCl and 150 mM NaCl. This is connected to a hyperosmotic solution with an osmolality of 798 mOsmol/kg. As the intended route of administration is a topical application on the nasal mucosa, this high salt content could possibly irritate the nasal mucosa. Therefore, the salt content was reduced in a next step of liquid formulation development. Three different variations of the original formulation with reduced salt contents were tested in a stability study and compared to the current formulation. All formulations contained 25 mM HEPES, 10 mM $CaCl_2$, 10 mM methionine and 0.05% Poloxamer 188. These excipients were already determined to be crucial for the stability of HY-133 and were not

changed. The initial formulation further contained 300 mM arginine and 150 mM NaCl. The amount of NaCl and Arginine-HCl was modified in each formulation variation (Table 12). The protein concentration in all formulations were kept constant at 0.5 mg/ml.

Table 12: Concentrations of Arg-HCl and NaCl in each formulation variation.

Excipient	Original	Variation #1	Variation #2	Variation #3
Arg-HCl	300 mM	150 mM	0 mM	300 mM
NaCl	150 mM	75 mM	150 mM	0 mM

The measured osmolalities of the different HY-133 formulations are shown in Table 13. Arginine-HCl was determined to have the highest impact on the formulation osmolality due to the higher concentration compared to NaCl. A mix of both excipients resulted in an intermediate osmolality. Variation #2 was hereby the formulation variation resulting in values closest to isotonicity.

Table 13: Osmolalities of HY-133 salt variations.

Formulation	Osmolality [mOsmol/kg]
Original HY-133 formulation	798
Variation #1 (150 mM Arg-HCl; 75 mM NaCl)	447
Variation #2 (150 mM NaCl)	336
Variation #3 (300 mM Arg-HCl)	543

The four different formulations were stored at 4 °C and 40 °C over a period of up to 7 months. Chemical and conformational stability (with RP and SEC), development of concentration (UV), particle formation (FlowCam) and specific activity (FRET) were measured.

3.1 Particle formation and physical stability

No major differences in concentrations of the respective samples were observed upon storage at 4°C and 40°C for 4 months. Also, light scattering measured at 350 nm did not vary during the stability study (Figure 35).

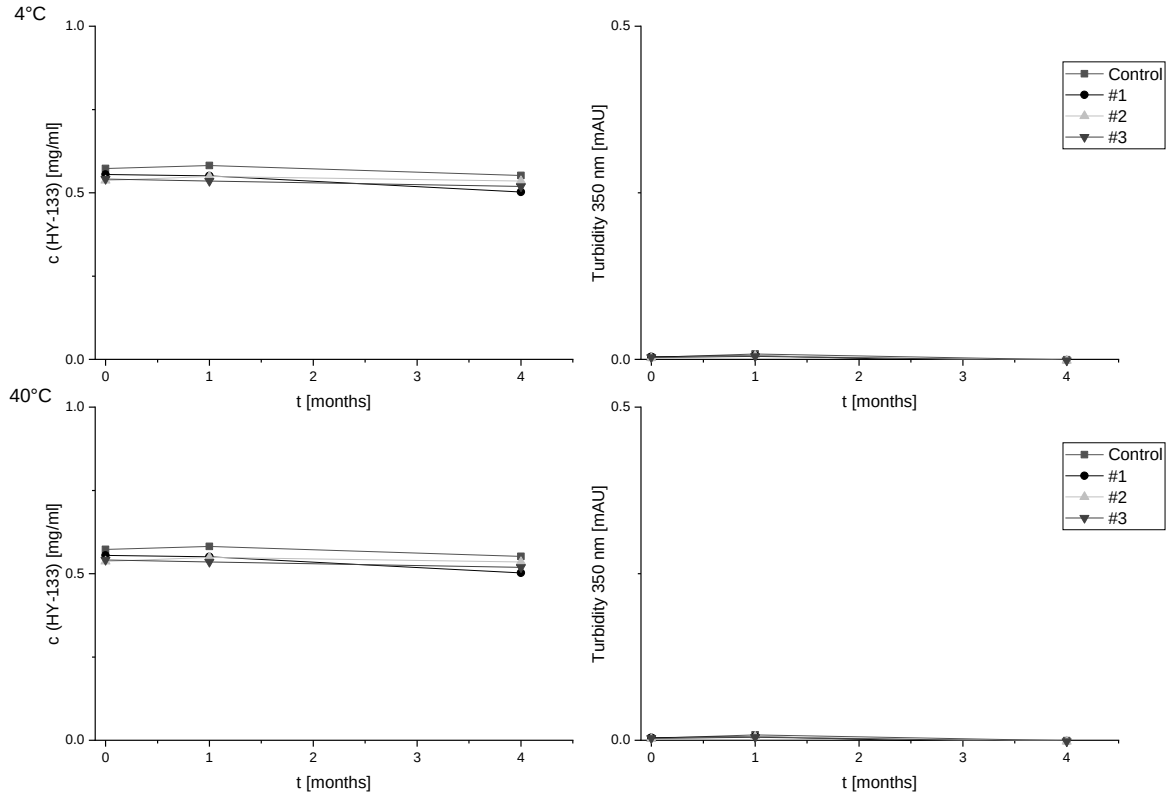

Figure 35: Determination of concentration (280 nm) and turbidity (350 nm) of the different HY-133 formulation variations.

Exemplary pictures of the corresponding samples are shown in Figure 36. All formulations were free of visible particles and did not develop any visible turbidity upon storage for 1 months, irrespective of the storage condition.

Figure 36: Visual appearance of different HY-133 salt variations after 1-month storage at 4 °C (left) and 40 °C (right).

In general, low subvisible particle counts ≥ 1 µm/ml were determined in all formulations (Figure 37). Particle numbers remained unchanged in all formulations upon storage at 4 °C for up to 7 months. Storage at 40°C led to higher particle counts in the majority of the samples over time. The overall subvisible particle counts in these samples was still low, as the particle numbers did not exceed 2,500 particles per ml.

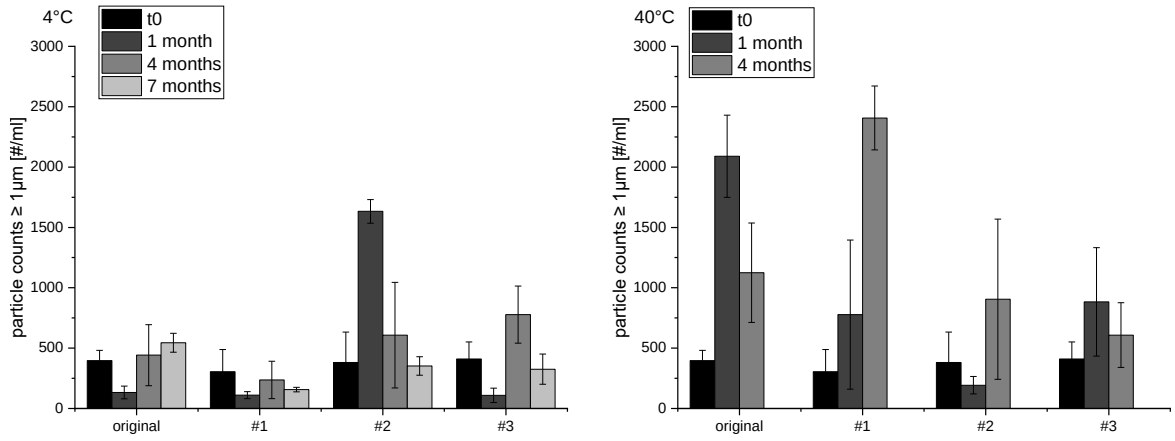

Figure 37: Subvisible particles counts ≥ 1µm of HY-133 salt variations.

SE-HPLC was used to determine the total protein recovery rate (Figure 38), the monomer content (Figure 39) and lower and higher molecular weight contents (Figure 40).

Stable total protein recovery rates were determined in all formulations upon storage at 4 °C for up to 7 months, indicating no major loss in total protein content upon storage. All formulations showed a major loss in total protein amount upon storage at 40 °C. The first variation showed the highest remaining protein content after 1 month of storage, followed by variations #2 and #3. The high salt formulation showed the highest loss in protein content after 1 month. Overall, very low protein amounts were determined after 4 months of storage, with a slight trend towards higher recovery rates of HY-133 in the first variation.

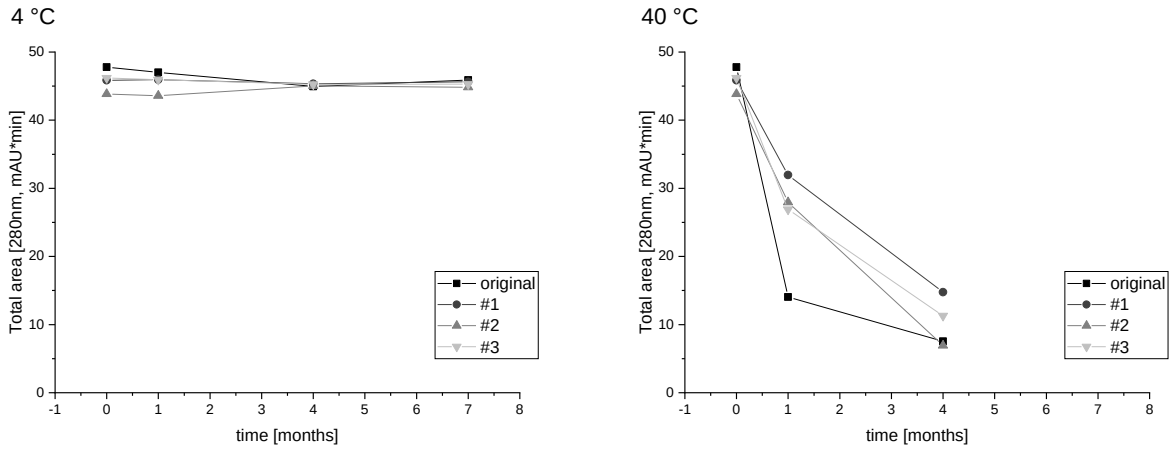

Figure 38: Total area indicating total protein recovery obtained by SE-HPLC.

Initial monomer contents at T0 were above 90% in all three variations and slightly lower in the original formulation. Monomer contents were stable of the course of the study, no differences between the formulation variations and the different time points were found. Storage at elevated temperatures

revealed no differences in monomer content after 1 month of storage and increased degradation after 4 months. Thereby, the original formulation showed the highest monomer loss and the variation #2 with only NaCl yielded in the lowest loss with more than 70% remaining monomer content.

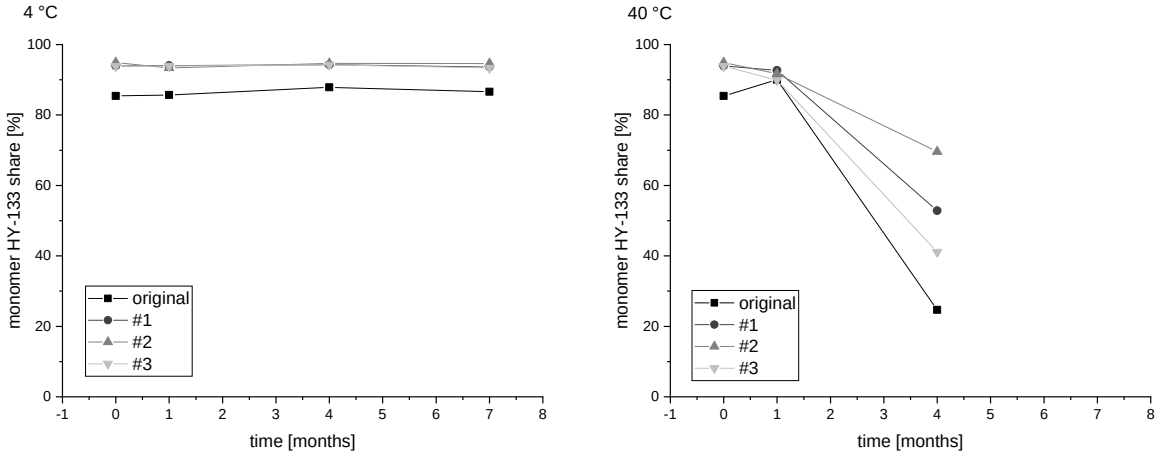

Figure 39: HY-133 monomer contents of salt variations determined by SEC.

Lower and higher molecular weight species remained stable and unchanged after storage at refrigerated conditions for up to 7 months. LMW content was comparable between the different formulations. Low HMW contents were determined in the three formulation variations, whereas slightly higher HMW contents were observed in the original formulation starting from the beginning of the study. Storage at elevated temperatures led to an increase in both LMW and HMW contents in the majority of the formulations. Only a minor increase in LMW content was observed in three salt content variations and slightly more in the original formulation. The amount of HMW were highly increased in all formulations upon storage for 40 °C. Lowest increase was thereby observed in variation #2 and highest in the original formulation.

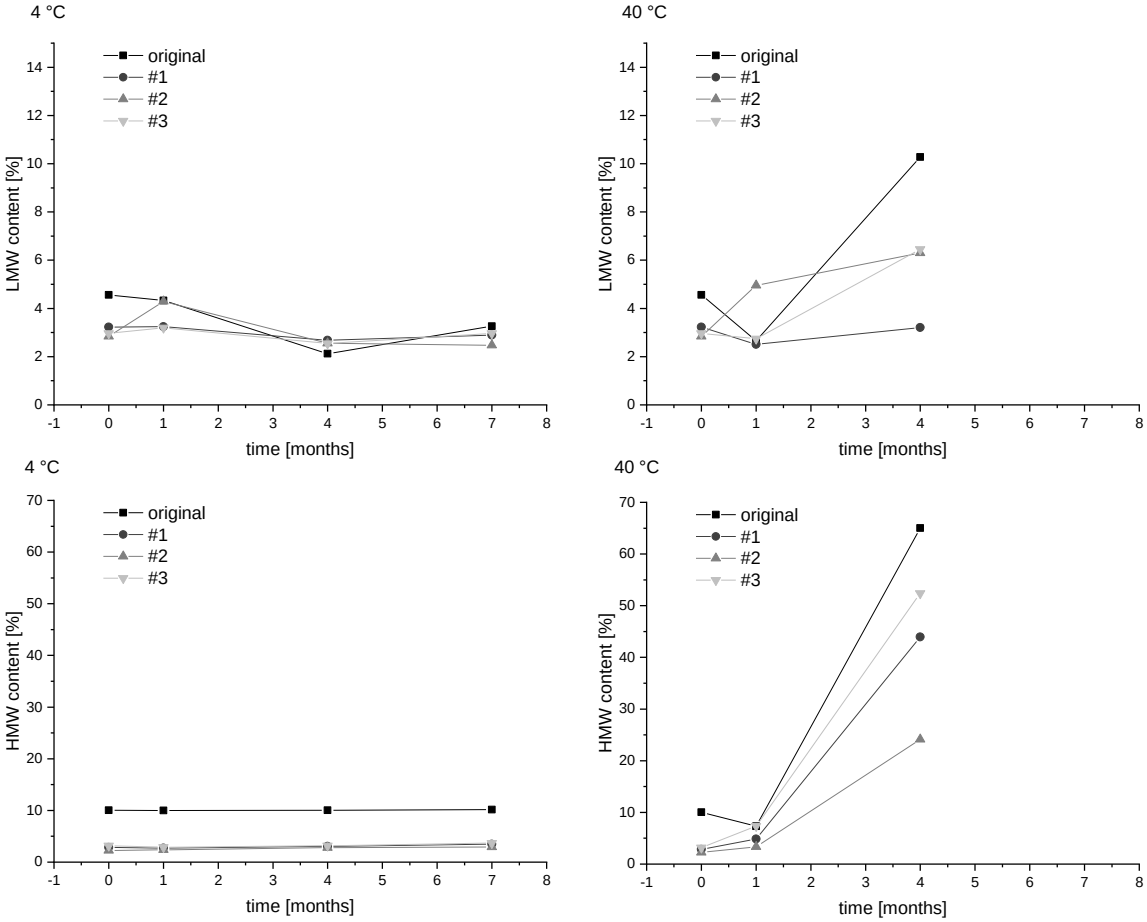

Figure 40: HY-133 LMW (top) and HMW (bottom) contents of salt variations determined by SEC.

3.2 Chemical stability

The native HY-133 amount was determined by RP-HPLC, the results are displayed in Figure 41. In general, all formulation variations of the original HY-133 formulation resulted in a slightly higher native protein amount. No differences in native HY-133 content were determined in any of the formulations upon storage at 4 °C for up to 7 months. Storage at 40 °C led to a decrease in native HY-133 in all samples, with highest degradation observed in the original formulation and reduced degradation in all three variations.

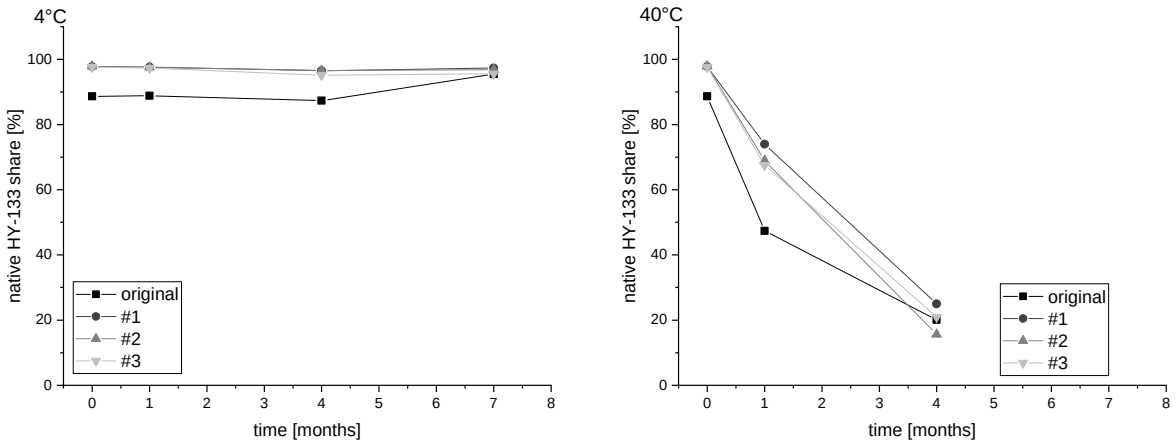

Figure 41: Native HY-133 contents of HY-133 salt variations determined by RP-HPLC.

3.3 HY-133 activity measurement

All formulations showed comparable specific activities of HY-133 after storage at 4 °C for 7 months. In contrast, the specific activity was highly reduced in the original control formulation after storage at 40 °C after 1 month. All three formulation variations showed only minor reduction of the specific activity after 1 month of storage at 40 °C.

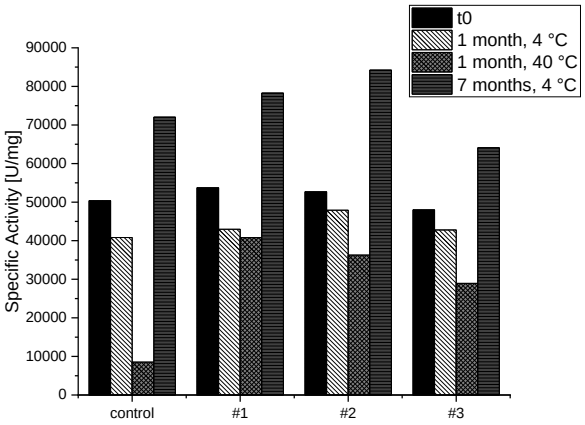

Figure 42: Specific activity of HY-133 in the different formulation variations.

3.4 Summary of HY-133 salt concentrations

In general, all three formulation variations provided adequate stability over the course of the study at refrigerated condition. Reduction of the salt content led to comparable stability as the original formulation after storage for up to 7 months at 4 °C. In fact, all salt reduced formulations showed higher initial monomer contents and higher native HY-133 share.

Compared to the high salt formulation, all salt reduced formulation variations showed higher stability of HY-133 upon storage at 40 °C. Thereby, variation #1 represented the most stable formulation in terms of chemical stability and activity. The specific activity of HY-133 could be maintained for 1 month

at elevated temperatures in variation #1. Subvisible and visible particles, as well as turbidity values were comparable in the different salt variations and the original formulation.

The aim of reducing the drastic hyperosmolality of the final formulation while maintaining or improving HY-133 stability, could be achieved with formulation variation #1. The liquid formulation development could therefore be finalized with the following composition: 25 mM HEPES, 10 mM $CaCl_2$, 10 mM methionine, 150 mM Arg-HCl, 75 mM NaCl, and 0.05% Poloxamer 188 at a pH of 6.0.

4. Stability dependence on primary packaging material

So far, all different formulations in the previous stability studies were stored in 2R fiolax glass vials with rubber serum stoppers. In general, compatibility of protein formulations with glass containers is high and well investigated. Protein adsorption to the container wall is low and gas intake reduced. However, administration into the nasal cavity comes with different challenges and vials are not the intended primary packaging materials [34]. For the administration into the nasal cavity, several possible primary packaging systems were evaluated. Some are based on glass containers and were not further examined within this study, while others are made of different polymers. In this study, the compatibility of HY-133 with the 3K system by Ursapharm was tested. These containers consist of HD-PE. In total, 2 ml of either the 0.5 mg/ml or the 1 mg/ml formulation were filled into the 10 ml bottles of this primary packaging material and analyzed upon 4 months at 4 °C and 40 °C.

4.1 Particle formation and physical stability

Overall protein concentration did not change upon storage at 4 °C for up to 4 months (Figure 43). Storage at elevated temperatures led to an apparent increase in protein concentration, which could be caused by scattering of aggregated protein. Since optical evaluation of the solution in this primary packaging system was not possible, an increase in turbidity can only be detected by scattering effects measured at 350 nm. Turbidity was constant upon storage at 4 °C. In contrast, elevated scattering values were determined in both formulations after 4 months of storage at 40 °C. This increase was concentration dependent as higher turbidity was observed in the 1 mg/ml formulation.

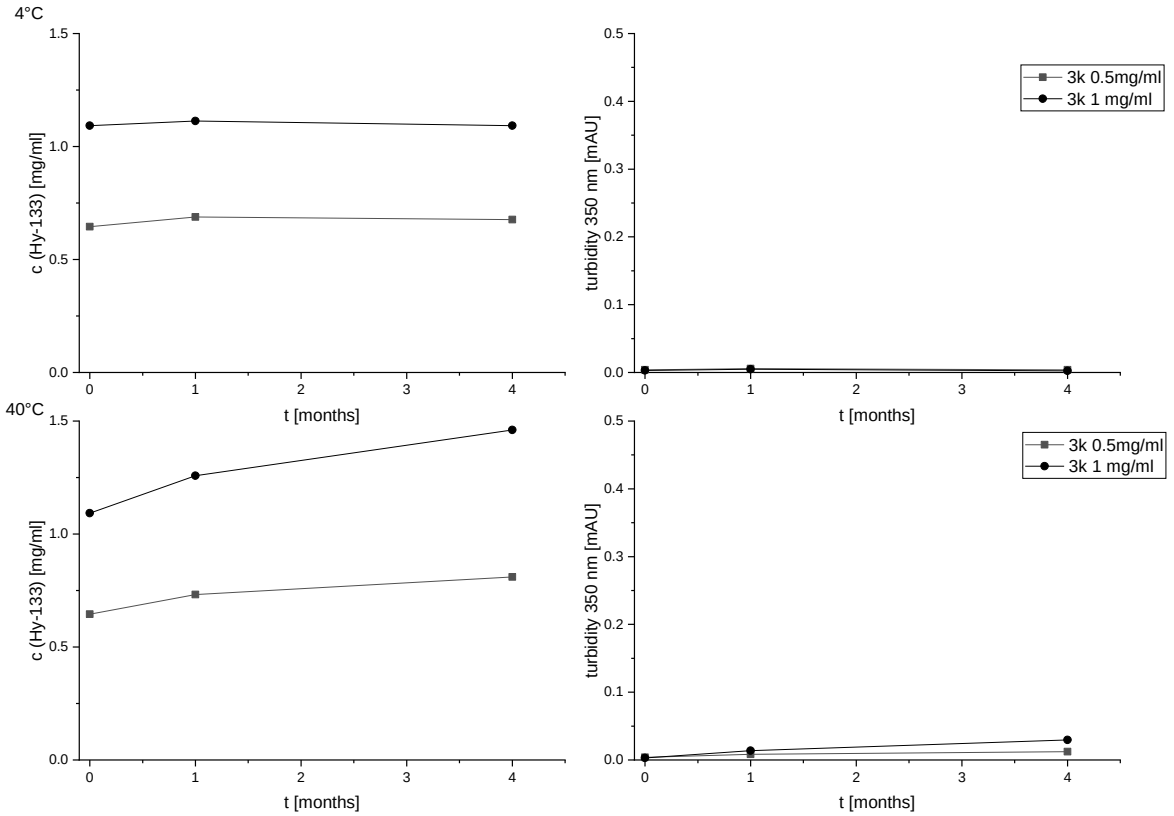

Figure 43: Determination of concentration (280 nm) and turbidity (350 nm) of the different HY-133 concentrations.

Both formulations stored in HD-PE containers showed low subvisible particle counts upon storage at 4 °C for up to 7 months and upon storage at 40 °C for 4 months. At both storage conditions, no changes in subvisible particle numbers were observed after 4 months of storage. Slightly elevated subvisible particle counts were determined in both formulations after storage for 7 months at 4 °C.

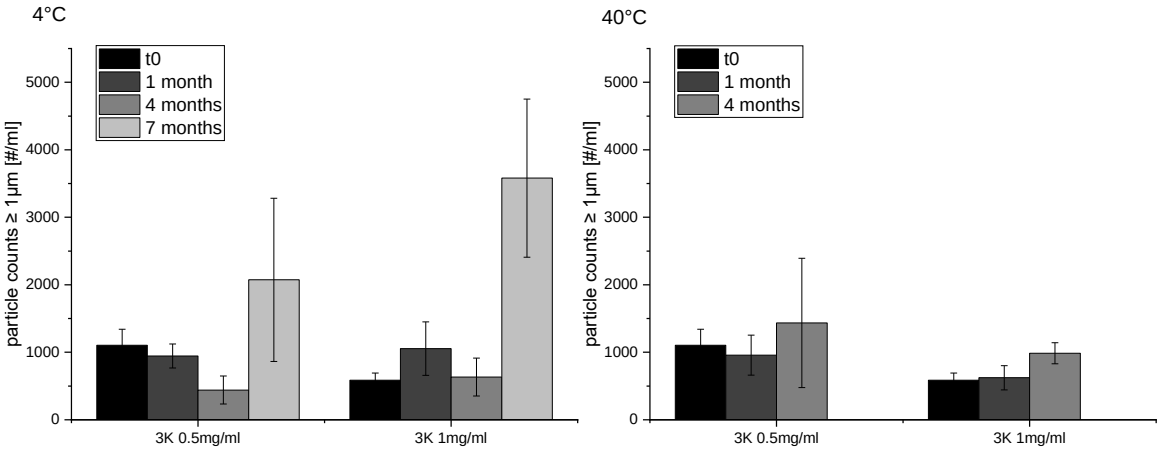

Figure 44: Subvisible particle counts ≥ 1µm of HY-133 formulations stored in 3K containers for up to 7 months.

SE-HPLC was used to determine the total protein recovery rate (Figure 45), the monomer content (Figure 46), and lower and higher molecular weight contents (Figure 47).

No changes in total protein recovery were determined in any of the formulations upon storage for up to 7 months at 4 °C. The determined protein content was highly reduced after 1 month of storage at 40 °C.

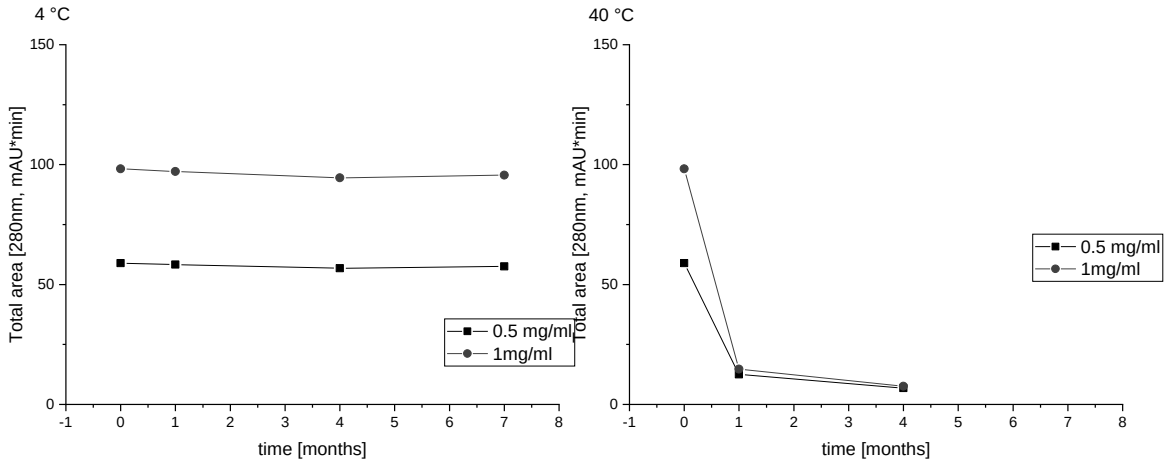

Figure 45: Total protein recovery determined by SE-HPLC.

Stable monomer content was determined upon storage at 4 °C for up to 7 months. The monomer content did not differ between the different presentations and primary packaging systems. In contrast, the monomer content was highly reduced upon storage at 40 °C for 4 months.

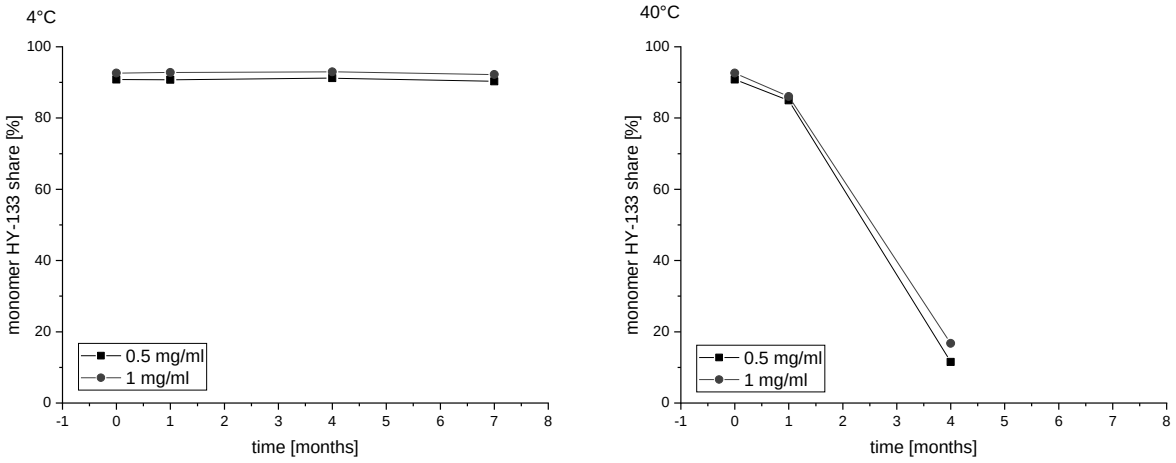

Figure 46: Monomer content of HY-133 formulations stored in 3K containers determined by SE-HPLC.

Storage at 4 °C for up to 7 months did not lead to major changes of both LMW and HMW contents in formulations stored in 3K containers. HY-133 formulations with a concentration of 0.5 mg/ml showed slightly higher HMW contents compared to the higher concentrated presentation. Storage at 40 °C led to an increase in both LMW and HMW contents, irrespective of the protein concentration. HMW increase was substantially higher compared to the increase of the LMW species.

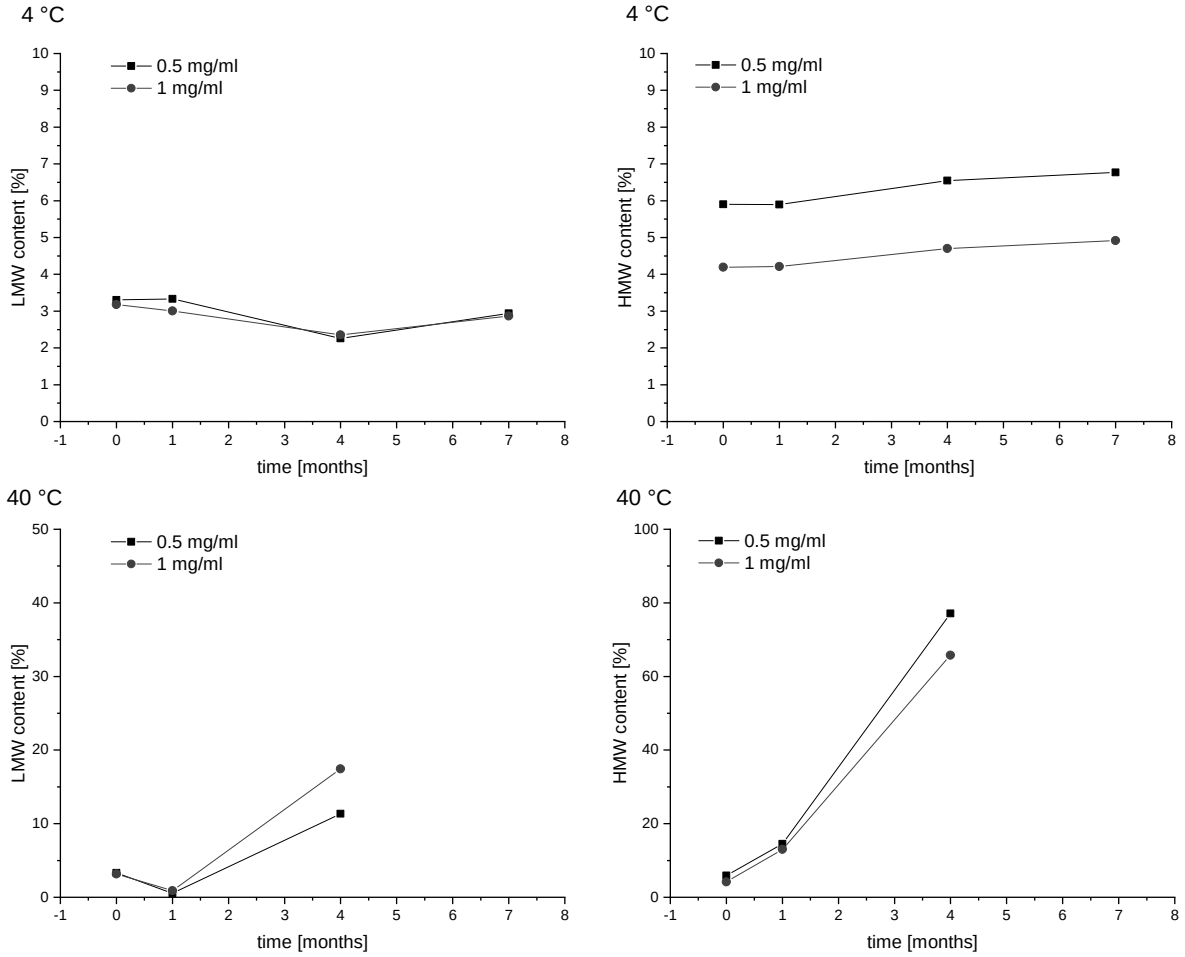

Figure 47: Lower molecular weight (LMW) species and higher molecular weight (HMW) species of HY-133 stored in 3K containers upon storage at 4 °C and 40 °C.

4.2 Chemical stability of HY-133

Native HY-133 content of both presentations remained stable over a storage time of 7 months at refrigerated conditions (Figure 48). Storage at elevated conditions led to rapid decrease in native protein content, which was comparable to formulations stored in glass vials.

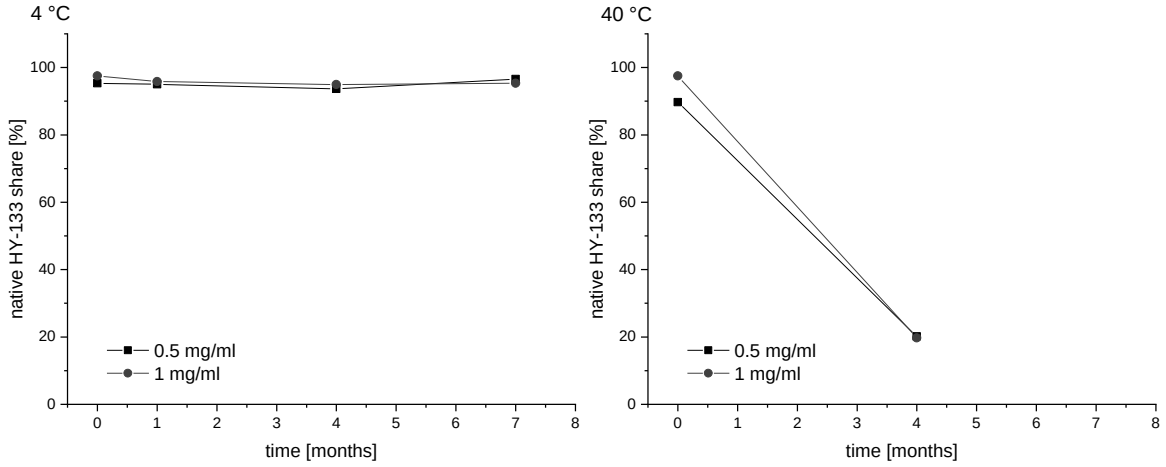

Figure 48: Native HY-133 content in HD-PE containers, determined by RP-HPLC.

4.3 HY-133 activity measurement

Specific activity was slightly reduced after 1-month storage at 4 °C and highly reduced after 1-month storage at 40 °C (Figure 49).

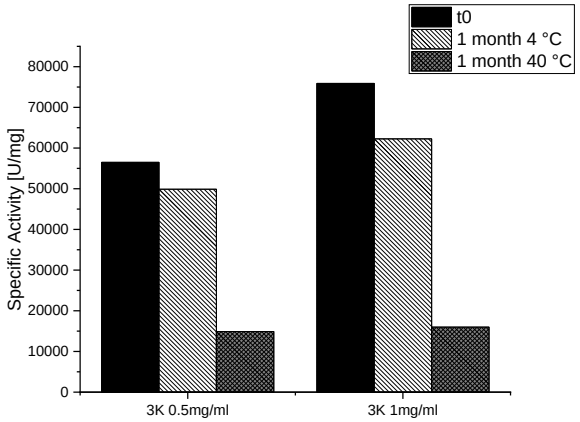

Figure 49: Specific activity of HY-133 in the designated primary packaging material.

4.4 Summary of HY-133 stability in different packaging materials

In general, physicochemical stability of HY-133 in HD-PE containers was comparable to storage in glass containers. No major differences were determined with any of the analytical methods upon storage at 4 °C over a period of 7 months. Storage at an elevated temperature of 40 °C led to major changes in chemical and colloidal stability of the protein, both comparable to similar formulations stored in glass containers. Thus, it was concluded that storage of liquid HY-133 drug product in the designated HD-PE container is also possible. However, as for the formulation stored in glass container, refrigerated storage conditions are recommended to maintain protein stability.

5. References

[1] S. Li, C. Schöneich, and R. T. Borchardt, "Chemical instability of protein pharmaceuticals: Mechanisms of oxidation and strategies for stabilization," *Biotechnol. Bioeng.*, vol. 48, no. 5, pp. 490–500, 1995.

[2] E. Vasilyeva *et al.*, "Development of a chip-based capillary gel electrophoresis method for quantification of a half-antibody in immunoglobulin G4 samples," *Electrophoresis*, vol. 25, no. 21–22, pp. 3890–3896, 2004.

[3] Z. Zhu, J. Lu, and S. Liu, "Protein Separation by Capillary Gel Electrophoresis: A Review," *Anal. Chem.*, vol. 709, no. 9, pp. 21–31, 2012.

[4] W. Wang, "Instability, stabilization, and formulation of liquid protein pharmaceuticals," *Int. J. Pharm.*, vol. 185, no. 2, pp. 129–188, 1999.

[5] S. J. Shire, *Monoclonal Antibodies*. Elsevier, 2015.

[6] W. Wang, S. Nema, and D. Teagarden, "Protein aggregation-Pathways and influencing factors," *Int. J. Pharm.*, vol. 390, no. 2, pp. 89–99, 2010.

[7] M. C. Manning, D. K. Chou, B. M. Murphy, R. W. Payne, and D. S. Katayama, "Stability of protein pharmaceuticals: An update," *Pharm. Res.*, vol. 27, no. 4, pp. 544–575, 2010.

[8] S. Frokjaer and L. Hovgaard, *Pharmaceutical Formulation Development of Peptides and Proteins*. London: Taylor & Francis, 2000.

[9] T. J. Kamerzell, R. Esfandiary, S. B. Joshi, C. R. Middaugh, and D. B. Volkin, "Protein-excipient interactions: mechanisms and biophysical characterization applied to protein formulation development.," *Adv. Drug Deliv. Rev.*, vol. 63, no. 13, pp. 1118–59, Oct. 2011.

[10] W. Wang and C. J. Roberts, "Protein aggregation – Mechanisms, detection, and control," *Int. J. Pharm.*, vol. 550, no. 1–2, pp. 251–268, 2018.

[11] C. J. Roberts, T. K. Das, and E. Sahin, "Predicting solution aggregation rates for therapeutic proteins: Approaches and challenges," *Int. J. Pharm.*, vol. 418, no. 2, pp. 318–333, 2011.

[12] C. J. Roberts, "Therapeutic protein aggregation : mechanisms , design , and control," *Trends Biotechnol.*, vol. 32, no. 7, pp. 372–380, 2014.

[13] T. A. Khan, H.-C. Mahler, and R. S. K. Kishore, "Key interactions of surfactants in therapeutic protein formulations: A review.," *Eur. J. Pharm. Biopharm.*, vol. 97, no. Pt A, pp. 60–67, Nov. 2015.

[14] A. Martos *et al.*, "Trends on Analytical Characterization of Polysorbates and Their Degradation Products in Biopharmaceutical Formulations," *J. Pharm. Sci.*, vol. 106, no. 7, pp. 1722–1735, 2017.

[15] V. Hampl *et al.*, "A Newly Identified Impurity in Polysorbate 80, the Long-Chain Ketone 12-Tricosanone, Forms Visible Particles in a Biopharmaceutical Drug Product," *J. Pharm. Sci.*, vol. 107, pp. 1552–1561, 2018.

[16] S. Uchiyama, "Liquid formulation for antibody drugs," *Biochim. Biophys. Acta - Proteins Proteomics*, vol. 1844, no. 11, pp. 2041–2052, 2014.

[17] D. A. Parkins and U. T. Lashmar, "The formulation of biopharmaceutical products," *Pharm. Sci. Technol. Today*, vol. 3, no. 4, pp. 129–137, 2000.

[18] B. K. Muralidhara and M. Wong, "Critical considerations in the formulation development of parenteral biologic drugs," *Drug Discov. Today*, vol. 25, no. 3, pp. 574–581, 2020.

[19] T. Arakawa *et al.*, "Suppression of protein interactions by arginine: A proposed mechanism of the arginine effects," *Biophys. Chem.*, vol. 127, no. 1–2, pp. 1–8, 2007.

[20] E. A. Idelevich *et al.*, "The Recombinant Bacteriophage Endolysin HY-133 Exhibits In Vitro Activity against Different African Clonal Lineages of the Staphylococcus aureus Complex, Including Staphylococcus schweitzeri," *Antimicrob. Agents Chemother.*, vol. 60, no. 4, pp. 2551–2553, Apr. 2016.

[21] M. Sanz-Gaitero, R. Keary, C. Garcia-Doval, A. Coffey, and M. J. van Raaij, "Crystal structure of the lytic CHAPK domain of the endolysin LysK from Staphylococcus aureus bacteriophage K," *Virol. J.*, vol. 11, no. 1, p. 133, 2014.

[22] S. Y. Jun *et al.*, "Antibacterial properties of a pre-formulated recombinant phage endolysin, SAL-1.," *Int. J. Antimicrob. Agents*, vol. 41, no. 2, pp. 156–61, Feb. 2013.

[23] T. J. Zbacnik *et al.*, "Role of Buffers in Protein Formulations," *J. Pharm. Sci.*, vol. 106, no. 3, pp. 713–733, 2017.

[24] M. J. Akers, "Excipient-drug interactions in parenteral formulations," *J. Pharm. Sci.*, vol. 91, no. 11, pp. 2283–2300, 2002.

[25] J. G. Moloughney and N. Weisleder, "Poloxamer 188 (P188) as a Membrane Resealing Reagent in Biomedical Applications," *Recent Pat. Biotechnol.*, vol. 6, no. 3, pp. 200–211, 2013.

[26] R. J. Falconer, C. Chan, and T. P. Munro, "Stabilization of a monoclonal antibody during

purification and formulation by addition of basic amino acid excipients," *J Chem Technol Biotechnol*, vol. 86, pp. 942–948, 2011.

[27] N. A. Kim, S. Hada, R. Thapa, and S. H. Jeong, "Arginine as a protein stabilizer and destabilizer in liquid formulations Arginine as a protein stabilizer and destabilizer in liquid formulations," *Int. J. Pharm.*, vol. 513, no. 1–2, pp. 26–37, 2016.

[28] B. M. Baynes, D. I. C. Wang, and B. L. Trout, "Role of Arginine in the Stabilization of Proteins against Aggregation," *Biochemistry*, vol. 44, pp. 4919–4925, 2005.

[29] S. Ohtake, Y. Kita, and T. Arakawa, "Interactions of formulation excipients with proteins in solution and in the dried state," *Adv. Drug Deliv. Rev.*, vol. 63, no. 13, pp. 1053–1073, 2011.

[30] S. Hada *et al.*, "Evaluation of antioxidants in protein formulation against oxidative stress using various biophysical methods," *Int. J. Biol. Macromol.*, vol. 82, pp. 192–200, 2016.

[31] V. Gervasi, R. Dall Agnol, S. Cullen, T. McCoy, S. Vucen, and A. Crean, "Parenteral protein formulations: An overview of approved products within the European Union," *Eur. J. Pharm. Biopharm.*, vol. 131, pp. 8–24, 2018.

[32] A. M. Wade and H. N. Tucker, "Antioxidant characteristics of L-histidine 11The work described in this manuscript was partially sponsored and funded by Cytos Pharmaceuticals, LLC.," *J. Nutr. Biochem.*, vol. 9, no. 6, pp. 308–315, 1998.

[33] H. L. Kim, A. McAuley, B. Livesay, W. D. Gray, and J. McGuire, "Modulation of protein adsorption by poloxamer 188 in relation to polysorbates 80 and 20 at solid surfaces," *J. Pharm. Sci.*, vol. 103, no. 4, pp. 1043–1049, 2014.

[34] P. G. Djupesland, "Nasal drug delivery devices: Characteristics and performance in a clinical perspective-a review," *Drug Deliv. Transl. Res.*, vol. 3, no. 1, pp. 42–62, 2013.

Chapter 6

Stabilization of a novel recombinant bacteriophage endolysin by protein-excipient interaction with HEPES and other Good's buffers

Simon Eisele, Carolin Berner, Gerhard Winter

Department of Pharmacy, Pharmaceutical Technology and Biopharmaceutics, Ludwig-Maximilians-Universität München, Munich, Germany

Author statements: Conceptualization: SE, GW; Experiment design: SE, GW; Methodology: SE; CB Investigation: SE, CB; Data analysis: SE, CB; *In silico* investigation: CB; Visualization: SE, CB; Writing- Original draft: SE, GW; Writing- Review & Editing: SE, CB, GW; Resources: SE, CB, GW

The study presented in this chapter was conducted as part of a collaborative work between the authors. Simon Eisele investigated the stabilizing effect of the Good's buffers by physicochemical characterizations, whereas Carolin Berner investigated and performed the *in silico* study. The scope of the study can be considered as the continuation of the research presented in Chapter 5, hence it was included in this thesis. This chapter is in preparation for submission as a manuscript.

Table of Contents

1. Abstract

The novel antibacterial drug HY-133 is a recombinant bacteriophage endolysin which specifically targets various *staphylococcus aureus (S. aureus)* strains. As chemical degradation was found to be a major issue in early development phases, different buffer excipients were evaluated for their stabilizing effect and HEPES was found to be the most stabilizing one. Commonly used buffers for biopharmaceutics like citrate or histidine buffers at pH 6.0 did not lead to equally stabilized formulations. So far, HEPES is commonly used in drug substance upstream processes but rarely in drug product formulations. It was shown that HEPES rapidly binds to the protein without changing the light scattering second virial coefficient (A_2), which was determined by homo- and heteroassociation CG-MALS experiments. With HEPES belonging to the Good's buffer series, the influence of structurally similar excipients such as POPSO, MES, MOPS, PIPES, and EPPS was analyzed and compared to a buffer composition without any of these piperazinic or morpholinic derivatives. HEPES and its derivatives increased the protein's conformational and chemical stability. All investigated Good's buffers were able to increase the T_m values and further increased chemical stability upon storage for 16 weeks compared to a buffer free formulation. The investigated zwitterionic N-substituted aminosulfonic acids behaved similarly. Because HEPES is already used in protein expression, the need for a final buffer exchange to obtain the drug product might be redundant.

2. Introduction

The successful development of therapeutic proteins depends on the design of stable and robust formulations to sustain stability of the drug product during shelf life. Reduced protein stability can lead to a loss of efficacy and potency, and also to harmful effects like enhanced immunogenicity [1]. Therefore, potential chemical and physical protein instabilities are addressed by the adaption of the formulation composition during drug product development [2]. Oxidation of proteins is often reduced by the addition of antioxidants, such as methionine [3]. Deamidation is another typical degradation pathway of proteins and can often be reduced by pH adaption [4]. In addition, the pH has an impact on the protein colloidal stability by changing the charge distribution on the protein surface and thereby affecting the protein-protein interactions in solution [5]. These can further be mitigated by the addition of salts, specifically anions of the Hofmeister salt series [6],[7].

Furthermore, changes in the conformation or partial unfolding of the protein can lead to loss in activity and non-native aggregation [8]. Various excipients like specific ligands, amino acids, buffers and osmolytes are commonly used to increase the conformational stability [7]. The selection is usually limited to excipients that are well characterized to avoid further safety and efficacy study examinations [9]. The excipients either stabilize the conformation of the protein by preferential exclusion or by

preferential binding to the native state of the protein [2], [10]. Preferential exclusion is usually achieved with high concentrations of sugars, polyols or amino acids [5]. In contrast, excipients that preferentially bind to the protein with a certain affinity are applied in lower concentrations [10]. While protein-excipient binding can enhance protein stability when the interaction is weak and transient, stronger-interacting excipients were found to mostly destabilize proteins [11]. Moreover, the binding needs to be reversible to assure the proteins therapeutic efficacy after administration.

Since excipient effects are protein specific, finding the optimal excipients to achieve a stable drug product is generally done using a trial-and-error approach. However, there have been recent approaches to apply computational tools in the context of formulation design. A virtual screen has been presented that could identify new compounds which bind to predicted aggregation hotspots, thus inhibiting protein-protein interactions [12]. Furthermore, molecular dynamics (MD) simulations are now commonly used to study proteins in the presence of excipients to identify the local effects on the proteins. Thus, the mechanisms by which certain excipients, for example a dipeptide [13], arginine [14], arginine-salts [15], cyclodextrins [16] and surfactants [17] stabilize proteins have been elucidated.

Whereas larger proteins like monoclonal antibodies and antibody-drug-conjugates (ADCs) are rather well characterized, the stabilization mechanisms for new, structurally variable proteins must be examined on an individual basis. Here, we present a combined study of experimental and computational approaches on the stabilization of the novel antibacterial drug candidate HY-133, a bacteriophage lysin which specifically targets various *S. aureus* strains. The drug substance is a recombinant chimeric lysin with two functional modules: an enzymatic active domain (EAD) and a cell wall binding domain (CBD) which are linked via a synthetic peptide linker (Figure 1). Analysis of the electrostatic and hydrophobic surface properties reveal negatively and positively charged surface patches in both domains and a large hydrophobic patch in the CB domain. These properties make HY-133 not only prone to intermolecular interactions but also to inter-domain interactions which brings additional challenges to the development. Both domains can be varied according to the drug substance's intended specificity. Topical administrations of HY-133 in the nasal cavity and on the skin is intended.

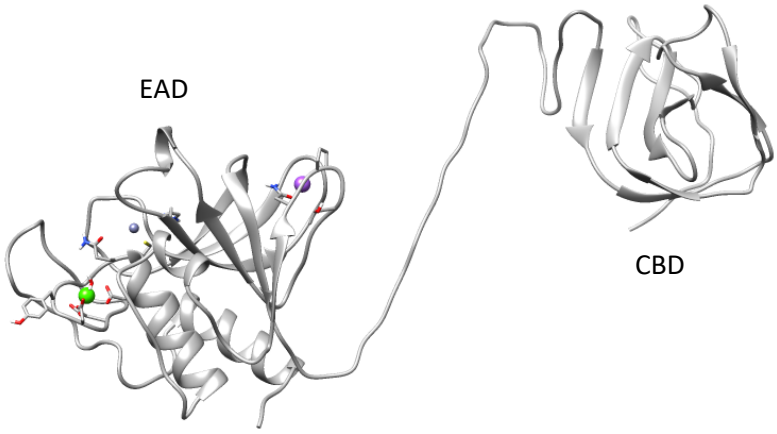

Figure 1: Homology model of HY-133 with the enzymatic active domain (EAD) from the endolysin of phage K (PDB code: 4CSH) and the cell wall binding domain (CBD) from lysostaphin (PDB code: 4LXC) with bound ions.

Early development phases revealed chemical degradation as a critical parameter of HY-133. However, a pH of 6.0 and methionine as antioxidant could maintain the protein's chemical stability in combination with a HEPES buffer. In addition, Poloxamer 188 effectively increased the colloidal stability. We furthermore found that the buffer substance N-2-hydroxyethylpiperazine-N'-ethanesulfonic acid (HEPES) had an advantage over the commonly used buffer systems citrate and histidine at the same pH. HEPES is part of the Good's buffers family, which was developed in 1966 by Good et al. with the background of providing highly water soluble buffer systems in the physiological pH range [18]. It belongs to the piperazinic subgroup and has wide structural similarities with piperazine-N,N′-bis(2-hydroxypropanesulfonic acid) (POPSO). Whereas 2-(N-morpholino)-ethanesulfonic acid (MES) and 3-(N-morpholino)propanesulfonic acid (MOPS) belong to the morpholinic subgroup, they all share the N-substituted aminosulfonic acid. The zwitterionic character of these substances provides adequate buffer capacities between pH 5.5 and 8.5 [19]. Interestingly, it has been shown that the addition of these buffers in high concentrations, in particular HEPES, can stabilize the native structure of BSA [20], sustain the activity of G-CSF [21], and increase the stability of RecA [22]. However, HEPES is not widely used in drug product formulations, despite being frequently used in protein expression. As a rare example, the smallpox vaccine ACAM200 contains HEPES as a buffering agent [23].

To gain a deeper understanding of the stabilizing effect, the interaction of the protein and HEPES was analyzed by CG-MALS. Moreover, we performed MD simulations to elucidate the stabilizing effect of HEPES on HY-133 at atomistic detail. Here, we determined HEPES-interaction sites, the strength of these interactions and what impact the binding has on the protein structure. HEPES and histidine were both found to interact with the charged and aromatic side chains of surface exposed residues via salt-bridge formation and cation-π interaction. The simulations also showed that the EAD and CBD tend to

interact in the absence of the excipient which is prevented by the binding of HEPES but not histidine. This self-interaction gives an indication about the mechanism of protein-protein interaction and aggregation.

3. Materials and methods

3.1 Protein and chemicals

The bacteriophage lysin HY-133 was produced by HyPharm GmbH, Bernried, Germany, in a concentration of 5 mg/mL at pH 8.0. The protein was dialyzed using a Spectra/Por dialysis membrane with a molecular weight cut-off of 10 kDa (SpectrumLabs) and a 4-fold buffer exchange to achieve the basic, buffer-free formulation. The formulation contained 0.5 mg/mL HY-133, 10 mM $CaCl_2$ and 10 mM methionine (both from Merck KGaA, Darmstadt, Germany), 150 mM NaCl (Bernd Kraft, Duisburg, Germany), 300 mM arginine hydrochloride (AppliChem PanReac) and 0.05 % Poloxamer 188 (Kolliphor 188, BASF, Ludwigshafen, Germany) at a pH of 6.0. HEPES (VWR International, Ismaning, Germany), MES, MOPS, POPSO, PIPES, EPPS (all from Sigma Life Science) citrate and histidine were spiked to the buffer-free formulation to achieve a final concentration of 25 mM, respectively, and the pH was adjusted thereafter. All chemicals were of molecular biology or multi compendial grade. Prior to use, all formulations were filtrated with 0.2 µm PVDF membrane syringe filters (VWR International).

3.2 Reversed phase high pressure liquid chromatography (RP-HPLC)

An Ultimate 3000 system (Thermo Fisher, Dreicheich, Germany) and a Jupiter C4, 5 µm 300A, 250 x 4.6 mm column (Phenomenex, Torrence, USA) were used for RP-HPLC. Protein detection was performed by fluorometric detection at 280/343 nm. The column oven temperature was set to 37 °C. Mobile phase A consisted of 10% acetonitrile and 0.1% triflouroacetic acid in highly purified water. 100% acetonitrile with 0.1% triflouroacetic acid were used as mobile phase B. A stepwise gradient with a flowrate of 1 ml/min for 22 min was applied, 10 µl of each sample was injected.

3.3 Ion exchange chromatography (IEX)

A Dionex Summit system (Thermo Fischer) with a ProPac WCX-10 BioLC Analytical 4x250 mm column with an attached column guard ProPac WCX-10G (Thermo Fisher) was used for ion exchange chromatography (IEX). 50 mM Tris buffer pH 8.0 (mobile phase A) and mobile phase A plus 300 mM NaCl (mobile phase B) were used as a stepwise gradient with a flowrate of 1 ml/min for 60 min. All samples were diluted 1:10 with highly-purified water prior to injection, 100 µl of each sample was injected. A fluorescence detector (280/343 nm) was used to detect the analyte variants.

3.4 Size exclusion chromatography (SEC)

An Ultimate 3000 system (Thermo Fisher) with a GE Superdex 75 Increase 10/300 GL column (General Electric, Boston, MA, USA) was used for size exclusion chromatography. A filtered buffer solution containing 50 mM Na_3PO_4 and 300 NaCl in highly purified water at pH 7.0 was used as a mobile phase at a flow rate of 0.5 ml/min for 45 min. Detection was performed with a UV-detector at 280 nm. The injection volume was 50 µl. A gel filtration standard (#1511901, Bio-Rad Laboratories, Hercules, CA, USA) was used for regular column tests.

3.5 Subvisibile particle analysis (FlowCam)

Subvisible particles were analyzed using a FlowCam 8000 with an attached 10x magnification cell (Fluid Imaging, Scarborough, USA). Triplicates of 200 µl samples were analyzed at a flowrate of 0.15 ml/min. Particles were defined by a dark segmentation threshold of 10 and a light segmentation threshold of 13.

3.6 Intrinsic differential scanning fluorimetry (nanoDSF)

NanoDSF was used to study the thermal unfolding of HY-133 with different excipients. The samples were filled in standard glass capillaries. A Prometheus® NT.48 (NanoTemper Technologies, Munich, Germany) was used with a ramp of 1 °C/min from 25 °C to 95 °C. Intrinsic protein fluorescence intensity at 330 nm and 350 nm was measured after excitation at 280 (± 10) nm. Back-reflection intensity was measured to detect protein aggregation and precipitation. The fluorescence ratio (FI350/F330) was used to determine protein thermal unfolding, calculated by PR.ThermControl V2.1 software (NanoTemper).

3.7 Circular dichroism (CD) spectroscopy

A Jasco J-810 spectrometer (Jasco Deutschland GmbH, Pfungstadt, Germany) was used to obtain near-UV circular dichroic spectra. Quartz cuvettes (Hellma GmbH, Muellheim, Germany) with 10 mm pathlengths were installed and measurements were performed with 10 accumulations per sample at a scanning speed of 20 nm/min. Each spectrum was buffer subtracted and curve smoothing was performed using the Savitzky-Golay algorithm with 7 smoothing points. For each sample, the molar ellipticity was calculated according to [24]. The molecular weight of the HY-133 was 31,045.8 Da.

3.8 Composition-gradient multi-angle light scattering (CG-MALS)

Homo-association experiments by CG-MALS were performed with 0 – 10 mg/ml HY-133 in the basic formulation at pH 6.0 with and without 25 mM HEPES. Before use, all samples were filtrated using 0.2 µm PES filters. Light scattering was detected with an automated CG-MALS instrument which was equipped with a dual syringe-pump (Calypso-II) sample and preparation unit, a Dawn Heleos-II multi-

angle laser light scattering detector, and an OptiLab® T-rEX dRI detector (all Wyatt Technologies, Santa Barbara, CA, USA). The Calypso 2.1.5 software was used to obtain Zimm Plots, K_D and A_2 values [25].

In addition, hetero-association experiments were performed by varying both the HY-133 and the HEPES concentration from 0 – 10 mM and 0 – 25 mM, respectively. The experimental settings were similar to the ones described above.

3.9 Activity: FRET-Assay

Activity of HY-133 was determined with an enzymatic assay (HY-133 Activity Assay, Microcoat, Bernried, Germany). A short peptide sequence with attached fluorophore and quencher was used as a substrate. The substrate mimics the murein cell wall of the bacteria and is specific to *S. aureus*. The substrate is hydrolyzed by HY-133, which results in elimination of the fluorescence quenching. The fluorescence signal was obtained at an excitation wavelength of 340 nm and detected at an emission wavelength of 440 nm. The specific activity can be calculated according to the protocol.

3.10 Storage stability study

The basic, buffer-free HY-133 formulation and the formulations containing 25 mM of the respective buffers were sterile filtered with 0.22 µm PVDF syringe filters (Millex-GV, Merck Millipore Ltd, Ireland), filled into sterilized 2R type I glass vials (MGlass AG, Germany) and closed with rubber chlorobutyl stoppers with FluroTec coating (West Pharmaceutical Servies, USA). The samples were stored at 4 °C, 30 °C and 40 °C for subsequent analysis for up to 4 months.

3.11 Molecular dynamics (MD) simulations

A homology model of HY-133 was generated with the EAD from the endolysin of phage K (PDB code: 4CSH) and the CBD from lysostaphin (PDB code: 4LXC) using the software MODELLER 9.21 [26]. The protonation states of ionizable residues at pH 6.0 were adjusted using the H++ server [27]. The protonated form of HEPES as well as the protonated and deprotonated forms of histidine (HIP/HIS) were parametrized with antechamber using GAFF2 for bonded and non-bonded parameters. Atomic partial charges were calculated with the AM1-BCC charge model in antechamber.

All-atom simulations were performed with the Amber19 program in a periodic box with explicit solvent [28]. The ff14SB force field for proteins was employed in combination with the TIP3P water model. Packmol and tleap were used to solvate the homology model of HY-133 in a cubic water box including 150 mM NaCl, 10 mM $CaCl_2$ without and with 25 mM of HEPES and histidine, respectively. All bonds involving hydrogen atoms were constrained using the SHAKE algorithm. Non-bonded electrostatic interactions were treated using the particle mesh ewald algorithm with a direct space cutoff of 9 Å. The system was energy minimized with the steepest descent algorithm for the first 5,000 cycles,

followed by 5,000 cycles using the conjugate gradient method. System equilibration was carried out for 1 ns in NVT ensemble to stabilize the temperature of 300 K using the Langevin thermostat, and subsequently for 1 ns in NPT ensemble to adjust the density of the system using the Berendsen barostat. The simulations were performed for 300 ns with a time step of 2 fs. The coordinates were saved every 10 ps. Each system was simulated in duplicates starting from a random seed number to estimate the statistical uncertainty of the results. All trajectories were analyzed using the CPPTRAJ module of Amber19 and VMD [29]. In order to identify effects of the buffer molecules on the conformation of HY-133, each frame of a trajectory was grouped into one of five discrete clusters by an agglomerative hierarchical clustering approach based on the conformational similarity defined by the root-mean-square deviation (rmsd). To estimate the binding of the HEPES and histidine molecules to the protein residues, we calculated the interaction score probability ($P(I_{score})$) defined as

$$P(I_{score}) = n / (N \cdot \alpha)$$

where n is the number of frames either HEPES or histidine was in contact with a certain residue over simulation time, N is the total number of frames, and α is a normalization factor to convert the interaction score into a probability.

4. Results and discussion

4.1 Influence of buffer excipients on chemical stability

At first, the protein's chemical stability with different buffer excipients was assessed. The 25 mM HEPES buffer was compared to a 25 mM citrate buffer and a 25 mM histidine buffer, respectively. In addition, combinations of 12.5 mM HEPES with 12.5 mM citrate or with 12.5 mM histidine were tested. All three formulations containing HEPES showed a constant native protein level upon storage for 16 weeks at 4 °C, irrespective of whether HEPES was used alone or in combination with a second buffer substance (Figure 2). In contrast, the formulations containing only citrate or only histidine showed a reduced native protein recovery of either 96% (citrate) or 84% (histidine). Storage at an elevated temperature of 40 °C led to a decrease of the native protein content over time in all formulations. This was most pronounced in formulations without HEPES, where only 20% protein recovery was achieved after 16 weeks. The highest native protein content (> 60%) was determined in the formulation containing solely HEPES. Both buffer combinations, HEPES + citrate and HEPES + histidine, resulted in native protein contents between the single buffer compositions. These results show that HEPES could not be replaced by commonly used buffer systems which would be more suitable for this pH range. Therefore, the stabilizing effect is independent of the buffering capacity and HEPES is not acting only as a buffering agent. A specific stabilizing effect of HEPES is clearly indicated.

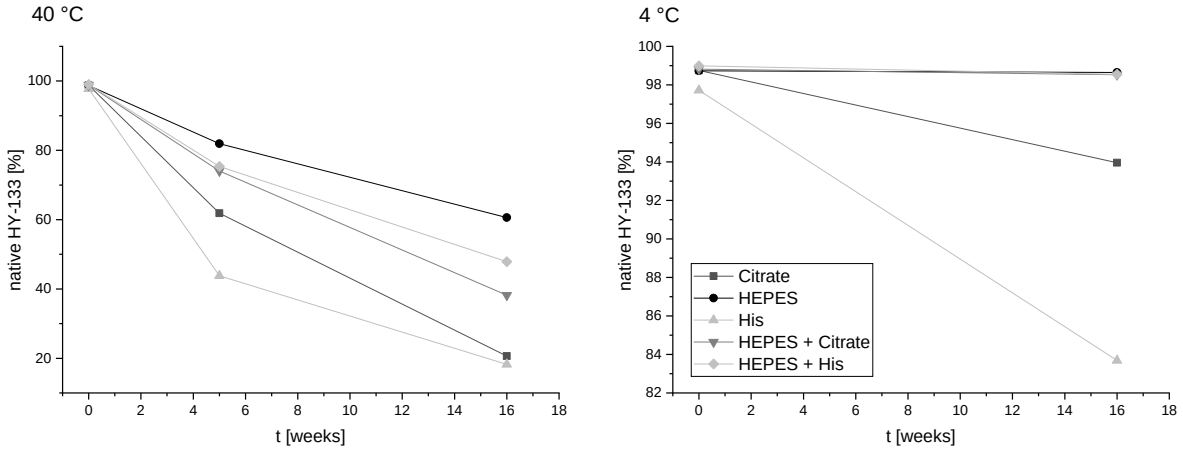

Figure 2: Native HY-133 amount over time dependent on different excipients. The pre-test was performed with each a citrate, histidine and HEPES buffer or the respective HEPES combinations and analyzed with RP-HPLC.

4.2 Function of HEPES as stabilizing excipient

To elucidate the role of HEPES in the HY-133 formulation, the interaction of the protein and HEPES was analyzed by CG-MALS. CG-MALS provides quantification of both self- and hetero-association of either a protein or a protein and another molecule and allows the determination of A_2, K_D and M_w. First, protein self-association was measured via the light scattering second virial coefficient (A_2) in the presence of HEPES and without HEPES (Figure 3). The typical step-wise decrease in light scattering signal resulted from the stop-flow injection of the different compositions. A visible difference between the two experiments was the delay until a stable light scattering signal was reached, which was more pronounced at higher protein concentrations. The delay appeared as an initially small increase in light scattering followed by a major signal decrease until the signal stabilized. Normalized A_2 values of -2.52 and -2.38 were determined without HEPES and with HEPES, respectively. A negative A_2 is associated with attractive forces between two protein molecules [30], which were prevalent in this formulation, irrespective of the presence of HEPES.

However, HEPES influenced the light scattering signal. The rapid set of the plateau and the initially observed peak at each step indicated a rapid binding of HEPES to protein hotspots. To gain a deeper understanding of the binding of HEPES to the protein, a hetero-association experiment was performed.

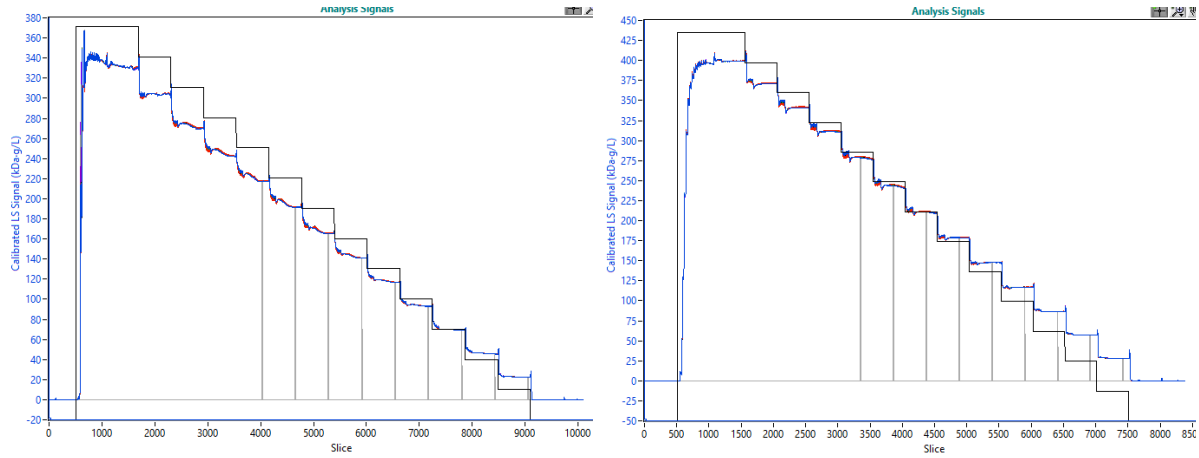

Figure 3: CG-MALS data for HY-133 with HEPES (left) and without HEPES (right). Light scattering data of HY-133 dependent on the protein concentration with and without HEPES. The black line shows the concentration signal, the blue line the light scattering signal. Grey bars represent measurement points.

In hetero-association experiments, a series of different composition ratios of HY-133 and HEPES were fitted to determine K_D and kinetic data. During the fitting process, the monomer molecular mass of both analytes and the associations stoichiometries can be modelled [31]. The best fit of HY-133 with HEPES was found to be a 1:1 stoichiometry model, also represented by the plateau with the highest amount of complex formation. The overlap of the light scattering data in the stepwise decrease in HY-133 concentration and the stepwise increase in HEPES concentration resulted in a K_D of $0.7 \cdot 10^{-3}$ mM. The data indicated an almost immediate binding of a HEPES molecule to a HY-133 molecule.

We were interested in whether we could confirm HEPES-binding, identify the local effects of HEPES on the protein and explain the stabilization mechanism. We therefore built a homology model of HY-133 and performed MD simulations to study the protein in the absence and presence of HEPES and histidine at atomistic detail. The interaction sites of HEPES and histidine were determined by calculating the interaction score $P(I_{score})$ per residue (Figure 4A). The $P(I_{score})$ reveals that both HEPES and histidine bind to charged and aromatic side chains of surface exposed residues of HY-133 via salt-bridge formation and cation-π interactions. Moreover, hydrogen bonds between HEPES and polar residues occurred. Considering the zwitterionic character of HEPES and histidine, this behavior was expected. We, however, observed different binding sites for the two molecules. Histidine mainly interacted with charged residues in the EA domain and with the termini of HY-133. HEPES showed some interaction with residues in the EA domain but also interacted with the more hydrophobic CB domain and linker residues. Histidine therefore altered the electrostatic surface properties of the protein to a higher extent than HEPES which may influence the inter-domain and intermolecular interactions. Nevertheless, this finding alone does not explain why HEPES is superior to histidine in stabilizing the protein.

Next, the effects of HEPES and histidine binding on the conformation of HY-133 were examined by grouping each frame of the trajectory into one of five clusters, based on the conformational similarity defined by the RMSD. A representative structure of the highest occupied cluster for each condition is shown in Figure 4C. Comparing these structures, it became apparent that the orientation and the distance of the domains substantially differed between the three conditions. For the simulations of HY-133 in water only, the initially elongated linker collapses and formed a hydrogen bond network to residues in the CB domain. Thus, the two domains were in close contact. Due to the sequence composition of the linker, this behavior is not surprising. Studies on intrinsically disordered peptides in water uncovered more compact structures for sequences with a high glycine content, supposedly because intrapeptide interactions out-compete backbone-solvent interactions [32], [33]. The simulations with histidine also revealed a collapse of the linker but with less hydrogen bonding to residues of the EA or CB domain than in the simulation with water only. Again, there was an interaction of the two domains but with a different orientation. The CB domain was rotated in a way that a hydrophobic region at its C-terminus is exposed to the surface. In the two other conditions, this region was located at the interface between the domains and mostly shielded from the surface. Only in simulations containing HEPES, the linker almost maintained the initial extended configuration with only a short bend around a HEPES molecule. Hydrogen bonds of this HEPES molecule to residues in the linker and a salt-bridge to residue 246 in the CB domain seemed to prevent the collapse of the linker. Thus, the linker was able to keep the domains separated. For a better understanding of intramolecular domain-domain interactions and the influence of the solvent conditions, we compared fluctuations in the distance between the two domains over simulation time (Figure 4B). In water only, the distance between the two domains rapidly decreased. Histidine molecules delayed the collapse of the linker but after 150 ns of simulation time, a similar distance as for the water simulations was reached. Only the simulations with HEPES showed an almost stable domain distance of approximately 30 Å.

In summary, the ability of HEPES to maintain the extended linker configuration and saturate hydrogen bond sites in the linker was the reason for the increased stability of HY-133. In the two other conditions, the linker collapsed which could even lead to the exposure of a hydrophobic region, as seen for histidine. Notably, also the changes in electrostatic properties of the protein surface upon binding of a zwitterion could influence the stability.

Due to the several binding sites identified, we cannot confirm a 1:1 stoichiometry as shown by the CG-MALS data. However, several of the binding events were only transient throughout the simulation and only a few were stable until the end of the simulation. Based on a previous study showing that weak and transient protein-excipient binding could enhance protein stability, whereas strong interactions

were found to mostly destabilize proteins [11], we could conclude that the lack of strong HEPES-binding did not hinder a stabilizing effect but rather promotes it.

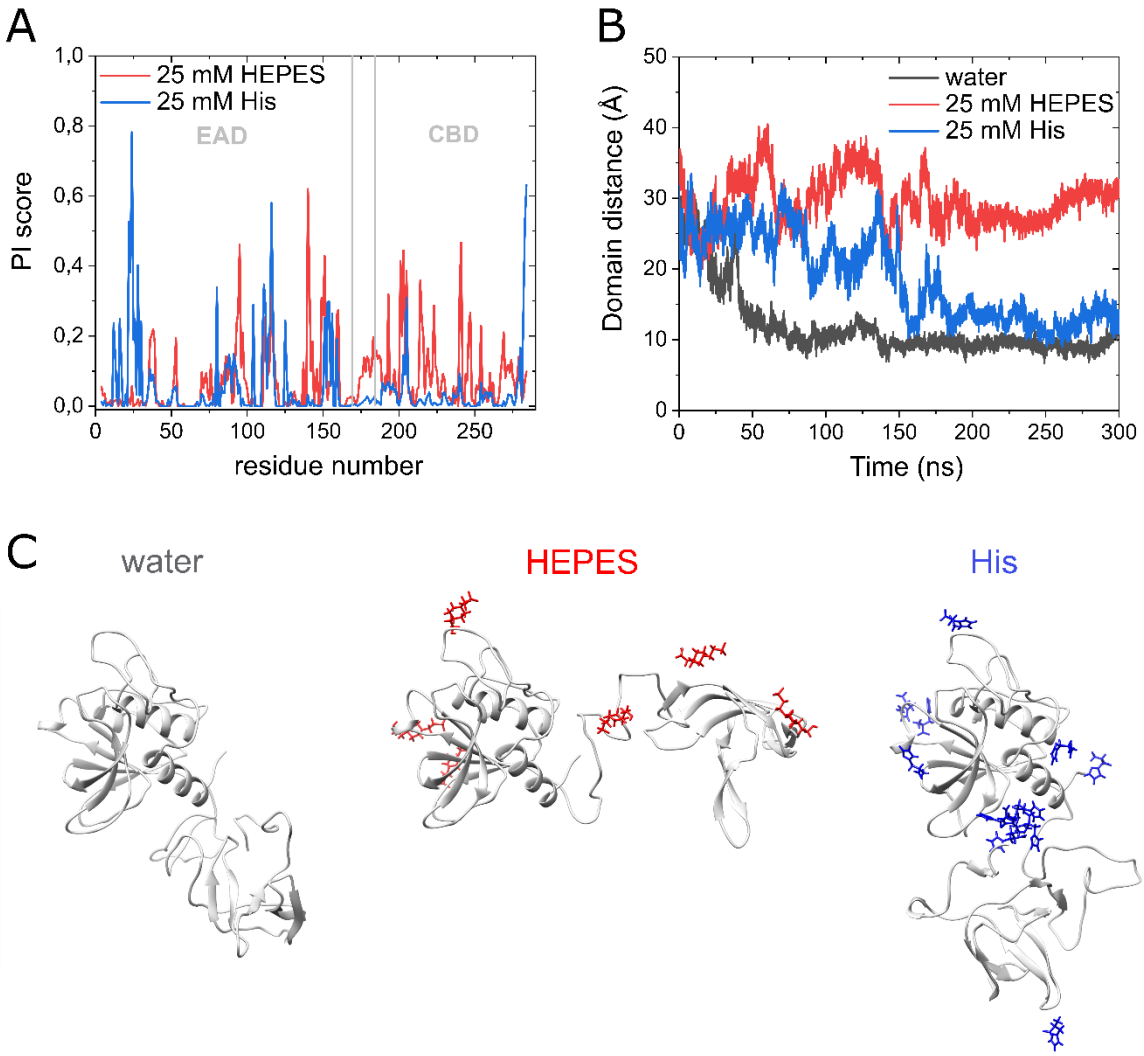

Figure 4: MD simulations of HY-133 without excipient, with 25 mM HEPES and 25 mM histidine. (A) Interaction scores P(I score) calculated per residue for HEPES and histidine averaged over the two replicates. (B) Distance of the last residue of the EA domain and the first residue of the CB domain over simulation time. (C) Representative structures of the highest occupied clusters for the three studied conditions (water: 61.1%. HEPES 62.2%, His: 74.6%) with aligned EAD domains. HEPES molecules are colored in red, protonated and deprotonated histidine molecules are colored in blue.

4.3 Influence of different Good's buffers on protein-excipient interactions

HEPES is a zwitterionic N-substituted aminosulfonic acid and part of the Good's buffer series. This series can be separated into several subgroups. The most prominent ones are the morpholinic, piperazinic and the TRIS family [19]. The structural similarities of buffers from the morpholinic and piperazinic family are most pronounced. All side chains of the buffers in these families contain sulfonic acid groups and have specific lengths. The piperazinic buffers contain two side chains instead of the one side chain in morpholinic buffers. Due to structural similarities, these buffers might be able to sufficiently stabilize protein to a similar extent as HEPES.

Six different Good's buffers of the above-mentioned groups were selected to examine their ability to replace HEPES and provide comparable stability of HY-133: four piperazine derivatives, HEPES, POPSO, PIPES and EPPS, and two morpholine derivatives, MES and MOPS. These buffers were characterized as non-metal binding and therefore fully compatible with $CaCl_2$, which is included in the formulation buffer and directly attached to one binding site at the protein. PIPES, HEPES, and MOPS are also reported to be non-metal binding [18] [34]. Only MES is potentially Ca^{2+} binding, a fact that is contrarily discussed in the literature [18], [19].

The thermal stability of proteins can be expressed by their melting temperature (T_m). The T_m values of the different formulations could be ranked, with a higher T_m representing a thermally more stable product [7]. The different buffer excipients were screened with nDSF to evaluate the thermal stability of HY-133 depending on the respective excipient. Without an additional excipient, a T_m of 46.4 °C was obtained (Table 1). Citrate and histidine buffers showed only minor changes in T_m, whereas the Good's buffers increased the respective T_m values. The highest value of 52.6 °C was found for PIPES which, along with HEPES, EPPS, and POPSO, belongs to the group of piperazine derivatives. Thus, the Good's buffers indicated a conformational protein stabilizing efficiency [35].

As shown before, T_m values of various proteins can depend on different N-based buffers [5], [36]. Both 20 mM MES and HEPES increased the conformational stability of RecA. Thermal stability was reported to be higher when the pH was above the pK_a of the respective buffer substance. This effect was stronger at lower pH, when the protein showed higher positive net charge, indicating a direct interaction of the buffer with the protein under these conditions [22]. In addition, MOPS showed a higher propensity to increase the thermal stability of BSA than MES when used in high concentrations of 1 M. It was shown that these buffers interact with the peptide backbone leading to net stabilization [37]. Furthermore, HEPES and EPPS were also stabilizing the conformational stability of BSA by interacting with the hydration layers of the peptide backbone [20]. In contrast, HY-133 already showed an increase in T_m at much lower concentrations, which indicates direct interaction of the excipient with the protein rather than stabilization due to preferential exclusion.

Table 1: T_m values of HY-133 dependent on the added excipient (excipient concentration = 25 mM).

Excipient	**Tm [°C]**
Without excipient	46.4
HEPES	51.5
Citrate	47.9
Histidine	45.0
MES	48.1
MOPS	51.1
EPPS	51.5
POPSO	52.4
PIPES	52.6

As described above, the T_m increase depends on the respective excipient at a fixed concentration of 25 mM. To determine the necessary ligand concentration, a thermal shift assay was performed. 12 different concentrations of HEPES, EPPS, POPSO, PIPES, MES, MOPS, citrate and histidine, respectively, ranging from 0 to 50,000 µM were spiked to the buffer-free formulation. The T_m of HY-133 in each buffer and excipient concentration was determined and plotted as a function of the respective excipient concentration (Figure 5). Formulations containing PIPES and POPSO resulted in higher overall T_m values and a faster increase of T_m. These two curves are followed by HEPES, EPPS, and MOPS, which all showed a similar curve profile. An overall higher concentration of the respective excipient was needed to achieve similar T_m values. The MES buffer system showed only a minor increase in T_m. Both citrate and histidine buffered formulations showed a non-sigmoidal shaped curve. The histidine buffered formulation resulted in an atypical curve with a local T_m minimum of about 34 °C. Citrate resulted in a local T_m maximum at 3,000 µM with decreasing T_m values at higher citrate concentrations.

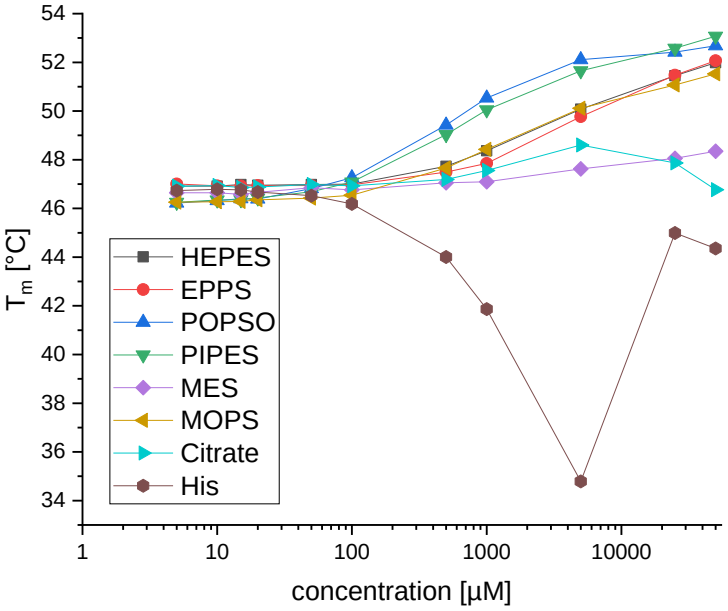

Figure 5: Overlay of the T_m values of the different excipients depending on their concentration.

For better comparison, the thermal shift curves were fitted with the Hill1-function (see Figure 6). The inflection point *k* is given in µM and equals the concentration, which is necessary for a significant increase in T_m. As described elsewhere, the inflection point equals K_d [36], [38], [39].

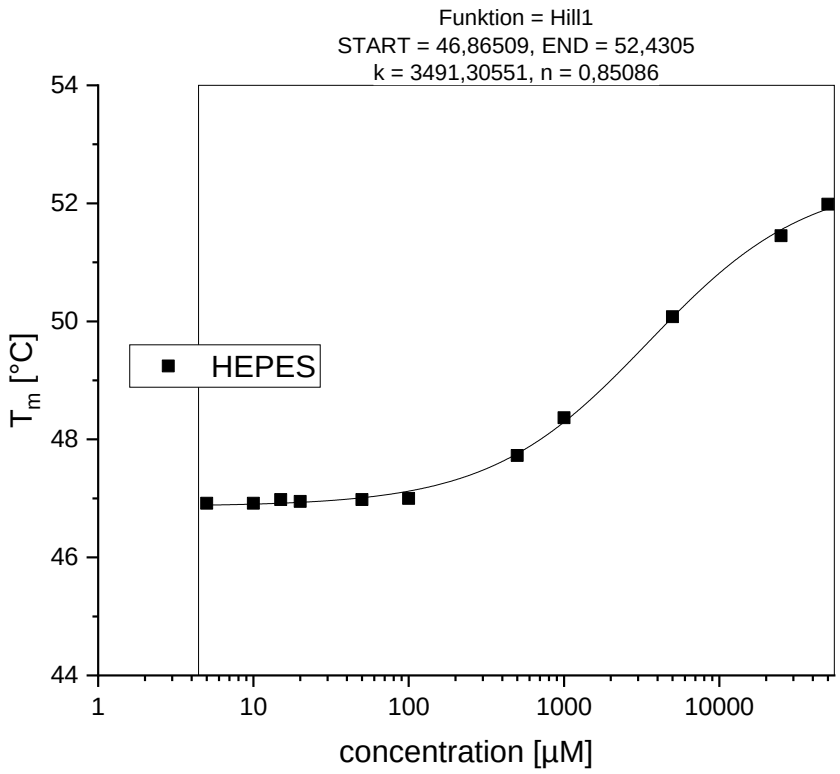

Figure 6: Tm values as a function of HEPES concentration. The curve was fitted with the Hill1 equation; the inflection point was calculated as k=3491 µM.

The K_d values were calculated for the different excipients and are shown as $c(Ligand)_k$ in [mM] in Table 2. As histidine and citrate buffers did not show a sigmoidal shaped curve, fitting and calculation of K_d was not possible. The lowest $c(Ligand)_k$ was obtained for POPSO (0.5 mM) and PIPES (0.8 mM), followed by MOPS (1.6 mM). HEPES (3.5 mM) and EPPS (5.1 mM) were comparable, whereas MES (30.5 mM) showed a substantially higher $c(Ligand)_k$.

These results were used to select four different ligands for further evaluation of the physical and chemical stability of HY-133 in formulations containing different buffer excipients. HEPES and POPSO were selected representing the piperazine buffer excipients, differing in their respective $c(Ligand)_k$. MES and MOPS were selected as morpholine derivatives. The 4 different excipients were compared to the basic formulation with only arginine-HCl, methionine, NaCl, $CaCl_2$, and Poloxamer 188.

Table 2: K_d values of the different excipients calculated in the thermal shift assay.

Ligand	**c(Ligand)k**
POPSO	0.5 mM
PIPES	0.8 mM
MOPS	1.6 mM
HEPES	3.5 mM
EPPS	5.1 mM
MES	30.5 mM

4.4 Stability study of HY-133 with HEPES and further Good's buffers

Subsequent to the determination of the influence of Good's buffers on the conformational stability, chemical degradation, protein aggregation (soluble and insoluble), and structural changes of the protein depending on the different formulations were analyzed over the course of up to 16 weeks at different storage conditions. Different Good's buffers were compared to a buffer free formulation. The formulations were stored at 2-8 °C, 30 °C, and 40 °C.

All formulations exhibited a characteristic near-UV CD-spectrum with a large negative peak at around 285 nm. In addition, three less prevalent peaks at 268 nm, 276 nm and 290 nm could be observed in all spectra. However, a decrease in molar ellipticity in the near-UV region was noted in the formulation without buffer excipient at T0. This structural difference can be linked to the missing additional excipient. The presence of HEPES and its structural similar entities affect the tertiary structure of the protein. Similar to the aforementioned CG-MALS experiments and MD simulations, where rapid binding of HEPES to the protein was shown, structural changes of the protein are caused by ligand binding to the protein [24]. In general, CD is a very precise tool to determine even minor changes in the protein's conformation [7] and changes in the higher order structure caused by the addition of sucrose were reported before [40].

After 2-week storage at 30 °C, this initially shifted CD-spectrum was further altered, which resulted in a spectrum without a large, distinct peak. Minor changes were observed in the POPSO formulation in this storage condition, whereas the three other formulations remained unchanged. In contrast, 40 °C storage for two weeks led to a loss in molar ellipticity in all formulations. However, the characteristic near UV CD-spectrum was maintained for all formulations containing excipient. The formulation without an additional excipient showed further alteration.

After 16-week storage at 4 °C, the characteristic near-UV CD-spectrum were maintained in all formulations after 16-week storage at 4 °C.

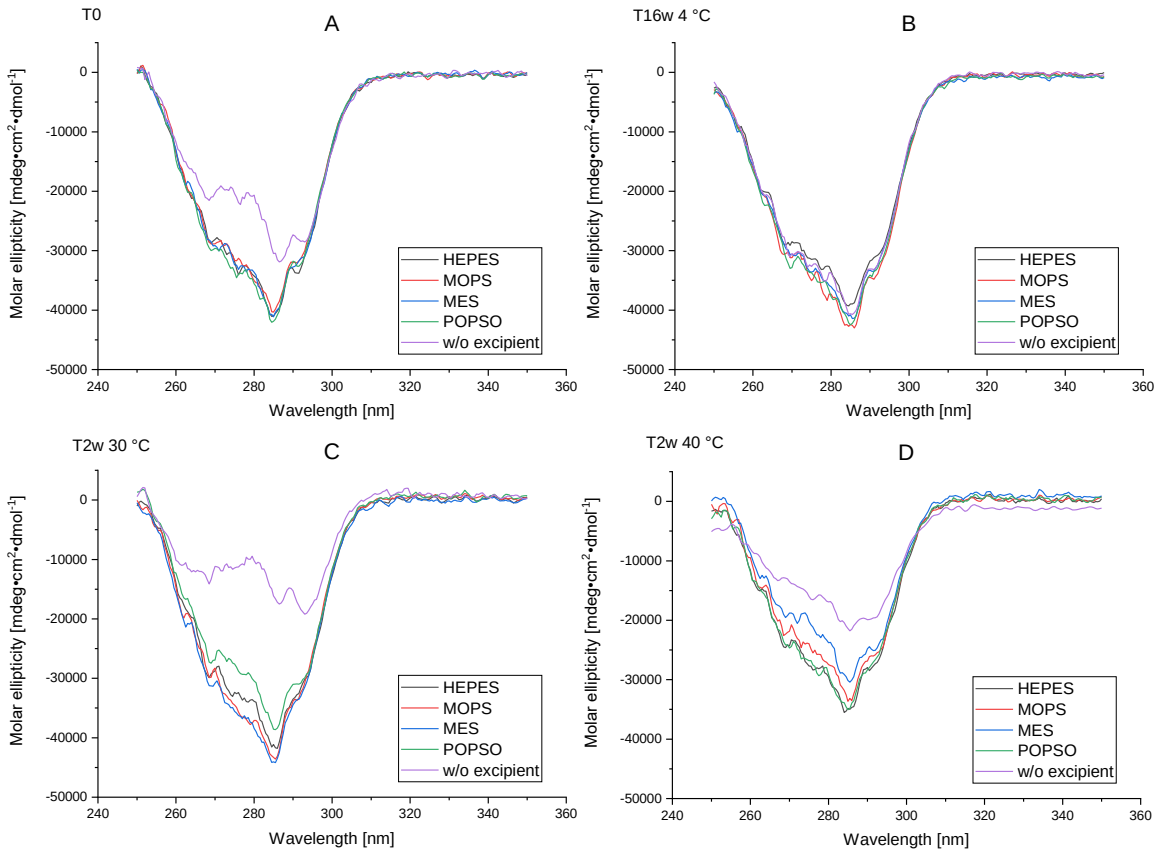

Figure 7: Molar ellipticity of formulations incl. HEPES, MOPS, MES and POPSO compared to a formulation without an additional buffer excipient. A. T0, B. after 16 weeks storage at 4 °C. C. 2 weeks storage at 30 °C. D. 2 weeks storage at 40 °C.

Subvisible particle counts remained low throughout the stability study. Storage at 4 °C did not lead to a major increase in particle counts, irrespective of the formulation. Elevated storage temperatures resulted in a slight increase in particle counts. Higher particle numbers were observed in formulations containing MOPS and MES at 30 °C storage. Storage at 40 °C led to an increase in particle numbers in the formulations containing MES and in the formulation without an additional excipient at the 9-week time point. Yet, this increase could not be confirmed at the following time points, indicating no clear stability trend. The structural differences in protein folding shown in the CD experiment was apparently not sufficient to cause particle formation through the formation of larger oligomers [41]. The presence of the surfactant Poloxamer 188 in a suitable concentration effectively inhibited subvisible particle formation by improving the colloidal stability of the protein [42].

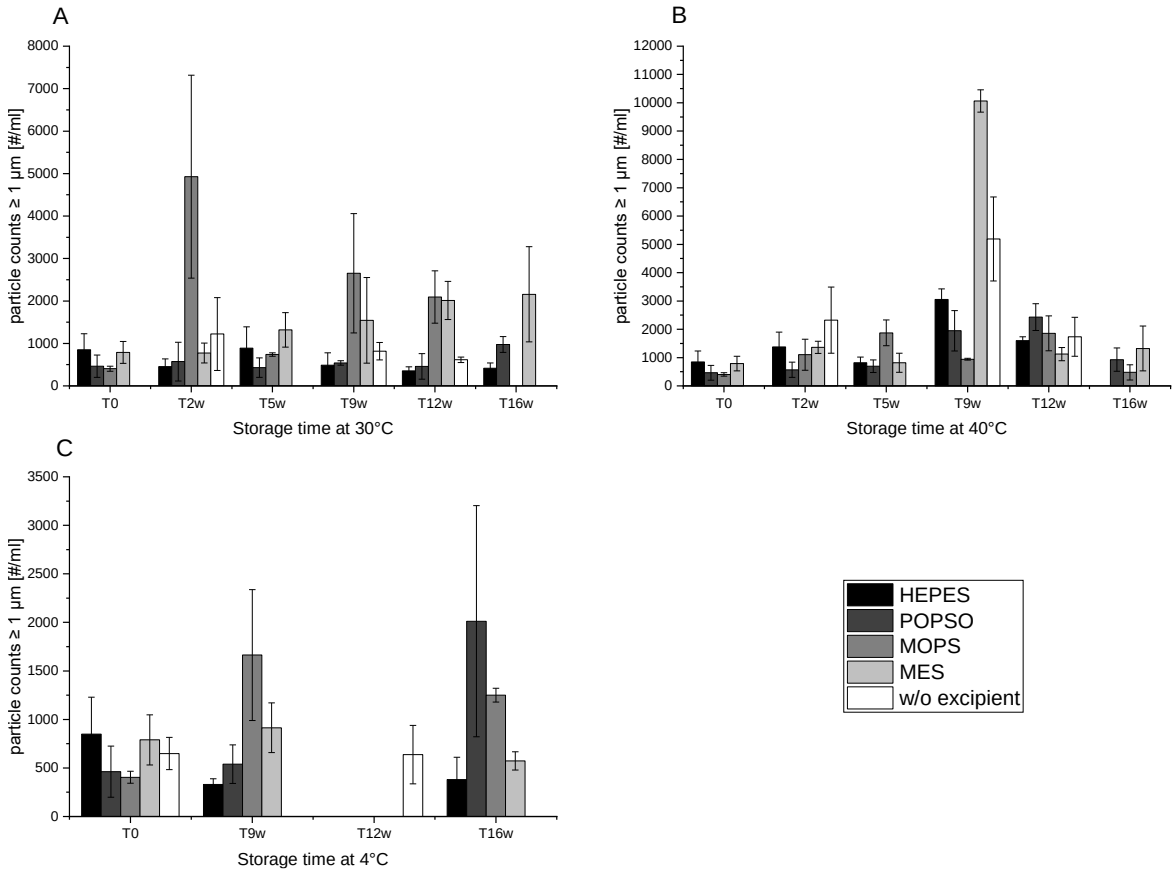

Figure 8: Particle counts of the different formulations upon storage at 30 °C (A), 40 °C (B), and 4 °C (C).

Size exclusion chromatography was used to determine the monomer content of each HY-133 formulation (Figure 9). An initially lower monomer content was determined in the formulation without excipient. Storage at 4 °C provided a stable monomer content over the course of the study, as no further decrease was observed in any of the formulations. However, storage at elevated temperatures led to a loss in relative monomer content. A comparable, small decrease in monomer content was determined in all formulations stored at 30 °C, differing only in the initially lower monomer content of the formulation without an additional excipient. Storage at 40 °C led to substantial loss in monomer content over time, which was more pronounced in the formulation without an additional excipient. HEPES performed best and its similar excipients stabilized the protein to a comparable extend.

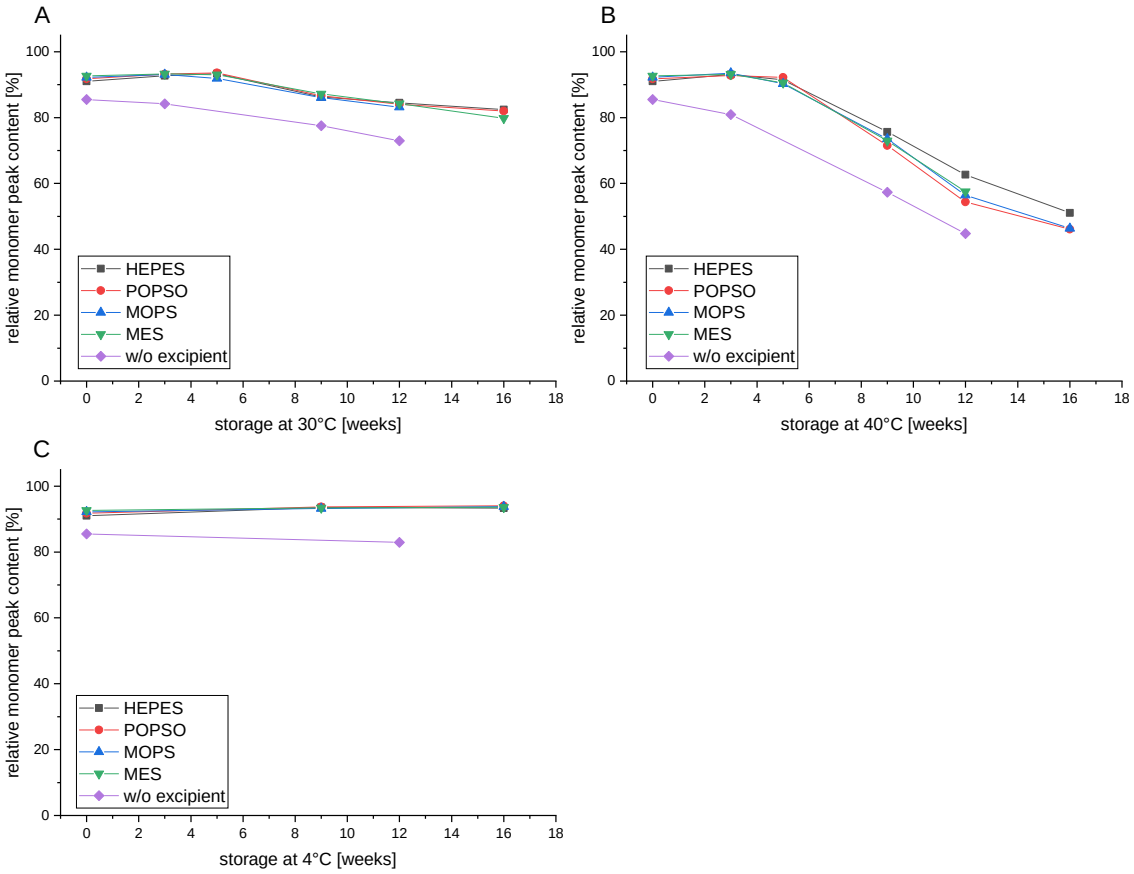

Figure 9: SEC data of the different HY-133 formulations upon storage at 30 °C (A), 40 °C (B) and 4 °C (C).

Chemical changes, such as oxidation and deamidation, of HY-133 were detected with RP-HPLC. The relative protein content is displayed in Figure 10. The formulation without an additional excipient showed an immediate loss in native protein content after dialysis at T0, followed by an accelerated degradation at early time points. Chemical changes were further highly dependent on storage temperature. While only minor changes of the protein were observed in any of the formulations during storage at 4 °C and 30 °C for up to 16 weeks, storage at 40 °C led to a drastic degradation in all the formulations. These changes were the least pronounced in formulations containing HEPES and MES, followed by POPSO and MOPS and most pronounced in the formulation without an additional excipient. Thus, all the derivatives and in particular HEPES and MOPS were able to stabilize HY-133 against chemical denaturation.

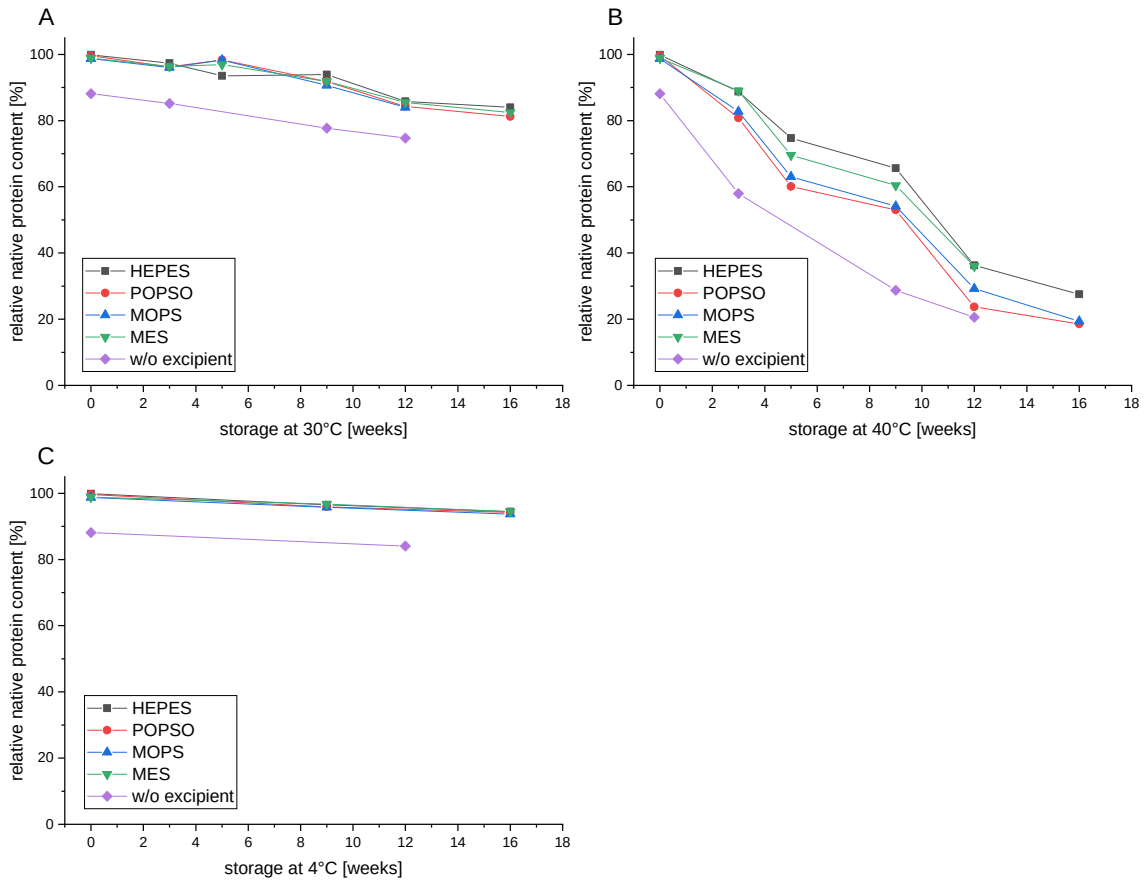

Figure 10: RP-HPLC data of the different HY-133 formulations upon storage at 30 °C (A), 40 °C (B) and 4 °C (C).

Charge variant formation, i.e. the formation of specific acidic and basic species of HY-133 upon storage, was determined by cation exchange chromatography (CEX) as shown in Figure 11. In general, the loss in main peak content of HY-133 is connected to an increase in pre-peak content, reflecting more acidic species of the protein. No change in the protein main peak was determined after storage at 4 °C in any of the formulations over the course of the study. Storage at 30 °C led to only minor changes in protein main peak with about 90% remaining after 16 weeks of storage, irrespective of the formulation. Storage at 40 °C led to a major loss in main peak content in all formulations over time. Larger loss was observed in the formulation without an additional excipient, indicating lower chemical stability compared to formulations with an additional HEPES-like excipient. For example, after 12 weeks of storage, formulations with an additional excipient resulted in more than 80% remaining main peak area, contrary to less than 30% main peak area in the HEPES-free formulation.

Several chemical alterations are known that are predominantly connected to the development of more acidic species. The most common one is deamidation of asparagine (Asn) residues, which is reflected by higher acidic species rates [43]. In addition to Asn residues, glutamine (Glu) residues can also be affected. Deamidation is connected to possible changes in the secondary and tertiary structure and therefore changes in the functionality of the protein [4], [44].

Thus, our results show that an HEPES-like excipient is crucial to increase the stability of HY-133 compared to a formulation without one of these excipients.

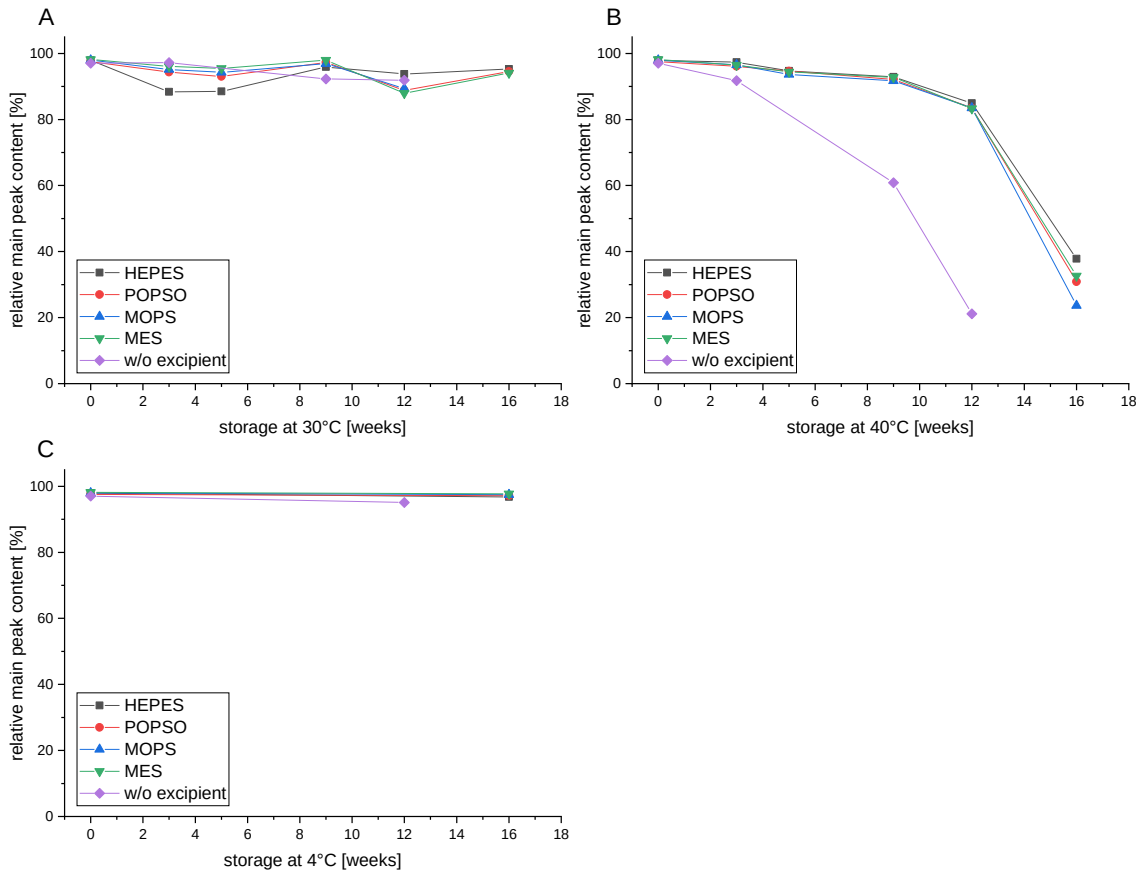

Figure 11: CEX data of the different HY-133 formulations upon storage at 30 °C (A), 40 °C (B) and 4 °C (C).

Finally, an enzymatic FRET-assay was applied as an activity assay (Figure 12). Storage at 4 °C and 30 °C did not lead to a loss in activity in any of the formulations after 16 weeks. In contrast, storage at 40 °C led to a decrease in activity in all formulations with differences between the formulations and storage durations. The highest and fastest loss in activity was determined in the formulation without an additional excipient. A decrease in specific activity of more than 50% was observed after 2 weeks and it further decreased over the course of the study until inactivity.

With the addition of HEPES or a HEPES-like buffer substance, the decrease in activity during storage at 40 °C was decelerated until 9 weeks. However, after 16 weeks at 40 °C, all formulations showed a substantial loss in activity.

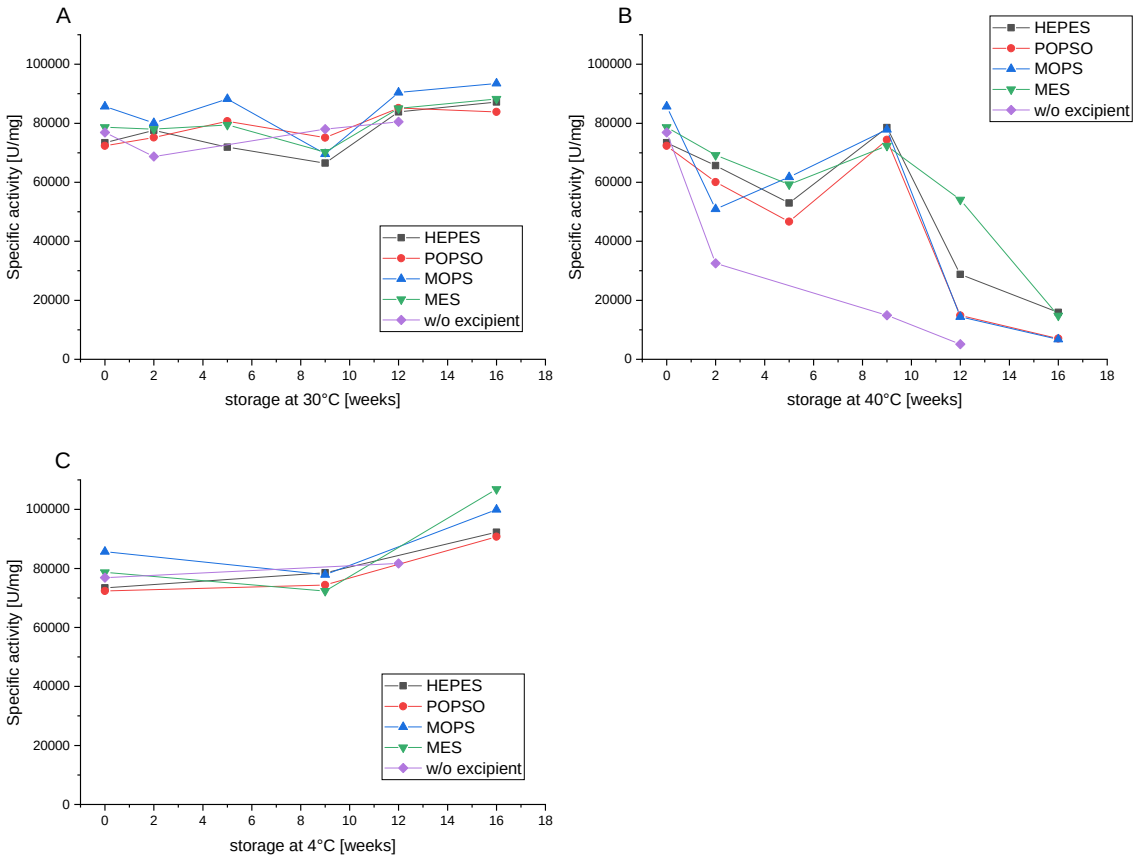

Figure 12: Activity of the different HY-133 formulations upon storage at 30 °C (A), 40 °C (B) and 4 °C (C).

5. Conclusion

The aim of this study was to identify and further examine the influence of HEPES on the protein stability of HY-133, a novel antibacterial drug specifically targeting various *S. aureus* strains. Furthermore, HEPES was compared to other Good's buffers used as excipients in a liquid biopharmaceutical formulation. So far, HEPES is mainly used as a buffer in protein expression. However, here we investigated the potential advantage of HEPES in formulation development.

Compared to commonly used histidine and citrate buffer systems, HEPES was clearly superior in stabilizing the protein HY-133 regarding its chemical and conformational stability. While HEPES did not change the second virial coefficient A_2, a rapid binding of HEPES to the protein was observed in CG-MALS. MD simulations could confirm the binding of HEPES to HY-133, thereby preventing the collapse of the linker and inter-domain interactions. This effect could not be reproduced with histidine, even though binding was also detected.

In the second part of the study, HEPES was substituted by various other Good's buffers with morpholinic and piperazinic ring systems: MOPS, POPSO, MES, EPPS, and PIPES. Whereas histidine and

citrate buffers were not able to increase T_m of HY-133, HEPES and the respective derivatives increased T_m by up to 6 °C.

Furthermore, thermal shift assays with the examined formulations were used to calculate K_d based on the Hill1-equation. POPSO showed the lowest concentration to increase T_m of HY-133 with 0.5 µM, followed by PIPES (0.8 µM), MOPS (1.5 µm), and HEPES (3.5 µm). K_d could not be calculated for citrate and histidine buffers.

Near-UV CD spectroscopy revealed that the conformational stability is sustained in formulations containing Good's buffers. Differences in the tertiary structure of the protein in the formulation without a Good's buffer was already determined at T0, indicating structural changes during the dialysis. Looking at different chemical and physical degradations, similar trends were found for different LC methods, such as SEC, RP, and CEX. The loss in protein activity was also reduced by the addition of HEPES and related buffer substances.

Overall, HY-133 highly benefits from the addition of HEPES or a similar Good's buffers due to sustained activity and substantially reduced chemical degradation. The studied Good's buffer substances performed similar. However, this study showed that the selection of an optimal buffer system is not limited to the buffer capacity at the perfect buffering range of the compounds. Instead, direct effects on the protein stability must also be considered. We showed that buffer substances could directly interact with a protein and could lead to improved chemical and conformational stabilization for new and pharmaceutical highly relevant protein classes.

6. References

[1] C. J. Roberts, "Therapeutic protein aggregation: Mechanisms, design, and control," *Trends in Biotechnology*, vol. 32, no. 7. 2014.

[2] M. C. Manning, D. K. Chou, B. M. Murphy, R. W. Payne, and D. S. Katayama, "Stability of protein pharmaceuticals: An update," *Pharm. Res.*, vol. 27, no. 4, pp. 544–575, 2010.

[3] W. Wang, S. Singh, david l. Zeng, K. R. King, and S. Nema, "Antibody Structure, Instability, and Formulation," *J. Pharm. Sci.*, vol. 96, pp. 1–26, 2007.

[4] D. Gervais, "Protein deamidation in biopharmaceutical manufacture: understanding, control and impact," *J. Chem. Technol. Biotechnol.*, vol. 91, pp. 569–575, 2016.

[5] T. J. Zbacnik *et al.*, "Role of Buffers in Protein Formulations," *J. Pharm. Sci.*, vol. 106, no. 3, pp. 713–733, 2017.

[6] W. Wang, S. Nema, and D. Teagarden, "Protein aggregation-Pathways and influencing factors," *Int. J. Pharm.*, vol. 390, no. 2, pp. 89–99, 2010.

[7] T. J. Kamerzell, R. Esfandiary, S. B. Joshi, C. R. Middaugh, and D. B. Volkin, "Protein-excipient interactions: mechanisms and biophysical characterization applied to protein formulation development.," *Adv. Drug Deliv. Rev.*, vol. 63, no. 13, pp. 1118–59, Oct. 2011.

[8] H. J. Lee, A. McAuley, K. F. Schilke, and J. McGuire, "Molecular origins of surfactant-mediated stabilization of protein drugs," *Adv. Drug Deliv. Rev.*, vol. 63, no. 13, pp. 1160–1171, 2011.

[9] D. P. Elder, M. Kuentz, and R. Holm, "Pharmaceutical excipients — quality, regulatory and biopharmaceutical considerations," *Eur. J. Pharm. Sci.*, vol. 87, no. 25, pp. 88–99, Dec. 2015.

[10] S. N. Timasheff, "Control of protein stability and reactions by weakly interacting cosolvents: The simplicity of the complicated," *Adv. Protein Chem.*, vol. 51, pp. 355–432, 1998.

[11] M. Zalar, H. L. Svilenov, and A. P. Golovanov, "Binding of excipients is a poor predictor for aggregation kinetics of biopharmaceutical proteins," *Eur. J. Pharm. Biopharm.*, vol. 151, pp. 127–136, 2020.

[12] A. Tosstorff, H. Svilenov, G. H. J. Peters, P. Harris, and G. Winter, "Structure-based discovery of a new protein-aggregation breaking excipient," *Eur. J. Pharm. Biopharm.*, vol. 144, pp. 207–216, 2019.

[13] A. Tosstorff, G. H. J. Peters, and G. Winter, "Study of the interaction between a novel, protein-stabilizing dipeptide and Interferon-alpha-2a by construction of a Markov state model from

molecular dynamics simulations," *Eur. J. Pharm. Biopharm.*, vol. 149, pp. 105–112, 2020.

[14] D. Shukla and B. L. Trout, "Interaction of Arginine with Proteins and the Mechanism by Which It Inhibits Aggregation," *J. Phys. Chem. B*, vol. 114, no. 42, pp. 13426–13438, Oct. 2010.

[15] C. P. Schneider, D. Shukla, and B. L. Trout, "Arginine and the Hofmeister Series: The Role of Ion–Ion Interactions in Protein Aggregation Suppression," *J. Phys. Chem. B*, vol. 115, no. 22, pp. 7447–7458, Jun. 2011.

[16] M. Rospiccio, A. Arsiccio, G. Winter, and R. Pisano, "The Role of Cyclodextrins against Interface-Induced Denaturation in Pharmaceutical Formulations: A Molecular Dynamics Approach," *Mol. Pharm.*, vol. 18, no. 6, pp. 2322–2333, Jun. 2021.

[17] A. Arsiccio, J. McCarty, R. Pisano, and J.-E. Shea, "Effect of Surfactants on Surface-Induced Denaturation of Proteins: Evidence of an Orientation-Dependent Mechanism," *J. Phys. Chem. B*, vol. 122, no. 49, pp. 11390–11399, Dec. 2018.

[18] N. E. Good, G. D. Winget, W. Winter, T. N. Connolly, S. Izawa, and R. M. M. Singh, "Hydrogen Ion Buffers for Biological Research *," *Biochemistry*, vol. 5, no. 2, pp. 467–477, Feb. 1966.

[19] C. M. H. Ferreira, I. S. S. Pinto, E. V. Soares, and H. M. V. M. Soares, "(Un)suitability of the use of pH buffers in biological, biochemical and environmental studies and their interaction with metal ions-a review," *RSC Adv.*, vol. 5, no. 39, pp. 30989–31003, 2015.

[20] B. S. Gupta, M. Taha, and M. J. Lee, "Buffers more than buffering agent: Introducing a new class of stabilizers for the protein BSA," *Phys. Chem. Chem. Phys.*, vol. 17, no. 2, pp. 1114–1133, 2015.

[21] K. Kasraian *et al.*, "Sustained In Vivo Activity of Recombinant Bovine Granulocyte Colony Stimulating Factor (rbG-CSF) Using HEPES Buffer," *Pharm. Dev. Technol.*, vol. 6, no. 3, pp. 441–447, 2001.

[22] M. A. Metrick, J. E. Temple, and G. Macdonald, "The effects of buffers and pH on the thermal stability, unfolding and substrate binding of RecA," *Biophys. Chem.*, vol. 184, pp. 29–36, 2013.

[23] B. W. Petersen, T. J. Harms, M. G. Reynolds, and L. H. Harrison, "Use of Vaccinia Virus Smallpox Vaccine in Laboratory and Health Care Personnel at Risk for Occupational Exposure to Orthopoxviruses — Recommendations of the Advisory Committee on Immunization Practices (ACIP), 2015," *MMWR. Morb. Mortal. Wkly. Rep.*, vol. 65, no. 10, pp. 257–262, 2016.

[24] S. M. Kelly, T. J. Jess, and N. C. Price, "How to study proteins by circular dichroism," *Biochim. Biophys. Acta - Proteins Proteomics*, vol. 1751, no. 2, pp. 119–139, 2005.

[25] J. Arora *et al.*, "Charge-mediated Fab-Fc interactions in an IgG1 antibody induce reversible self-association, cluster formation, and elevated viscosity," *MAbs*, vol. 8, no. 8, pp. 1561–1574, 2016.

[26] B. Webb and A. Sali, "Comparative Protein Structure Modeling Using MODELLER," *Curr. Protoc. Bioinforma.*, vol. 54, no. 1, pp. 5.6.1-5.6.37, Jun. 2016.

[27] R. Anandakrishnan, B. Aguilar, and A. V Onufriev, "H++ 3.0: automating pK prediction and the preparation of biomolecular structures for atomistic molecular modeling and simulations," *Nucleic Acids Res.*, vol. 40, no. W1, pp. W537–W541, Jul. 2012.

[28] H. D.A. Case, I.Y. Ben-Shalom, S.R. Brozell, D.S. Cerutti, T.E. Cheatham, III, V.W.D. Cruzeiro, T.A. Darden, R.E. Duke, D. Ghoreishi, G. Giambasu, T. Giese, M.K. Gilson, H. Gohlke, A.W. Goetz, D. Greene, R Harris, N. Homeyer, Y. Huang, S. Izadi, A. Kovalenko, C. L. Nguyen, A. Onufriev, F. Pan, R. Qi, D.R. Roe, A. Roitberg, C. Sagui, S. Schott-Verdugo, J. Shen, Y. Simmerling, J. Smith, J. Swails, R.C. Walker, J. Wang, H. Wei, L. Wilson, R.M. Wolf, X. Wu, L. Xiao, D. M. Y. Xiong, and P. A. Kollman, *AMBER 2019*. University of California, San Francisco, 2019.

[29] W. Humphrey, A. Dalke, and K. Schulten, "VMD: Visual molecular dynamics," *J. Mol. Graph.*, vol. 14, no. 1, pp. 33–38, 1996.

[30] Y. Ma *et al.*, "Determination of the second virial coefficient of bovine serum albumin under varying pH and ionic strength by composition-gradient multi-angle static light scattering," *J. Biol. Phys.*, vol. 41, no. 1, pp. 85–97, 2015.

[31] D. Some and S. Kenrick, *Characterization of Protein-Protein Interactions via Static and Dynamic Light Scattering*. Protein Interactions, InTech, 2012.

[32] D. P. Teufel, C. M. Johnson, J. K. Lum, and H. Neuweiler, "Backbone-Driven Collapse in Unfolded Protein Chains," *J. Mol. Biol.*, vol. 409, no. 2, pp. 250–262, 2011.

[33] S. Doose, "Importance of Backbone and Solvent Properties for Conformational Dynamics in Polypeptides," *ChemPhysChem*, vol. 9, no. 18, pp. 2687–2689, Dec. 2008.

[34] N. E. Good and S. Izawa, "Hydrogen Ion Buffers," *Methods Enzymol.*, vol. 24, no. C, pp. 53–68, 1972.

[35] R. L. Remmele Jr., N. S. Nightlinger, S. Srinivasan, and W. R. Gombotz, "Interleukin-1 receptor (IL-1R) liquid formulation development using differential scanning calorimetry," *Pharmaceutical Research*, vol. 15, no. 2. pp. 200–208, 1998.

[36] K. Huynh and C. L. Partch, "Analysis of protein stability and ligand interactions by thermal shift

assay," *Curr. Protoc. protein Sci.*, vol. 79, no. February, pp. 28.9.1-28.9.14, 2015.

[37] M. Taha, B. S. Gupta, I. Khoiroh, and M. J. Lee, "Interactions of biological buffers with macromolecules: The ubiquitous 'smart' polymer PNIPAM and the biological buffers MES, MOPS, and MOPSO," *Macromolecules*, vol. 44, no. 21, pp. 8575–8589, 2011.

[38] A. Zubriene *et al.*, "Measurement of nanomolar dissociation constants by titration calorimetry and thermal shift assay - Radicicol binding to Hsp90 and ethoxzolamide binding to CAII," *Int. J. Mol. Sci.*, vol. 10, no. 6, pp. 2662–2680, 2009.

[39] M. Vivoli, H. R. Novak, J. A. Littlechild, and N. J. Harmer, "Determination of protein-ligand interactions using differential scanning fluorimetry," *J. Vis. Exp.*, no. 91, pp. 1–13, 2014.

[40] S. V. Thakkar *et al.*, "Excipients differentially influence the conformational stability and pretransition dynamics of two IgG1 monoclonal antibodies," *J. Pharm. Sci.*, vol. 101, no. 9, pp. 3062–3077, 2012.

[41] S. Amin, G. V. Barnett, J. A. Pathak, C. J. Roberts, and P. S. Sarangapani, "Protein aggregation, particle formation, characterization & rheology," *Curr. Opin. Colloid Interface Sci.*, vol. 19, no. 5, pp. 438–449, 2014.

[42] T. A. Khan, H.-C. Mahler, and R. S. K. Kishore, "Key interactions of surfactants in therapeutic protein formulations: A review.," *Eur. J. Pharm. Biopharm.*, vol. 97, no. Pt A, pp. 60–67, Nov. 2015.

[43] S. Fekete, A. Beck, J. Veuthey, and D. Guillarme, "Ion-exchange chromatography for the characterization of biopharmaceuticals," *J. Pharm. Biomed. Anal.*, vol. 113, pp. 43–55, 2015.

[44] Y. Du *et al.*, "Chromatographic analysis of the acidic and basic species of recombinant monoclonal antibodies," *MAbs*, vol. 4, no. 5, pp. 578–585, 2012.

Chapter 7

Topical application formulation of HY-133: Hydrogel development

Table of Contents

1. Hydrogel formulation development

1.1 Introduction

Topical administration of HY-133 in the nasal cavity is intended to target the main carrier site of *staphylococcus aureus (S. aureus)*, the anterior nares [1]. This site is often colonized by the bacteria without an associated disease [2]. However, nasal *S. aureus* carriers have a higher risk of serious infections. It has been described that the eradication of *S. aureus* in the nasal cavity with mupirocin reduces the risk of autoinfection of high-risk patients [3]. *S. aureus* predominantly adheres to the mucosa and mucin-coated epithelial cells, but non-specific bindings like hydrophobic interactions are also known to exist [1], [4]. As the bacteria are strongly bound to the target site, a suitable residence time of the drug product in the anterior nares needs to be ensured. In general, drug products with the nasal cavity as intended administration site are often administered as nasal spray or nasal drops. These drug products often have the disadvantage of short retention times because dripping out leads to a rapid loss of the drug product [5]. As the deposition of the drug product in the nasal cavity is of special importance in an eradication therapy, quick clearance of the HY-133 drug product must be avoided. The residence time of drugs is vastly dependent on the nasal mucociliary clearance [6]. Cilia transports the mucus layer towards the throat, which is causing rapid clearance of a nasal spray. A 50% dose clearance of a liquid dosage form within 20 minute, as shown before [6], would therefore not be suitable for a topical application of HY-133.

To overcome fast clearance times, the development of the drug product targeted two main aspects: prolonging the residence time of the API on the target site and an effective distribution of the product in the nasal cavity.

Both objectives can be addressed by a HY-133 formulation with an elevated viscosity and mucoadhesive properties. The mucoadhesive effect is mostly based on the interactions of the API formulation with the mucosa via hydrogen bonds [7]. Polymers with a high number of carboxyl and hydroxy groups are particularly suitable to build up these hydrogen bonds with the nasal mucosa. Various excipients with these characteristics can additionally form highly viscous solutions and hydrogels. Consequently, the same excipient can provide the required combination of elevated viscosity and the mucoadhesive effect which is beneficial for an enhanced residence time of HY-133, leading to an improved efficacy.

Derivates of cellulose would fulfill such requirements. Several different cellulose derivates such as hydroxypropyl methylcellulose (HPMC), carboxymethylcellulose sodium (NaCMC), hydroxyethyl-cellulose (HEC), and methylcellulose (MC) were described as suitable adhesive adjuvants [8]–[10]. For example, the addition of HPMC increased the clearance halftime in liquid nasal sprays [6]. Another

commonly used excipient is the polysaccharide gellan gum, which forms gels in the presence of cations [11]. Another frequently used polymer is poly(vinylpyrrolidone) (PVP). Concentrations of 3% to 6% PVP were already used as a suitable delivery vehicle to nasally administer penciclovir [12]. In general, hydrogels can be formed with all aforementioned excipients. However, the viscosity is highly dependent on the concentration of each excipient and must be adapted to match the requirements of the drug product.

The necessary modifications of the drug product formulation composition could possibly influence the API stability and therefore needs to be evaluated carefully. In a first step, the following requirements were defined for the hydrogel drug product: the hydrogel itself should comprise a mucoadhesive excipient and has an elevated viscosity with a non-newtonian shear thinning effect. During the development, an upper viscosity limit was determined which still allowed administration by spraying and an adequate dosing of the drug product. The excipient must be compatible with the formulation buffer, and the hydrogel should be transparent and odorless. Finally, the manufacturing process should be controllable, and sterility of the final drug product must be ensured. Sterility could be provided by either final sterilization of the drug product or by aseptic compounding.

As several new excipients had to be tested during the final drug product definition, this phase was divided into two parts: (I) the development of a nasal spray with elevated viscosity and (II) the compatibility of the excipients forming the nasal spray with the drug substance without impairing the protein stability.

1.2 Development of a sprayable hydrogel prototype

Nasal sprays are often aqueous formulations with low viscosity which can be delivered via mechanical spray pumps. Depending on the intended dose, either metered-dose spray pumps or single-dose spray devices can be used [5]. The resulting drug-device combinations are often characterized by their emitted dose, spray pattern and droplet size distribution (DSD) [13]. These parameters are used to assess the performance of the drug-device combination during the developmental phase. They are of special importance to ensure an evenly distributed drug product in the nose. Thereby, aerosol droplets should be larger than 10 µm to avoid deposition of the drug in the lung [14]. In hydrogel nasal sprays, DSD was found to be particularly affected as droplet size increased with higher CMC concentrations [14]. It was also reported that the addition of low-viscosity grade CMC increased the drug product viscosity, which resulted in a changed spray pattern and plume geometry, but an unchanged spray content [15]. However, the viscosities of the tested 1% - 2% CMC hydrogels were with 7.5 to 19.4 mPa·s still below a suitable and intended viscosity for HY-133 nasal spray development. A more localized deposition in the anterior regions of the nose was shown before with higher concentrations of methylcellulose [16]. As the local drug product delivery of HY-133 specifically targeted the anterior

part of the nasal cavity, hydrogels with higher viscosities, but accurate and precise dosing, needed to be developed.

Sprayability poses a particular difficulty in hydrogels. Both shear thinning and thixotropy are important factors enabling dosing of highly viscous hydrogels through mechanical spray pumps [17]. Thereby, the spraying pattern could change from a spray plume to a more jet stream like spray geometry. Very low HPMC concentrations of 0.1% to 0.3% were reported to substantially decrease the spray area and the width of the spray plume [18]. While this differs from the normally yielding spray plume, it eases the drug product delivery and ideally provides a stable content uniformity.

Shear stress is applied on the hydrogel during expulsion through the spray nozzle [14]. Ideally, the shear stress leads to shear thinning of the hydrogel and subsequently to an eased application of the drug product. Additionally, the flow of the formulation is improved at the target site, which enables rapid distribution within the nasal cavity. However, rapid rebuilding of the hydrogel structure is important to facilitate adherence of the drug product on the mucosa [17]. Complete viscosity recovery should occur fast, thixotropic effects therefore minimized and shear destruction must be avoided [17].

1.3 Hydrogel preparation

Different methods for the preparation of the hydrogels were tested. In general, hot and cold dispersion of the different excipients were tested with different devices. In the following, the description of the methods will be subdivided into the preparation in lab-scale and a scale-up method using a modular laboratory reactor.

1.3.1 Lab scale preparation

Depending on the excipient, the preparational methods varied regarding their temperature during the dissolution process. Whereas HPMC and NaCMC could be dispersed at cooled conditions and at room temperature, xanthan and gellan gums were required to be heated to over 80 °C to form a hydrogel. The respective excipient was slowly dispersed in either purified water or the formulation buffer. The mixture was stirred at medium revolutions (speed settings 5 of 10) overnight and visible agglomerations were manually dissolved with a spatula. After complete dissolution, a viscous, but still fluid hydrogel was obtained. Possibly enclosed air bubbles were removed by quick centrifugation (2,000 rpm for 10 minutes).

For the preparation of the drug substance containing hydrogel, HY-133 was mixed to the placebo hydrogel by gentle stirring. Thereby, a concentrated HY-133 stock solution was volumetrically added to the hydrogel.

1.3.2 Scale-up manufacturing

An IKA Lab Reactor LR 1000 attached with an Ultraturrax T25 digital (both IKA, Staufen, Germany) was used for the preparation of the placebo hydrogel. The Lab Reactor consisted of a 1 L borosilicate glass vessel which included an anchor stirrer with scrapers made of PTFE, ensuring proper mixing during the process. The lid was made of stainless steel and provided various gas-tight connections. Besides the ultraturrax, a PT-100 temperature sensor was permanently installed to monitor and control the temperature during the process. In addition, a pH electrode could be attached. All devices were vacuum-sealed and were in direct contact with the placebo hydrogel during the process. The vessel temperature could be set between 5 °C and 120 °C with a temperature control unit. For effective cooling below room temperature, a cooling device was attached to the lab reactor. The vacuum pump was directly attached to the vessel of the lab reactor by a vacuum valve. The vessel pressure was directly controlled via the rpm-regulated pump. All components which were in contact with the drug product consisted of either stainless steel, perfluorinated rubber (FFKM), PTFE, PEEK or borosilicate glass 3.3.

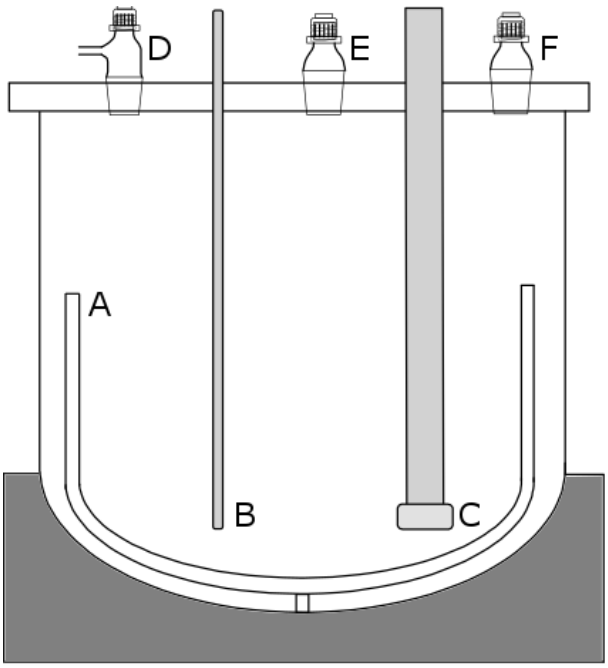

Figure 1: Design of the IKA Lab Reactor LR 1000. The vessel was installed on a temperature-controlled assembly unit (grey). The following attachments were installed for the manufacturing of the different hydrogels: (A) Anchor stirrer; (B PT-100 Temperature sensor; (C) Rotor-stator device (ultraturrax); (D) Pressure valve; (E) Funnel port; (F) Tubing port.

At least 300 ml of the respective formulation buffer were filled into the glass vessel and pre-cooled to 10 °C. The buffer was stirred at maximum speed (150 rpm) and the pre-weighed gelling agent (e.g., HPMC, see following paragraphs) was filled into the vessel through a funnel. A 10% gelling agent surplus was used to compensate the dilution effect which was caused by the addition of the drug substance. The vessel was closed and a vacuum of 350 mbar was applied. Subsequently, the gelling agent was dispersed by the ultraturrax at a speed of 25,000 rpm for a maximum of 2 minutes. The

dispersion was further stirred, and it was visually ensured that no agglomerated excipient residues were present. However, dispersion with the ultraturrax can be repeated if solid residues are observed. A turbid hydrogel, which was caused by the enclosure of small air bubbles, was formed. Afterwards, the hydrogel was stirred overnight at 20 rpm and 10 °C to remove the remaining air bubbles. A clear, slightly yellowish hydrogel was obtained.

1.3.3 Aseptic fill and finish process

A concept to ensure a sterile drug product was developed. As the drug product is not heat resistant and cannot be sterilized by filtration only, aseptic compounding can be used as a concept for the manufacturing process. Therefore, the placebo hydrogel was autoclaved and the drug substance was filtered with a 0.2 µm sterile syringe filter prior to aseptically combining hydrogel and drug substance. Both compounds were then mixed in a sterilized vessel and filled under aseptic conditions in the respective primary packing material.

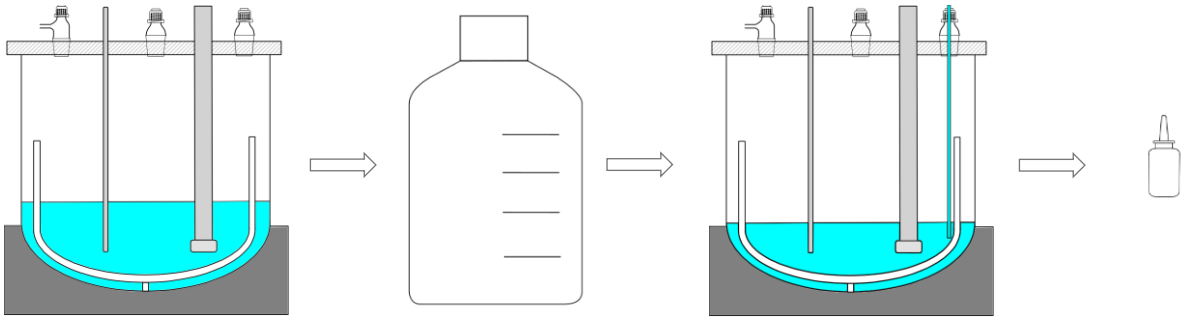

Figure 2: Visualization of the sterile manufacturing process of the HY-133 hydrogel. In a first step, the placebo hydrogel is manufactured by dispersion of HPMC, for example, in the formulation buffer at 350 mbar at 10 °C. The dispersion is stirred overnight until complete gel formation. The placebo hydrogel is filled into a 1L Schott bottle and steam sterilized. The sterilized hydrogel is then filled into the sterilized mixing vessel and the filtered drug product is added via a sterile port and properly mixed. In the final step, the HY-133 hydrogel is pumped via a sterile tubing from the vessel into a sterile nasal spray device.

The hydrogel was filled into a 1 L borosilicate glass bottle and sterilized in an autoclave at 121 °C for 15 minutes. The hydrogel was checked for visible changes and subsequently aseptically transferred into the pre-sterilized Lab Reactor. The drug substance stock solution with a concentration of 10 mg/ml was filtered with a 0.22 µm PVDF syringe filter (Millex-GV, Merck-Millipore) and thereafter filled via a sterile port into the vessel. To obtain a final drug product concentration of 1 mg/ml, the filtered drug substance was diluted at a ratio of 1:10 with the hydrogel. The mixing was performed in the lab reactor with a mixing speed of 20 rpm for 10 minutes.

A sterile tube could be attached to one of the ports on the lid and inserted to the hydrogel. By using a rotary piston pump, the drug product could be directly filled into either single- or multi-dose containers.

1.4 Primary packaging material

Two different primary packaging systems were evaluated as possible devices for the application of HY-133 hydrogels. Because no final decision was made on the dosing frequency and duration, two different dosing systems, a single- and a multi-dose container, were tested. As the HY-133 hydrogel was developed as a preservative-free formulation, the containers needed to ensure sufficient microbial integrity. Further requirements include the possibility of sterilization of the primary packaging material and the compatibility with the aseptic filling process developed in this study. In addition, content uniformity is of special importance, since the viscosity of the hydrogel formulation is much higher than the viscosity of a usually administered liquid nasal formulation. The selected single- and multi-dose containers fulfilled these general requirements.

The Aptar UDS-L (AptarGroup Inc., Illinois, US) was selected as the single-dose system to target the anterior part of the nasal cavity. A delivered dose volume of 125 µl can be achieved with a very small overfill of 15 µl, as no priming of the administration device is necessary. The container consists of fiolax glass and is closed with a bromobutyl stopper (Figure 3). The glass container can be directly filled with the pump included in the aseptic filling process line. Container closing could be performed using a tube-rod system, similar to those commonly used to close pre-filled syringes.

Figure 3: The Aptar UDS-L (left) was implemented as a single-dose container for the administration of a HY-133 hydrogel. The drug product is filled into a glass container (right).

The Ursatec 3K system (Ursatec GmbH, Tholey, Germany) was selected as the multi-dose container. Similar to the UDS-L system of Aptar, this system is designed for preservative-free formulations. The system consists of a HD-PE container which is closed by a non-airless pumping nozzle. This nozzle prevents a possible contamination of the drug product by (I) external liquids using a valve and (II) air, which flows back into the container via a filter. As the device requires priming, the length of the priming phase and the content uniformity after the priming phase was determined. Therefore, two hydrogels with different gelling agent contents were filled into the container. Both hydrogels had a priming phase of 3 pump strokes. The sprayed hydrogel content was not differing between the two hydrogels (e.g., 0.139 g ± 0.003 g for a 1% HPMC hydrogel and 0.137 g ± 0.002 g for a 1.5% HPMC hydrogel).

In summary, both containers can be used for the application of the preservative-free HY-133 hydrogel. The systems can be selected according to the dosing frequency. Multi-dose containers needed more drug product material as the overfill is substantially higher. They are therefore only recommended for more than 3 sequential doses.

2. Hydrogel excipient screenings

2.1 Limitations of sprayable hydrogels

In a pre-test, gels with different viscosities were evaluated in terms of their sprayability with the designated applicator system. Hydrogels with a viscosity of maximum 2 Pa·s were considered to be sprayable. Higher viscosities required either higher forces or resulted in inadequate dosing. Therefore, the limit of 2 Pa·s was set for the further development of the hydrogels.

2.1.1 Viscosity determination and limits of different excipients

In a pre-test, hydrogels consisting of 1% NaCMC (Cekol 2,000 P), HPMC K4M, gellan gum, or xanthan gum, respectively, were prepared as described. All hydrogels were clear and without visible excipient residues. NaCMC (Cekol 2,000 P) and HPMC K4M hydrogels resulted in visibly lower viscosities than xanthan and gellan gum hydrogels.

Figure 4 displays the viscosity data of the 4 hydrogels with increasing shear rates from 1 s^{-1} to 100 s^{-1}. All 4 samples showed non-Newtonian, shear thinning behavior to a different extent. They all differed in their overall viscosities and rheology properties. NaCMC (Cekol 2,000 P) and HPMC K4M hydrogels had a similarly low viscosity with distinct pseudoplastic behavior. Viscosity was fully reversible without a hysteresis effect. The xanthan hydrogel showed higher initial viscosity with rapid shear thinning at already low shear rates. The viscosity plateau was reached with shear rates of 40 s^{-1} and higher. The viscosity of this hydrogel was also fully reversible. These 3 hydrogels could be administered by a multi-dose nasal spray device. In contrast, the gellan gum hydrogel was not sprayable, although a pronounced shear thinning effect was determined. The initial viscosity was very high, which prevented an effective device priming. In contrast to the other tested hydrogels, the decrease in viscosity was irreversible. This prevented a rapid rebuilding of the hydrogel structure and could not provide a prolonged residence time in the nasal cavity. In summary, gellan gum hydrogels were not a suitable drug product matrix for HY-133.

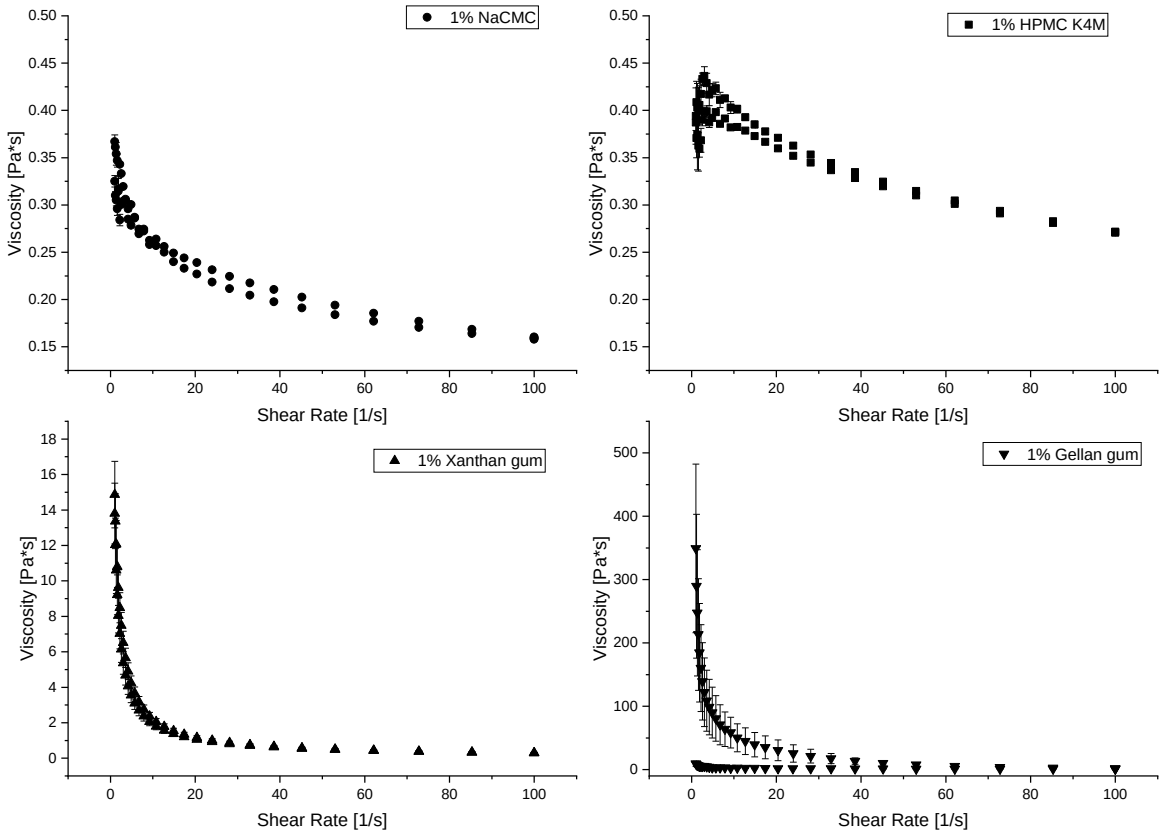

Figure 4: Viscograms of 1% NaCMC (Cekol 2,000 P), HPMC K4M, xanthan or gellan gum, respectively, in purified water. Three single runs were averaged and the standard deviations were calculated.

The rheological characteristics and the viscosities at low and high shear rates of the NaCMC (Cekol 2,000 P) and HPMC K4M hydrogels were highly dependent on the amount of gelling agent (Figure 5). Similar excipient concentrations resulted in higher viscosities in HPMC K4M hydrogels compared to NaCMC (Cekol 2,000 P) hydrogels. Besides an increased viscosity with higher excipient concentrations, the shear thinning effect was also more pronounced with higher concentrations. However, a comparably low viscosity was not reached at higher shear rates.

All concentration variations of these NaCMC (Cekol 2,000 P) and HPMC hydrogels could be administered by spraying with the designated spraying device and nozzle. In particular, correct dosing was possible with a 1.5% HPMC hydrogel and a viscosity of up to 2 Pa·s. Hydrogels with higher viscosities, as it was shown for the xanthan and gellan gums hydrogels, could not be sprayed reproducibly by determining the applied dose by weight. Therefore, a maximum viscosity of 2 Pa·s was specified as an upper viscosity limit.

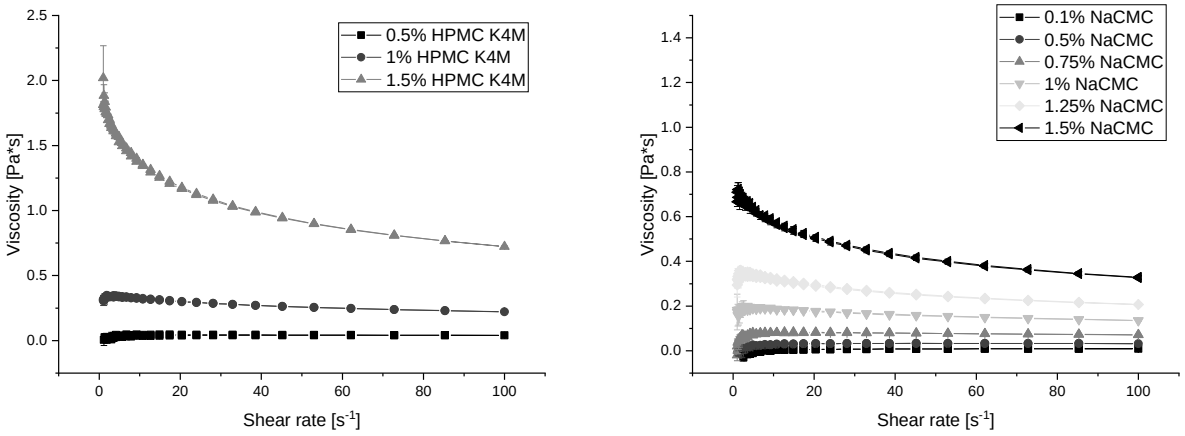

Figure 5: Viscograms of concentration variations of HPMC K4M (left) and NaCMC (Cekol 2,000 P) (right) hydrogels prepared in purified water.

2.1.2 Influence of formulation buffer composition on the rheology of HPMC hydrogels

In a next step, the influence of composition changes on the rheology of a 1.5% HPMC hydrogel were investigated. Poloxamer 188 (PX 188) had previously shown to be beneficial for the overall protein stability. However, the addition of surfactants to hydrogels could lead to viscosity changes [15]. Therefore, the addition of PX 188 to a 1.5% HPMC placebo gel was tested (Figure 6). Compared to a surfactant-free hydrogel, the addition of 0.05% PX 188 led to overall lower viscosities, whereas the shear thinning effect was not influenced. Overall, the viscosity changes after the addition of PX 188 were neglectable with regard to the further hydrogel development. Using the basic HY-133 formulation buffer instead of highly purified water as a dissolution media had only a minor impact on the rheology of the hydrogel. The substantially higher salt content in the buffer solution led to slightly lower viscosities. During the preparation of the hydrogel in a lab-scale manufacturing device (LabReactor), the excipient was dispersed by a rotor-stator device. This was accompanied with substantially higher shear stress during the preparation. However, the rheological characteristic of the resulting hydrogel was not influenced as the viscosity could be fully recovered.

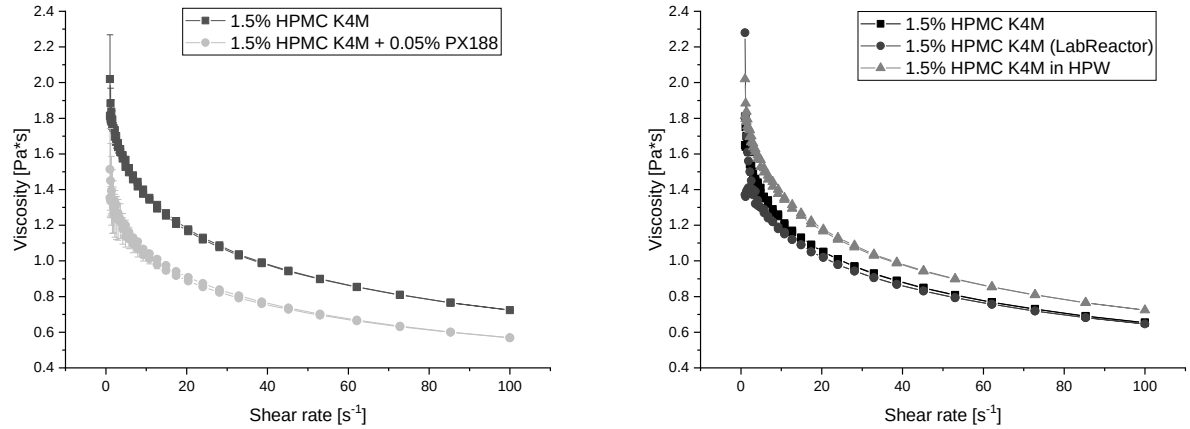

Figure 6: Influence on the rheology of HPMC hydrogels by the addition of PX 188 (left). Viscograms of 1.5% HPMC hydrogels dependent on the dissolution media (right).

A potential way to reduce a possible negative influence of HPMC on HY-133 stability was to reduce the overall HPMC concentration. Thereby, HPMC grades with higher gelling properties (e.g., 2% K15M: 13 Pa·s) could be used in lower concentrations (Figure 7). The overall viscosity of 0.5% HPMC K15M in the formulation buffer was only slightly increased compared to the formulation buffer itself and shear thinning could not be observed. In contrast, 0.5% K100M resulted in a shear-thinning viscosity profile which was comparable to a 1% HPMC K4M solution (compare Figure 7 with Figure 5). Thus, the lower K100M excipient concentration would suffice to overcome potential interactions with HY-133 which in turn result in API instabilities.

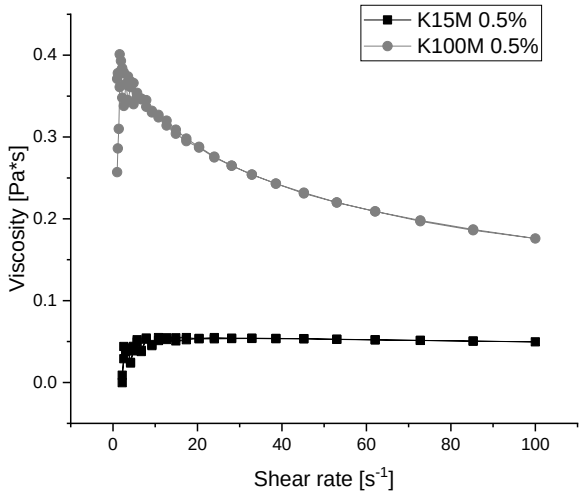

Figure 7: Viscograms of hydrogels consisting of low concentrations of K15M and K100M HPMC.

2.1.3 Pre-test summary

The pre-tests gave an overall impression of the possibilities but also limitations of a hydrogel as a delivery system for a nasal drug product. Variations in excipient concentrations allow precise adjustment of the hydrogel viscosity. This tool allows quick adaption to viscosity setpoints found throughout the developmental process. However, a viscosity limit of 2 Pa·s should not be exceeded to ensure that the final product is sprayable.

2.2 Hydrogel excipient screening studies

2.2.1 Hydrogel excipient screening study I – Short-term stability study with polysaccharides hydrogels

In a first preliminary screening study, several polysaccharides were tested for their compatibility with HY-133. Different hydrogels were prepared by dispersing 1% NaCMC, HPMC, xanthan gum and Gellan gum in the bulk formulation buffer. The hydrogels were mixed with HY-133 bulk solution to yield in a final drug concentration of 0.5 mg/ml. Mixing of the protein with Xanthan and Gellan gum hydrogels led to visible protein aggregation. Therefore, both hydrogels were excluded from further studies due to the apparent incompatibilities.

In a short-term stability study, the chemical stability of HY-133 in HPMC and NaCMC was determined after preparation at T0 and after 2 weeks of storage at 4 °C, 25 °C, and 40 °C. For this study, 1.5% of the respective gelling agent was dissolved in the formulation buffer. Within this study, the bulk formulation buffer as described in Chapter 5 was used. The buffer consisted of 25 mM HEPES, 150 mM NaCl, 10 mM $CaCl_2$, and 300 mM arginine at a pH of 6.5.

Chemical stability of HY-133 was determined by RP-HPLC after storage. The native HY-133 contents in NaCMC and HPMC hydrogel formulations are shown in Figure 8. Only 2 weeks of storage at 4 °C already led to a loss in native HY-133 content of about 25% in the NaCMC hydrogel. Storage at both 25 °C and 40 °C resulted in a near total loss in native protein content. In contrast, only a slight loss in native protein content was determined in the HPMC hydrogel at 4 °C storage after 2 weeks. Native HY-133 loss in HMPC was increased upon 25 °C and 40 °C storage, but to a much lesser extent compared to the NaCMC hydrogel.

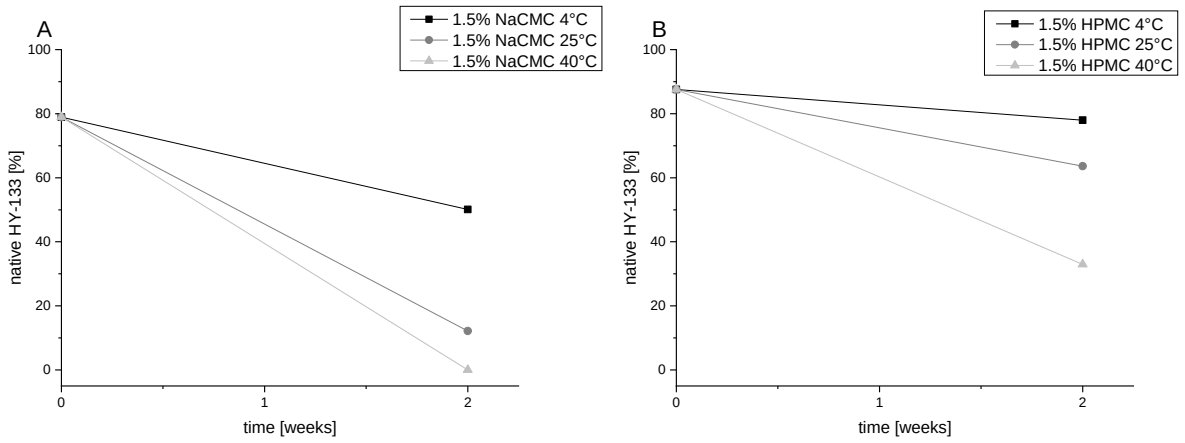

Figure 8: Native HY-133 content in NaCMC (A) and HPMC (B) hydrogels upon storage for two weeks determined by RP-HPLC.

Chemical stability of HY-133 in HPMC hydrogels was superior compared to NaCMC hydrogels. The ionic character of NaCMC, which is caused by the carboxy groups, might lead to an increased protein interaction compared to the non-ionic HPMC. Such strong electrostatic interactions of NaCMC with lysozyme were reported before [19]. Similar interactions might also explain the observed elevated loss in native HY-133. HPMC was therefore selected for the further studies.

2.2.2 Hydrogel excipient screening study II – Short-term stability study with polyvinylpyrrolidone (PVP) hydrogels

Different hydrogel matrices with 5 different polyvinylpyrrolidone (PVP) concentrations were evaluated as a possible drug product matrix in a second excipient screening study. These 5 variations included PVP concentrations from 1% to 20% in the formulation buffer. Again, a HY-133 stock solution was mixed with the PVP hydrogel to obtain a drug concentration of 0.5 mg/ml. The manufactured hydrogels were stored for 3 weeks at 4 °C and 40 °C and the stability was evaluated thereafter.

In Figure 9, the native HY-133 contents determined by RP-HPLC in the different PVP-hydrogels are displayed. After preparation (T0), an initial native HY-133 of about 80% was determined in most of the formulations. However, when compared to a reference HY-133 substance, native HY-133 was already reduced at T0. After storage at 4 °C for 3 weeks, a stable native protein content was determined in both lower concentrated PVP hydrogels (1% and 2.5% PVP). The other formulations had decreasing native protein contents dependent on the PVP concentration. Storage at 40 °C led to an accelerated decrease in HY-133 content with less than 30% remaining native protein content after 3 weeks of storage in formulations with ≥ 5% PVP.

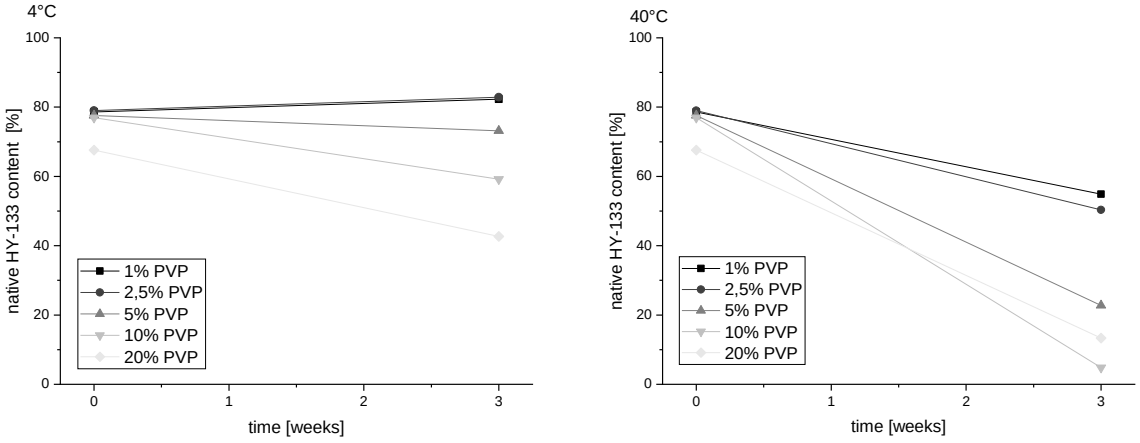

Figure 9: Native HY-133 contents of PVP hydrogel variations after storage at 4 °C (left) and 40 °C (right) determined by RP-HPLC

The main peak contents of HY-133 in PVP-hydrogels determined by IEX upon storage at 4 °C and 40 °C are shown in Figure 10. Here, no differences in main peak contents were observed upon storage, irrespective of the storage condition. However, the total protein recovery declined in the 20% PVP hydrogel upon storage at 4 °C, as it is shown in Figure 11. Storage at an elevated temperature of 40 °C led to a decrease in HY-133, dependent on the respective PVP concentration.

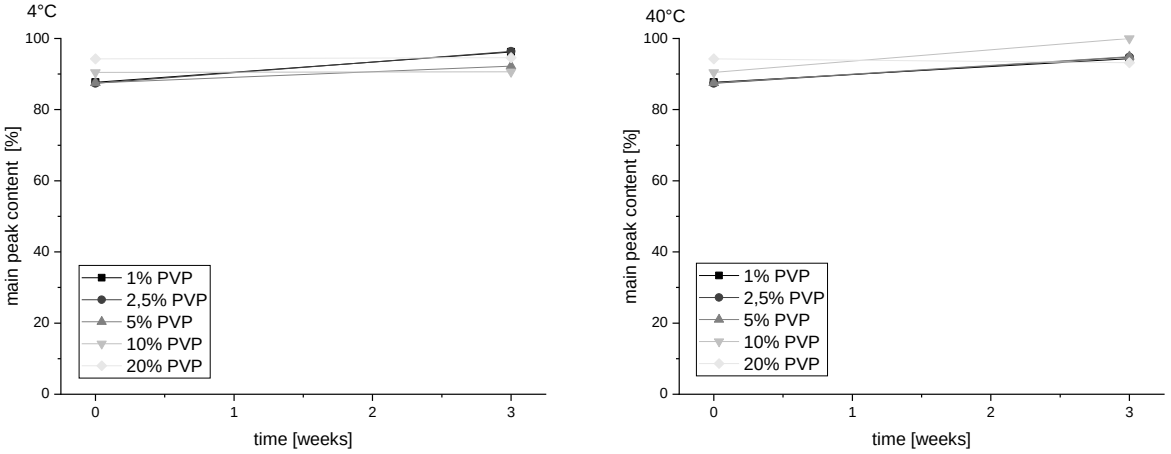

Figure 10: Native HY-133 contents of PVP hydrogel variations after storage at 4 °C (left) and 40 °C (right) determined by IEX-HPLC.

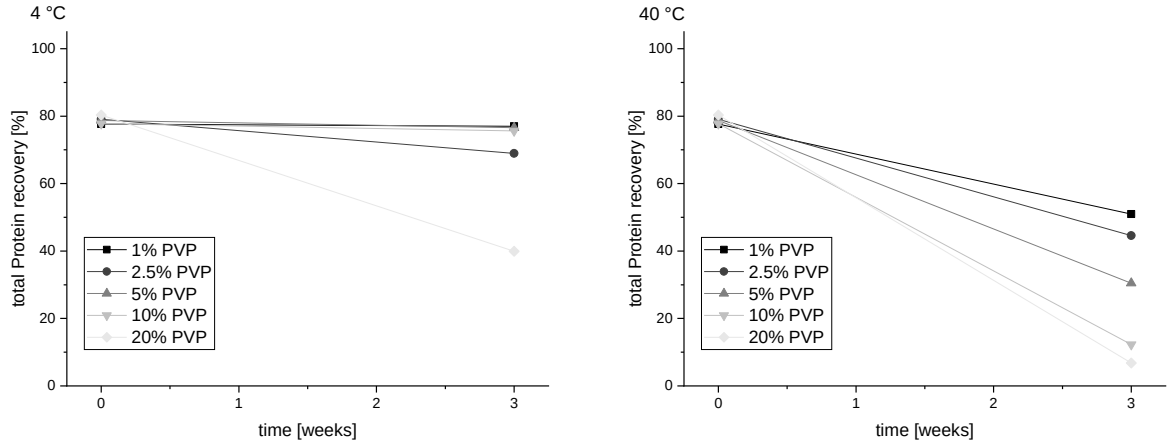

Figure 11: Total protein recovery of HY-133 in PVP hydrogel variations after storage at 4 °C (left) and 40 °C (right) determined by IEX-HPLC.

HY-133 stability in PVP-hydrogels was determined by SEC upon storage for 3 weeks at 4 °C and 40 °C and is displayed in Figure 12. Storage at 4 °C did not lead to the formation of higher or lower molecular weight species. In contrast, storage at 40 °C resulted in both aggregation and fragmentation of the protein dependent on higher PVP concentrations. The protein recovery varied from 80-100% at 4 °C storage and from 0-30% at 40 °C storage and tended to be lower with higher PVP concentrations.

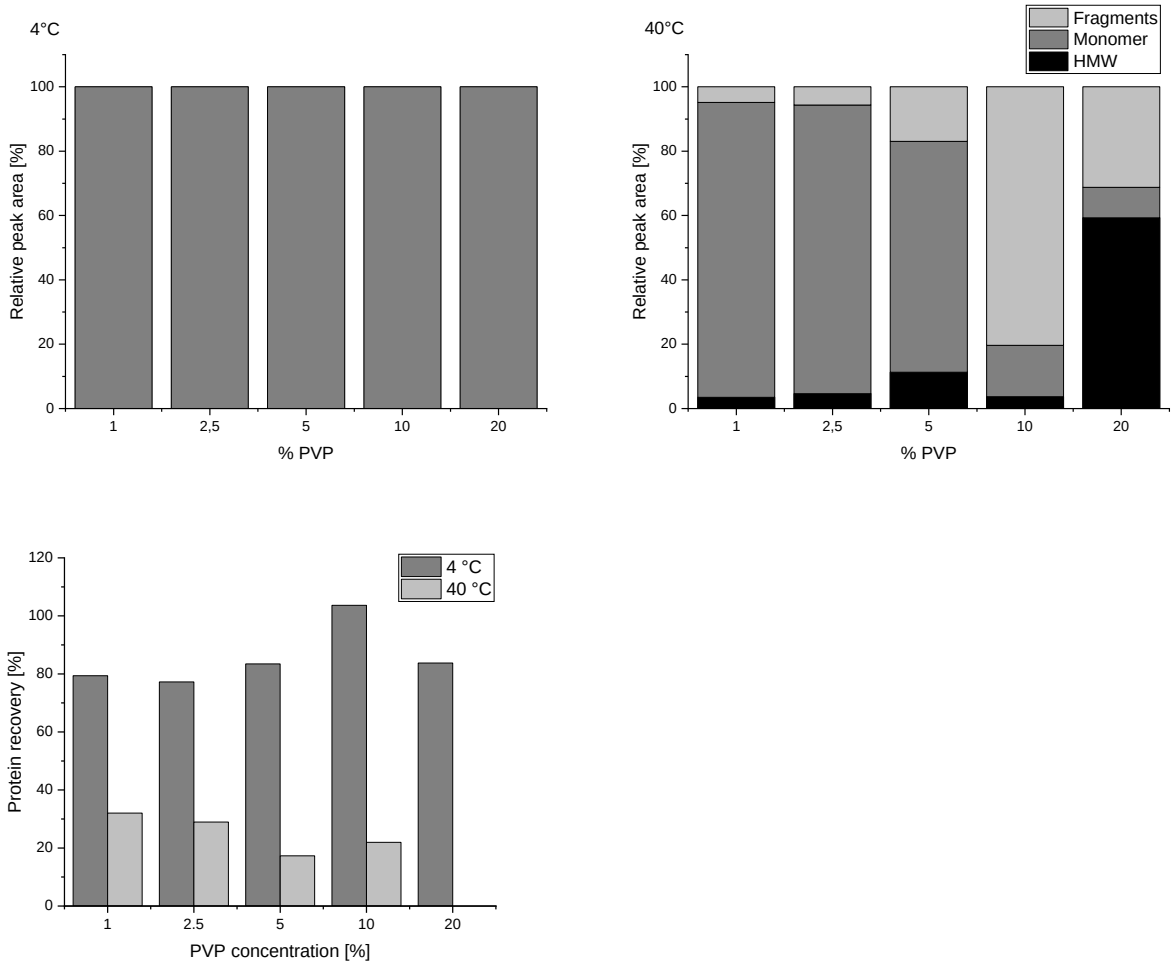

Figure 12: SEC results of PVP hydrogels containing 0.5 mg/ml HY-133 after 3 weeks of storage at 4 °C (top left) and 40 °C (top right). Protein recovery (monomer) determined with SEC (bottom).

A high increase of HMW species and fragmentated protein was determined with the Bioanalyzer after 2 weeks of storage at both storage conditions. Here, protein degradation was visible even upon storage at refrigerated condition. However, no clear trend towards a concentration dependent degradation was prevalent. The loss in monomer content was tremendous in all hydrogel variations and, compared to the results obtained by SEC, the amount of higher molecular weight species was increased in all of the formulations, independent of the storage condition (Figure 13).

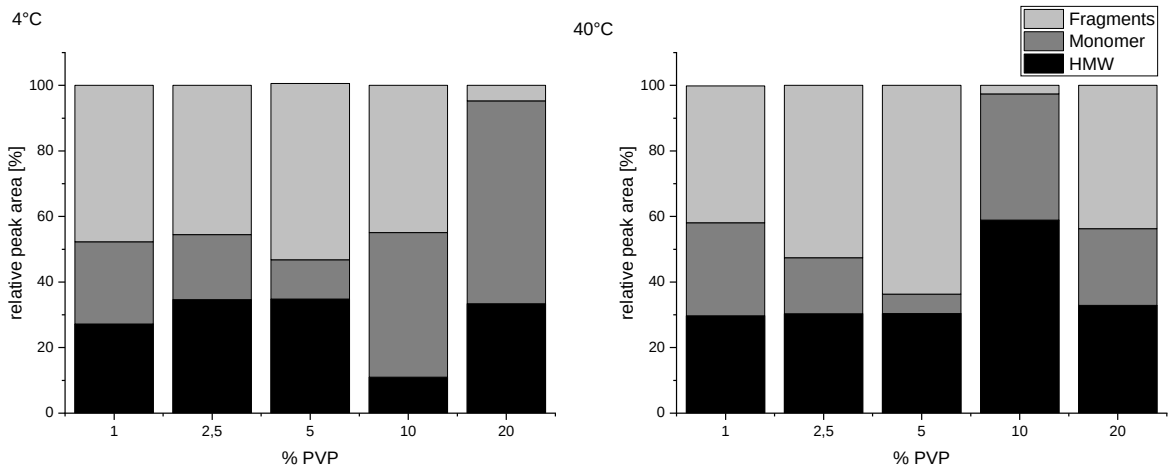

Figure 13: Relative HY-133 monomer, fragment and HMW content determined by Bioanalyzer. The results are shown after 2 weeks of storage at 4 °C (left) and 40 °C (right).

2.2.3 Screening study I & II summary

The pre-tests gave an overall first impression of the possibilities but also limitations of a hydrogel as a delivery system of a nasal drug product. All tested excipients were able to form hydrogels, therefore being in principal suitable for further investigations. However, Gellan gum was not suitable due to overall too high viscosities and its lack in rebuilding its viscosity upon shear stress. 1% NaCMC and 1% HPMC K4M resulted in less than 1 Pa·s, while Xanthan gum had a high initial viscosity of approximately 15 Pa·s.

Further, PVP hydrogels were not suitable as a drug product matrix for a HY-133 containing hydrogel. An initially lower native protein amount and increased chemical changes were measured especially at higher PVP concentrations. In addition, the monomer content of HY-133 was strongly reduced after 2 weeks of storage.

Based on the results of the pre-tests, HPMC was selected as a starting formulation matrix for further evaluation. The first test showed a generally good compatibility with the drug substance, a design space which allowed precise adjustment of hydrogel viscosity and variability in excipient grades.

3. Development of a HY-133 containing hydrogel (HyGel)

3.1 HyGel I – Definition of HPMC concentration, hydrogel pH and surfactant content

The first stage of the hydrogel (HyGel) formulation study was designed to evaluate the stability dependence of HY-133 on different hydrogel parameters like the HPMC concentration, the hydrogel pH and the surfactant content.

In this study, hydrogels with HPMC K4M as gelling agent were manufactured. The gelling agent was dissolved in the buffer which is described in Table 1. The 4 different HPMC concentration variations

ranged from 0.5% to 2.5% and were tested at a pH of 5.0 and 6.0. In addition, polysorbate 80 was added to the formulation and compared to the corresponding surfactant-free alternative. At the time of conducting this study, PX 188 was not set as the surfactant as stated in Chapter 5.

Table 1: HY-133 formulation compositions in the first HyGel study. All formulations were manufactured at a pH of 5.0 and 6.0. Each variation was examined with and without PS 80.

Excipient	Concentration
HEPES	25 mM
NaCl	150 mM
$CaCl_2$	10 mM
Arginine-HCl	300 mM
Methionine	10 mM
HPMC K4M (USP, Colorcon)	0.5%; 1%; 1.5%; 2.5%
pH	5.0 and 6.0
± Polysorbate 80	0.1 %

3.1.1 Surfactant-free formulations

The following section describes the evaluation of the stability of the surfactant-free formulations for up to 20 weeks at 4 °C, 25 °C, and 40 °C.

Chemical changes of the different hydrogel formulations over a storage time are shown in Figure 14. The native protein content decreased by up to 25% after storage at 4 °C. The decrease was independent of the formulation pH and the HPMC concentration with only minor differences between the formulation variations.

Elevated storage temperatures led to more distinct differences between the formulations. The loss in native protein was already more pronounced upon storage at 25 °C. The lower concentrated hydrogels resulted in more than 60% native protein content remaining, whereas in the two highest concentrations (1.5% and 2.5% HPMC) roughly 55% remaining native protein was found. These differences were even more pronounced at 40 °C. Already after 1 week of storage, 15% to 20% less native protein was found in all formulations. After 7 weeks of storage, a trend for higher loss in formulations with a higher HPMC concentration and lower pH values was observed. The lowest remaining protein content after 7 weeks was found in a 2.5% HPMC hydrogel at pH 5.0. After 7 weeks of storage at 40 °C, the analysis of the samples was discontinued.

Thus, higher HPMC concentrations tended to be unfavorable for the chemical stability of the protein.

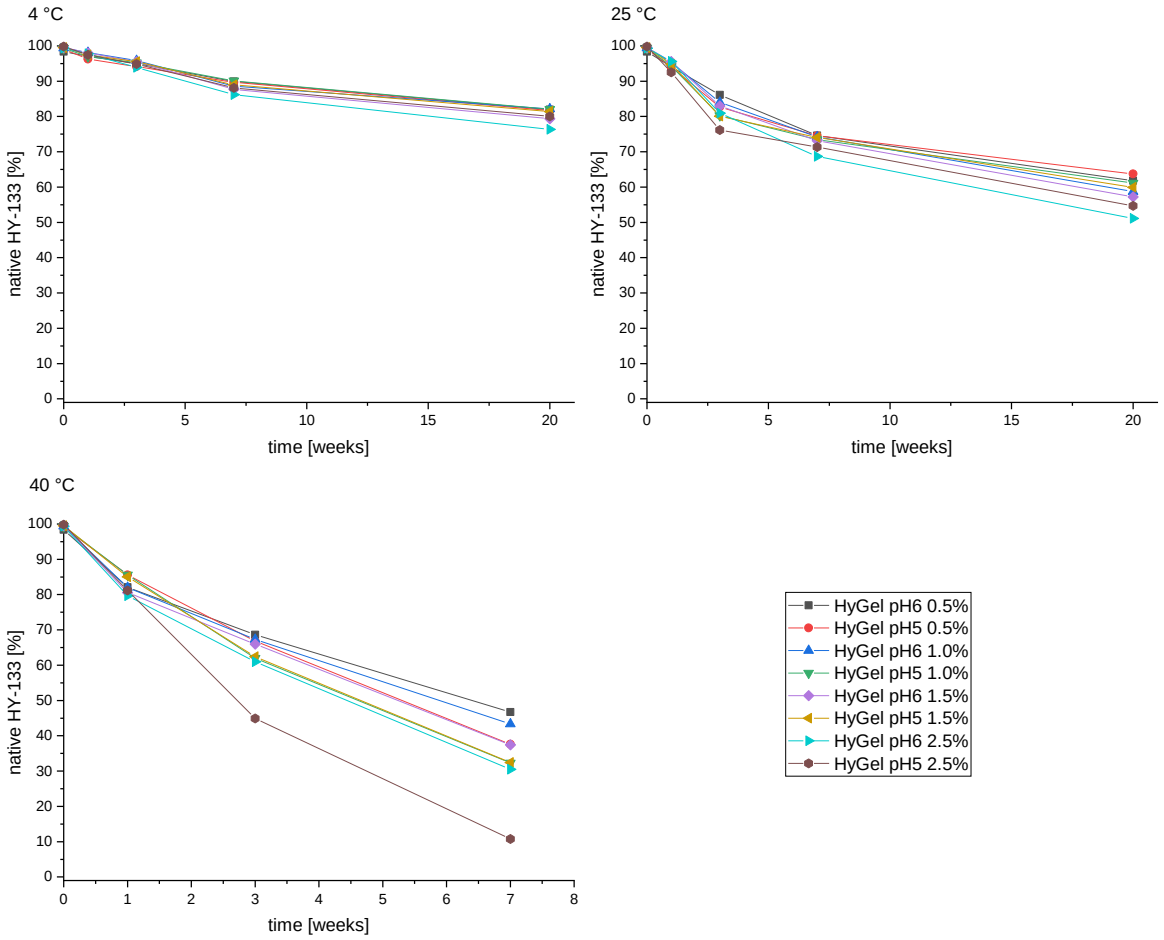

Figure 14: Native HY-133 of the different HY-133 in HPMC hydrogels determined by RP-HPLC. Samples stored at 4 °C and 25 °C were analyzed up to 20 weeks, while the 40 °C stored samples were not analyzed after 7 weeks due to the drastic decrease in native HY-133 content.

SEC (Figure 15) was used to determine the total recovery of the protein in a hydrogel after preparation (T0). In hydrogels containing ≤ 1% HPMC, the total protein content could be extracted out of the formulation matrix. Higher HPMC concentrations led to an extractable protein content of only about 75%. The separation of monomer from lower and higher molecular weight species was not implemented in this study due to insufficient separation and therefore missing higher and lower molecular weight species with the used column. It was hypothesized that higher HPMC concentration might not lead to full dosing of the API in the nasal cavity due to the lower extractable protein content. A final HMPC concentration of 1% might therefore be favorable.

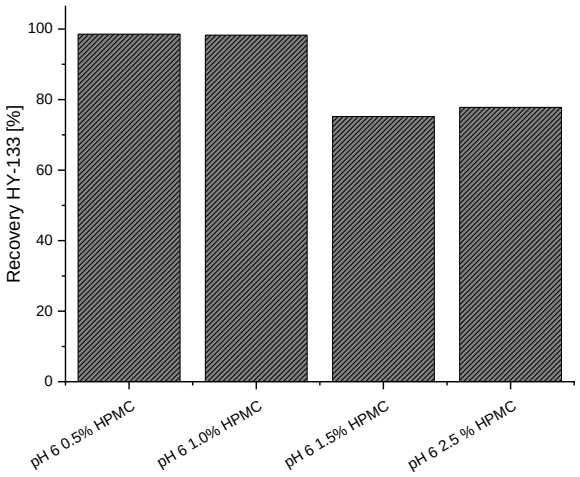

Figure 15: Total recovery of HY-133 determined with SE-HPLC after preparation at T0.

An overview of the activity of HY-133 in different hydrogel formulations is shown in Figure 16. In general, higher K_m values were observed in all formulations with pH 5.0, indicating lower HY-133 activity. In these formulations, the K_m gradually decreased with higher HPMC concentrations. All pH 6.0 hydrogels showed lower K_m values indicating higher activity. V_{max} varied throughout the different formulations with overall lower V_{max} values in higher concentrated hydrogel, indicating lower activity. Thus, formulations with pH 6.0 and 1-1.5% HPMC were favorable.

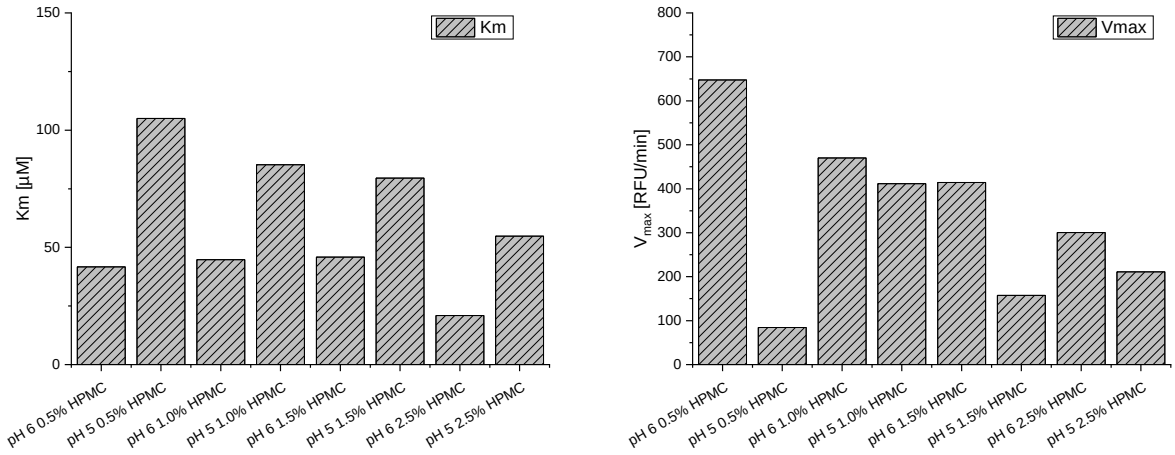

Figure 16: Activity measurements of the different HY-133 hydrogels at T0. Activity is given in K_m and V_{max}.

3.1.2 Formulations with Polysorbate 80 (PS 80)

In the following part, the stability of the formulations containing a surfactant (PS 80) was evaluated for up to 20 weeks at 4 °C, 25 °C, and 40 °C.

Rapid chemical degradation of HY-133 upon the addition of polysorbate 80 (PS 80) was determined in all hydrogel formulations. The loss of the native protein content over storage at different temperatures is displayed in Figure 17. Directly after the formulation of the drug substance, tremendously decreased

native HY-133 contents were determined in all of the formulations. The initial native protein content was around 60% for the lowest HPMC concentration, but already substantially reduced to 20% at the highest HPMC concentration. A further rapid loss of native HY-133 was observed at refrigerated conditions. Between 2% and 25% remaining native protein, dependent on the HMPC content, were determined after only 1 week of storage. At later time points, less than 10% protein content were determined. Storage at 25 °C and 40 °C led to near total loss in native HY-133 after only 1 week.

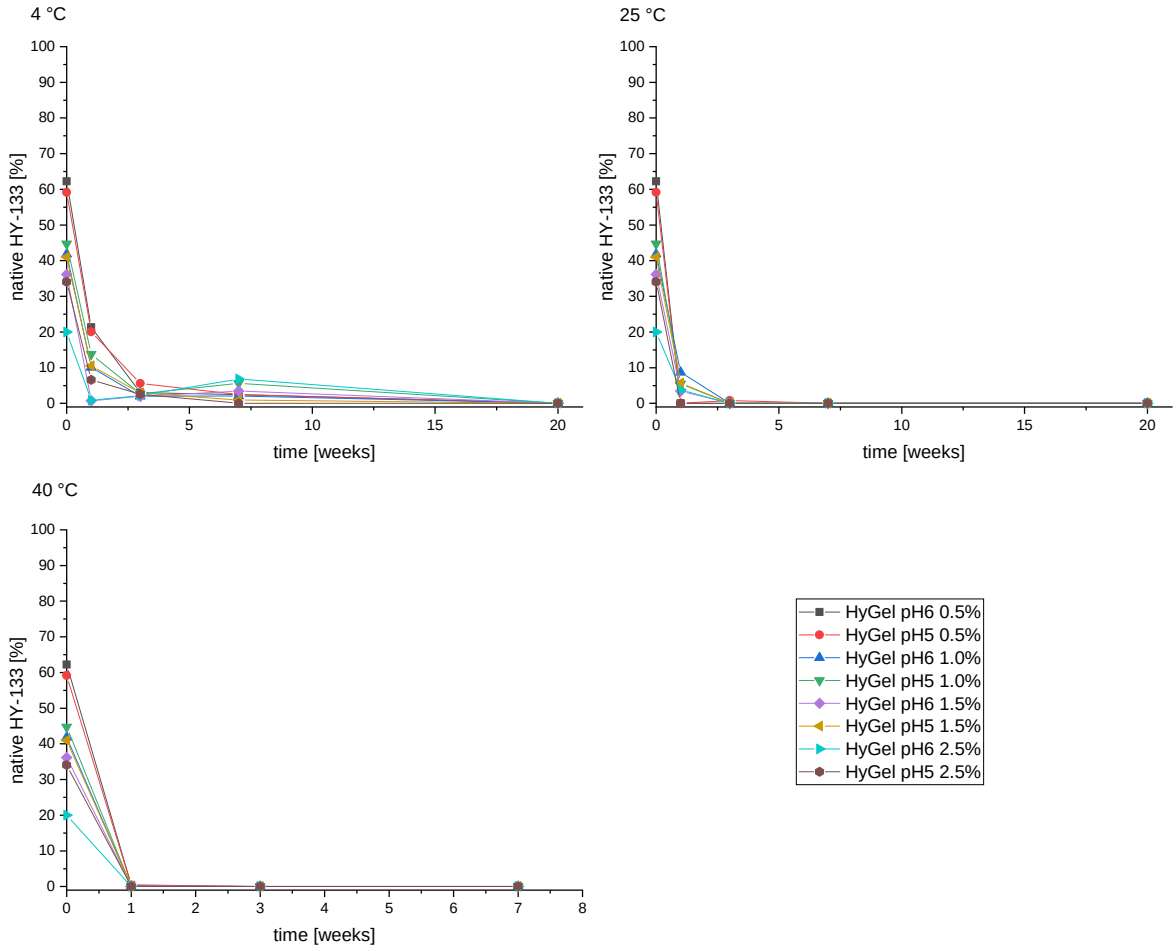

Figure 17: Native HY-133 of the different HY-133 containing PS80 in HPMC hydrogels determined by RP-HPLC.

An overview of the determined activities of the different hydrogel formulations after preparation is shown in Figure 18. Less activity can be observed compared to surfactant-free formulations (compare Figure 18 and Figure 16).

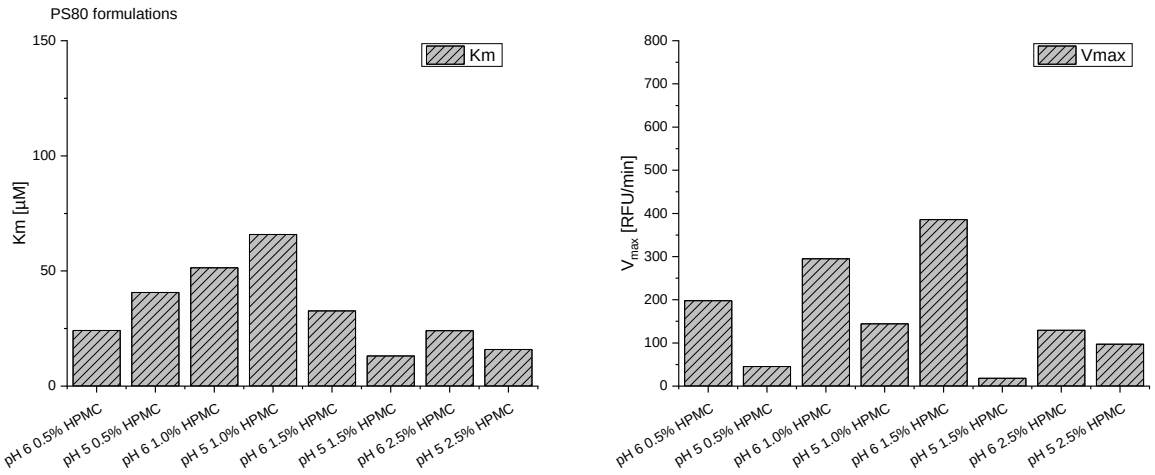

Figure 18: K_m and V_{max} measurements of the different HY-133 hydrogels with added PS 80 at T0.

3.1.3 HyGel I summary

In summary, it was shown that the addition of the gelling agent HPMC K4M can lead to changes in the physicochemical stability and the activity of HY-133. With respect to the surfactant-free formulations, the pH 5.0 variation showed lower chemical stability and higher K_m values compared to the pH 6 variation. Higher K_m values could be linked to a reduced activity, which could either be caused by the reduced amount of native HY-133 or by changed ionization rates connected to the lower pH value. The chemical stability was further reduced with higher HPMC concentrations at both pH values, indicating adverse effects caused by the presence of the gelling agent. Free radicals can form during the manufacturing process of HPMC, which can not only reduce the viscosity of the hydrogel, but also adversely affect the chemical stability of the API [20]. These free radicals might also be the reason for higher degradation profiles of HY-133 in HPMC hydrogels. The addition of methionine could mitigate the effect of these free radicals [20]. However, HPMC with a higher purity profile might also solve this formulation challenge.

PS 80 containing formulations showed already lower chemical stability at T0 compared to the surfactant-free hydrogels. Over the course of the stability study, fast degradation of all hydrogel variations indicated highly compromised formulation stability resulting from the addition of PS 80. Residual peroxides in PS 80 can trigger and enhance chemical changes of proteins [21]. Free radicals present in certain HPMC excipients might amplify the formation of peroxyl radicals and therefore lead to a substantial increase of chemically degraded HY-133.

Thus, the addition of PS 80 to the HY-133 hydrogel formulation was not feasible regarding the overall stability of the drug product and was dismissed from further examination.

In summary, PS 80-free, low concentrated HPMC hydrogels with a pH of 6.0 were determined as the most stable formulation. Yet, the overall stability of the drug product was still not comparable to the liquid HY-133 formulation. Therefore, a second hydrogel formulation study was performed.

3.2 HyGel II – Selection of different HPMCs

Previous steps of the hydrogel development have shown that HY-133 is not equally stable in a HPMC hydrogel compared to the liquid formulation. So far, it is not known whether the accelerated decrease in active HY-133 was caused by direct interaction of HY-133 with HPMC or by impurities originating from different HPMC qualities. Therefore, we screened the market for different HPMC manufacturers and included different HPMC substitution grades and lots. A follow-up study was designed to evaluate the usability of different HPMC types and manufacturers as a hydrogel matrix for the final drug product.

In general, HPMC types can be divided into different substitution types and grades. Four different substitution types are described in the USP, of which 2 were selected due to their general suitability [22]. Type 2208, also referred to as type "K", is used in most of the formulations within this study. This type is known to have a high hydrophilicity [23]. Type 2910, also known as the "E" type with medium hydrophilicity, is used in 2 formulations within this study [24]. The different HPMC types differ in their substitution grade, specifically in their methoxyl and hydroxypropyl contents. For example, type 2910 refers to an average methoxyl group content of 29% and an average hydroxypropyl content of 10% [22]. In addition, up to 4 different grades, which reflect the viscosity of a 2% solution and correspond to different average molecular weights, were examined throughout this study. This selection ranged from very low viscosity to the high viscosity HPMC grade, e.g., E50 to K200M, respectively.

In total, 14 different HPMCs from 4 different manufactures were used in this formulation study. An overview of the different HPMC types is shown in Table 2. All excipients are multi-compendial and fulfil the requirements of EP, USP and JP.

Table 2: Overview of the different HPMCs used for the 2nd HyGel stability study.

#	Manufacturer	HPMC type	Lot	Average Molecular weight [kDa]	Nominal viscosity [mPa·s] of 2% solutions in water
1	Ashland	Benecel K100M	1726998	1,000	75,000 - 140,000
2	Ashland	Benecel K200M	1895171	1,200	150,000 - 280,000
3	Ashland	Benecel K4M	1681277	400	2,700 - 5,040
4	Ashland	Benecel K200M	1993913	1,200	150,000 - 280,000
5	Colorcon	Methocel K100M	DT 429501	1,000	75,000 - 140,000
6	Colorcon	Methocel K15M	DT 427044	575	13,500 - 25,200
7	Colorcon	Methocel K4M	DT 420749	400	2,300 – 3,750
8	Colorcon	Methocel K4M	DTR 452622	400	2,300 – 3,750
9	Colorcon	Methocel E4M	DT 443604	400	2,300 – 3,750
10	Parmentier	Mantrocel K4M	2015-10-180B	400	2,700 - 5,040
11	Parmentier	Mantrocel K100M	2015-10-180C	1,000	75,000 - 140,000
12	JRS Pharma	Vivapharm K4M	14277/17	400	2,700 - 5,040
13	JRS Pharma	Vivapharm K15M	13878/17	575	13,500 - 25,200
14	JRS Pharma	Vivapharm E50	13093/16	91.3	50

It was defined in the pre-tests that a viscosity of up to 2.0 Pa·s was suitable for adequate spray dosing when using a commercial nasal spray container. Within the second HyGel development study, the content of the different HMPCs was kept constant at 1% and changes in viscosity, even when exceeding 2.0 Pa·s, were neglected. The different formulations were formulated in the final formulation buffer (Table 3) and a HY-133 stock solution was spiked to a final drug concentration of 0.5 mg/ml. The formulations were stored in glass vials at 4 °C and 40 °C for up to 7 months.

Table 3: Formulation composition used in the second hydrogel study.

#	Excipient	Concentration	pH	Surfactant
1	HEPES	25 mM		
2	NaCl	150 mM		
3	$CaCl_2$	10 mM	6.0	+ 0.1% PX188
4	Arginine-HCl	300 mM		
5	Methionine	10 mM		

3.2.1 Viscosity measurements

Figure 19 displays the viscograms of the lower viscosity HPMC types. 1% HPMC E50 in the formulation buffer did not form a hydrogel and therefore did not show enhanced viscosity values. In contrast, all K4M and E4M variations resulted in solutions with comparable viscosities. At a shear rate of 10 s^{-1} and viscosities of about 0.3 to 0.4 Pa·s were determined, with trends towards higher viscosities for the E4M variation. All formulations showed comparable shear thinning behaviors. With viscosity values < 2 Pa·s, all K4M and E4M variations were sprayable.

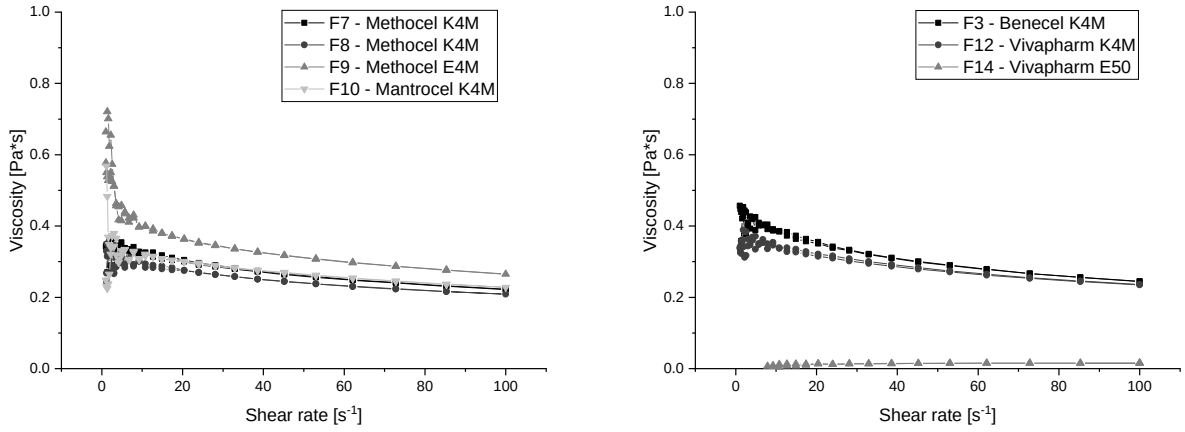

Figure 19: Viscograms of hydrogels including 1% HPMC K4M, E4M or E50, respectively.

The viscograms of the medium grade HPMC variation K15M are shown in Figure 20. While nominal grades are similar, the obtained viscosities differ between the two excipients. Methocel K15M from Colorcon showed substantially higher viscosities compared to the K4M grade from the same manufacturer. In contrast, Vivapharm K15M showed much lower viscosities, which were comparable to K4M grade HPMCs.

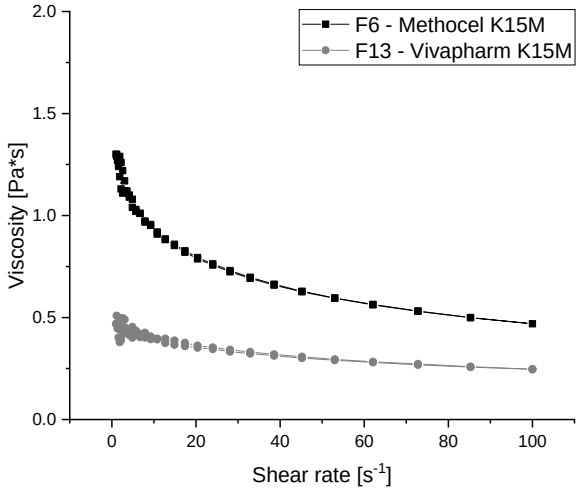

Figure 20: Viscograms of hydrogels including 1% HPMC K15M from two different manufacturers.

The viscograms of the K100M and K200M grade HPMC hydrogels are shown in Figure 21. All 3 K100M grades showed comparable viscosities and shear thinning effects. The viscosities were substantially lower at higher shear rates. Here, no rheological variations between the different manufacturers were evident. Both K200M variations resulted in much higher viscosities. The shear thinning effect was more pronounced as in K100M hydrogels and the obtained viscosities were comparable to the K100M variation at high shear rates. However, all 5 hydrogel variations could not be sprayed due to the high initial viscosities and were therefore not suitable as a sprayable hydrogel drug product. Nevertheless, all variations were included in the stability study to determine possible incompatibilities.

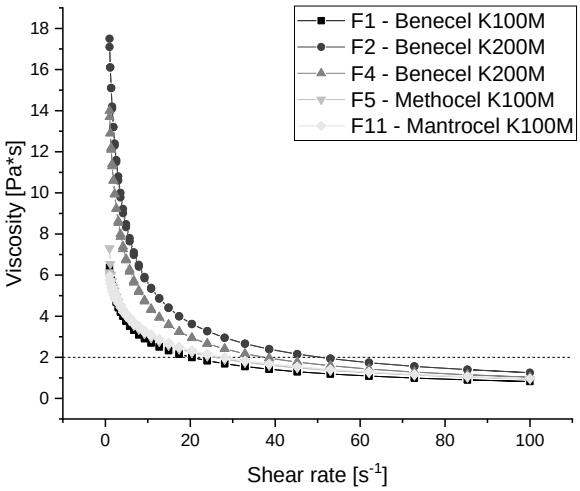

Figure 21: Viscograms of hydrogels including 1% HPMC K100 or K200M, respectively. The dotted line represents the viscosity limit for the hydrogel being able to be sprayed.

3.2.2 Physicochemical characterization of the different HPMC hydrogels

Chemical and conformational stability of HY-133 in the 14 different hydrogel variations were analyzed over a storage period of up to 23 weeks. The hydrogel formulations were compared to a reference standard in the same formulation buffer (Chapter 5, Table 11) without HPMC. Previous stability studies of the drug substance formulation showed that HY-133 may not only face difficulties maintaining its chemical integrity over time, but that aggregation and fragmentation can also occur over time.

The chemical stability of HY-133 in different hydrogels upon storage for up to 23 weeks at 4 °C and 40 °C was determined with RP-HPLC and IEX-HPLC.

The results of the RP-HPLC measurements are summarized in Figure 22. Native protein contents were determined to be 80-95% after 6 months storage at 4 °C, with formulation F8 performing best. Formulation F5 resulted in <40% after 6 months.

Storage at an elevated temperature of 40 °C showed total degradation of HY-133 over time. However, the degradation profile differed between the formulations and over time. The first time point after 6 weeks is of highest interest, as the observed differences between the formulations are most pronounced. Here, formulation F1, F3, F5-F8 and F11 were the most stable formulations. These formulations were comparable to the reference sample. Most degradation was observed in formulation F10, which was not comparable to 4 °C results.

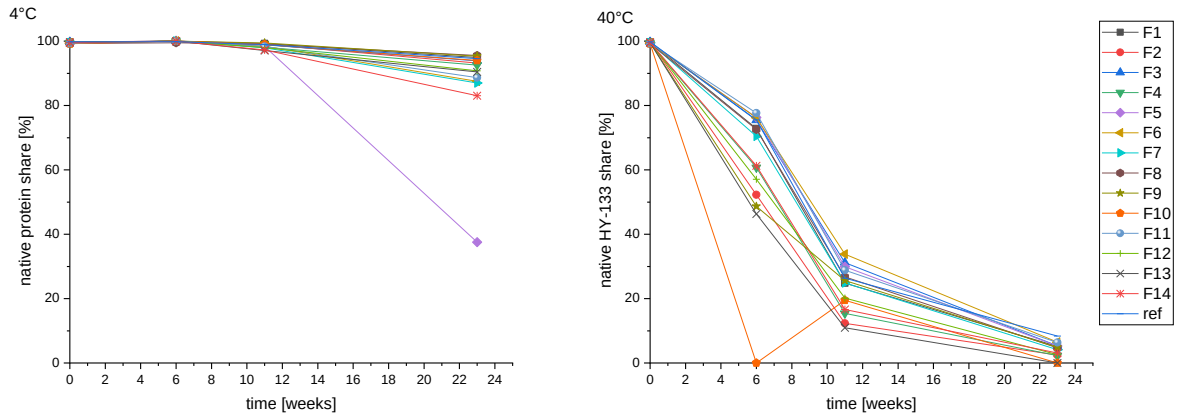

Figure 22: Native protein share [%] of the hydrogel formulations upon storage at 4 °C (left) and 40 °C (right) for up to 23 weeks determined by RP-HPLC.

Additionally, the chemical degradation of HY-133 was determined with IEX-HPLC. The results are displayed in Figure 23. All formulations showed high main peak contents, which were comparable with the 97% main peak content in the reference sample upon storage at refrigerated condition for up to 23 weeks. Storage at 40 °C led to a higher decrease in the main peak content in formulation F9 and F13 after only 6 weeks of storage. The remaining formulations showed more than 85% main peak content after 6 weeks without major differences between the formulations. Similar results were

obtained after 11 weeks of storage with approximately 50% main peak content left in all of the formulations. None of the samples could be evaluated after 23 weeks of storage due to their complete loss in main peak content. Therefore, no results are shown after 23 weeks of storage at 40 °C.

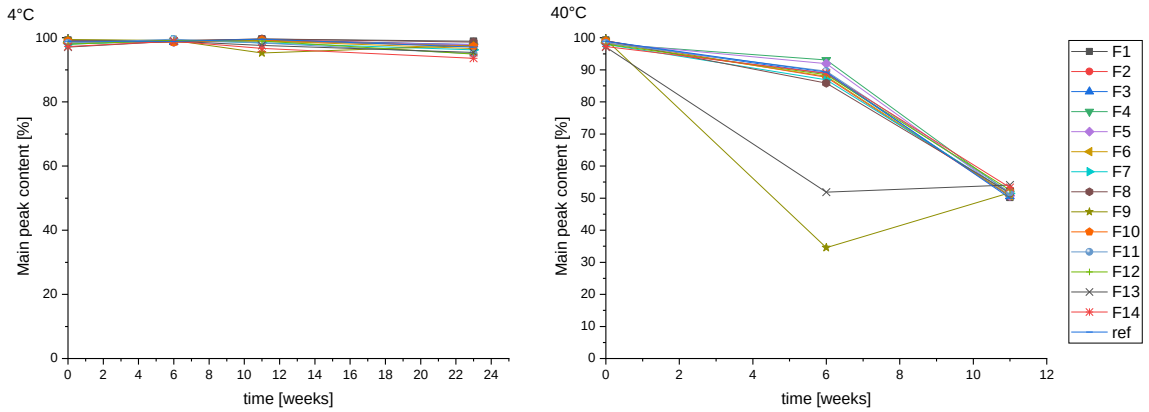

Figure 23: Main peak contents [%] of the hydrogel formulations upon storage at 4 °C and 40 °C for up to 23 weeks determined by IEX-HPLC. Data from 40 °C after 23 weeks of storage were not evaluable and are therefore not shown.

3.2.3 Conformational stability

Aggregation and fragmentation rates of HY-133 in the different hydrogels were determined by SE-HPLC after 6 months of storage at 4 °C and 40 °C (Figure 24). In general, the different formulations showed no aggregation and only slight fragmentation upon storage at 4 °C. No major differences were apparent between the different formulations, only a minor trending towards higher aggregation rates in formulation F12 and F13 was observed. Storage at 40 °C resulted in 35 – 55% fragmented protein species, irrespective of the formulation. In addition, elevated contents of higher molecular weight species were determined in formulations F2, F4, F12 and F13.

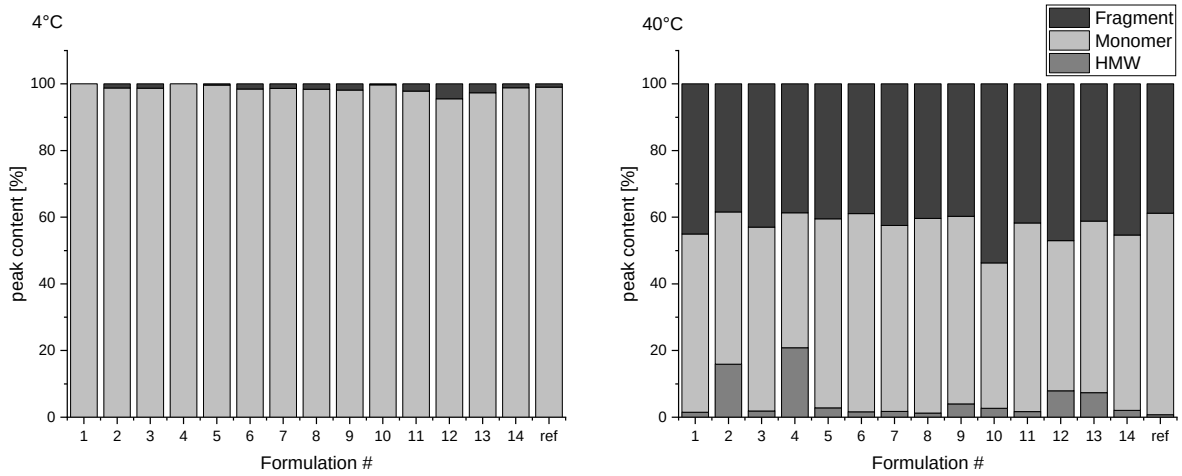

Figure 24: Fragment-, monomer- and HMW-shares of HY-133 hydrogel formulations upon storage at 4 °C (left) and 40 °C (right) for 23 weeks determined by SE-HPLC.

3.2.4 Protein recovery

In Figure 25, the total protein recovery determined by SEC upon storage for 6 months is illustrated. Protein recovery was compared to a freshly thawed reference substance, which is marked with the 100% line in red. In general, the majority of the formulations showed high protein recovery after 6 months of storage at 4 °C. The recovery was reduced in formulations F1-F4. In F1, 90% remaining protein was determined, whereas an even higher decrease was observed in F2-F4. Except for formulation F3, all of these excipients were K100M and K200M HPMC types, which resulted in hydrogels with higher viscosities and might affect the overall protein recovery rate. The total protein recovery decreased in most of the formulations to 80 – 90% upon storage at 40 °C. Formulation F10 showed a substantially lower protein amount with only 50% remaining. Formulation F4 showed an apparently increased protein content, which might be caused by scattering effects originating from higher molecular weight species at this storage condition. Interestingly, the recovery rate was lowest in this sample after storage at 4 °C, indicating an overall compromised protein stability. Overall, formulations F5, F6, and F9 were performing best with respect to protein recovery.

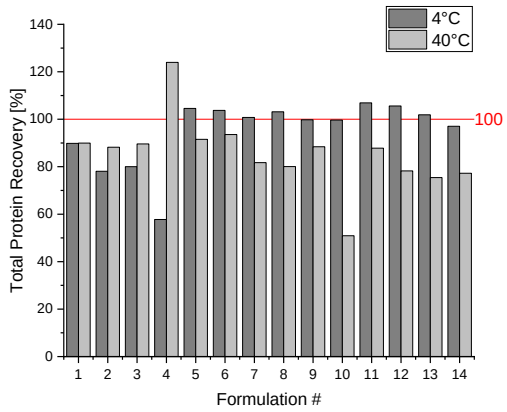

Figure 25: Total protein recovery after 23 weeks of storage, determined by SEC.

3.2.5 Specific activity of HY-133 hydrogels

The specific activity of the different HY-133 hydrogel variations was determined with the non-validated FRET-method. Therefore, the different time-points could not be directly compared. However, the results can be compared to the activity of the reference substance. Figure 26 shows the K_m values of the different hydrogel formulations upon storage at 4 °C for 11 and 23 weeks. All formulations showed a specific activity after storage for up to 23 weeks and were comparable to the activity of the reference substance. Slight variations were determined between the hydrogel formulations, but were within the measuring accuracy. The different HMPC qualities and viscosities did not result in larger activity differences upon storage.

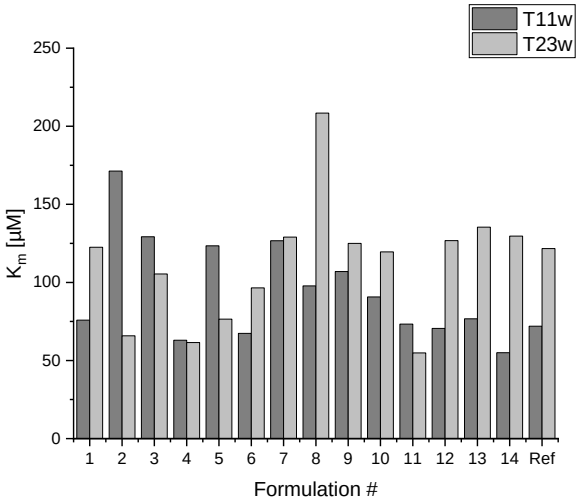

Figure 26: Specific activity of the HY-133 hydrogel formulations and the reference substance upon storage at 4 °C for 11 and 23 weeks.

3.2.6 Summary of selected HyGel II formulation and direct comparison with the drug substance

In general, formulations with 1% HPMC K4M, E4M, K15M or E50M could be sprayed using a commercial multi-dose delivery system and were therefore overall suitable for nasal administration. In contrast, the higher viscosity grade HPMC variations, 1% K100M and K200M, could not be sprayed with the respective device, but compatibility with the protein was evaluated, nevertheless. The combination of the chemical and physical characterization of the different hydrogels enabled a precise selection of excipients, with comparable stability as the reference substance. To demonstrate the differences of the tested HPMC excipients, summarizing radar plots are shown in Figure 27. RP- and IEX-HPLC showed chemically instabilities of HY-133 in formulations F5 (K100M), F6 (K15M), F7 (K4M), and F14 (E50). However, as only few of the used excipients of each grade led to a decrease in protein stability, a general incompatibility with these excipients can be excluded. Presumably, differences in excipient quality between the different manufacturers could cause the observed variations in chemical stability of HY-133. This phenomenon was also evident in formulation F7 and F8, which both contained HPMC K4M from Colorcon from two different lots. These two hydrogels showed small differences in the chemical stability of HY-133 upon storage, which might be caused by batch-to-batch variations of the gelling agents.

It can be concluded that despite the small differences in HY-133 stability with different HPMC grades, sufficient protein stability could be provided at 4 °C in the majority of the formulations. Therefore, storage of the final HyGel formulation is recommended at refrigerated conditions. In general, low viscosity HPMC grades (K4M, E4M) perform better compared to high viscosity HPMC grades (K100M, K200M).

In this study, F8 and F9 showed the overall highest physicochemical stability and protein recovery over time (Figure 27). Also, both formulations showed no differences in activity at the end of the study.

However, stability differences were apparent in 40 °C storage conditions, where intermediate time points showed a higher chemical degradation in F9 compared to F8. Therefore, formulation F8 was selected as excipient to be used in the final drug product.

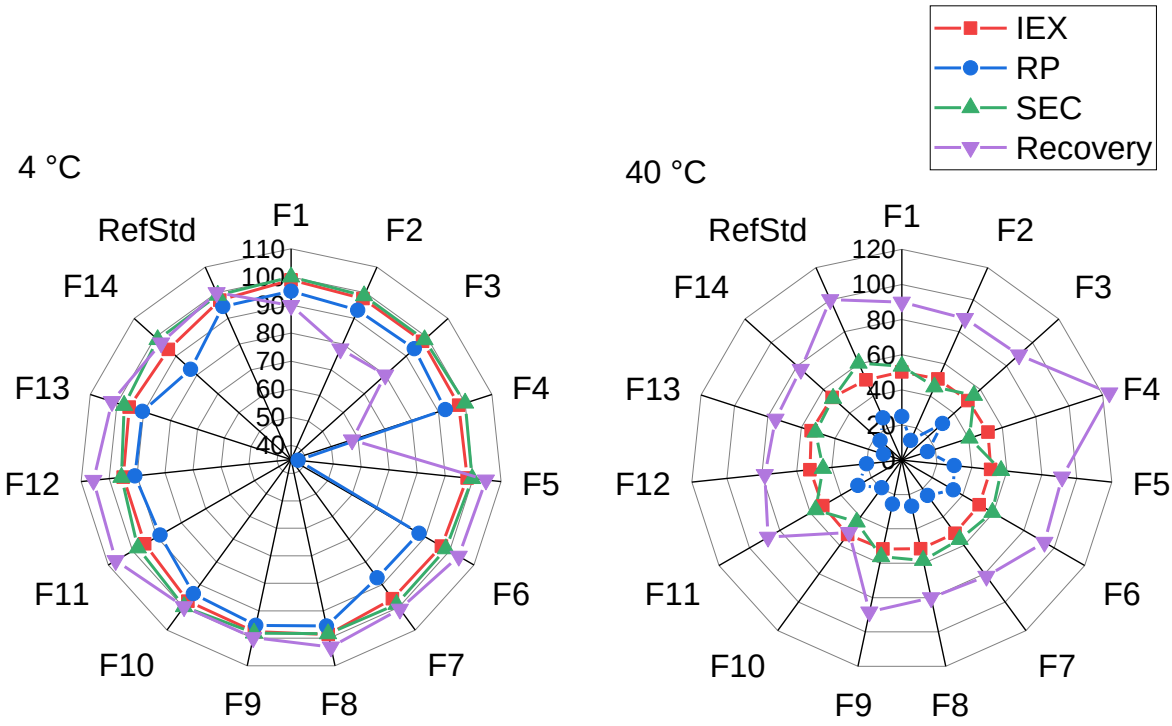

Figure 27: Summary of the results of the second hydrogel study. Radar plots show physical and chemical stability of HY-133 in the different hydrogels upon storage for 23 weeks at 4 °C and 11 weeks at 40 °C.

3.2.7 Stability indicating study of selected formulation

After 6 months of storage at 4 °C, the chemical stability of the selected hydrogel formulation was compared to an equally stored reference (Figure 28A). The final liquid formulation of HY-133 (see Table 1, pH=6.0) was used as reference material. The native HY-133 share in the hydrogel was similar compared to the reference. Therefore, it can be concluded that the hydrogel formulation did not change the chemical stability of HY-133. In addition, the activity of the selected hydrogel formulation (F8) was determined after 6 months of storage at 4 °C with the validated activity method and compared to the equally stored reference and a freshly thawed drug substance. The results are shown in Figure 28B. The specific activity of HY-133 was comparable in all three variations. Therefore, the drug product can be considered as equally stable as the reference regarding its specific activity and its physicochemical stability.

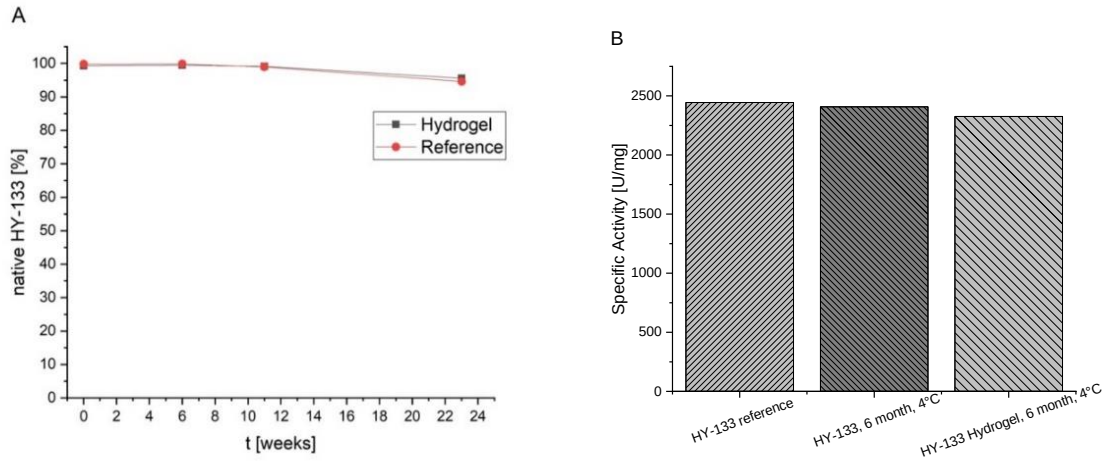

Figure 28: Compared to the reference substance (drug substance), chemical stability was not affected by the addition of Methocel K4M (A). Additionally, the specific activity of HY-133 as on the same level as a freshly thawed sample and the similar stressed reference substance (B).

The reference and the hydrogel were additionally tested using a disk diffusion test. An agar plate was inoculated with *S. xylosus* and the HY-133 reference substance as well as the HY-133 hydrogel at 0.5 mg/ml were directly pipetted in pre-defined sectors of the agar plate. All 4 tested samples were able to effectively inhibit the bacterial growth on the agar plate, which could be characterized by defined zones of inhibitions. The sizes of these zones of inhibition varied with the administered doses. As the HY-133 reference (Figure 29, A) was able to freely spread on the agar plate, the zone of inhibition was larger compared to that of a hydrogel of similar volume.

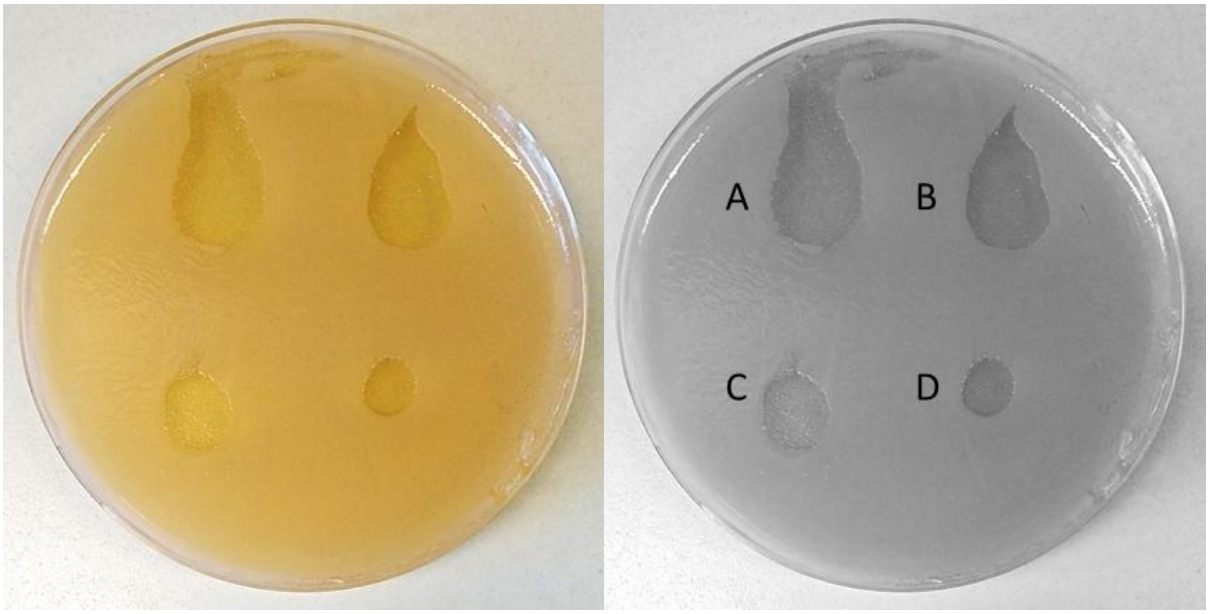

Figure 29: Disk diffusion test with 20 µl of a 0.5 mg/ml HY-133 liquid formulation (A) compared to 3 different doses of the respective hydrogel formulation. Each 20 µl (B); 10 µl (C) and 2 µl (D) of a 0.5mg/ml in 1.5% HPMC K4M hydrogel were compared with the liquid formulation. The same agar plate is shown in its original (left) and as a colorless variation (right).

3.3 Release testing of HY-133 containing HPMC hydrogels

The release of HY-133 from a HPMC K4M hydrogels (F8) was determined in two different HPMC concentrations. A 1.5% and a 2.5% HPMC concentration were used as low and high viscosity variations of the developed formulation. For this, a fluorometric release test was developed in-house (Chapter 3). Briefly summarized, an exact amount of a HY-133 hydrogel was surrounded by an acceptor medium and the concentration per well was determined fluorometrically over time. The fluorometric release method was used because well-established release testing methods for topical systems normally target transdermal delivery of small molecules. Such test methods are based on the diffusion of a drug product through a membrane, which was not intended for the treatment of *S. aureus*. In addition, such membrane systems are not available for medium sized proteins such as HY-133, which is intended to directly target surface-bound *S. aureus*. Therefore, a direct measurement method which is based on the release of a drug from a matrix system, such as a hydrogel, was established. For this, the surrounding acceptor medium was specifically selected to provide a composition and an ionic strength comparable to a typical nasal fluid. Early tests showed that the hydrogel erodes only slowly and that the drug release was mostly based on diffusion. These diffusion effects are mainly driven by the concentration of the diffusing substance, in this case the drug substance HY-133. This effect was first described by Fick's first law of diffusion with the following equation: $J = -D \cdot (dC/dx)$ [25].

In-vitro release testing (see Chapter 3, section 2.17) was performed with two hydrogels: a 1.5% HPMC K4M and a 2.5% HPMC K4M hydrogel, each containing 0.5 mg/ml HY-133. The respective cumulative release curve is shown as an average of 3 independent measurements with the corresponding standard deviation in Figure 30. Both hydrogels showed a reproducible release with very low standard deviations. The release itself was clearly dependent on the HPMC concentration. The 1.5% HPMC hydrogel showed an almost complete release after 10 minutes. This indicates that a generally complete release of the drug product is possible and substantial retention of HY-133 at this HPMC concentration is not likely. By contrast, the higher HPMC concentration of 2.5% led to a substantial prolongation of the HY-133 release. After 10 minutes, only 60% of the contained drug product was released. Contrary to the lower concentrated hydrogel, the HY-133 release was not completed by the end of the measurement after 23 minutes. The lower concentrated hydrogel also showed a burst release with more than 20% initially available drug product, compared to only 10% in the 2.5% HPMC hydrogel.

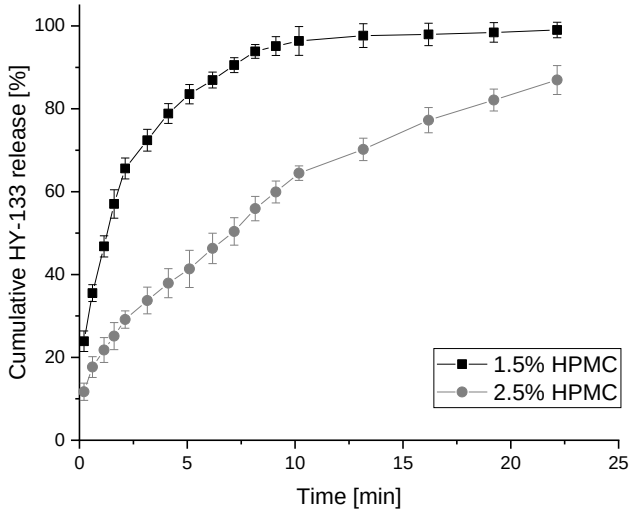

Figure 30: HY-133 release profile of 1.5% and 2.5% HPMC hydrogels (n=3).

The release data of the two exemplary hydrogels indicate that in addition to the increased residence time of the hydrogel, a slightly sustained release of HY-133 in the hydrogel can be achieved. With this, the HY-133 hydrogel provides a prolonged effective time. However, the cumulative release curve from the lower concentrated HPMC hydrogel indicated that a decrease of the gelling agent leads to a faster release of HY-133, eventually reaching a non-sustained release behavior. A further reduction of the HPMC concentration to 1% was tested in a later stage of the hydrogel development. There, substantially lower viscosities were determined, which would increase the HY-133 release speed even further.

To determine the overall release kinetic, the in-vitro release data was fitted to 4 commonly used release models: Zero order, First order, Higuchi and Korsmeyer-Peppas. The respective equations are shown in Table 4, with Ct being the drug concentration released at time t, C0 being the concentration at the start of the release curve, k being the release constant and n the release exponent of the Korsmeyer-Peppas equation. The release models were ranked according to the adjusted R2, which serves as a goodness of fit measurement. In general, the release curve of the 2.5% HPMC hydrogel showed a better fit to the tested models than the 1.5% HPMC hydrogel. The best fit for both hydrogel concentrations was achieved with the Korsmeyer-Peppas model (Figure 31), followed by the first order model and the Higuchi model.

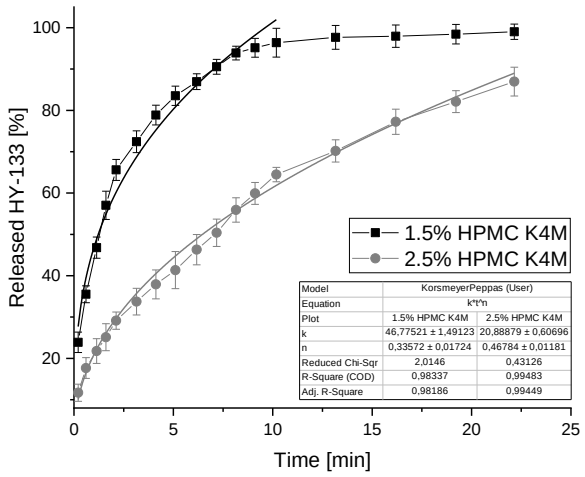

Figure 31: Release curves of 1.5% and 2.5% HPMC K4M hydrogels containing HY-133. The curves were fitted using the Korsmeyer-Peppas release model.

As shown in Table 4, the Korsmeyer-Peppas model not only takes the release constant into account, but also includes a release exponent *n* [26]. This release exponent allows to draw further conclusions about the release mechanism [27]. A release exponent n ≤ 0.5 indicates that Fickian diffusion rather than erosion is the main release mechanism [28]. A release exponent of n = 0.5 represents a special case as this denotes the Higuchi model. At n values > 0.5, swelling and erosion rather than diffusion is the dominant release mechanism [29], [30]. The estimation of the Korsmeyer-Peppas model suggested a release exponent value of 0.34 and 0.46 for the 1.5% and 2.5% HPMC hydrogels, respectively. The estimated release exponent values are in line with results from the first description of the Korsmeyer-Peppas model, where n values as low as 0.3 were observed [26]. Furthermore, Fickian diffusion was also found to be the main release mechanism in a related study on hydrogels and microemulsions [31].

Table 4: Release models with t being the time, C_0 being the HY-133 concentration at the start of the release study and C_t being the concentration at the respective time.

	1.5% HPMC K4M			**2.5% HPMC K4M**		
	K	n	Adj. R^2	K	n	Adj. R^2
Zero Order $C_t = C_0 + k \cdot t$	5.9	-	0.79	3.6	-	0.93
First Order $C_t = C_0 \cdot e^{-kt}$	0.3	-	0.98	0.08	-	0.99
Higuchi $C_t = C_0 + k \cdot t^{0.5}$	34.9	-	0.83	19.1	-	0.99
Korsmeyer-Peppas $C_t = C_0 + k \cdot t^n$	46.8	0.34	0.98	20.9	0.46	0.99

Based on the results of the release modelling, both hydrogels could therefore be described as diffusion-based systems with a sustained release kinetic. However, it was also shown that a lower HPMC concentration leads to a faster release and thus that the release might no longer be sustained at even lower HPMC concentrations, as they were later introduced in this study.

In general, the determination of the release model enabled further insight on the release mechanism, which is mainly diffusion controlled and therefore dependent on the concentration of HY-133 [25]. This means that a higher API concentration will be connected to a faster release rate. Furthermore, the release rate can be adjusted by precisely changing the HPMC concentration. With this, the release rate can be prolonged to react on a change in the intended application site during the developmental process.

4. Aseptic manufacturing and stability of a sterile HY-133 hydrogel

Formulations intended for nasal administration in multidose containers should contain preservatives to inhibit microbial growth in the drug product. However, although sterile manufacturing is not necessary for nasal multi-dose formulations, changing to preservative-free formulations will lead to special demands to ensure microbial integrity of the formulation. In many cases, aseptic manufacturing and an adequate primary packaging system can replace the use of preservatives. Aseptic compounding is described in USP <1211> as a suitable method for the preparation of sterile drug products. An aseptic compounded drug product is defined as a combination of sterilized components, which includes the drug substance, any excipient and the primary packaging material. Without a terminal sterilization step, a risk assessment must be carried out which specifically includes all surfaces which come in contact with the product during the mixing and filling process. Aseptic compounding is further discussed in USP <797>, where in particular personnel training, personal hygiene, sterile compounding facilities and equipment are described and regulated.

In clinical phase studies of new antimicrobial APIs, preservative-free dosage forms are of special interest [32]. Since preservatives can reduce or even inhibit bacterial growth, determination of the efficacy of the new antimicrobial APIs would be disturbed. This could subsequently lead to a false-positive response and poorly interpretable results. For example, in a small sample cohort the topical treatment with benzylalkonium chloride, a typically used preservative, effectively reduced bacterial growth in the nasal cavity [33]. Further, preservatives can cause aggregation of proteins and might therefore also influence the outcome of the stability study [34]. However, the aqueous-based dosage form of the current drug product formulation is prone for microbial contamination, which must be reduced by an aseptic manufacturing process. Hence, a sterile and preservative-free HY-133

formulation was developed to mitigate on the one side false-positive effects by the use of preservatives and on the other side prevent microbial growth in the drug product.

The final drug product cannot be heat sterilized, as the protein API has a denaturation temperature well below the sterilization temperature (Chapter 5). Final sterile filtration of the drug product is also not possible due to the elevated viscosity of the hydrogel. Therefore, an aseptic compounding process was implemented and the sterilization of the compounds was divided into two different steps. First, the pre-produced placebo hydrogel was autoclaved and filled into a sterile vessel. The drug substance was sterilized by a 0.2 µm PVDF filter and subsequently aseptically mixed in the sterile vessel with the hydrogel. In a smart setup, the sterile filter can be used as an inline filter, ensuring a self-contained system.

In the following section, the stability of HY-133 in sterile and non-sterile hydrogels is tested. In addition, the viscosity of the hydrogel over time is determined. The two final buffer compositions, the original and the salt reduced variation (Chapter 5), are used as a basis for the 1% HPMC hydrogel. The reduction in HPMC content to 1% was a strategic decision of the project board. The salt reduced formulation variation was included in this study to verify the stability findings in chapter 5. The different drug products underwent further testing regarding the physicochemical stability of the protein and the viscosity of the hydrogel.

4.1 Viscosity of sterilized hydrogels upon storage

The heat stability of HPMC hydrogels and the possibility to sterilize them by autoclaving was reported before [35]. As the viscosities of the used low-concentration HPMC hydrogels are lower than published ones, the rheological behavior of the placebo hydrogels was investigated. The viscograms of the hydrogels in both buffer variations (final and salt reduced) before and after the sterilization process are shown in Figure 32. In both cases, sterilization of the placebo hydrogel did not lead to changes in the viscograms. Viscosities are comparable to those determined in the screenings described above. The shear-thinning effect is evident in both hydrogel variations before and after the autoclaving process. Therefore, the rheology of the hydrogel was considered to be not affected by the sterilization process.

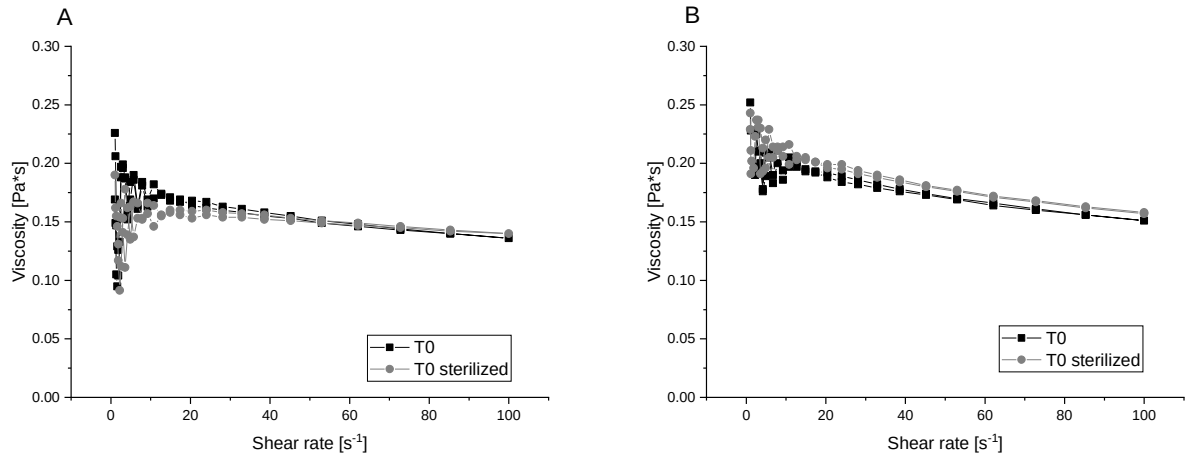

Figure 32: Viscograms of sterilized and non-sterilized hydrogels in (A) the final formulation buffer and (B) the final salt reduced formulation buffer. Each hydrogel contained 0.5 mg/ml HY-133 and 1% HPMC K4M.

The rheological characterizations of sterilized and non-sterilized HY-133 hydrogels in both formulation variations over a storage time of 6 months are shown in Figure 33 and Figure 34. The salt reduced formulations (Figure 34) showed slightly higher viscosities compared to the samples with the higher salt content (Figure 33). A 6-month storage at 40 °C led to reduced viscosities in both formulation variations, independent of the pre-sterilization of the hydrogel. The viscosity reduction was more pronounced in the final formulation buffer. After 6 months of storage at 4 °C, no viscosity changes could be observed in the non-sterilized hydrogels. However, slightly lower viscosities could be observed in both sterilized hydrogel variations. Overall, the changes in viscosities after storage at 4 °C were of only minor extent.

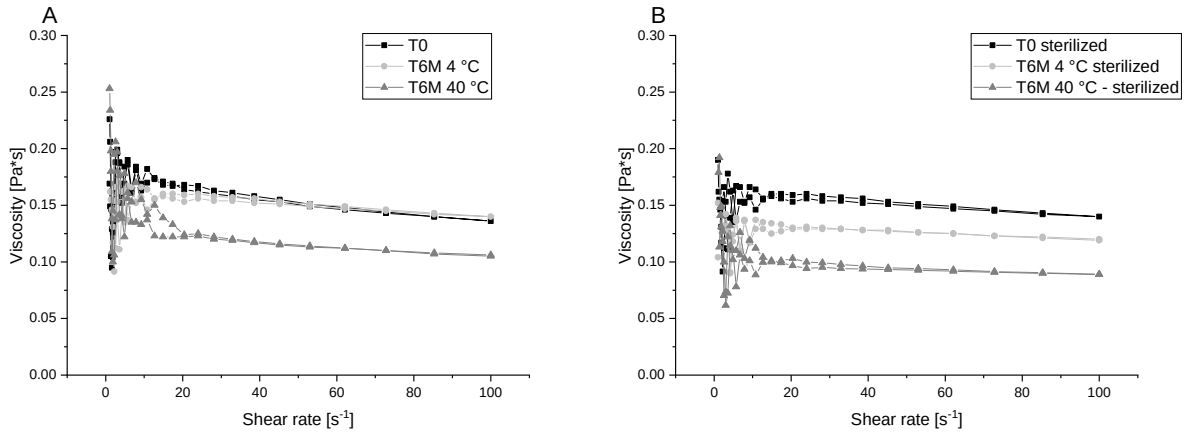

Figure 33: Viscograms of hydrogels in the final formulation buffer (non-sterilized (A) and sterilized (B)), determined at T0 and after 6-month storage at 4 °C and 40 °C. Each hydrogel comprised 0.5 mg/ml HY-133 and 1% HPMC K4M.

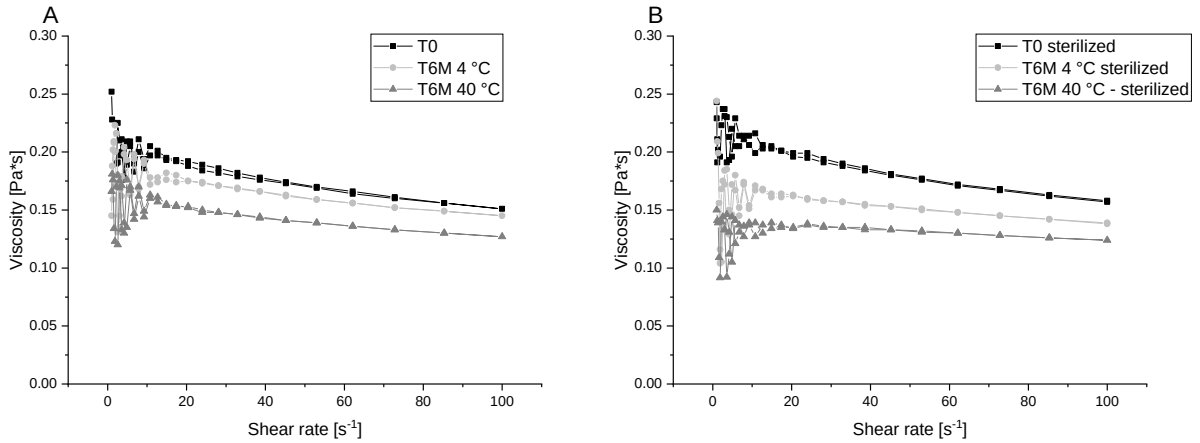

Figure 34: Viscograms of hydrogels in the salt reduced formulation buffer (non-sterilized (A) and sterilized (B)), determined at T0 and after 6-month storage at 4 °C and 40 °C. Each hydrogel comprised 0.5 mg/ml HY-133 and 1% HPMC K4M.

4.2 Chemical stability

The chemical stability of HY-133 was assessed by RP-HPLC and IEX-HPLC. The respective results are displayed in Figure 35 and Figure 36. In general, no change in native HY-133 was determined with RP-HPLC upon storage at 4 °C upon 7 months, irrespective of the hydrogel formulation (final buffer or salt reduced buffer) and sterility. At this storage condition, also main peak contents determined by IEX-HPLC were comparable between the different hydrogels. As both methods showed a similar stability of the HY-133 drug product compared to the reference (HY-133 in liquid solution), sterilization of the placebo hydrogel did not lead to degradation, which could have influenced the stability of HY-133. This is particularly important, as free radicals could form during the autoclaving process in HPMC hydrogels [20].

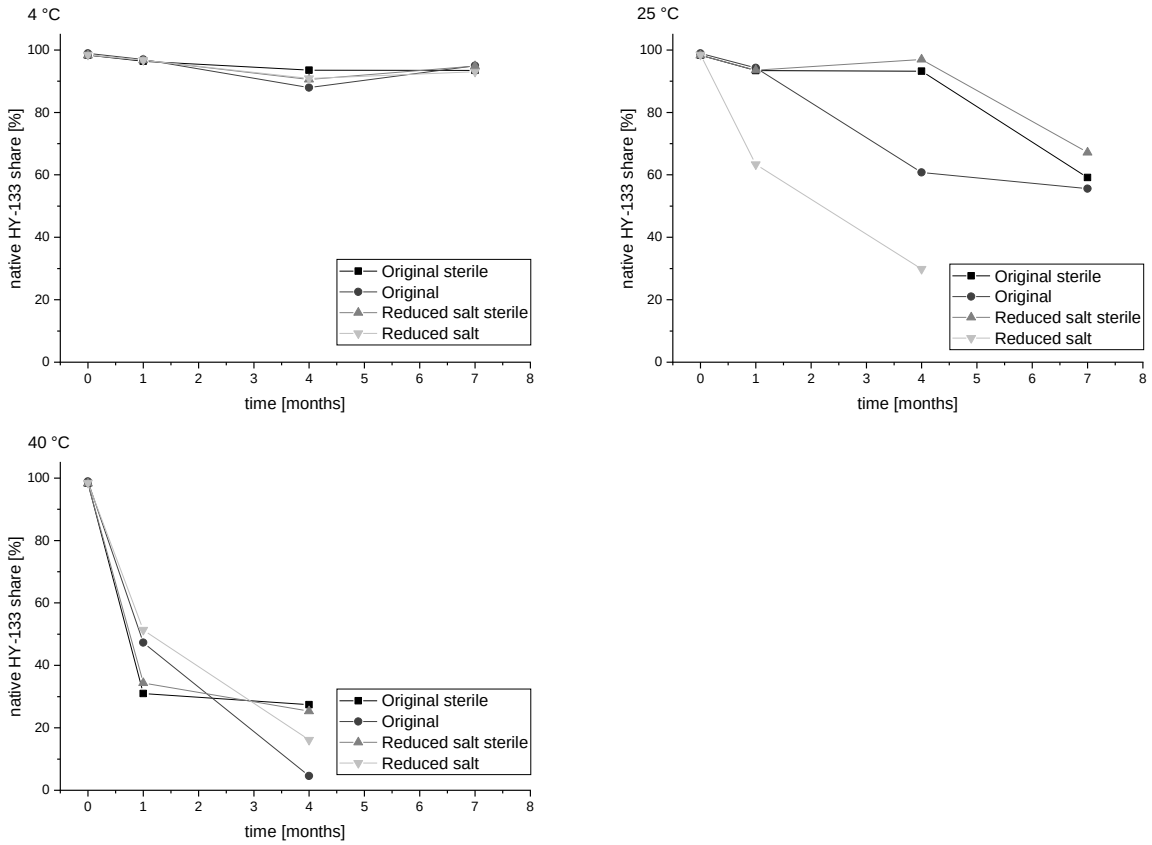

Figure 35: Native HY-133 content in sterilized and non-sterilized HPMC hydrogel variations determined by RP-HPLC upon storage of up to 7 months at 4 °C, 25 °C, and 40 °C.

Upon storage at 25 °C and 40 °C, HY-133 degradation was more pronounced and faster in non-sterilized gels, as well as in the salt-reduced formulation variation. Sterilization improved protein stability in both final and salt-reduced formulations.

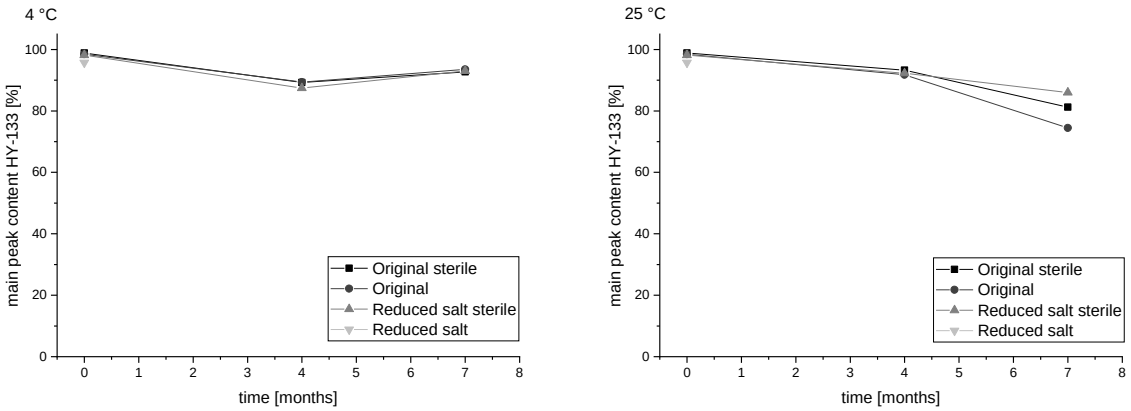

Figure 36: Native HY-133 content in sterilized and non-sterilized HPMC hydrogel variations determined by IEX-HPLC upon storage of up to 7 months at 4 °C and 25 °C.

4.3 Physical stability

The monomer contents of HY-133 in the different HyGel formulations are shown in Figure 37. Results are only available until 4 months of storage, as data after 7 months was not reproducible. Storage at 4 °C led to no major changes in monomer content of the different formulations, except for the salt reduced variation. There, a substantial decrease to 25% monomer content was observed. A similar trend was observed upon storage at 25 °C, with only slightly decreasing monomer contents for all variations, except of the salt reduced, non-sterile HyGel. This formulation variation showed a large decrease already after 1 month of storage at 4 °C. No clear trend in monomer contents was observed upon storage at 40 °C, with first decreasing and then increasing monomer contents determined in both original formulations.

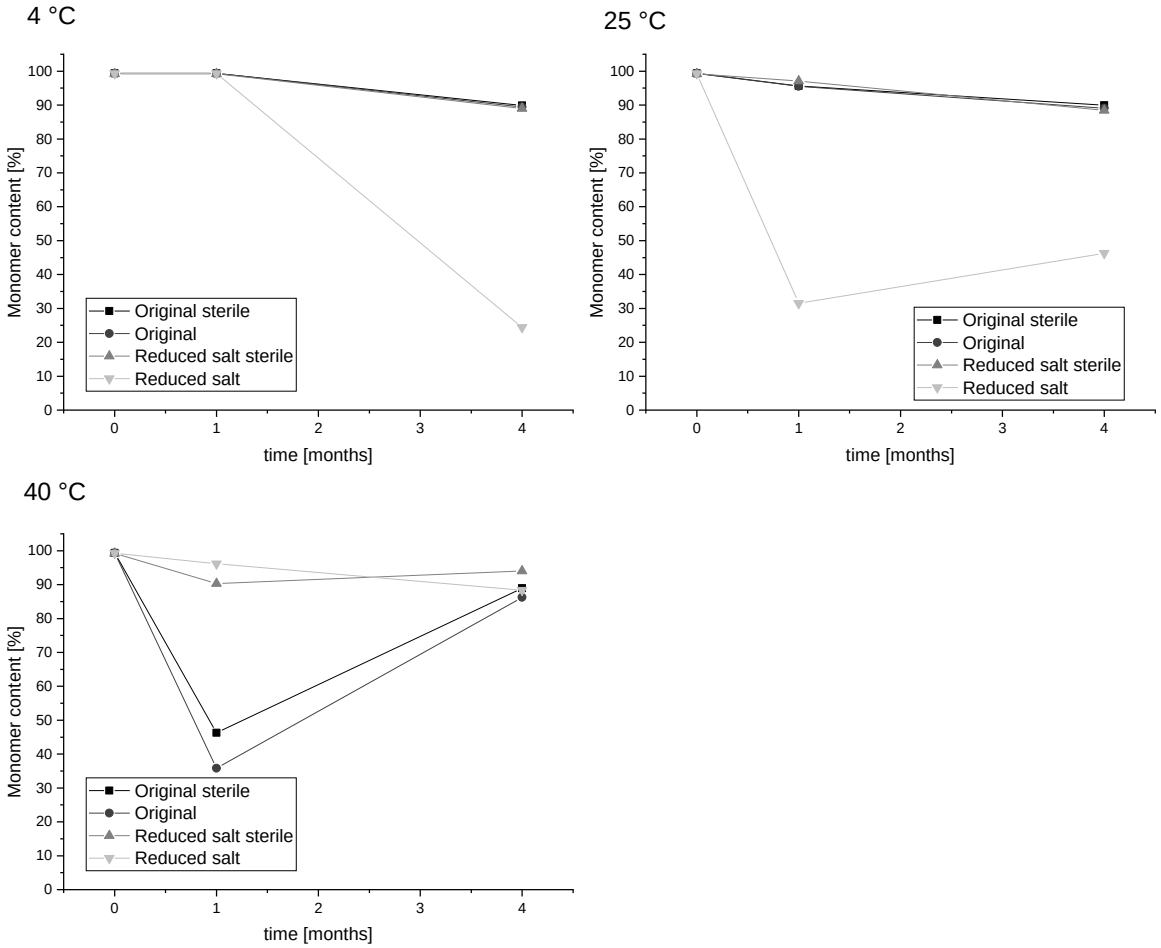

Figure 37: Total monomer content of HY-133 in sterilized and non-sterilized HPMC hydrogel variations upon storage of 4 months at 4 °C, 25 °C, and 40 °C analyzed by SE-HPLC.

To understand the monomer content results, reference must be made to the total protein recovery, which is shown in Figure 38. Storage at 4 °C showed minor changes in protein recovery upon storage for 4 months without clear tendency towards higher or lower recovery rates. The total protein recovery was constant at all samples stored at 25 °C for up to 4 months. A sharp decrease in total protein content

was shown for all samples stored at 40 °C, which could then lead to an incorrect determination of the relative monomer contents.

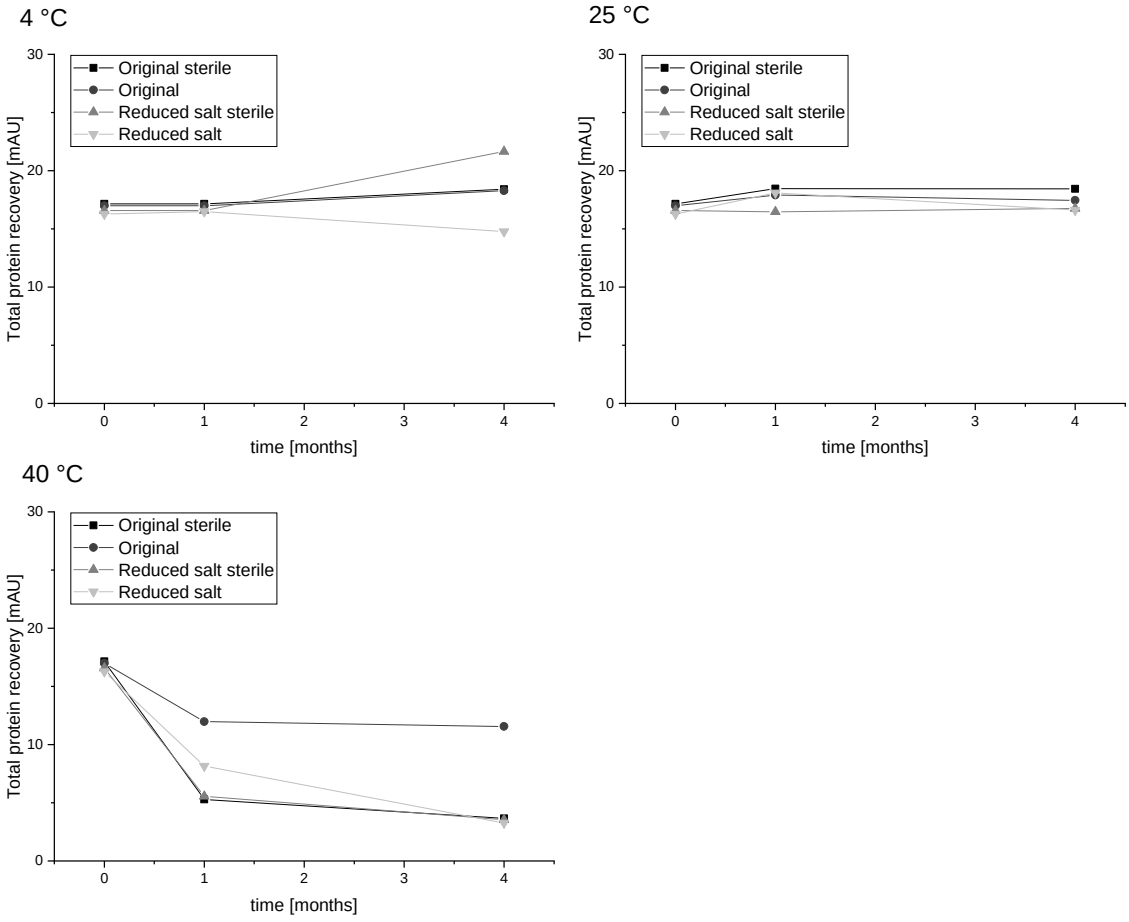

Figure 38: Total protein recovery of HY-133 in sterilized and non-sterilized HPMC hydrogel variations upon storage of 4 months at 4 °C, 25 °C, and 40 °C analyzed by SE-HPLC.

4.4 Summary of the effect of gel sterilization

In summary, the sterilization the hydrogels had no impact on the stability of HY-133. Refrigerated conditions provide an adequate stability of the sterilized drug product and can therefore be considered as similarly stable as a HY-133 solution, although specific activity was not determined.

5. Summary

The development of a hydrogel formulation comes with several challenges. The viscosity of the hydrogel should low enough to still facilitate spraying of the drug product, but also high enough to ensure proper administration without fast clearance of the drug product in the nasal cavity. Maximum viscosity levels were determined at 2 Pa·s; higher viscous gels were not sprayable with the tested nasal spraying devices (Ursatec 3K and Aptar UDS-L). Hydrogel preparation via cold dispersion was successfully implemented in lab-scale and also in larger scale. However, as final sterilization of the drug

product was not possible, an aseptic compounding concept was developed. A placebo gel was prepared in a first step, followed by autoclaving. Subsequently, the API was added aseptically. Sterilizing the gel by autoclaving resulted in an improved HY-133 stability compared to a non-sterile gel.

Different excipients for hydrogel formation from different vendors are available on the market comprising a broad range of different viscosities. The excipients should further provide full recovery of viscosity after shear stress. This was achieved with different HPMC types, while PVP, xanthan gum, gellan gum, and NaCMC did not provide suitable viscosities or lacked in sufficient protein stability upon storage at different conditions (4 °C, 25 °C, and 40 °C). However, any gelling agent can lead to changes in the physicochemical stability and activity of HY-133. A trend towards decreased protein stability was observed with higher gelling agent contents. Gels with pH 6 showed higher protein stability and activity. Free radicals in HPMC hydrogels were thought to alter protein stability [20]. Addition of methionine or higher purity grades of HPMC were thought to mitigate these effects. The surfactant PS 80 negatively influenced HY-133 stability already at T0 and showed a complete loss in HY-133 main peak area already at early time points as residual peroxides in PS 80 could enhance chemical changes of HY-133 [21]. In summary, polysorbate-free, low concentrated HPMC hydrogels with a pH of 6.0 were determined as the most stable formulation.

In general, formulations with 1% HPMC K4M, E4M, K15M or E50M could be sprayed using a commercial multi-dose delivery system and were therefore overall suitable for nasal administration. The HPMC grade itself had no impact on the chemical stability of the protein and a general incompatibility with these excipients was excluded. However, differences were seen in excipient quality between different manufacturers and lots. With respect to different HPMC grades, K4M and E4M from Colorcon resulted in the best protein stability, characterized by SE-HPLC, RP-HPLC, and IEX. A stability study recommended to store the gels at 4 °C maintaining protein stability longest.

The HPMC gels were sufficient to slightly sustain the release of HY-133 from the gels with slower release curves at higher HPMC contents. The release was mainly diffusion controlled and is therefore dependent on the HY-133 concentration.

6. References

[1] H. F. Wertheim *et al.*, "The role of nasal carriage in Staphylococcus aureus infections," *Lancet Infect. Dis.*, vol. 5, no. 12, pp. 751–762, 2005.

[2] F. R. DeLeo, M. Otto, B. N. B. Kreiswirth, and H. F. H. Chambers, "Community-associated meticillin-resistant *Staphylococcus aureus*," *Lancet*, vol. 375, no. 9725, pp. 1557–1568, 2010.

[3] T. Coates, R. Bax, and A. Coates, "Nasal decolonization of Staphylococcus aureus with mupirocin: Strengths, weaknesses and future prospects," *J. Antimicrob. Chemother.*, vol. 64, no. 1, pp. 9–15, 2009.

[4] S. J. Peacock, I. De Silva, and F. D. Lowy, "What determines nasal carriage of Staphylococcus aureus?," *Trends Microbiol.*, vol. 9, no. 12, pp. 605–610, 2001.

[5] P. G. Djupesland, "Nasal drug delivery devices: Characteristics and performance in a clinical perspective-a review," *Drug Deliv. Transl. Res.*, vol. 3, no. 1, pp. 42–62, 2013.

[6] E. Marttin, N. G. M. Schipper, J. C. Verhoef, and F. W. H. . Merkus, "Nasal mucociliary clearance as a factor in nasal drug delivery," *Adv. Drug Deliv. Rev.*, vol. 29, pp. 13–38, 1998.

[7] N. A. Peppas, P. Bures, W. Leobandung, and H. Ichikawa, "Hydrogels in pharmaceutical formulations," *Eur. J. Pharm. Biopharm.*, vol. 50, no. 1, pp. 27–46, 2000.

[8] R. Donnelly, R. Shaikh, T. Raj Singh, M. Garland, and Ad. Woolfson, "Mucoadhesive drug delivery systems," *J. Pharm. Bioallied Sci.*, vol. 3, no. 1, p. 89, Jan. 2011.

[9] A. Fortuna, G. Alves, A. Serralheiro, J. Sousa, and A. Falcão, "Intranasal delivery of systemic-acting drugs: Small-molecules and biomacromolecules," *Eur. J. Pharm. Biopharm.*, vol. 88, no. 1, pp. 8–27, Sep. 2014.

[10] S. a Sharpe *et al.*, "Comparison of the flow properties of aqueous suspension corticosteroid nasal sprays under differing sampling conditions.," *Drug Dev. Ind. Pharm.*, vol. 29, no. 9, pp. 1005–12, 2003.

[11] M. H. Mahdi, B. R. Conway, and A. M. Smith, "Development of mucoadhesive sprayable gellan gum fluid gels," *Int. J. Pharm.*, vol. 488, no. 1–2, pp. 12–19, 2015.

[12] A. Das, P. B. K. Gupta, and B. Nath, "Mucoadhesive Polymeric Hydrogels for Nasal Delivery of Penciclovir," *J. Appl. Pharm. Sci.*, vol. 2, no. 12, pp. 158–166, 2012.

[13] S. P. Newman, G. R. Pitcairn, and R. N. Dalby, "Drug Delivery to the Nasal Cavity: In Vitro and In Vivo Assessment," *Crit. Rev. Ther. Drug Carrier Syst.*, vol. 21, no. 1, p. 46, 2004.

[14] P. Dayal, M. S. Shaik, and M. Singh, “Evaluation of different parameters that affect droplet-size distribution from nasal sprays using the Malvern Spraytec®,” *J. Pharm. Sci.*, vol. 93, no. 7, pp. 1725–1742, Jul. 2004.

[15] C. Guo, K. J. Stine, J. F. Kauffman, and W. H. Doub, “Assessment of the influence factors on in vitro testing of nasal sprays using Box-Behnken experimental design,” *Eur. J. Pharm. Sci.*, vol. 35, no. 5, pp. 417–426, Dec. 2008.

[16] A. S. Harris, E. Svensson, Z. G. Wagner, S. Lethagen, and I. M. Nilsson, “Effect of viscosity on particle size, deposition, and clearance of nasal delivery systems containing desmopressin,” *J. Pharm. Sci.*, vol. 77, no. 5, pp. 405–408, 1988.

[17] G. M. Eccleston, M. Bakhshaee, N. E. Hudson, and D. H. Richards, “Rheological Behavior of Nasal Sprays in Shear and Extension,” *Drug Dev. Ind. Pharm.*, vol. 26, no. 9, pp. 975–983, Jan. 2000.

[18] Y. Pu, A. P. Goodey, X. Fang, and K. Jacob, “A comparison of the deposition patterns of different nasal spray formulations using a nasal cast,” *Aerosol Sci. Technol.*, vol. 48, no. 9, pp. 930–938, 2014.

[19] Z. Li *et al.*, “Effect of substitution degree on carboxymethylcellulose interaction with lysozyme,” *Food Hydrocoll.*, vol. 62, pp. 222–229, 2017.

[20] L. Basumallick, J. A. Ji, N. Naber, and Y. J. Wang, “The fate of free radicals in a cellulose based hydrogel: Detection by electron paramagnetic resonance spectroscopy,” *J. Pharm. Sci.*, vol. 98, no. 7, pp. 2464–2471, Jul. 2009.

[21] S. Li, C. Schoneich, and R. T. Borchardt, “Chemical Instability of Protein Pharmaceuticals : Mechanisms of Oxidation and Strategies for Stabilization,” *Biotechnol. Bioeng.*, vol. 48, pp. 490–500, 1995.

[22] E. Mašková *et al.*, “Hypromellose – A traditional pharmaceutical excipient with modern applications in oral and oromucosal drug delivery,” *J. Control. Release*, vol. 324, no. February, pp. 695–727, 2020.

[23] K. Mitchell, J. L. Ford, D. J. Armstrong, P. N. C. Elliott, J. E. Hogan, and C. Rostron, “The influence of substitution type on the performance of methylcellulose and hydroxypropylmethycellulose in gels and matrices,” *Int. J. Pharm.*, vol. 100, pp. 143–154, 1993.

[24] M. B. Schulz and R. Daniels, “Hydroxypropylmethylcellulose (HPMC) as emulsifier for submicron emulsions: Influence of molecular weight and substitution type on the droplet size after high-pressure homogenization,” *Eur. J. Pharm. Biopharm.*, vol. 49, no. 3, pp. 231–236, 2000.

[25] A. Fick, “Ueber Diffusion,” *Ann. Phys.*, vol. 170, no. 1, pp. 59–86, 1855.

[26] P. L. Ritger and N. A. Peppas, “A simple equation for description of solute release I. Fickian and non-fickian release from non-swellable devices in the form of slabs, spheres, cylinders or discs,” *J. Control. Release*, vol. 5, no. 1, pp. 23–36, Jun. 1987.

[27] S. Qian, Y. C. Wong, and Z. Zuo, “Development , characterization and application of in situ gel systems for intranasal delivery of tacrine,” *Int. J. Pharm.*, vol. 468, no. 1–2, pp. 272–282, 2014.

[28] J. Siepmann and N. A. Peppas, “Modeling of drug release from delivery systems based on hydroxypropyl methylcellulose (HPMC),” *Adv. Drug Deliv. Rev.*, vol. 48, no. 2–3, pp. 139–157, 2001.

[29] P. Costa and J. M. Sousa Lobo, “Modeling and comparison of dissolution profiles,” *Eur. J. Pharm. Sci.*, vol. 13, no. 2, pp. 123–133, May 2001.

[30] M. P. Paarakh, P. A. N. I. Jose, C. M. Setty, and G. V Peter, “Release kinetics - concepts and applications,” *Int. J. Pharm. Res. Technol.*, vol. 8, no. 1, pp. 12–20, Jan. 2019.

[31] V. Cojocaru *et al.*, “Formulation and evaluation of in vitro release kinetics of na3cadtpa decorporation agent embedded in microemulsion-based gel formulation for topical delivery,” *Farmacia*, vol. 63, no. 5, pp. 656–664, 2015.

[32] J. D. Ehrick *et al.*, *Sterile Product Development*, vol. 6. New York, NY: Springer New York, 2013.

[33] O. Onerci Celebi and A. R. C. Celebi, “The effect of ocular lubricants containing benzalkonium chloride on nasal mucosal flora,” *Cutan. Ocul. Toxicol.*, vol. 37, no. 3, pp. 305–308, 2018.

[34] L. Jorgensen, S. Hostrup, E. H. Moeller, and H. Grohganz, “Recent trends in stabilising peptides and proteins in pharmaceutical formulation - considerations in the choice of excipients.,” *Expert Opin. Drug Deliv.*, vol. 6, no. 11, pp. 1219–1230, 2009.

[35] M. N. Anurova, E. O. Bakhrushina, and N. B. Demina, “Review of Contemporary Gel-Forming Agents in the Technology of Dosage Forms,” *Pharm. Chem. J.*, vol. 49, no. 9, pp. 627–634, 2015.

Chapter 8

Sustained release of HY-133 using nanoparticles

Table of Contents

1. Introduction

Various resistance mechanisms of *S. aureus* against common antibiotics are known and well characterized. Mostly, these resistances are caused by mutations in binding sites or the introduction of plasmids carrying resistance genes [1]. In addition, *S. aureus* can further use physical escape mechanisms like the formation of biofilms and encapsulations, which both are more difficult to target by therapeutic agents compared to planktonic bacteria [2], [3]. The formation of small-colony variants (SCV) of *S. aureus* were reported to effectively decrease the exposure to antibiotics and to therefore reduce the effectiveness of those [4]. SCVs were also shown to substantially contribute to the formation and the stabilization of *S. aureus* biofilms [5].

Despite being characterized as highly active, selective and bactericidal against *S. aureus*, time-kill curves of HY-133 revealed a regrowth of different strains of *S. aureus* [6]. This was also evident in samples, where more than 99.9% of the initial bacterial load was killed [6]. A direct comparison of HY-133 with daptomycin showed that the regrowth effect was lower in daptomycin treated colonies [7]. However, the concentrations used in these studies were with up to 0.004 mg/ml still substantially lower than the drug product described in this thesis [6], [7]. The regrowth phenomenon was dependent on the HY-133 concentration and on the bacterial strain used in the different experiments and could be observed after 1 to 2 h after treatment and initial reduction of the bacteria below LOD [6]. So far, it is not known whether this phenomenon can only be found in in-vitro experiments, or would also occur in-vivo. A similar regrowth phenomenon was also observed in another endolysin SAL200, showing that this phenomenon is not specific to HY-133 [8]. Its predecessor, the endolysin SAL-1, has already shown its effectivity against these types of adherent *S. aureus* [9].

The encapsulation of an active agent to increase the effectivity in *S. aureus* biofilms was already used with several small molecules like daptomycin, vancomycin or cefazolin [10], [11]. Selenium nanoparticles provided a substantial inhibition of the formation of *S. aureus* biofilms and the disruption of those biofilms [12]. The endolysin LysRODI was successfully encapsulated in pH-sensitive liposomes and substantially decreased the *S. aureus* load in planktonic cultures as well as in biofilms [13].

A sustained release formulation of HY-133 could be beneficial to overcome the regrowth of *S. aureus* in the first hours upon treatment with HY-133. Therefore, a drug delivery system which provides an extended release of HY-133 for several hours should be developed. A longer release over days was not intended. Nanoparticles are a well described and researched class of drug delivery systems, with various systems already known. Additionally, the mucoadhesive effect of nanoparticles could pose an additional benefit for a nasal administration of HY-133 [14].

Different materials like poly (lactic-co-glycolic acid) (PLGA), dextran or mesoporous silica are well examined to prepare protein loaded nanoparticles [15], [16]. Nanoparticles can be prepared via nanoprecipitation, coacervation-phase separation, desolvation, reverse-phase and emulsification-solvent evaporation [15]. Many preparational methods of nanoparticles involve organic solvents, which poses a major difficulty for the incorporation of proteins [17]. Also, the salt composition, the nanoparticle material itself and the preparational steps are factors which need to be considered during the preparation of protein loaded nanoparticles.

Here, two different HY-133 loaded nanoparticles were investigated, namely alginate and gelatin nanoparticles. Both nanoparticles were biodegradable, well-established systems, which were loaded via electrostatic interactions either after or during the preparation of the nanoparticles. As HY-133 is positively charged due to its formulation pH below the pI, this interaction enabled an effective loading without further changes of the protein.

The different nanoparticles were characterized regarding their zeta-potential and mean size using DLS, as well as its drug release via photometry and RP-HPLC. RP-HPLC also confirmed the integrity of the protein after release.

2. Gelatin-Nanoparticles

Gelatin has a long history as an excipient in solid dosage forms, like capsules and tablets. Therefore, gelatin is generally regarded as safe and is, as a GRAS substance, generally suitable for pharmaceutics [18], [19]. It has a low antigenicity, is biodegradable and can be chemically modified [19]. In the last years, the use of gelatin as an excipient for the formation of nanoparticles was investigated. Gelatin nanoparticles were long prepared via a two-step desolvation method, with the common disadvantages of low particle yield and a complicated process scale-up [20]. The method was later improved by using a customized high molecular weight gelatin type A, which enabled to prepare nanoparticles with only one desolvation step. This increased the particle yield and provided the basis for the later scale-up process [21]. The one-step desolvation method was used here to prepare HY-133 loaded gelatin nanoparticles. Glutaraldehyde was used as a crosslinker. The prepared nanoparticles were loaded via ionic interaction [22], [23]. This was possible as HY-133 (pos.) and the nanoparticles (neg.) are oppositely charged.

2.1 Preparation of Gelatin-Nanoparticles

HY-133 loaded gelatin nanoparticles were prepared according to Geh et. al. [21]. A 3% gelatin type B Bloom 300 solution in purified water was prepared and stirred for 15 minutes at 900 rpm. Complete dissolution was achieved via heating of the gelatin dispersion to 50 °C and the pH was adjusted to a

value between 6.0 and 8.0. Subsequently, acetone was added dropwise to start the desolvation process and therefore the formation of the nanoparticles. The nanoparticles were then crosslinked with a 25% glutaraldehyde solution and the solution was stirred overnight. To remove all residual organic components, the nanoparticle suspension was washed three times with water in an ultrafiltration cell with a 100 kDa cutoff membrane.

During the development, different pH values between 6.0 and 8.0 were tested in 16 different batches.

2.2 Characterization of Gelatin-Nanoparticles

Sixteen different nanoparticle batches were characterized regarding their concentration, purity and the median size and zeta-potential.

The nanoparticle suspensions were dried in aliquots of 20 µl each at 60 °C and the mass of the nanoparticles was recorded. All prepared nanoparticle batches achieved a high yield of 18 to 21 mg/ml, which corresponds to a particle yield of about 80%. The purity of the gelatin nanoparticles was assessed via a specific RP-HPLC method. Here, the main aspect was residual acetone and glutaraldehyde. All nanoparticle batches showed a distinct acetone peak, indicating major organic residues which could affect the protein stability over time. The acetone content was later reduced by an additional centrifugation step.

Median size and the zeta-potential were measured with a Zetasizer Nano (Malvern, UK). Therefore, the samples were diluted 100-fold with a 10 mM phosphate buffer, pH 7.0. The different batches had Z-averages ranging from 170 to 280 nm with PDI values of below 0.25. Overall, a slight trend for smaller nanoparticles was obtained with higher pH values during the preparation of the nanoparticles due to the increased charge of the gelatin molecules (Figure 1). This caused higher repulsion of the molecules and therefore smaller nanoparticles [21].

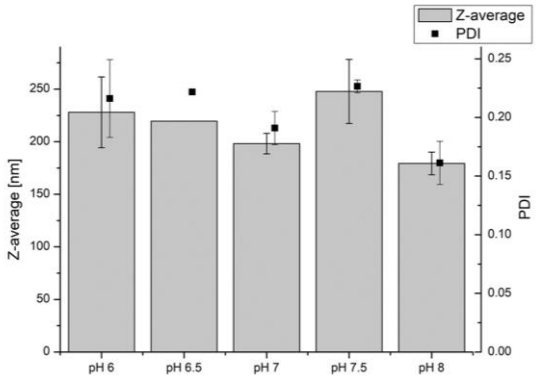

Figure 1: Average median sizes (z-average) and PDI values, depending on the selected pH values during preparation.

The zeta-potential of all gelatin nanoparticle batches was around -18 mV, providing a proper basis for stable nanoparticle suspensions.

2.3 HY-133 loaded Gelatin-Nanoparticles

To load the gelatin nanoparticles, HY-133 in a concentration of 0.5 mg/ml was mixed with the pre-prepared nanoparticle suspension. The loading efficiency was determined via fluorometric measurement using the Cary Eclipse fluorescence spectrophotometer (Agilent, Santa Clara, California, USA) with an excitation wavelength of 280 nm and an emission wavelength of 343 nm. Using this setup, a measurement range between 0.01 and 0.5 mg/ml was covered. The loaded nanoparticles were centrifuged at 14,000 g for 30 minutes and the supernatant was analyzed.

In addition, the median size of the HY-133 loaded nanoparticles was checked. No changes regarding the Z-average value and the PDI could be observed. The zeta potential was slightly reduced by an average value of 2 mV from -18.1 mV to -16.5 mV.

Loading of the nanoparticles with 0.5 mg/ml HY-133 was efficient and reached a maximum at a gelatin nanoparticle concentration of 10 mg/ml, where a loading efficiency of 95% was reached. The oppositely charged nanoparticles were well suited for an effective protein loading via ionic interaction.

However, the solution medium was drastically changed compared to the formulation buffer of HY-133. As the formulation buffer was diluted during the loading of the nanoparticles by 1:20, the stabilizing effect of the formulation buffer was reduced, which could potentially alter the stability of HY-133 over time. This was shown in stability experiments, where HY-133 loaded nanoparticles were incubated over 4 weeks. A substantial loss in native HY-133 content was determined in these samples.

To address the decreased stability of HY-133, the storage buffer of the HY-133 loaded nanoparticles was adapted to match the HY-133 formulation buffer. For this, the nanoparticle suspension was centrifuged as described above, the supernatant was removed and the nanoparticles were resuspended in formulation buffer. Again, 0.5 mg/ml HY-133 was mixed with the gelatin nanoparticle suspension. In this mixture, only 10% of the available protein amount could be loaded to the nanoparticles in all cases. The interaction of HY-133 and the nanoparticles was decreased due to the high salt concentration in the formulation buffer, which shielded the surface charge of the nanoparticles and prevented an ionic interaction between nanoparticle and protein. Further experiments showed that the loading efficiency was highly dependent on the excipient concentration coming from the formulation buffer in the sample. Only 20% excipient concentration of the original formulation buffer substantially decreased the loading efficiency to around 40%, illustrating the correlation between salt concentration in the nanoparticle storage buffer and the loading efficiency.

The activity of HY-133 loaded nanoparticles was compared to unloaded nanoparticles and a HY-133 reference solution. The HY-133 loaded nanoparticles showed a comparable activity as the reference solution. However, a distinct extended release could not be observed. The lytic activity was fast and

did not vary over time. Unloaded gelatin nanoparticles, used as a control, showed no specific lytic activity.

The stability of HY-133 in the presence of gelatin nanoparticles was assessed over a storage time of up to 4 weeks at temperatures of 4 °C and 40 °C. For this, the nanoparticle suspension was centrifuged and chemical integrity of the protein in the supernatant was determined. Storage at 4 °C led to a loss in native HY-133 in gelatin nanoparticles after 4 weeks of storage (Figure 2). The loss was substantially higher when the nanoparticles were loaded and stored in water compared to a storage in formulation buffer. The results clearly indicated that the stability of HY-133 was affected by the addition of gelatin nanoparticles.

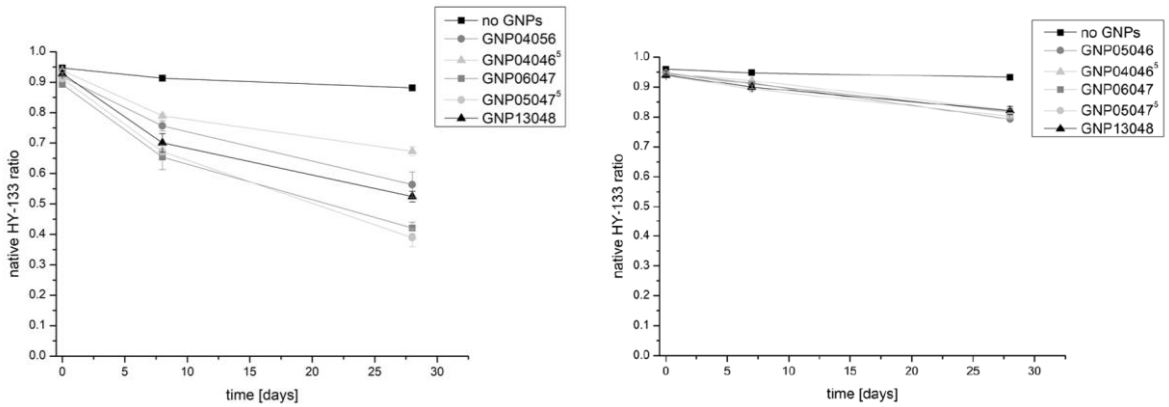

Figure 2: Chemical stability of HY-133 in gelatin nanoparticles stored at 4 °C, prepared in water (left) and formulation buffer (right).

3. Manufacturing of Alginate-Nanoparticles

Alginate nanoparticles and microspheres are versatile carriers of different drug species, including proteins. They were already described as insulin carriers [24]–[26], but also model proteins like BSA, chymotrypsin or lysozyme could be loaded successfully [17], [27]. A recent publication describes the loading of alginate nanoparticles with endolysins [28].

Alginate nanoparticles can be prepared by using two different mechanisms, complexation and emulsification [29]. In general, alginate nanoparticles are formed by mixing dissolved sodium alginate with divalent ions like calcium chloride or tripolyphosphate (TPP) [29], [30]. The nanoparticles can be coated by adding a polycation solution such as chitosan to form a polyelectrolyte complex [24]. The method is based on self-assembly of different charged species, which is the most widely used method to prepare alginate nanoparticles by complexation. Proteins can be loaded during the initial crosslinking step or by simple incubation of the pre-formed nanoparticles with the protein [27]. High protein concentrations were reported to results in precipitation of the components. A concentration of 0.046 mg/ml insulin could be loaded during the crosslinking steps [31]. A concentration dependency

was observed only recently in the endolysin LysMR-5-loaded nanoparticles resulting in small nanoparticle sizes and a complete release of protein at a concentration of 0.14 mg/ml protein. An increase of protein to 0.29 mg/ml yielded in a substantial increase in nanoparticle size [28].

To reduce the required HY-133 amount for the nanoparticle binding studies, the "batch" volume was adapted to fit in a 6-well plate with a batch size of 9.5 ml per formulation. A peristaltic pump was used to dispense the respective excipient solutions stepwise into the wells. To reduce the droplet size of the added components, tubing size was reduced to a small nozzle at the outlet. This approach required 4.7 mg HY-133 per batch.

Different to the normally used NP-preparation method, the alginate solution was not prepared in water, but in an adapted formulation buffer of HY-133. The addition of HY-133 to an aqueous alginate solution led to an immediate precipitation of HY-133 due to the rapid dilution of the protein in water. Therefore, the alginate solution contained only the following excipients of the regular formulation buffer of HY-133: methionine, arginine-HCl and NaCl (Table 1). The concentration of PX 188 was increased to 0.1% to reach a lower PDI of the formed nanoparticles. $CaCl_2$ was not included in the alginate solution, as this polycation would immediately cause the formation of nanoparticles. Therefore, the necessary amount of $CaCl_2$ was added together with HY-133 in the second step of the preparation process. Subsequently, the nanoparticles were coated with chitosan to make use of literature-stated advantages such as physicochemical stability and controlled release as reported in literature [32].

Table 1: Exemplary composition and preparation sequence of coated alginate nanoparticles containing HY-133. Different variations were examined over the course of the study.

#	Step	Excipients	Concentrations
1	Alginate solution pH 4.9 **7.83 ml**	Alginate NaCl Arginine-HCl HEPES Methionine Poloxamer 188	0.1% 75 mM 150 mM 25 mM 10 mM 0.1%
2	Polycation solution with HY-133 Added dropwise with a peristaltic pump **0.85 ml**	$CaCl_2$ HY-133	5 mM 13.5 mg/ml
3	Coating solution **0.8 ml**	Chitosan (LMW)	0.05% in 1% acetic acid

The excipients were solved in purified water and then filtered with a 0.2 µm filter. In an exemplary mixture, 7.83 ml alginate solution was stirred in a 6-well plate. A mixture of 0.5 ml of 5 mM $CaCl_2$ and 0.35 ml of 13.5 mg/ml HY-133 was added with a peristaltic pump. The dropping speed was adjusted to

75 µl/min. A slight turbidity was apparent after few minutes and increased over time, indicating the formation of nanoparticles. After complete addition of the protein-$CaCl_2$ mixture, the solution was stirred for further 30 minutes for allowing complete nanoparticle formation. In the final step, 0.8 ml chitosan solution was added to obtain coated nanoparticles. Large agglomerates were removed by filtration with a 5 µm filter.

Figure 3: Preparation of alginate nanoparticles in a 6-well plate. The protein-$CaCl_2$ mixture was added dropwise and caused turbidity of the solution.

To determine the loading efficiency, the nanoparticle suspension was centrifuged at 5,000 x g and the protein concentration in the obtained supernatant was measured by RP-HPLC. The loading efficiency was calculated via the following equation:

$$Loading\ efficiency\ [\%] = \frac{c(HY133) - c(HY133_{supernatant})}{c(HY133)} * 100\%$$

An additional loading of the protein after the nanoparticle formation was not possible. As the nanoparticles were negatively charged, the positively charged protein in high concentrations led to an immediate precipitation of both components.

3.1 Loading efficiency and release determination of HY-133 from nanoparticles

The release of each formulation was determined with the following procedure: an aliquot of 0.5 ml of the nanoparticle suspension was mixed with 1.5 ml 50 mM Tris buffer at pH 7.0. Subsequently, the mixture was centrifuged at 5,000 x g and the supernatant was further analyzed as a starting point for

the release study. The remaining pellet was resuspended with the Tris buffer and incubated at 37 °C in a rocker shaker. At each time point, the mixture was centrifuged as described above, the supernatant was completely removed and the pellet resuspended with 0.5 ml Tris buffer.

A positive reference sample was generated by releasing the protein out of the alginate nanoparticles with 1 M NaOH. Thereby, 90% of the protein was found, corresponding to a mean loading efficiency of around 90%, while 10% were not encapsulated and remained in the liquid phase.

3.2 Development approach of nanoparticles

During the development, different parameters during the preparation of nanoparticles were evaluated to improve size, zeta potential, loading efficiency and release behavior. These parameters included formulation factors like the addition of Poloxamer 188, the concentration of chitosan and $CaCl_2$ and process factors like volume, mixing speed and mixing approach. Variations of parameters and the effect on the nanoparticles are listed in Table 2. The maximal released protein amount is noted as well.

Table 2: Exemplary formulations tested during the alginate nanoparticle research.

#	Variation / changed parameter	Effect
	Starting values: 0.1% alginate 13.5 mg/ml HY-133 5 mM $CaCl_2$ 0.1% PX188 0.05% chitosan	Concentrations in final NP solution: 0.08% alginate 0.5 mg/ml HY-133 0.3 mM $CaCl_2$ 0.08% PX188 0.0004% chitosan
1	0.1-0.5 mg/ml HY-133 Pre-mix of HY-133 with alginate, without formulation buffer components 0.1% alginate, 18 mM $CaCl_2$	Precipitation after addition of $CaCl_2$. Not analyzed further.
2	0.1-0.5 mg/ml HY-133 Pre-mix of HY-133 with $CaCl_2$ Without formulation buffer components	Precipitation after addition of $CaCl_2$. Not analyzed further.
3	0.5 mg/ml HY-133 Alginate:Chitosan 20:1 Alginate:Chitosan 10:1	Size: < 900 nm PDI: < 0,3 Zeta: < -40 mV Release: max. 20% (120 h)
4	0.5 mg/ml HY-133 Alginate:Chitosan 10:1	Size: < 900 nm PDI: < 0,3 Zeta: < -40 mV Release: max. 20% (120 h)
5	0.5 mg/ml HY-133 w/o Chitosan	Size: < 700 nm PDI: < 0.2 Zeta: < -40 mV Release: max. 20% (6 h)
6	0.5 mg/ml HY-133 Alginate:Chitosan 10:1	Size: < 700 nm PDI: < 0.2 Zeta: < -40 mV Release: max. 20% (6 h)

#	Variation / changed parameter	Effect
7	0.5 mg/ml HY-133 w/o Chitosan With increased PX188 (0.5%)	Size: ~ 400 nm PDI: < 0,1 Release: max. 10% (6 h)
8	0.5 mg/ml HY-133 Alginate:Chitosan 10:1 With increased PX188 (0.5%)	Size: <700 nm PDI: ~ 0,2 Zeta: ~ -40 mV Release: max. 10% (6 h)
9	0.5 mg/ml HY-133 Alginate:Chitosan 1:1	Neutral zeta potential
10	0.5 mg/ml HY-133 Alginate:Chitosan 0.2:1	Slightly positive zeta potential
11	1.0 mg/ml HY-133 Alginate:Chitosan 5:1	Neutral to slightly positive zeta potential Loading: 15%
12	1.0 mg/ml HY-133 Alginate:Chitosan 2:1	Neutral to slightly positive zeta potential Loading: 10%
13	2.0 mg/ml HY-133 Alginate:Chitosan 5:1	Neutral to slightly positive zeta potential Loading: 25%
14	2.0 mg/ml HY-133 Alginate:Chitosan 2:1	Neutral to slightly positive zeta potential Loading: 5%
15	0.5 mg/ml HY-133 Alginate:Chitosan 5:1 $CaCl_2$ 50-200 µl	Neutral to slightly positive zeta potential Loading: 25-40%
16	0.5 mg/ml HY-133 Alginate:Chitosan 5:1 $CaCl_2$ 0-100 µl	0 µl $CaCl_2$: 30% loading (slight amount of $CaCl_2$ in sample due to HY-133 intake) 50 µl $CaCl_2$: 65-80% loading 100 µl $CaCl_2$: 0% loading
17	1.0 mg/ml HY-133 Chitosan 0.1% Alginate:Chitosan 50:1	Negative zeta potential Loading: 77% Release: 37%

3.3 Final approach in larger batch size

The last approach (#17, Table 2) was selected for further analysis. For this, the batch size was increased to yield a larger nanoparticle load.

To evaluate the storage stability and to characterize the release of the produced nanoparticles, the selected formulation composition was prepared in 50 ml batch size. Particles around 1.2 µm were obtained with a medium polydispersity index. The zeta potential was below -40 mV, indicating negatively charged particles. A loading efficiency of 77% was obtained.

To assess the storage stability of the nanoparticles, aliquots were stored at 4 °C and 25 °C and the particle sizes and zeta potentials were measured over the course of 4 weeks (Figure 4). An increase in mean particle size and PDI was observed at both temperatures over time. A higher storage temperature could be associated with a larger mean particle size. The zeta potential was constant over time, showing zeta potentials of around -40 mV.

Figure 5 shows the release curve of the nanoparticles at the start of the stability study. The release rate showed a fast onset with the majority of the protein released within the first hour. Afterwards, the release rate slowed down and the study was terminated after 3 h. However, only around 37% of the overall loaded protein content was released after 3 h. Together with the rather low loading efficiency, an overall very small HY-133 amount was released. In further experiments it was tried to increase protein loading to yield a higher protein release. Contrarily, a higher protein load resulted in a decrease of protein release. However, the overall released protein amount could be adjusted by increasing the amount of loaded nanoparticles in the release experiment by up-concentration of nanoparticles.

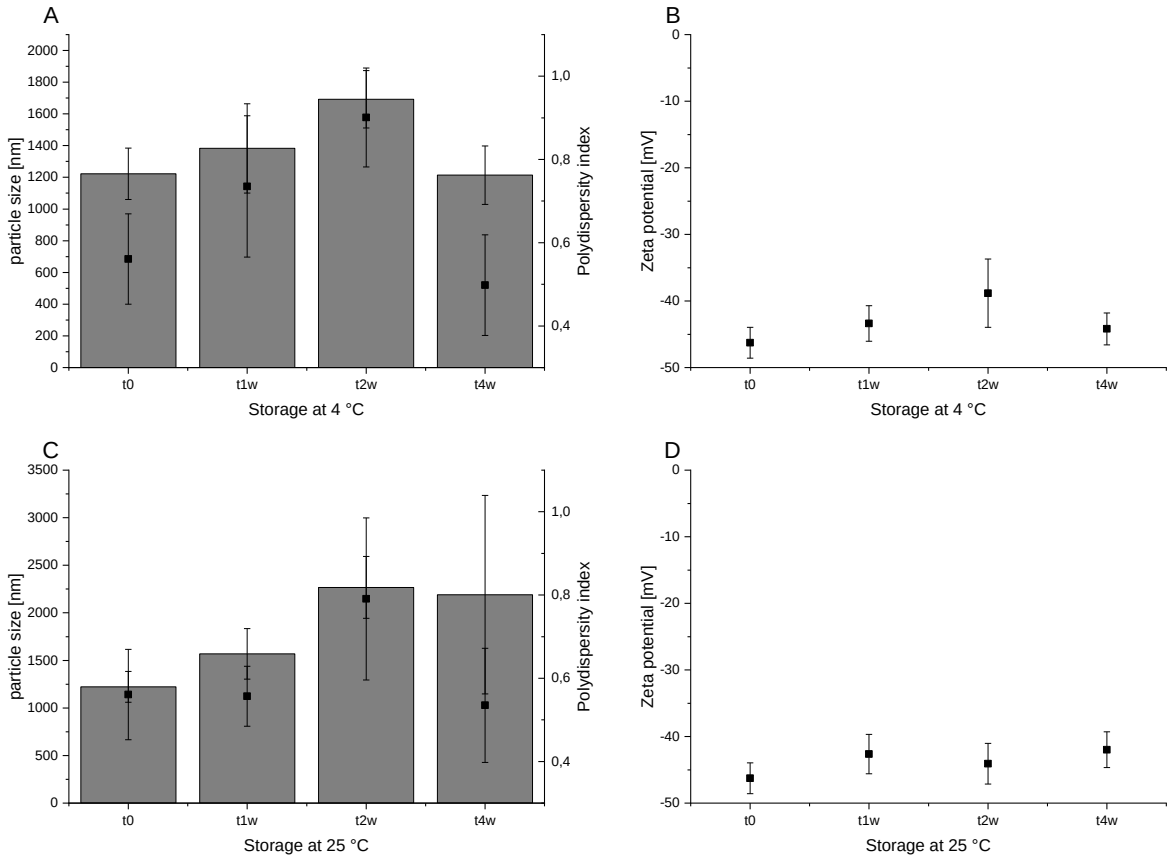

Figure 4: Particle sizes and corresponding PDIs determined by DLS measurements after storage at 4 °C (A) and 25 °C (C). The corresponding zeta potential is shown in (B) and (D).

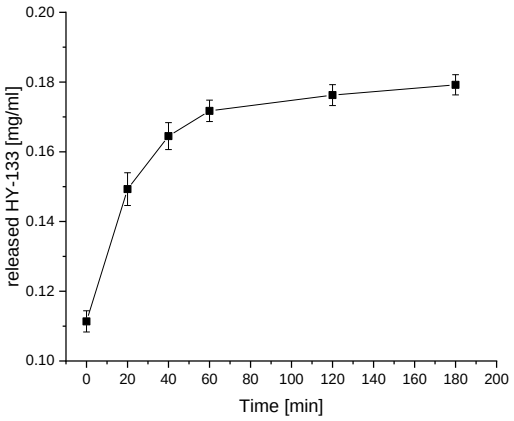

Figure 5: Release curve of the final nanoparticle formulation (n=2).

3.4 Concentration of nanoparticles

To evaluate the influence of the amount of nanoparticles present during a release test, the concentration of the nanoparticles was increased by reducing the suspension volume after a centrifugation step. A new batch was used with about 90% loading efficiency of the initially used 0.5 mg/ml HY-133. Two different HY-133 concentrations, 1 mg/ml and 2.5 mg/ml, were then prepared via up-concentration through centrifugation. Subsequently, the release was studied with all three variations.

Figure 6 shows the release curve of the nanoparticle suspension with an initial amount of 0.5 mg/ml HY-133. A small amount of protein was released in the first 60 min of the study, but stops thereafter. The study was terminated after 240 min with about 13% of the overall loaded protein released.

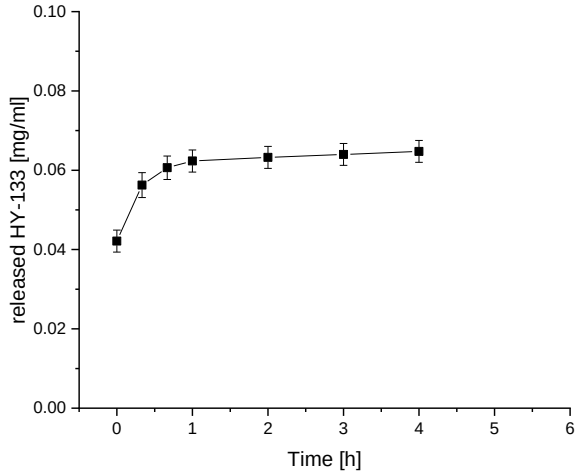

Figure 6: Release curve of a HY-133 nanoparticle batch loaded with 0.5 mg/ml HY-133.

The higher concentrated nanoparticle variations showed a strong release onset in the first 60 min, but again constant protein concentrations after this time (Figure 7). Nevertheless, more protein was released when a higher nanoparticle concentration was available.

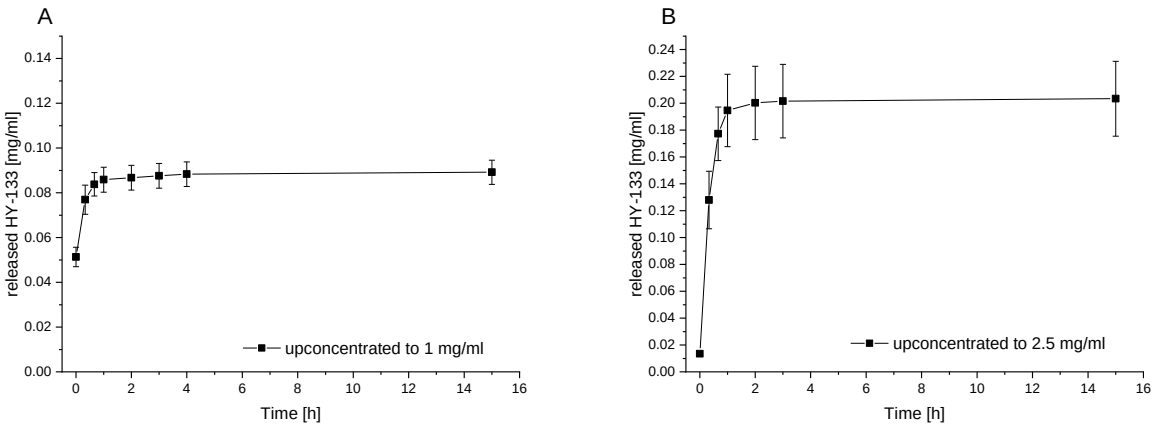

Figure 7: Release curve of a HY-133 nanoparticle batch containing 1 mg/ml HY-133 (A) and 2.5 mg/ml HY-133 (B).

4. Discussion and outlook

Different observations could be made throughout the nanoparticle study.

A major point for consistent nanoparticle preparation is a reproducible loading procedure with a constant protein load. Repeats of various batches applying the same parameters did not result in a reliable protein load. Variation of the protein concentration did not yield in an improved protein load. Particle formation is based on self-assembly of different charged components. Thus, the protein concentration might be reduced below 0.5 mg/ml HY-133 to result in constant protein load >90%.

It was further observed that the zeta potential of the nanoparticles had an influence on protein loading, protein release, as well as protein stability. Only negatively charged particles (zeta potential of -40 mV and lower) had sufficient protein load, a slight protein release and maintained protein stability. Particles with zeta potentials between -15 mV and +15 mV could not fulfill any of the above-mentioned points. For further studies, a more negative zeta potential should be used with respect to protein load, release, and stability.

The results of the alginate nanoparticle study did not result in sufficiently high protein release with smaller particle sizes. As stated above, a decrease in protein concentration is thought to reduce particle sizes further, which might improve protein release. In this study, particle size had no influence on protein quality attributes. The low release rate of HY-133 from the nanoparticles could not be solved and needs to be addressed in further studies. To achieve the required HY-133 dose in future studies, particle formation with lower protein concentration followed by an up-concentration step might be beneficial. However, aggregation of nanoparticles due to high nanoparticle counts needs to be avoided.

5. References

[1] S. Khoshnood *et al.*, "A review on mechanism of action, resistance, synergism, and clinical implications of mupirocin against Staphylococcus aureus," *Biomed. Pharmacother.*, vol. 109, no. October 2018, pp. 1809–1818, 2019.

[2] K. M. Craft, J. M. Nguyen, L. J. Berg, and S. D. Townsend, "Methicillin-resistant Staphylococcus aureus (MRSA): antibiotic-resistance and the biofilm phenotype," *Medchemcomm*, vol. 10, no. 8, pp. 1231–1241, 2019.

[3] F. R. DeLeo, B. A. Diep, and M. Otto, "Host Defense and Pathogenesis in Staphylococcus aureus Infections," *Infect. Dis. Clin. North Am.*, vol. 23, no. 1, pp. 17–34, 2009.

[4] F. Kipp, K. Becker, G. Peters, and C. Von Eiff, "Evaluation of Different Methods to Detect Methicillin Resistance in Small-Colony Variants of Staphylococcus aureus," *J. Clin. Microbiol.*, vol. 42, no. 3, pp. 1277–1279, 2004.

[5] Z. A. Mirani, M. Aziz, and S. I. Khan, "Small colony variants have a major role in stability and persistence of Staphylococcus aureus biofilms," *J. Antibiot. (Tokyo).*, vol. 68, no. 2, pp. 98–105, 2015.

[6] N. Schleimer *et al.*, "In Vitro Activity of the Bacteriophage Endolysin HY-133 against Staphylococcus aureus Small-Colony Variants and Their Corresponding Wild Types," *Int. J. Mol. Sci.*, vol. 20, no. 3, p. 716, Feb. 2019.

[7] D. Knaack *et al.*, "Bactericidal activity of bacteriophage endolysin HY-133 against Staphylococcus aureus in comparison to other antibiotics as determined by minimum bactericidal concentrations and time-kill analysis," *Diagn. Microbiol. Infect. Dis.*, vol. 93, no. 4, pp. 362–368, Apr. 2019.

[8] N. H. Kim *et al.*, "Effects of phage endolysin SAL200 combined with antibiotics on staphylococcus aureus infection," *Antimicrob. Agents Chemother.*, vol. 62, no. 10, pp. 1–10, 2018.

[9] S. Y. Jun *et al.*, "Antibacterial properties of a pre-formulated recombinant phage endolysin, SAL-1.," *Int. J. Antimicrob. Agents*, vol. 41, no. 2, pp. 156–61, Feb. 2013.

[10] I. Santos Ferreira *et al.*, "Encapsulation in Polymeric Microparticles Improves Daptomycin Activity Against Mature Staphylococci Biofilms—a Thermal and Imaging Study," *AAPS PharmSciTech*, vol. 19, no. 4, pp. 1625–1636, 2018.

[11] K. Bhise *et al.*, "Combination of vancomycin and cefazolin lipid nanoparticles for overcoming

antibiotic resistance of MRSA," *Materials*, vol. 10, no. 7, 2018.

[12] K. Cihalova *et al.*, "Staphylococcus aureus and MRSA growth and biofilm formation after treatment with antibiotics and SeNPs," *Int. J. Mol. Sci.*, vol. 16, no. 10, pp. 24656–24672, 2015.

[13] S. Portilla, L. Fernández, D. Gutiérrez, A. Rodríguez, and P. García, "Encapsulation of the antistaphylococcal endolysin lysrodi in ph-sensitive liposomes," *Antibiotics*, vol. 9, no. 5, pp. 1–8, 2020.

[14] R. Donnelly, R. Shaikh, T. Raj Singh, M. Garland, and Ad. Woolfson, "Mucoadhesive drug delivery systems," *J. Pharm. Bioallied Sci.*, vol. 3, no. 1, p. 89, Jan. 2011.

[15] B. Mishra, B. B. Patel, and S. Tiwari, "Colloidal nanocarriers: a review on formulation technology, types and applications toward targeted drug delivery," *Nanomedicine Nanotechnology, Biol. Med.*, vol. 6, no. 1, pp. 9–24, 2010.

[16] I. I. Slowing, J. L. Vivero-Escoto, C. W. Wu, and V. S. Y. Lin, "Mesoporous silica nanoparticles as controlled release drug delivery and gene transfection carriers," *Adv. Drug Deliv. Rev.*, vol. 60, no. 11, pp. 1278–1288, 2008.

[17] U. Bilati, E. Allémann, and E. Doelker, "Strategic approaches for overcoming peptide and protein instability within biodegradable nano- and microparticles," *Eur. J. Pharm. Biopharm.*, vol. 59, no. 3, pp. 375–388, 2005.

[18] N. Sahoo, R. K. Sahoo, N. Biswas, A. Guha, and K. Kuotsu, "Recent advancement of gelatin nanoparticles in drug and vaccine delivery," *Int. J. Biol. Macromol.*, vol. 81, pp. 317–331, 2015.

[19] A. O. Elzoghby, W. M. Samy, and N. A. Elgindy, "Protein-based nanocarriers as promising drug and gene delivery systems," *J. Control. Release*, vol. 161, no. 1, pp. 38–49, 2012.

[20] C. J. Coester, K. Langer, H. van Briesen, and J. Kreuter, "Gelatin nanoparticles by two step desolvation--a new preparation method, surface modifications and cell uptake.," *J. Microencapsul.*, vol. 17, no. 2, pp. 187–193, 2000.

[21] K. J. Geh, M. Hubert, and G. Winter, "Optimisation of one-step desolvation and scale-up of gelatine nanoparticle production," *J. Microencapsul.*, vol. 33, no. 7, pp. 595–604, 2016.

[22] I. Wagner *et al.*, "Preliminary evaluation of cytosine-phosphate-guanine oligodeoxynucleotides bound to gelatine nanoparticles as immunotherapy for canine atopic dermatitis," *Vet. Rec.*, vol. 181, no. 5, p. 118, 2017.

[23] J. Sharma and H. B. Bohidar, "Gelatin-glutaraldehyde supramolecular structures studied by

laser light scattering," *Eur. Polym. J.*, vol. 36, no. 7, pp. 1409–1418, 2000.

[24] C. M. Silva, A. J. Ribeiro, D. Ferreira, and F. Veiga, "Insulin encapsulation in reinforced alginate microspheres prepared by internal gelation," *Eur. J. Pharm. Sci.*, vol. 29, no. 2, pp. 148–159, 2006.

[25] B. Sarmento, S. Martins, A. Ribeiro, F. Veiga, R. Neufeld, and D. Ferreira, "Development and comparison of different nanoparticulate polyelectrolyte complexes as insulin carriers," *Int. J. Pept. Res. Ther.*, vol. 12, no. 2, pp. 131–138, 2006.

[26] A. W. Chan and R. J. Neufeld, "Tuneable semi-synthetic network alginate for absorptive encapsulation and controlled release of protein therapeutics," *Biomaterials*, vol. 31, no. 34, pp. 9040–9047, 2010.

[27] L. A. Wells and H. Sheardown, "Extended release of high pI proteins from alginate microspheres via a novel encapsulation technique," *Eur. J. Pharm. Biopharm.*, vol. 65, no. 3, pp. 329–335, 2007.

[28] J. Kaur, A. Kour, J. J. Panda, K. Harjai, and S. Chhibber, "Exploring Endolysin-Loaded Alginate-Chitosan Nanoparticles as Future Remedy for Staphylococcal Infections," *AAPS PharmSciTech*, vol. 21, no. 6, pp. 1–15, 2020.

[29] J. P. Paques, E. Van Der Linden, C. J. M. Van Rijn, and L. M. C. Sagis, "Preparation methods of alginate nanoparticles," *Adv. Colloid Interface Sci.*, vol. 209, pp. 163–171, 2014.

[30] A. Rampino, M. Borgogna, P. Blasi, B. Bellich, and A. Cesàro, "Chitosan nanoparticles: Preparation, size evolution and stability," *Int. J. Pharm.*, vol. 455, no. 1–2, pp. 219–228, 2013.

[31] B. Sarmento, D. C. Ferreira, L. Jorgensen, and M. van de Weert, "Probing insulin's secondary structure after entrapment into alginate/chitosan nanoparticles," *Eur. J. Pharm. Biopharm.*, vol. 65, no. 1, pp. 10–17, 2007.

[32] L. A. Frank, G. R. Onzi, A. S. Morawski, A. R. Pohlmann, S. S. Guterres, and R. V Contri, "Chitosan as a coating material for nanoparticles intended for biomedical applications," *React. Funct. Polym.*, vol. 147, p. 104459, 2020.

Chapter 9

Final Summary

The present thesis mainly focused on the formulation development of the novel bacteriophage endolysin HY-133 for MRSA treatment, which has not been explored yet in detail: i) analytical challenges (Chapter 3) and investigation of physicochemical properties (Chapter 4) to ii) develop liquid formulation of HY-133 (Chapter 5) including the effect of Good's buffers on protein stability (Chapter 6), followed by iii) studies on prolonged release in hydrogels including a scale-up procedure (Chapter 7) and nanoparticulate systems (Chapter 8).

In order to understand the protein stability of the novel bacteriophage HY-133, an analytical tool set was adapted and extended covering several stability indicating methods (Chapter 3). Due to the uncommon 2-domain structure of the protein, the physicochemical properties of HY-133 were characterized further to understand purity, protein integrity and conformation of the protein (Chapter 4).

During drug product development, a suitable and stable liquid formulation of the novel bacteriophage endolysin HY-133 was developed (Chapter 5). Four different formulation screenings and stability studies were conducted to identify a formulation composition providing sufficient protein stability. Thereby, a final composition of a HEPES buffer with poloxamer 188 at pH 6.0 proved better stability compared to histidine, citrate, or combined buffer systems while keeping the salt content ($CaCl_2$, methionine, Arg-HCl and NaCl) unchanged. Further, protein stability was concentration dependent, showing best stability with the lowest tested concentration (0.5 mg/ml HY-133). Using only half of the originally Arg-HCl and NaCl concentrations yielded in an improved protein stability as well as only slightly hypertonic formulation. The liquid formulation further proved to be stable in the intended primary packaging material; nasal sprays in HD-PE containers, stored at 4 °C for over 6 months.

HEPES as crucial formulation component was compared to other Good's buffers, testing if a similar protein stability profile could be achieved (Chapter 6). The exceptional stabilizing effect was thought to be similar in structurally similar excipients, such as POPSO, MES, MOPS, PIPES, and EPPS. All piperazinic or morpholinic derivatives increased the protein stability compared to a buffer composition without any of these derivatives. Still, HEPES resulted in better protein stability due to its outstanding effect on rapidly binding to the protein without changing k_D, detected in homo- and heteroassociation CG-MALS experiments. The advantage of HEPES against the other Good's buffers was seen in the already existing use in protein expression, up- and downstream, making the need for diafiltration or

dialysis during drug substance manufacturing to other stabilizing agents potentially redundant. These findings were supported by in-silico analysis. The concept of the formulation was patented.

Based on the liquid formulation, a step towards the application as nasal spray was done by developing a sprayable hydrogel drug product. In placebo trials, a suitable spraying behavior including a suitable viscosity was established, subsequently followed by a stability study of HY-133 in the hydrogels (Chapter 7). Thereby, the buffer explored within Chapter 5 was utilized and gelling agents, such as NaCMC, various HPMC types, PVP, gellan gum, and xanthan gum. Best performing critical parameters with respect to viscosity, protein stability, and slightly sustained release were achieved with HPMC hydrogels. Different HPMC types were suitable although they showed differences when sourced from different vendors or varying batches. However, HPMC K4M (Methocel) was chosen as final excipient for the hydrogel formulation. Sterilization of the placebo gel by autoclaving and later aseptic compounding of HY-133 in the gel was established successfully.

An improvement of sustained release of HY-133 on the nasal cavity was planned to be implemented by nanoparticulate systems. A formulation development was performed with gelatin and alginate nanoparticles (Chapter 9). The generated particles could not release a sufficient amount of protein, irrespective of the release duration. Particle size, protein concentration, and ionic strength of the composition are thought to be the main factors of not releasing the protein. Further and extensive development would be required, if this approach would be still considered of interest by the sponsors.

In summary, this thesis provided several new findings regarding the handling and stabilization requirements of the novel bacteriophage endolysin HY-133. A suitable liquid and also hydrogel formulation were discovered, proving stability at 4 °C for several months, while a sustained release out of nanoparticulate systems could not be achieved.